The genetics of adaptation

at a species' southern range edge

Inauguraldissertation

zur

Erlangung der Würde eines Doktors der Philosophie

vorgelegt der

Philosophisch-Naturwissenschaftlichen Fakultät

der Universität Basel

von

Jessica Heblack

2024

Genehmigt von der Philosophisch-Naturwissenschaftlichen Fakultät auf Antrag von

Erstbetreuerin: Prof. Yvonne Willi (Universität Basel)

Zweitbetreuer: PD Dr. Daniel Berner (Universität Basel)

Externer Experte: Dr. Jake Alexander (ETH Zürich)

Basel, den 27.02.2024

Prof. Dr. Marcel Mayor

Dekan

Table of contents

Abstract

This study investigates the factors influencing the geographic distribution and adaptive potential of *Arabidopsis lyrata* subsp. *lyrata*, a plant species with a restricted distribution in Northern America. The research addresses questions posed by ecologists and evolutionary biologists regarding the limitations of species adaptation and the drivers of geographic distribution. The study integrates ecological and evolutionary perspectives. On the one hand, by exploring the interplay of ecological constraints resulting from steep environmental gradients. On the other hand, evolutionary challenges of genetic drift, reduced genetic diversity, and trade-offs between adaptive traits. The focus is on the southern range edge, where climate change is expected to impose rapid and frequent environmental shifts.

Chapter I investigates how genetic diversity is maintained in a dynamic dune landscape, revealing signs of local adaptation through a genome-wide association study. The analyses identify outlier genes associated with reproductive development, highlighting the role of landscape features and climate in driving genetic differentiation.

Chapter II explores genetic constraints on traits of adaptation using a greenhouse stress experiment that simulates climatic conditions at the southern range edge. While phenotypic performance differences suggest synergistic effects under multi-stress conditions, genetic variance-covariance matrices reveal complex patterns with potential limitations to multivariate genetic variation. Constraints between growth traits and their divergence from selection pressure emphasize the challenges of adapting to changing environmental conditions.

Chapter III examines the genomic basis of the differences in performance using a natural selection experiment along the southern range edge in the USA. Family effects within the greenhouse experiment explain a high fraction of the observed variance, emphasizing the complexity of natural environments. Gene-level analysis reveals low overlap between

treatment and common garden sites for the same trait, highlighting the intricate genetic pathways involved in trait establishment.

In conclusion, the study highlights the complexity of genetic processes shaping adaptive potential. While genetic variability is present under range edge conditions, the multi-environmental nature introduces genetic constraints. The study underscores the importance of considering landscape context and genetic complexities in understanding a species' adaptive responses to environmental changes. The speed of adaptation remains a question, demanding further experiments focusing on real-time evolution. Additionally, broader genetic analyses and microclimate studies may provide deeper insights into the traits and genes underlying adaptive potential at the southern range edge.

Acknowledgements

Foremost I would like to thank my supervisor Yvonne Willi for offering me the opportunity to do my PhD. I highly appreciate your confidence in my work, your support, and the scientific knowledge you taught me.

I like to thank my committee members Daniel Berner and Jake Alexander for accepting to be part of my thesis committee, for their participation and contribution. I would also like to thank Judith Schepers and Kay Lucek for their support in analysing data, discussing results, writing, and publishing. Many thanks also to Jana Flury, Aaditya Narasimhan, and Thomas Dorey for your valuable inputs during various parts of my thesis.

A very special and warm thank you to my lab besties, Olivier Bachmann, and Markus Funk, without your jolly friendship my PhD would only have been half as funny. Thank you, Olivier, also for your excellent help during lab work and plant crossing – the group would not be the same without you. Same goes for Susanna Riedl, endless thanks for your help during plant raising and crossing and for being such a great "office-mum" for me. I would also like to thank Georg Armbruster – I miss your Wednesday cakes, Theofania Patsiou, and Hannah Augustijnen – the office would have been lonely without you.

I highly appreciate the help and commitment of all the students and professors in the United States: Brooks Saville, Sara Childs, Tom Craven and his crew at Duke Forest, Carole Goodwillie, John Gill, Brian Tew, and the whole facility team at ECU, Jeffrey Derr and Rob Holz, the Virginia Department of Conservation and Recreation as well as Charlie Whalen and his team at York River State Park, David Marsh, Nicole Poulin, Bill Hamilton, and finally, Aleks H., Marisa F., Nadia S., Christy C., Marleigh M., Adam N., Steven H., Jordan B., Ni'Dajah B., Josh G., Jensen R., and Tanner H. Same goes for all the helpers from the University of Basel: Xenia Q., Charlotta M., Flurina S., Elis B., Elias T., and Siro E.

Special thanks also to Katja, und Niels – my master supervisors – you first showed me how field work could be like, and I learned so much from you. Despite the distance you still care about my future and believe in me. Thank you so much.

Lastly, I would like to thank my family and friends for all your help, believe, and encouragement during all the ups and downs of my PhD. Special thanks to my parents, for all the things you have taught me and that have brought me so far. To my partner, for fighting with me through this though PhD times but also through all real-life problems – I cannot thank you enough. To my besties: Nadine, Kaarina, Sam, and Kay – thank you for always having a friendly ear for my problems and struggles.

A thousand times thank you.

Jessica Heblack

General introduction

An ecological niche is described by the environmental conditions where a species can maintain viable populations (Hutchinson, 1957), and if dispersal limitation can be ruled out, coincides with species distribution limits (Hargreaves et al., 2014). Since decades, it has been an open question in ecology and evolutionary biology why species cannot broaden their niche easily.

On the one hand, ecologists propose that distribution limits occur due to restricted dispersal abilities of species and restrictions to their ecological niche (Lee-Yaw et al., 2018; Paccard et al., 2016; Willi & Van Buskirk, 2019). Evolutionary biologists, on the other hand, posit that distribution limits occur due to limits to adaptation. Adaptation can be limited because of increased genetic drift and decreased genetic diversity at range edges, reducing the ability of species to adapt to new environmental conditions (Lee-Yaw et al., 2018; Paccard et al., 2016; Willi & Van Buskirk, 2019). Alternatively, biased dispersal from diverse central populations may cause maladaptation at range edges (Kirkpatrick & Barton, 1997), which can occur in species with high dispersing capabilities over relatively short and steep environmental gradients. A further hypothesis is that a species' niche is the result of trade-offs in environmental tolerances that constrain adaptation and thus manifest as range limits (MacArthur, 1972). Due to this interplay of ecological restrictions coupled with the mentioned evolutionary problems species at range limits are especially vulnerable to environmental change.

A systematic change in environmental conditions is involved in many range limits (Tomasini et al., 2022). Environments within a species' distribution are heterogeneous, but along a latitudinal or elevational gradient they change gradually (Leinonen et al., 2009). This can include, increasing day lengths towards the poles during summer, higher temperatures to the equator, and lower precipitation starting from mid-latitude regions (excluding rain forests; Ritter, 2024), and stronger radiation and shorter vegetation periods at higher altitudes (Billings,

1974). As these changes deviate from the optimal conditions a species requires, we observe reduced species abundances at boundaries of their distribution. This pattern has been described as the abundant-centre hypothesis (Brown, 1984). As a result, fewer individuals are capable of surviving in these suboptimal conditions, reducing the number of successful gene variants, thus enhancing genetic drift, and reducing genetic diversity necessary for species to adapt to new environments or fluctuating conditions (Eckert et al., 2010; Willi & Van Buskirk, 2019). Further, as these edge populations are smaller and more isolated from the centre, probably through biased dispersal by steep selection gradients, gene flow is restricted and the chance for the fixation of maladaptive genes is increased, leading to reduced local adaptation (Kawecki, 2008; Whitlock, 2000; Willi & Van Buskirk, 2019).

Another reason for range limits may involve trade-offs – genetic correlations between adaptive traits. They can be caused by pleiotropic antagonism, one gene controls more than one trait, with traits having conflicting effects (Rose, 1983) or linkage – alleles do not segregate independently (Pulst, 1999). Historically, trade-offs between life-history traits have been studied extensively (Stearns, 1992), and most trade-offs emerge related to growth and development (Lande, 1980; Stearns, 1989). Examples are manifold, e.g., increased thermal resistance in ectotherms with the cost of reduced growth or longevity (Burraco et al., 2020), constraints between longevity and body size in Drosophila (Norry & Loeschcke, 2002) or defence investment reduces growth in multiple plant species (Lind et al., 2013). Recent work on 100 Brassicaceae species across the Alps revealed that faster growth under heat resulted in reduced leaf and plant size, indicating the presence of a trade-off which might constrain adaptation to warming conditions (Maccagni & Willi, 2022) and the evolution of favourable traits at species margins (Hoffmann & Blows, 1994). Genetic constraints can be tested by determining genetic variance-covariance matrices (G-matrices) between different traits of adaptation (Arnold, 1992; Lande, 1979), with the dimensionality of the G-matrix indicating the

level of genetic constraint (Kirkpatrick, 2009). The divergence of a G-matrix from vector of population divergence can further be used to estimate the direction (Schluter, 1996) and the response of selection (Blows & Hoffmann, 2005; Hansen & Houle, 2008), indicating the selective potential of the species under the giving environmental pressures.

Species distribution models have been used to predict a species persistence under ongoing climate change (e.g., Cursach et al., 2020; Heikkinen et al., 2006; Lee-Yaw et al., 2018). These models focused on the known restriction of distributions by steep environmental conditions and reduced genetic variation (Phillips, 2012; Polechová & Barton, 2015). However, consider selection to be multivariate, nor that selection occurs on suites of correlated characters (Antonovics, 1976; Lande & Arnold, 1983). In recent years, and with the development of efficient, affordable, and fast sequencing techniques it is now possible to investigate the underlying genetics and involved traits in adaptive responses to environmental stress on a wider range of traits, individuals, and species using genome-wide association studies (GWAS). Adding these insights to existing distribution model approaches can help to better predict the reaction of a species under climate change (Capblancq et al., 2020; Exposito-Alonso, 2023), as well as indicate possible starting points for assisted gene flow in threatened species, reducing the potential of introducing maladapted genes (Aitken & Whitlock, 2013).

In summary, species distributions, especially distributions coinciding with a species' ecological niche, can be explained by an interplay of multiple ecological as well as evolutionary factors. However, under ongoing climate change it is essential to know the specific underlying genetics and genetic constraints that could limit species' distributions, to further predict the survival of populations and species at their range edges.

Study system

In this thesis, I use *Arabidopsis lyrata* ssp. *lyrata*, as the model species to investigate the

genetics of adaptation at its range margins. I study genetic trade-offs under multi-environmental stress, and the genomic backbone of selection at the southern edge of its distribution. *Arabidopsis lyrata* has become a commonly used species in genome- and adaptation-related studies (Leinonen et al., 2011; Ross-Ibarra et al., 2008). One reason for this is that the three subspecies of *A. lyrata* have a circumpolar distribution with, *A. l. kamchatica* in Canada and northern Asia, *A. l. petraea* in north-central Europe, and *A. l. lyrata* in northern America (Al-Shehbaz & O'Kane, 2002), and are found in a wide range of different habitats. This opens the possibility of studying adaptations to different climatic conditions in populations sharing a closer genomic background. Further, *A. lyrata* is a sister species of the model organism *A. thaliana* (L.) Heynh., with a relatively short divergence time of approximately 10-11 million years (Hanada et al., 2018), and a sequence identity of values greater than 80%, which provides a powerful toolbox for genetic studies (Hu et al., 2011). *Arabidopsis l. lyrata* in North America is mainly outcrossing, with some selfing populations at the range margins. In previous studies, it was shown that *A. l. lyrata* in North America is genetically divided into two clusters, an eastern and a western one, with some evidence of admixture in the Lake Erie region (Griffin & Willi, 2014; Willi & Määttänen, 2010).

The distribution of *Arabidopsis lyrata* ssp. *lyrata*, henceforth referred to as *A. lyrata*, in the United States and Canada is known to be restricted in the north and south by niche limitations (Lee-Yaw et al., 2018). Under ongoing climate change, frequent changes of temperature, and precipitation patterns are expected, and have already changed drastically along the southern range edge of species distributions (Dore, 2005). Increased species extinctions at the warm ends of species' distributions have already been observed, e.g., in plant species of the Alps and marine ecosystems (Fredston-Hermann et al., 2020; Pinsky et al., 2019; Rumpf et al., 2019). Therefore, *A. lyrata* is a prime candidate to investigate which climatic, phenotypic, and genetic factors might hinder adaptation at its southern range limit.

As a pioneer species, *A. lyrata* occurs on nutrient poor, sandy dunes or rocky outcrops along riverbanks and shorelines. The species is perennial with a basal rosette and 10 mm long white flowers. Flowering mainly occurs in early spring, but autumn flowering can be seen. *Arabidopsis lyrata* is mostly pollinated by bees and flies, e.g., Syrphids, and Bombyliids (Sánchez-Castro et al., 2022). Seeds mainly germinate in the autumn of seed set, and seedlings produce a sufficient rosette before winter onset.

This thesis will mainly work with one population in the southern centre of the species distribution, which harbours a high level of genetic diversity (Griffin & Willi, 2014; Willi & Määttänen, 2010, 2010). Interestingly, despite its central location, it harbours the same clinal variation in the four traits varying the most along the latitudinal gradient, including reproductive development and size (Paccard et al., 2014; Wos & Willi, 2015), making it the prime study population.

Research questions

Based on the described theories I investigated in my thesis, whether local adaptation to a dynamic landscape helps to maintain a high level of genetic variance in fitness related traits (**Chapter I**). Secondly, I conducted a greenhouse stress experiment to assess the genetic variances and covariances matrices (G-matrix) of life cycle related growth traits, Hereby, I want to reveal possible trade-offs that might reduce the evolutionary potential of a plant species reacting to different environmental selection pressures (**Chapter II**). Lastly, I performed a natural selection experiment along the southern range edge of a plant species to assess the genomic basis of performance differences, and whether responses to selection can be predicted (**Chapter III**).

References

Aitken, S. N., & Whitlock, M. C. (2013). Assisted gene flow to facilitate local adaptation to climate change. *Annual Review of Ecology, Evolution, and Systematics*, *44*(1), 367–388. https://doi.org/10.1146/annurev-ecolsys-110512-135747

Al-Shehbaz, I. A., & O'Kane, S. L. (2002). Taxonomy and phylogeny of Arabidopsis (Brassicaceae). *The Arabidopsis Book*, *1*, e0001. https://doi.org/10.1199/tab.0001

Antonovics, J. (1976). The nature of limits to natural selection. *Annals of the Missouri Botanical Garden*, *63*(2), 224. https://doi.org/10.2307/2395303

Arnold, S. J. (1992). Constraints on phenotypic evolution. *The American Naturalist*, *140*, S85–S107. https://doi.org/10.1086/285398

Billings, W. D. (1974). Adaptations and origins of alpine plants. *Arctic and Alpine Research*, *6*(2), 129–142. https://doi.org/10.1080/00040851.1974.12003769

Blows, M. W., & Hoffmann, A. A. (2005). A reassessment of genetic limits to evolutionary change. *Ecology*, *86*(6), 1371–1384. https://doi.org/10.1890/04-1209

Brown, J. H. (1984). On the relationship between abundance and distribution of species. *The American Naturalist*, *124*(2), 255–279. https://doi.org/10.1086/284267

Burraco, P., Orizaola, G., Monaghan, P., & Metcalfe, N. B. (2020). Climate change and ageing in ectotherms. *Global Change Biology*, *26*(10), 5371–5381. https://doi.org/10.1111/gcb.15305

Capblancq, T., Fitzpatrick, M. C., Bay, R. A., Exposito-Alonso, M., & Keller, S. R. (2020). Genomic prediction of (mal)adaptation across current and future climatic landscapes. *Annual Review of Ecology, Evolution, and Systematics*, *51*(1), 245–269. https://doi.org/10.1146/annurev-ecolsys-020720-042553

Cursach, J., Far, A. J., & Ruiz, M. (2020). Geospatial analysis to assess distribution patterns and predictive models for endangered plant species to support management decisions: A case study in the Balearic Islands. *Biodiversity and Conservation*, *29*(11–12), 3393–3410. https://doi.org/10.1007/s10531-020-02029-y

Dore, M. H. I. (2005). Climate change and changes in global precipitation patterns: What do we know? *Environment International*, *31*(8), 1167–1181. https://doi.org/10.1016/j.envint.2005.03.004

Eckert, A. J., Bower, A. D., González-Martínez, S. C., Wegrzyn, J. L., Coop, G., & Neale, D. B. (2010). Back to nature: Ecological genomics of loblolly pine (*Pinus taeda*, Pinaceae): Ecological genomics of loblolly pine. *Molecular Ecology*, *19*(17), 3789–3805. https://doi.org/10.1111/j.1365-294X.2010.04698.x

Exposito-Alonso, M. (2023). Understanding local plant extinctions before it is too late: Bridging evolutionary genomics with global ecology. *New Phytologist*, *237*(6), 2005–2011. https://doi.org/10.1111/nph.18718

Fredston-Hermann, A., Selden, R., Pinsky, M., Gaines, S. D., & Halpern, B. S. (2020). Cold range edges of marine fishes track climate change better than warm edges. *Global Change Biology*, *26*(5), 2908–2922. https://doi.org/10.1111/gcb.15035

Griffin, P. C., & Willi, Y. (2014). Evolutionary shifts to self-fertilisation restricted to geographic range margins in North American *Arabidopsis lyrata*. *Ecology Letters*, *17*(4), 484–490. https://doi.org/10.1111/ele.12248

Hanada, K., Tezuka, A., Nozawa, M., Suzuki, Y., Sugano, S., Nagano, A. J., Ito, M., & Morinaga, S.-I. (2018). Functional divergence of duplicate genes several million years after gene duplication in Arabidopsis. *DNA Research*, *25*(3), 327–339. https://doi.org/10.1093/dnares/dsy005

Hansen, T. F., & Houle, D. (2008). Measuring and comparing evolvability and constraint in multivariate characters. *Journal of Evolutionary Biology*, *21*(5), 1201–1219. https://doi.org/10.1111/j.1420-9101.2008.01573.x

Hargreaves, A. L., Samis, K. E., & Eckert, C. G. (2014). Are species' range limits simply niche limits writ large? A review of transplant experiments beyond the range. *The American Naturalist*, *183*(2), 157–173. https://doi.org/10.1086/674525

Heikkinen, R. K., Luoto, M., Araújo, M. B., Virkkala, R., Thuiller, W., & Sykes, M. T. (2006). Methods and uncertainties in bioclimatic envelope modelling under climate change. *Progress in Physical Geography: Earth and Environment*, *30*(6), 751–777. https://doi.org/10.1177/0309133306071957

Hoffmann, A. A., & Blows, M. W. (1994). Species borders: Ecological and evolutionary perspectives. *Trends in Ecology & Evolution*, *9*(6), 223–227. https://doi.org/10.1016/0169-5347(94)90248-8

Hu, T. T., Pattyn, P., Bakker, E. G., Cao, J., Cheng, J.-F., Clark, R. M., Fahlgren, N., Fawcett, J. A., Grimwood, J., Gundlach, H., Haberer, G., Hollister, J. D., Ossowski, S., Ottilar, R. P., Salamov, A. A., Schneeberger, K., Spannagl, M., Wang, X., Yang, L., … Guo, Y.-L. (2011). The *Arabidopsis lyrata* genome sequence and the basis of rapid genome size change. *Nature Genetics*, *43*(5), 476–481. https://doi.org/10.1038/ng.807

Hutchinson, G. E. (1957). Concluding remarks. *Cold Spring Harbor Symposia on Quantitative Biology*, *22*(0), 415–427. https://doi.org/10.1101/SQB.1957.022.01.039

Kawecki, T. J. (2008). Adaptation to marginal habitats. *Annual Review of Ecology, Evolution, and Systematics*, *39*(1), 321–342. https://doi.org/10.1146/annurev.ecolsys.38.091206.095622

Kirkpatrick, M. (2009). Patterns of quantitative genetic variation in multiple dimensions. *Genetica*, *136*(2), 271–284. https://doi.org/10.1007/s10709-008-9302-6

Kirkpatrick, M., & Barton, N. H. (1997). Evolution of a species' range. *The American Naturalist*, *150*(1), 1–23. https://doi.org/10.1086/286054

Lande, R. (1979). *Quantitative genetic analysis of multivariate evolution, applied to brain: Body size allometry*. 16.

Lande, R. (1980). The genetic covariance between characters maintained by pleiotropic mutations. *Genetics*, *94*(1), 203–215. https://doi.org/10.1093/genetics/94.1.203

Lande, R., & Arnold, S. J. (1983). The measurement of selection on correlated characters. *Evolution*, *37*(6), 1210. https://doi.org/10.2307/2408842

Lee-Yaw, J. A., Fracassetti, M., & Willi, Y. (2018). Environmental marginality and geographic range limits: A case study with *Arabidopsis lyrata* ssp. *lyrata*. *Ecography*, *41*(4), 622–634. https://doi.org/10.1111/ecog.02869

Leinonen, P. H., Remington, D. L., & Savolainen, O. (2011). Local adaptation, phenotypic differentiation, and hybrid fitness in diverged natural populations of *Arabidopsis lyrata*: Adaptation and hybrid fitness in *A. lyrata*. *Evolution*, *65*(1), 90–107. https://doi.org/10.1111/j.1558-5646.2010.01119.x

Leinonen, P. H., Sandring, S., Quilot, B., Clauss, M. J., Mitchell-Olds, T., Agren, J., & Savolainen, O. (2009). Local adaptation in European populations of *Arabidopsis lyrata* (Brassicaceae). *American Journal of Botany*, *96*(6), 1129–1137. https://doi.org/10.3732/ajb.0800080

Lind, E. M., Borer, E., Seabloom, E., Adler, P., Bakker, J. D., Blumenthal, D. M., Crawley, M., Davies, K., Firn, J., Gruner, D. S., Stanley Harpole, W., Hautier, Y., Hillebrand, H., Knops, J., Melbourne, B., Mortensen, B., Risch, A. C., Schuetz, M., Stevens, C., & Wragg, P. D. (2013). Life-history constraints in grassland plant species: A growth-defence trade-off is the norm. *Ecology Letters*, *16*(4), 513–521. https://doi.org/10.1111/ele.12078

MacArthur, R. H. (1972). *Geographical ecology: Patterns in the distribution of species*. Harper & Row, Publishers.

Maccagni, A., & Willi, Y. (2022). Trait divergence and trade-offs among Brassicaceae species differing in elevational distribution. *Evolution*, *76*(9), 1986–2003. https://doi.org/10.1111/evo.14554

Norry, F. M., & Loeschcke, V. (2002). Temperature-induced shifts in associations of longevity with body size in *Drosophila melanogaster*. *Evolution*, *56*(2), 299–306. https://doi.org/10.1111/j.0014-3820.2002.tb01340.x

Paccard, A., Fruleux, A., & Willi, Y. (2014). Latitudinal trait variation and responses to drought in *Arabidopsis lyrata*. *Oecologia*, *175*(2), 577–587. https://doi.org/10.1007/s00442-014-2932-8

Paccard, A., Van Buskirk, J., & Willi, Y. (2016). Quantitative genetic architecture at latitudinal range boundaries: Reduced variation but higher trait independence. *The American Naturalist*, *187*(5), 667–677. https://doi.org/10.1086/685643

Phillips, B. L. (2012). Range shift promotes the formation of stable range edges: Range shift and range edges. *Journal of Biogeography*, *39*(1), 153–161. https://doi.org/10.1111/j.1365-2699.2011.02597.x

Pinsky, M. L., Eikeset, A. M., McCauley, D. J., Payne, J. L., & Sunday, J. M. (2019). Greater vulnerability to warming of marine versus terrestrial ectotherms. *Nature*, *569*(7754), 108–111. https://doi.org/10.1038/s41586-019-1132-4

Polechová, J., & Barton, N. H. (2015). Limits to adaptation along environmental gradients. *Proceedings of the National Academy of Sciences*, *112*(20), 6401–6406. https://doi.org/10.1073/pnas.1421515112

Pulst, S. M. (1999). Genetic linkage analysis. *Archives of Neurology*, *56*(6), 667. https://doi.org/10.1001/archneur.56.6.667

Ritter, M. E. (2024). *The physical environment*. https://geo.libretexts.org/Bookshelves/Geography_(Physical)/The_Physical_Environment_(Ritter)

Rose, M. R. (1983). Further Models of Selection with Antagonistic Pleiotropy. In H. I. Freedman & C. Strobeck (Eds.), *Population Biology* (Vol. 52, pp. 47–53). Springer Berlin Heidelberg. https://doi.org/10.1007/978-3-642-87893-0_7

Ross-Ibarra, J., Wright, S. I., Foxe, J. P., Kawabe, A., DeRose-Wilson, L., Gos, G., Charlesworth, D., & Gaut, B. S. (2008). Patterns of polymorphism and demographic history in natural populations of *Arabidopsis lyrata*. *PLoS ONE*, *3*(6), e2411. https://doi.org/10.1371/journal.pone.0002411

Rumpf, S. B., Hülber, K., Wessely, J., Willner, W., Moser, D., Gattringer, A., Klonner, G., Zimmermann, N. E., & Dullinger, S. (2019). Extinction debts and colonization credits of non-forest plants in the European Alps. *Nature Communications*, *10*(1), 4293. https://doi.org/10.1038/s41467-019-12343-x

Sánchez-Castro, D., Armbruster, G., & Willi, Y. (2022). Reduced pollinator service in small populations of *Arabidopsis lyrata* at its southern range limit. *Oecologia*, *200*(1–2), 107–117. https://doi.org/10.1007/s00442-022-05237-1

Schluter, D. (1996). Adaptive radiation along genetic lines of least resistance. *Evolution*, *50*(5), 1766–1774. https://doi.org/10.1111/j.1558-5646.1996.tb03563.x

Stearns, S. C. (1989). Trade-offs in life-history evolution. *Functional Ecology*, *3*(3), 259. https://doi.org/10.2307/2389364

Stearns, S. C. (1992). *The evolution of life histories* (1st ed.). Oxford University Press.

Tomasini, M., Eriksson, M., Johannesson, K., & Rafajlović, M. (2022). *Shallow environmental gradients can cause range margins to form* [Preprint]. Evolutionary Biology. https://doi.org/10.1101/2022.03.19.484973

Whitlock, M. C. (2000). Local drift load and the heterosis of interconnected populations. *Heredity*, *84*(4), 452. https://doi.org/10.1046/j.1365-2540.2000.00693.x

Willi, Y., & Määttänen, K. (2010). Evolutionary dynamics of mating system shifts in Arabidopsis lyrata: Mating system shifts in A. lyrata. *Journal of Evolutionary Biology*, *23*(10), 2123–2131. https://doi.org/10.1111/j.1420-9101.2010.02073.x

Willi, Y., & Van Buskirk, J. (2019). A practical guide to the study of distribution limits. *The American Naturalist*, *193*(6), 773–785. https://doi.org/10.1086/703172

Wos, G., & Willi, Y. (2015). Temperature-stress resistance and tolerance along a latitudinal cline in North American *Arabidopsis lyrata*. *PLOS ONE*, *10*(6), e0131808. https://doi.org/10.1371/journal.pone.0131808

Chapter 1: **Transient genomic differentiation linked to micro-scale environmental heterogeneity in a population of *Arabidopsis lyrata***

Jessica Heblack[1], Kay Lucek[2] and Yvonne Willi[1]

[1] *Department of Environmental Sciences, University of Basel, 4056 Basel, Switzerland*

[2] *Institute of Biology, University of Neuchâtel, 2000 Neuchâtel, Switzerland*

Running title: Landscape association study

No. figures: 5

No. tables: 3

Supplementary: 5 figures, 11 tables

To be submitted to Molecular Ecology (MolEcol).

Abstract

Spatial variation in habitat features may lead to local adaptation even over short geographic scales and promote the maintenance of adaptive genetic diversity within populations. Here, we tested for the genomic footprint of such adaptation to different ecological aspects of a dune landscape by scanning for outlier genes associated with landscape parameters and phenotypic traits related to them. Our study system was a population of North American *Arabidopsis lyrata*. Seeds from across the dune landscape were collected, plants raised, and their phenology, growth, thermal resistance, and the shape and trichome of leaves assessed under greenhouse conditions. Using whole-genome sequences we performed genotype-environment and genotype-phenotype associations (GEAs and GPAs, respectively), quantified dispersal distances, and tested whether outlier genes harboured heightened diversity. We found several associations, despite marginal evidence for restricted gene flow over distance. The trait most commonly involved was time to flowering, and in line, out of the twelve overlapping candidate genes in GEAs and GPAs with known function, seven are involved in growth or reproductive development. Our findings further suggested that the transient patterns of adaptation likely involved genetic change at many loci each with small effect, and some evidence of weak dominance inheritance beyond additivity. Lastly, candidate genes had increased genetic diversity, but runs of homozygosity did not differ. Our study supports that transient adaptation over micro-habitat gradients can be polygenic with small effect genes, and that it increases the maintenance of adaptive genetic variation within populations, despite the homogenizing effect of gene flow.

Keywords: dispersal distance, genetic differentiation, genome-wide association, landscape genetics, microhabitat adaptation.

Introduction

Why populations harbor high genetic variation for expressed traits has remained an enigma for evolutionary biology (Hine et al., 2022). The drivers of genetic variation in isolated populations are mutation, genetic drift, and selection (Wright, 1969; Lacy, 1997). However, theoretical models considering these processes cannot easily explain e.g., the typically high heritability values of traits found in natural populations (Barton & Turelli, 1989; Johnson & Barton, 2005). Theory which aimed to resolve the enigma attributed a likely important role to antagonistic pleiotropy (Barton, 1990). Another potentially interfering role may play selection if it is not uniform across the population but variable, leading to spatial islands of possibly transient divergent adaptation (Bürger, 2010; Spichtig & Kawecki, 2004). Here we investigated on a genomic level fine-scale genetic differentiation associated with features of a heterogeneous habitat that may select for different traits and genotypes, leading to high genomic variation segregating within a population.

Selection can affect genetic variation in populations in diverse ways (Willi et al., 2006). Stabilizing selection, which is commonly a key player in theory of genetic variation for expressed traits, can maintain some genetic variation if it is not too strong (Charlesworth, 2015; Becker et al., 2022). Divergent selection, e.g., leading to local adaptation varying over space, can augment genetic variation as different genotypes are favored (Kingsolver & Pfennig, 2007; Nosil et al., 2009). Local adaptation is affected by and multi-entwined with habitat structure, the strength of selection and dispersal ability (Forester et al., 2016; Reisch et al., 2021). Local adaptation is favored if the habitat is heterogeneous, and dispersal relative to selection is low (Lenormand, 2002; Yeaman & Whitlock, 2011). Though some dispersal can also be favorable for local adaptation to evolve if a population harbors generally low levels of genetic variation (Barton, 2001).

Studies on local adaptation have traditionally focused on divergent selection across

mono-environmental gradients and phenotypic traits varying among populations of a species, both theoretically (e.g., Holt and Gaines, 1992; Kirkpatrick and Barton, 1997) and empirically (Kawecki & Ebert, 2004). Divergence among populations has been tested in many common garden experiments (Colautti et al., 2010; Leinonen et al., 2009) or transplant experiments in the field (Ågren & Schemske, 2012; Fournier-Level et al., 2011). Common garden experiments have the advantage of comparing populations of known environmental origins and therefore the possibility of associating traits with environment. However, such testing does not allow direct inference about whether trait differences are adaptive. Transplant experiments have the advantage of testing for adaptive differences, but it remains often unknown what the trait-environment associations are that lead to heightened fitness. More recently, landscape genetics has provided new tools to link traits with the environment, by testing for associations between genetic variants and environmental gradients (Challa & Neelapu, 2018; Jump & Peñuelas, 2005; Temesgen et al., 2021). Downstream analysis can indicate the genes and traits involved in differentiation (e.g., Thoen *et al.*, 2017; Verslues *et al.*, 2014). While this type of method has been commonly applied over large geographic ranges (e.g., Exposito-Alonso *et al.*, 2018; Rajendran *et al.*, 2021), it can also be used to study associations over close spatial gradients.

Genomic association studies over small spatial scales are promising but have remained rare. A study by Parisod and Christin (2008) revealed strong and mosaic-like, fine-scale population structure among *Biscutella laevigata* genotypes linked to specific habitat factors over an altitudinal range of 1850 – 2000 m, especially related to solar radiation. However, no causal genomic markers explaining the observed genotype-environment-association could be detected. More recent work by Roux and Frachon (2022) analyzed the association between disease resistance to plant pathogens along a 350 m meadow transect in *A. thaliana* that contained three physically and chemically distinct soil types. They found strong associations

between genotype and environment as well as seven candidate genes related to disease resistance of which two were known to be involved in the reaction to bacterial pathogens. These studies suggest that populations can maintain considerable amounts of adaptive genetic variation linked to environmental differences and genetic divergence.

In this study, we combined genotype-environment associations and genotype-phenotype associations over a heterogeneous dune landscape to detect the genes and traits linked to habitat divergence. Our study system was one population of *Arabidopsis lyrata*. The species is a short-lived perennial occurring in habitats with some disturbance. When it occurs in sand dune landscapes, it typically grows under several microhabitat conditions: in areas of open dunes and forested dunes, or on dune bottoms, tops and on the leeside. Areas may be covered by some other vegetation, or *A. lyrata* occurs as one of few plant species. We based our study on an 11-ha area in Saugatuck Dunes State Park, Michigan, USA. Previous experiments on plants from this area revealed that those originating from open dune tops compared to those from mostly forested dune bottoms grew to larger sizes but flowered later under mesic conditions, and they showed a less strong increase in stomata density in response to drought (Paccard et al., 2013). A follow-up study considering the gradients of distance from trees, vegetation cover and intraspecific density found plants on dune tops to flower later under benign conditions, but larger sizes under benign conditions was now associated with increased distance from trees (Wos & Willi, 2018). Furthermore, higher vegetation cover was associated with higher frost resistance and late flowering with low intraspecific density.

Here we build on these results by first reassessing links between habitat features and traits. We raised replicate plants of over 600 seed families collected in the field, which we phenotyped for phenology, growth, thermal resistance, leaf trichomes and shape, and which we whole-genome sequenced. Genotype-environment and genotype-phenotype association analyses (GEAs and GPAs, respectively) were performed. We narrowed down the likely SNPs

within candidate genes of divergent adaptation by focusing on those that overlapped between pairs of significantly associated habitat features and traits. We report on candidate genes with an accumulation of such outlier SNPs and their respective functions. For candidate genes with known physiological function, we tested for allelic effects and genomic diversity as compared to background diversity.

Methods

Seed material & environmental variables

Seeds of *A. lyrata* were collected over a dune landscape at the eastern shoreline of Lake Michigan, at Saugatuck Dunes State Park, Michigan, USA (42.70N 86.21W; 42.71N 86.20W; Figure 1). Former population genetic analyses had shown that the specific population – in comparison to others – had relatively high genomic diversity, despite evidence of a history of postglacial recolonization from the Driftless Area of Wisconsin (Willi & Määttänen, 2010, 2011; Griffin & Willi, 2014). The area is also the most likely source of the *A. lyrata* reference genome (Hu et al., 2011). Seeds of plants were collected in four years, in 2009, 2010, 2013, and 2014, with the sections of sampling (N = 3; see Figure 1) partially varying among years. Within each year, sampled plants were generally at least 3-6 m apart from each other. Seeds of several fruits per plant were collected and stored in separate paper bags. Seeds were stored at 4°C in a cold room, in containers with silica beads to reduce humidity.

At the site of each maternal plant, four habitat variables were assessed. These were, apart from precise location data, dune position, vegetation cover, distance from canopy, and intraspecific density. Dune position, quantified as the fraction down from the dune top, varied between 0 and 1, with 0 indicating that the plant grew on the top of a dune and 1 indicating that the plant grew at the bottom of a dune. Vegetation cover was the fraction of ground covered with lichens and herbaceous plants, projected on the ground on a 0.5 m x 0.5 m square. Distance

from canopy was the distance in meters from the ground-projected canopy edge to the plant. If a plant grew under the canopy of a tree, the value was set to 0. Intraspecific density was the number of bolted *A. lyrata* plants on the same square of 0.5 m x 0.5 m, with the collected plant in the centre.

Propagation and assessment of phenotypic traits

Field-collected seeds of about 600 maternal plants were raised in pots, first in climate chambers and then in a greenhouse, starting in November 2019. Three seeds per field-collected mother plant were sown in a pot with a 2:1 peat-sand mixture, arranged in 28-pot trays (pot width/height: 6.5/7.5 cm). They were stratified for 10 days at 4°C in dark climate chambers (ClimeCab 1400, KÄLTE 3000 AG, Landquart, Switzerland). Trays were kept wet, by having standing water in the trays, regular spraying of pots from above, and covering them with mesh nets. Then trays were moved to the greenhouse with a constant temperature of 20°C and increasing day length and light intensity. In the first week, only natural light was allowed (~8.45 h daylight). Then artificial light was set to increase day length by 1 h every 2-3 days until long-day conditions of 16 h light: 8 h dark were reached. Light intensity was kept at 200 $\mu Ms^{-1}m^{-2}$ (240 $\mu Ms^{-1}m^{-2}$ on plant level) throughout the study. Mesh nets were removed when ~60% of seeds per tray had germinated. Overall germination rate was 89 %. When most plants had reached the 4-leave stage, excessive plants were removed so that one individual per pot remained. Pots in which no germination had occurred were filled with a surplus plant of other pots (n = 10 of half- or full-sibs; sibship not considered in later analysis because of low number of such closely related plants), leading to a total of 570 plants on which traits were assessed (Table 1).

Trait measures focused on phenology, growth, thermal resistance, leave trichomes, and leave shape. Germination, defined as when green tissue of cotyledons became visible, was

scored daily. The day of bolting, first flowering, and plant death were scored every 2-3 days. Number of days from germination to the respective events were adjusted for the mid-point of checking. The growth trajectory was tracked by taking pictures of plants twice a week. The resulting pictures were used to measure the length of the two longest leaves using ImageJ v1.53 (Schneider et al., 2012). Size over time was explored for the best-supported growth model. Seven models (linear, exponential, logistic, two- and three-parameter logistic, van Bertalanffy, Gompertz) were compared based on AIC for each plant. Across plants, the Gompertz and three-parameter logistic models performed similarly, and we therefore chose to work with the simpler of the two, the three-parameter logistic model. For each plant, the three parameters were extracted: asymptotic size (s_{asym}), time till fastest growth/half-size (x_{mid}), and maximal growth rate (r_{max}).

Resistance to frost and heat was assessed by their effects on the photosystem (PS) II, by measuring its efficiency via fluorescence after stress exposure. We collected two leaves of each plant and put them in separate, empty 50 ml centrifuge tubes. For the assessment of frost resistance, tubes were put in a programmable, dark freezer with the following temperature regime: 4°C for 2 h for acclimatization, -4K/h during 4 h, constant -12°C for 1 h, +4K/h during 4 h to 4°C, and acclimatization at this temperature for 2 h. For the assessment of heat resistance, samples were submersed in a dark water bath of 48°C for 65 minutes. Then samples of the two treatments were dark-adapted for 20 minutes with a leave clip (DLC-8) and fluorescence was measured with a MINI-PAM-II (Heinz Walz GmbH, Effeltrich, Germany). Dark-adapted leaves were exposed to a 0.8-second-long saturation pulse during which the device measured minimum fluorescence levels on open PS II reaction centers (F_0) and the maximum fluorescence level on closed PS II reaction centers (F_M). The maximum photochemical quantum yield of PS II (F_V/F_M) could then be calculated as:

$$\frac{F_V}{F_M} = \frac{F_M - F_0}{F_M}$$

Values smaller 0.84 indicate stressed leaves (Genty et al., 1989).

During peak flowering, leaf hairiness (trichomes) and leaf shape were recorded in simple binary categories: leaf upper surface glabrous or with hair, shape lightly or strongly pinnate.

SNP data

When most plants had reached the 8-leave-stage and before flowering, one leaf per plant was collected and stored in a separate tube filled with ~10 glass beads at -20°C. DNA-extraction was done with the DNeasy Plant Mini Kit (Qiagen, Hilden, Germany), following the manufacturer's protocol with minor changes. Plant tissue was disrupted by freezing with liquid nitrogen and six to eight rounds of shaking for 13 seconds on a Silamat S6 universal mixing device (Ivoclar Vivadent, Schaan, Liechtenstein). Library preparation and sequencing was done on a NovaSeq 6000 (Illumina, San Diego, USA) at the ETH Zurich D-BSSE facility in Basel (S4 flow cell; 95 samples per lane; paired end 2x 150 bp).

Lists of single-nucleotide polymorphisms (SNPs) were generated by the following pipeline. Tails with excess poly-G were trimmed with *fastp* (Chen et al., 2018). Furthermore, heads and tails of sequence reads with mean quality lower than 20 were removed. Then reads were aligned to the *A. lyrata* reference genome (Hu et al., 2011) with the software *bwa mem* (Li & Durbin, 2009). Sorting of reads, combining of reads (second sequencing run when coverage was low after the first) and removal of duplicates was done with *SAMtools* (Li et al., 2009). Variants were called with *BCFtools* (Li, 2011). Lastly, using *VCFtools* (Danecek et al., 2011) polymorphic sites were filtered for the following: minimum read depth per individual of four, minimum phred quality score of 20, only biallelic sites, minor allele frequency of 5% (MAF), missing data of 5%, and removal of indels. This resulted in 747'538 SNPs across the 570 sequenced individuals.

Statistical analyses

Pre-investigation focused on the correlation structure of environmental variables, of phenotypic trait, and spatial autocorrelation in the four environmental variables measured in the field. Pearson correlations to analyze the former two and Mantel tests to analyze the later were run in R v4.0.5 (R Core Team, 2021). Then, the effect of the four environmental variables on each of the phenotypic traits was explored in linear models (proc GLM or proc logistic for binary traits in *SAS* v9.4 (SAS® Institute, Inc., Cary, NC). Before analysis, phenotypic data was corrected for tray, and the phenology variables of days to germination, bolting and days to flowering were $\log_{10}$-transformed. To condense the range of independent variables, vegetation cover, distance to canopy, and intraspecific density were also log_{10}-transformed. Further independent variables included section of sampling (northern area = 2, intermediate area = 3, southern area = 4), year of sampling (2009, 2010, 2013, 2014), and their three-way interactions with each of the habitat variables. Effects were evaluated by type-3 testing (GLM) or joint testing (logistic regression).

The extent to which local adaptation can evolve depends on dispersal (Kawecki & Ebert, 2004). Dispersal was analyzed by the decay of kinship among the lab-raised plants over space where they were collected as seeds. The area of collecting was divided into plots of ~25 x 25 m per sampling year and section. GPS coordinates of mother plants were used to calculate a geographic distance matrix between all pairs of individuals and the kinship matrix was produced by *KING* (Manichaikul et al., 2010) embedded in *PLINK* v2.0 (Purcell et al., 2007). Correlations between estimated kinship and log-transformed geographic distance were calculated for each section-year combination separately by pooling the plots within them. Linear models were fitted, and slopes compared.

For each of the significant phenotype-environment relationships as revealed in the linear models, input datasets for GEA and GPA were produced that included the year-section combinations that aligned with the main pattern more strongly. Association analyses were performed with the software *gemma* (Zhou & Stephens, 2012). For the samples of each association, a centered relatedness matrix was computed with *gemma*. Then, univariate linear mixed models were run, once for the environmental variable and once for the phenotypic variable (Zhou & Stephens, 2014). Output was p-Wald test statistics for each SNP. Overlapping outlier SNPs ($p < 0.005$ and MAF > 0.1) revealed in GEA and GPA and overlapping with a gene were kept. For putative outlier genes with at least two outlier SNPs, the respective function was checked in *phytozome* (https://phytozome-next.jgi.doe.gov/) and *tair* (Berardini et al., 2015).

Lastly, all outlier genes were investigated in more depth. SNPs were annotated by SnpEff (Cingolani et al., 2012) with the *A. lyrata* v2.1 (Rawat et al., 2015) reference genome. Furthermore, we tested whether their SNPs supported pure additive or some dominance inheritance. All outlier SNPs within outlier genes for individual plants of a GEA or GPA were coded as: -1 when homozygous for the reference allele, 0 when heterozygous, and 1 when homozygous for the alternative allele. Only SNPs with a MAF < 0.1 were included. Further input data was the phenotypic value of each retained individual standardized to the mean of 0 and variance of 1. Linear models were run and the dominance deviation from the mid-homozygous expectation revealed by contrast (*lmer*; Bates et al., 2014). Absolute dominance deviation values and standard error were saved und used as inputs in fixed-effects meta-analysis, once based on environmental variables and once based on phenotypic traits with the R package *metafor* (Viechtbauer, 2010). Finally, genomic diversity in outlier genes was compared to diversity in randomly picked genes adjacent to them by calculating expected heterozygosity per gene (*He*). One adjacent gene was 50 kb up- and the other downstream of

the candidate gene. Allele frequencies of the two alleles per SNP position within a gene were obtained by *VCFtools* (Danecek et al., 2011) and expected heterozygosity calculated by: H_e = 2pq, with p and q being the allele frequency of the respective alleles per SNP position. Single SNP heterozygosity was then averaged over all SNPs within each gene. Additionally, the location of outlier genes in respect to runs of homozygosity (ROHs), a sign for fixed haplotypes within the population, was assessed. ROHs were calculated with *homozyg* in *PLINK* v1.9 (Purcell et al., 2007). Settings for e.g., ROH length, scanning window or maximal number of heterozygotes per window can be found in Table S1.

Results

Relationship between environmental variables and phenotypic traits, and dispersal

Pearson correlations among environmental variables and among phenotypic variables were low ($r < 0.2$). Time to bolting and time to flowering ($r = 0.763$. $p < 0.001$, Table S2) showed the strongest correlations. Furthermore, spatial autocorrelations in environmental variables evaluated by Mantel-tests were significantly negative (Table S3).

Formerly known associations between environmental variables and phenotypic traits were mainly confirmed and some newly detected (Table 1, Figure 2, Table S4). Fraction down from dunes was negatively related with time to flowering, with plants from dune bottoms having a faster reproductive development, and as a trend with leave shape, with plants being less pinnate in dune bottoms. A strong negative relation between fraction down from dunes and plant size was detected in some year-section combinations, with increased plant size on the dune tops, and the pair of variables was therefore included in GEA/GPA analyses. Vegetation cover tended to be related to time to flowering, with plants flowering earlier when originating from denser vegetation, but patterns varied significantly among year-section combinations (significant 3-way interaction; Table S4). Additionally, vegetation cover was positively related

with frost resistance and leave trichomes, with plants being more frost resistant and hairy when originating from denser vegetation. For the distance from canopy, a significant overall relation with time to flowering was found, with plants growing faster with increasing distance from the tree canopy, though variation in this effect was indicated by a significant interaction with year-section. Unlike found previously though, plant size did not increase with distance from the canopy, but the association was positive and significant or nearly significant ($p < 0.1$) in multiple section-year combinations and therefore included in the GEA/GPA analysis. Lastly, local density of *A. lyrata* was also negatively related with time to bolting and time to flowering; plants of high-density spots had faster reproductive development.

Kinship values tended to be generally low, with a tendency of being higher for very close individuals and no strong change with increasing distance (Figure S3, Table S5). Kinship-dispersal analysis showed little difference between section-year combinations (Table S6). Gene flow within the population seems to be considerable.

Genome wide association study

Association analysis focused on the six highly significant environment-trait pairs (Figure 2) and four additional associations that showed strong section-year responses (*fD* – leave shape, *fD* - s_{aysm}, *BB* – t_{flo}, *dC* - s_{asym}). A minimum number of 35 (*BB* - res_{frost}) and a maximum number of 224 (*BB* - t_{flo}) outlier ($p < 0.005$) SNPs were identified that overlapped between GEA and GPA (Table 2). They were located in 93 genes with at least two such outlier SNPs. Applying a MAF of 0.1 per SNP, 77 outlier genes remained, and of these, twelve were candidate genes with known physiological function (Table 3, for the full list of genes see Table S9).

Nine candidate genes were found in associations with vegetative (size) or reproductive development (bolting, flowering). Two candidate genes were found for the environment-trait pair of dune position (*fD*) and maximum size (s_{asym}). *JMJ15* encodes a *H3K4* demethylase

which represses *FLC* levels (flowering locus C) and leads to early flowering in *A. thaliana* (Yang et al., 2012). *PIA1* encodes for a protein of the ankyrin repeat family and does not have a known function. Four genes were detected for the pair of vegetation cover (*BB*) and time to flowering. *HGL1* codes for a protein involved in the *FERONIA* (*FER*) signalling pathway, with major functions in pollen tube reception and vegetative growth (Choi et al., 2022). *SDG40* encodes for a methyltransferase that directly regulates *FLC* and affects time to flowering temperature-independently (Nasim et al., 2021). *EVE1* encodes a ubiquitin protein that influences the transition between vegetative and reproductive phase (Hwang et al., 2011). *VAR2* a metalloprotease involved in the repair of photosystem II after light stress (Liu & Guo, 2013; Wang et al., 2022), induces a mosaic of green and bleached leave surfaces (Martínez-Zapater, 1993). Three candidate genes were found for the environment-trait pairs of intraspecific density of *A. lyrata* (*dAlyr*) and time till bolting and flowering, respectively. *PATL4* is associated with bolting time (t_{bol}) and codes for a phospholipid-binding protein involved in stomatal regulation during oxidative stress (Melicher et al., 2023). *LSD1* and *JMJ14* are associated with time to flowering (t_{flo}). *LSD1*, together with other genes, controls plant water use efficiency (WUE) as well as vegetative growth and reproductive development (Bernacki *et al.*, 2019; Huang *et al.*, 2010; Schneider *et al.*, 1995). *JMJ14* influences the thermosensory response of plants, the flowering onset as well as a reduction of growth vigor (Lu et al., 2010; Li et al., 2011; Cui et al., 2021). Mutants show reduced growth as well as early flowering phenotypes (Rodrigues et al., 2021) and it appears to be antagonistic to *JMJ15* (Cattaneo et al., 2019). In summary most of these candidate genes show associations with reproductive development as well as physiological functions influencing it.

The remaining three genes were detected for the trait pair of vegetation cover (BB) and leaf trichomes. *LNG3* has an influence on the cell wall and seed mucilage synthesis (Yang et al., 2019, 2022). *ENO1* is an enolase with an effect on trichome and root-hair shape (Prabhakar

et al., 2009). The third is pseudogene *AT4G09360* that recognizes pathogens (Meyers et al., 2003; Sinapidou et al., 2004). Beyond, several of the twelve mentioned candidate genes also show physiological functions related to environmental stressors, e.g., *JMJ15* for thermal and salt stress tolerance, (Cui et al., 2021; Shen et al., 2014), *LSD1* in response and acclimatisation to drought and cold stress (Bernacki *et al.* (2019) or *HGL1* in response to abiotic as well as biotic stresses (Choi et al., 2022).

Haplotypes, deviation from the mid-homozygous phenotype, and heterozygosity

Lastly, outlier genes or candidate genes were investigated in more detail. Patterns of correlation between haplotypes and associated phenotypes or environmental factors were found and exemplarily shown for two cases (Figure 3). Two thirds of the 391 outlier SNPs of the 77 outlier genes were located at synonymous sites (25.8 %), up-stream of a transcribed region (23 %), or down-stream of a transcribed region (17.9%). Twenty SNPs were found in introns (5.1%). The remaining SNPs were missense variants (20.7 %; Table S7), splice variants (4.6 %), or in the 3' UTR (2.8 %) or the 5' UTR region (0.5 %). The predicted effects of the 391 outlier SNPs were: 29.7 % with likely low effect, 21.5 % with likely moderate effect, and the majority, 48.9 % with a modifier effect. None of the SNPs was predicted to have a likely high effect.

Contrasts and meta-analysis of the dominance deviation from the expected mid-homozygous phenotype, revealed evidence of overall weak dominance, supporting that effects are predominantly additive. Estimated mean effect size for environmental variables was 0.13 and for phenotypic traits 0.16 (Table S8, Figure 4). Furthermore, the variance explained by the SNP/allelic state was low, with a mean R^2 of 5.5% for environmental variables and 5.1% for phenotypic traits, again indicating low effect sizes (environmental traits: Table S10; phenotypic traits: Table S11).

As a measure of genetic diversity, expected heterozygosity (H_e) within each candidate

genes as well as two randomly picked genes 50k bp down- or upstream of the respective candidate gene were calculated. H_e of candidate genes was significantly higher compared to adjacent genes ($t_{1,201}$ = -2.458, p = 0.015; Figure 4). Therefore, the location of candidate genes was mostly outside of ROHs (Figure S5), with 21 (27 %) genes overlapping. Most overlaps could be found on chromosome 2 and 4 but only for few individuals (max. 12 of 570) (Figure 5).

Discussion

Genetic diversity within a population can predict adaptive potential, for example under climatic stress (Ørsted et al., 2019; Pluess et al., 2016). Maintenance of genetic diversity via relatively stable population size may be positively influenced by landscape features that promote local dispersal including connectivity between different landscape patches and the ability for population size resilience (Aavik & Helm, 2018). Apart, variation in selection over micro-scale gradients may contribute to the maintenance of genetic diversity and a higher response to novel selection (Huang et al., 2016). The goal of this study was to investigate genetic divergence associated with habitat features in a population of *A. lyrata* spread across a heterogeneous dune-landscape. We detected outlier genes associated with habitat features of which some had known biological and physiological function, and we compared outlier genetic variation to background genetic variation.

Phenotype-environment association

Previous research on our target population revealed high genomic diversity (Willi & Määttänen, 2011; Willi et al., 2018). Furthermore, environmental gradients in the field were associated with phenotypic trait variation when plants were raised under common environmental conditions, suggesting adaptive genetic divergence across the dune landscape

(Paccard et al., 2013; Wos & Willi, 2018). We could confirm these phenotype-environment associations and detected a couple additional ones (Fig. 2), in particular dune position with size and phenology, vegetation cover with trichomes and intraspecific density of *A. lyrata* with reproductive development. These links between phenotypes and environmental gradients were generally weak but consistent across the sections and years of sampling the seeds for this study. Though the strength of effect sometimes varied, probably linked to fluctuating environmental conditions across time and space (Fry, 2003). An alternative hypothesis is that pollen that fertilized the seeds we collected came from some distance and weakened patterns to variable extents.

Contrary to our prediction, the strength of phenotype-environment associations was not linked to evidence for variation in gene flow among the sections and years. Indeed, there was hardly any difference in the decay in relatedness over distance among sections and years of sampling across dunes. This suggests that pollen flow is probably good in this self-compatible population of *A. lyrata*. Simulations by Bonte et al. (2010) and North et al. (2011) showed the influence of landscape structure on dispersal form and evolution. Long and short distance dispersal evolve separately and depending on the surrounding landscape. For *A. lyrata*, results suggest that short as well as long distance dispersal are frequent. Therefore, dispersal is likely to erode phenotype-environment-associations during cycles of reproduction, but they may re-establish constantly by divergent local selection over the various gradients in our focal population.

Genotype-environment-association

For all the phenotypic-environment pairs, we found a number of outlier genes but none of the outlier SNPs explained a high fraction of variation in phenotypic expression, which is consistent polygenetic divergent adaptation. Also, most outlier SNPs in outlier genes had a low

(30%) or moderate predicted impact (21%) (Figure S4). In drought-related GWAS studies on e.g., peanut, papaya, rice, or bean, it was modifiers and high-impact variants that were the most common outliers (Bhat et al., 2022; Bohry et al., 2021; Jiang et al., 2023; Valdisser et al., 2020). This further suggest that variants have relatively minor effects. Apart from the linear and therefore additive effect of outlier SNPs, we found average contributions of dominance deviations between 0.13 and 0.16. All these results together support the common assumption of quantitative genetics: that variation in quantitative traits are controlled by a considerable number of loci and each locus has a small, predominantly additive effect (Barton & Keightley, 2002). Insights contrast to those by theoretical work, advocating that when gene flow is relatively high, alleles of large effect should be involved in adaptive divergence (Yeaman & Whitlock, 2011). In parallel, many studies have shown that within-population polymorphism under divergent selection is due to genes of large effects, as found for mice or the peppered moth (Keane et al., 2011; Van'T Hof et al., 2011). Here, we show that under considerable gene flow, adaptive divergence can still be based on many genes of small effect.

An important trait that we found to be related with all four environmental variables studied was time to flowering. Plants flowered earlier when they originated from dune bottoms, further away from tree canopies as well as under higher intraspecific density, and as a trend in denser vegetation. In line, we found that three of the outlier genes with known physiological function affected the shift to flowering namely *JMJ14*, *JMJ15* and *SDG40*. Selection on flowering may have different sources. Flowering is strongly determined by environmental factors in *Arabidopsis*. It may be that dune bottoms attract more snow in winter and melting takes longer, shortening the phase until the high summer temperatures start, which could be the reason why plants from dune bottoms flower earlier. Plants under trees may receive less light and a different light spectrum, and they may have adapted to induce the shift to reproduction at lower thresholds. Early flowering in the open could also be linked to thermal or drought

stress (Franks et al., 2007; Kenney et al., 2014). Finally, flowering early under intra- and interspecific competition is a typical adaptive direction that has been observed in many species of plants (Kehrberger & Holzschuh, 2019; Takeno, 2016; Vermeulen, 2015).

We predicted that outlier genes had heightened genomic diversity as compared to neighbouring genes – otherwise probably impacted similarly by recombination or genetic drift. Parallel to our prediction that divergent selection should maintain diversity, we found that the diversity of outlier genes was slightly elevated. However, outlier gene diversity was not much increased, which suggests weak linkage, or more likely, that the alternate variant of the causal variant is probably neutral and not under divergent selection in the opposite direction, that is at the other end of environmental gradients. This is further confirmed by the fact that outlier genes are mainly found outside of islands of homozygosity (ROH), indicating no increased haplotype accumulation in our focal population. The limited number of individuals showing an overlap between ROHs, and outlier genes also indicates that generally a high level of heterozygosity exists within the population.

Conclusion

Our results provide evidence that by combining phenotype-environment associations and performing GWAS on both identifies candidate genes of divergent adaptation. In our analysis, several of the parameters of the heterogenous dune landscape were linked with reproductive development and a few other traits, confirming the evolutionary lability of the timing of flowering. Adaptive divergence seemed to be based on many genes each of small effect, with predominantly additive genetic basis. And most importantly, we could confirm that adaptive divergence, even when transient and in the face of considerable gene flow can produce a genomic signature of increased adaptive genetic diversity.

Acknowledgements

Collection permits were granted by the Michigan Department of Natural Resources. O. Bachmann, S. Riedl and G. Armbruster helped measure plants, and O. Bachmann assisted with lab-work. We thank the team of the D-BSSE in Basel for the sequencing service, and the sciCORE facility at the University Basel for providing computational resources. We were supported by the Swiss National Science Foundation (grant no. 310030_184763 to Y.W.).

Data Accessibility

Data will be available on DRYAD. Genomic data will be stored on …

A**uthor Contributions**

Conceived and designed the experiments: JH, YW. Performed experiment: JH. Analysed the data: JH, KL, YW. Wrote the paper: JH, YW, with inputs of KL.

Benefit-Sharing statement

Benefits from this research accrue from the sharing of our data and results on public databases as described above.

References

Aavik, T., & Helm, A. (2018). Restoration of plant species and genetic diversity depends on landscape-scale dispersal. *Restoration Ecology*, *26*(S2). https://doi.org/10.1111/rec.12634

Ågren, J., & Schemske, D. W. (2012). Reciprocal transplants demonstrate strong adaptive differentiation of the model organism *Arabidopsis thaliana* in its native range. *New Phytologist*, *194*(4), 1112–1122. https://doi.org/10.1111/j.1469-8137.2012.04112.x

Barton, N. H. (1990). Pleiotropic models of quantitative variation. *Genetics*, *124*(3), 773–782. https://doi.org/10.1093/genetics/124.3.773

Barton, N. H. (2001). Adaptation at the edge of a species' range. *Integrating Ecology and Evolution in a Spatial Context*, 365–392.

Barton, N. H., & Keightley, P. D. (2002). Understanding quantitative genetic variation. *Nature Reviews Genetics*, *3*(1), 11–21. https://doi.org/10.1038/nrg700

Barton, N. H., & Turelli, M. (1989). Evolutionary quantitative genetics: How little do we know? *Annu. Rev. Genet.*, *23*, 337–370.

Bates, D., Mächler, M., Bolker, B., & Walker, S. (2014). Fitting linear mixed-effects models using lme4. *arXiv:1406.5823 [Stat]*. http://arxiv.org/abs/1406.5823

Becker, D., Barnard-Kubow, K., Porter, R., Edwards, A., Voss, E., Beckerman, A. P., & Bergland, A. O. (2022). Adaptive phenotypic plasticity is under stabilizing selection in Daphnia. *Nature Ecology & Evolution*, *6*(10), 1449–1457. https://doi.org/10.1038/s41559-022-01837-5

Berardini, T. Z., Reiser, L., Li, D., Mezheritsky, Y., Muller, R., Strait, E., & Huala, E. (2015). The arabidopsis information resource: Making and mining the "gold standard" annotated reference plant genome: Tair: Making and Mining the "Gold Standard" Plant Genome. *Genesis*, *53*(8), 474–485. https://doi.org/10.1002/dvg.22877

Bernacki, M. J., Czarnocka, W., Rusaczonek, A., Witoń, D., Kęska, S., Czyż, J., Szechyńska-Hebda, M., & Karpiński, S. (2019). *LSD1*-, *EDS1*- and *PAD4*-dependent conditional correlation among salicylic acid, hydrogen peroxide, water use efficiency and seed yield in *Arabidopsis thaliana*. *Physiologia Plantarum*, *165*(2), 369–382. https://doi.org/10.1111/ppl.12863

Bernacki, M. J., Czarnocka, W., Szechyńska-Hebda, M., Mittler, R., & Karpiński, S. (2019). Biotechnological potential of *LSD1*, *EDS1*, and *PAD4* in the improvement of crops and industrial plants. *Plants*, *8*(8), 290. https://doi.org/10.3390/plants8080290

Bhat, R. S., Shirasawa, K., & Chavadi, S. D. (2022). Genome-wide structural and functional features of single nucleotide polymorphisms revealed from the whole genome resequencing of 179 accessions of *Arachis*. *Physiologia Plantarum*, *174*(1), e13623. https://doi.org/10.1111/ppl.13623

Bohry, D., Ramos, H. C. C., Dos Santos, P. H. D., Boechat, M. S. B., Arêdes, F. A. S., Pirovani, A. A. V., & Pereira, M. G. (2021). Discovery of SNPs and InDels in papaya genotypes and its potential for marker assisted selection of fruit quality traits. *Scientific Reports*, *11*(1), 292. https://doi.org/10.1038/s41598-020-79401-z

Bonte, D., Hovestadt, T., & Poethke, H.-J. (2010). Evolution of dispersal polymorphism and local adaptation of dispersal distance in spatially structured landscapes. *Oikos*, *119*(3), 560–566. https://doi.org/10.1111/j.1600-0706.2009.17943.x

Bürger, R. (2010). Evolution and polymorphism in the multilocus Levene model with no or weak epistasis. *Theoretical Population Biology*, *78*(2), 123–138. https://doi.org/10.1016/j.tpb.2010.06.002

Cattaneo, P., Graeff, M., Marhava, P., & Hardtke, C. S. (2019). Conditional effects of the epigenetic regulator *JUMONJI 14* in *Arabidopsis* root growth. *Development*, *146*(23), dev183905. https://doi.org/10.1242/dev.183905

Challa, S., & Neelapu, N. R. R. (2018). Genome-wide association studies (GWAS) for abiotic stress tolerance in plants. In *Biochemical, Physiological and Molecular Avenues for Combating Abiotic Stress Tolerance in Plants* (pp. 135–150). Elsevier. https://doi.org/10.1016/B978-0-12-813066-7.00009-7

Charlesworth, B. (2015). Causes of natural variation in fitness: Evidence from studies of *Drosophila* populations. *Proceedings of the National Academy of Sciences*, *112*(6), 1662–1669. https://doi.org/10.1073/pnas.1423275112

Chen, S., Zhou, Y., Chen, Y., & Gu, J. (2018). fastp: An ultra-fast all-in-one FASTQ preprocessor. *Bioinformatics*, *34*(17), i884–i890. https://doi.org/10.1093/bioinformatics/bty560

Choi, J.-H., Kim, J.-W., & Oh, M.-H. (2022). Identification of Feronia-interacting proteins in *Arabidopsis thaliana*. *Genes & Genomics*, *44*(12), 1477–1485. https://doi.org/10.1007/s13258-022-01292-3

Cingolani, P., Platts, A., Wang, L. L., Coon, M., Nguyen, T., Wang, L., Land, S. J., Lu, X., & Ruden, D. M. (2012). A program for annotating and predicting the effects of single nucleotide polymorphisms, SnpEff: SNPs in the genome of *Drosophila melanogaster* strain w ^{1118}; iso-2; iso-3. *Fly*, *6*(2), 80–92. https://doi.org/10.4161/fly.19695

Colautti, R. I., Eckert, C. G., & Barrett, S. C. H. (2010). Evolutionary constraints on adaptive evolution during range expansion in an invasive plant. *Proceedings of the Royal Society B: Biological Sciences*, *277*(1689), 1799–1806. https://doi.org/10.1098/rspb.2009.2231

Cui, X., Zheng, Y., Lu, Y., Issakidis-Bourguet, E., & Zhou, D.-X. (2021). Metabolic control of histone demethylase activity involved in plant response to high temperature. *Plant Physiology*, *185*(4), 1813–1828. https://doi.org/10.1093/plphys/kiab020

Danecek, P., Auton, A., Abecasis, G., Albers, C. A., Banks, E., DePristo, M. A., Handsaker, R. E., Lunter, G., Marth, G. T., Sherry, S. T., McVean, G., Durbin, R., & 1000 Genomes Project Analysis Group. (2011). The variant call format and VCFtools. *Bioinformatics*, *27*(15), 2156–2158. https://doi.org/10.1093/bioinformatics/btr330

Exposito-Alonso, M., Vasseur, F., Ding, W., Wang, G., Burbano, H. A., & Weigel, D. (2018). Genomic basis and evolutionary potential for extreme drought adaptation in *Arabidopsis thaliana*. *Nature Ecology & Evolution*, *2*(2), 352–358. https://doi.org/10.1038/s41559-017-0423-0

Forester, B. R., Jones, M. R., Joost, S., Landguth, E. L., & Lasky, J. R. (2016). Detecting spatial genetic signatures of local adaptation in heterogeneous landscapes. *Molecular Ecology*, *25*(1), 104–120. https://doi.org/10.1111/mec.13476

Fournier-Level, A., Korte, A., Cooper, M. D., Nordborg, M., Schmitt, J., & Wilczek, A. M. (2011). A map of local adaptation in *Arabidopsis thaliana*. *Science*, *334*(6052), 86–89. https://doi.org/10.1126/science.1209271

Franks, S. J., Sim, S., & Weis, A. E. (2007). Rapid evolution of flowering time by an annual plant in response to a climate fluctuation. *Proceedings of the National Academy of Sciences*, *104*(4), 1278–1282. https://doi.org/10.1073/pnas.0608379104

Fry, J. D. (2003). Detecting ecological trade-offs using selection experiments. *Ecology*, *84*(7), 1672–1678. https://doi.org/10.1890/0012-9658(2003)084[1672:DETUSE]2.0.CO;2

Genty, B., Briantais, J.-M., & Baker, N. R. (1989). The relationship between the quantum yield of photosynthetic electron transport and quenching of chlorophyll fluorescence. *Biochimica et Biophysica Acta (BBA) - General Subjects*, *990*(1), 87–92. https://doi.org/10.1016/S0304-4165(89)80016-9

Griffin, P. C., & Willi, Y. (2014). Evolutionary shifts to self-fertilisation restricted to geographic range margins in North American *Arabidopsis lyrata*. *Ecology Letters*, *17*(4), 484–490. https://doi.org/10.1111/ele.12248

Hine, E., Runcie, D. E., Allen, S. L., Wang, Y., Chenoweth, S. F., Blows, M. W., & McGuigan, K. (2022). Maintenance of quantitative genetic variance in complex, multitrait phenotypes: The contribution of rare, large effect variants in 2 Drosophila species. *Genetics*, *222*(2), iyac122. https://doi.org/10.1093/genetics/iyac122

Holt, R. D., & Gaines, M. S. (1992). Analysis of adaptation in heterogeneous landscapes: Implications for the evolution of fundamental niches. *Evolutionary Ecology*, *6*(5), 433–447. https://doi.org/10.1007/BF02270702

Hu, T. T., Pattyn, P., Bakker, E. G., Cao, J., Cheng, J.-F., Clark, R. M., Fahlgren, N., Fawcett, J. A., Grimwood, J., Gundlach, H., Haberer, G., Hollister, J. D., Ossowski, S., Ottilar, R. P., Salamov, A. A., Schneeberger, K., Spannagl, M., Wang, X., Yang, L., … Guo, Y.-L. (2011). The *Arabidopsis lyrata* genome sequence and the basis of rapid genome size change. *Nature Genetics*, *43*(5), 476–481. https://doi.org/10.1038/ng.807

Huang, X., Li, Y., Zhang, X., Zuo, J., & Yang, S. (2010). The *Arabidopsis LSD1* gene plays an important role in the regulation of low temperature-dependent cell death. *New Phytologist*, *187*(2), 301–312. https://doi.org/10.1111/j.1469-8137.2010.03275.x

Huang, Y., Tran, I., & Agrawal, A. F. (2016). Does genetic variation maintained by environmental heterogeneity facilitate adaptation to novel selection? *The American Naturalist*, *188*(1), 27–37. https://doi.org/10.1086/686889

Hwang, H.-J., Kim, H., Jeong, Y.-M., Choi, M. Y., Lee, S.-Y., & Kim, S.-G. (2011). Overexpression of *EVE1*, a novel ubiquitin family protein, arrests inflorescence stem development in Arabidopsis. *Journal of Experimental Botany*, *62*(13), 4571–4581. https://doi.org/10.1093/jxb/err168

Jiang, C., Wang, Y., Zhou, J., Rashid, M. A. R., Li, Y., Peng, Y., Xie, L., Zhou, G., He, Y., Sun, W., Zheng, C., & Xie, X. (2023). Genome-wide scan for genetic signatures based on the whole-genome resequencing of salt- and drought-tolerant rice varieties. *Agronomy*, *13*(7), 1936. https://doi.org/10.3390/agronomy13071936

Johnson, T., & Barton, N. (2005). Theoretical models of selection and mutation on quantitative traits. *Philosophical Transactions of the Royal Society B: Biological Sciences*, *360*(1459), 1411–1425. https://doi.org/10.1098/rstb.2005.1667

Jump, A. S., & Peñuelas, J. (2005). Running to stand still: Adaptation and the response of plants to rapid climate change. *Ecology Letters*, *8*(9), 1010–1020. https://doi.org/10.1111/j.1461-0248.2005.00796.x

Kawecki, T. J., & Ebert, D. (2004). Conceptual issues in local adaptation. *Ecology Letters*, *7*(12), 1225–1241. https://doi.org/10.1111/j.1461-0248.2004.00684.x

Keane, T. M., Goodstadt, L., Danecek, P., White, M. A., Wong, K., Yalcin, B., Heger, A., Agam, A., Slater, G., Goodson, M., Furlotte, N. A., Eskin, E., Nellåker, C., Whitley, H., Cleak, J., Janowitz, D., Hernandez-Pliego, P., Edwards, A., Belgard, T. G., … Adams, D. J. (2011). Mouse genomic variation and its effect on phenotypes and gene regulation. *Nature*, *477*(7364), 289–294. https://doi.org/10.1038/nature10413

Kehrberger, S., & Holzschuh, A. (2019). How does timing of flowering affect competition for pollinators, flower visitation and seed set in an early spring grassland plant? *Scientific Reports*, *9*(1), 15593. https://doi.org/10.1038/s41598-019-51916-0

Kenney, A. M., McKay, J. K., Richards, J. H., & Juenger, T. E. (2014). Direct and indirect selection on flowering time, water-use efficiency (WUE , δ ^{13} C), and WUE plasticity to drought in *Arabidopsis thaliana*. *Ecology and Evolution*, *4*(23), 4505–4521. https://doi.org/10.1002/ece3.1270

Kingsolver, J. G., & Pfennig, D. W. (2007). Patterns and power of phenotypic selection in nature. *BioScience*, *57*(7), 561–572. https://doi.org/10.1641/B570706

Kirkpatrick, M., & Barton, N. H. (1997). Evolution of a species' range. *The American Naturalist*, *150*(1), 1–23. https://doi.org/10.1086/286054

Lacy, R. C. (1997). Importance of genetic variation to the viability of mammalian populations. *Journal of Mammalogy*, *78*(2), 320–335.

Leinonen, P. H., Sandring, S., Quilot, B., Clauss, M. J., Mitchell-Olds, T., Agren, J., & Savolainen, O. (2009). Local adaptation in European populations of *Arabidopsis lyrata* (Brassicaceae). *American Journal of Botany*, *96*(6), 1129–1137. https://doi.org/10.3732/ajb.0800080

Li, H. (2011). A statistical framework for SNP calling, mutation discovery, association mapping and population genetical parameter estimation from sequencing data. *Bioinformatics*, *27*(21), 2987–2993. https://doi.org/10.1093/bioinformatics/btr509

Li, H., & Durbin, R. (2009). Fast and accurate short read alignment with Burrows-Wheeler transform. *Bioinformatics*, *25*(14), 1754–1760. https://doi.org/10.1093/bioinformatics/btp324

Li, H., Handsaker, B., Wysoker, A., Fennell, T., Ruan, J., Homer, N., Marth, G., Abecasis, G., Durbin, R., & 1000 Genome Project Data Processing Subgroup. (2009). The Sequence Alignment/Map format and SAMtools. *Bioinformatics*, *25*(16), 2078–2079. https://doi.org/10.1093/bioinformatics/btp352

Li, W., Liu, H., Cheng, Z. J., Su, Y. H., Han, H. N., Zhang, Y., & Zhang, X. S. (2011). DNA methylation and histone modifications regulate de novo shoot regeneration in Arabidopsis by modulating *WUSCHEL* expression and auxin signaling. *PLoS Genetics*, *7*(8), e1002243. https://doi.org/10.1371/journal.pgen.1002243

Liu, F., & Guo, F.-Q. (2013). Nitric oxide deficiency accelerates chlorophyll breakdown and stability loss of thylakoid membranes during dark-induced leaf senescence in Arabidopsis. *PLoS ONE*, *8*(2), e56345. https://doi.org/10.1371/journal.pone.0056345

Lu, F., Cui, X., Zhang, S., Liu, C., & Cao, X. (2010). *JMJ14* is an H3K4 demethylase regulating flowering time in Arabidopsis. *Cell Research*, *20*(3), 387–390. https://doi.org/10.1038/cr.2010.27

Manichaikul, A., Mychaleckyj, J. C., Rich, S. S., Daly, K., Sale, M., & Chen, W.-M. (2010). Robust relationship inference in genome-wide association studies. *Bioinformatics*, *26*(22), 2867–2873. https://doi.org/10.1093/bioinformatics/btq559

Martínez-Zapater, J. M. (1993). Genetic analysis of variegated mutants in Arabidopsis. *Journal of Heredity*, *84*(2), 138–140. https://doi.org/10.1093/oxfordjournals.jhered.a111298

Melicher, P., Dvořák, P., Řehák, J., Šamajová, O., Pechan, T., Šamaj, J., & Takáč, T. (2023). Methyl viologen-induced changes in the Arabidopsis proteome implicate *PATELLIN 4* in oxidative stress responses. *Journal of Experimental Botany*, erad363. https://doi.org/10.1093/jxb/erad363

Meyers, B. C., Kozik, A., Griego, A., Kuang, H., & Michelmore, R. W. (2003). Genome-wide analysis of NBS-LRR–encoding genes in Arabidopsis. *The Plant Cell*, *15*(4), 809–834. https://doi.org/10.1105/tpc.009308

Nasim, Z., Fahim, M., Hwang, H., Susila, H., Jin, S., Youn, G., & Ahn, J. H. (2021). Nonsense-mediated mRNA decay modulates Arabidopsis flowering time via the *SET DOMAIN GROUP 40 – FLOWERING LOCUS C* module. *Journal of Experimental Botany*, *72*(20), 7049–7066. https://doi.org/10.1093/jxb/erab331

North, A., Cornell, S., & Ovaskainen, O. (2011). Evolutionary responses of dispersal distance to landscape structure and habitat loss: Evolution of dispersal distance under habitat loss. *Evolution*, *65*(6), 1739–1751. https://doi.org/10.1111/j.1558-5646.2011.01254.x

Nosil, P., Funk, D. J., & Ortiz-Barrientos, D. (2009). Divergent selection and heterogeneous genomic divergence. *Molecular Ecology*, *18*(3), 375–402. https://doi.org/10.1111/j.1365-294X.2008.03946.x

Ørsted, M., Hoffmann, A. A., Sverrisdóttir, E., Nielsen, K. L., & Kristensen, T. N. (2019). Genomic variation predicts adaptive evolutionary responses better than population bottleneck history. *PLOS Genetics*, *15*(6), e1008205. https://doi.org/10.1371/journal.pgen.1008205

Paccard, A., Vance, M., & Willi, Y. (2013). Weak impact of finescale landscape heterogeneity on evolutionary potential in *Arabidopsis lyrata*. *Journal of Evolutionary Biology*, *26*(11), 2331–2340. https://doi.org/10.1111/jeb.12220

Parisod, C., & Christin, P. (2008). Genome-wide association to fine-scale ecological heterogeneity within a continuous population of *Biscutella laevigata* (Brassicaceae). *New Phytologist*, *178*(2), 436–447. https://doi.org/10.1111/j.1469-8137.2007.02361.x

Pluess, A. R., Frank, A., Heiri, C., Lalagüe, H., Vendramin, G. G., & Oddou-Muratorio, S. (2016). Genome–environment association study suggests local adaptation to climate at the regional scale in *Fagus sylvatica*. *New Phytologist*, *210*(2), 589–601. https://doi.org/10.1111/nph.13809

Prabhakar, V., Löttgert, T., Gigolashvili, T., Bell, K., Flügge, U.-I., & Häusler, R. E. (2009). Molecular and functional characterization of the plastid-localized Phosphoenolpyruvate enolase (*ENO1*) from *Arabidopsis thaliana*. *FEBS Letters*, *583*(6), 983–991. https://doi.org/10.1016/j.febslet.2009.02.017

Purcell, S., Neale, B., Todd-Brown, K., Thomas, L., Ferreira, M. A. R., Bender, D., Maller, J., Sklar, P., De Bakker, P. I. W., Daly, M. J., & Sham, P. C. (2007). PLINK: A tool set for whole-genome association and population-based linkage analyses. *The American Journal of Human Genetics*, *81*(3), 559–575. https://doi.org/10.1086/519795

Rajendran, K., Coyne, C. J., Zheng, P., Saha, G., Main, D., Amin, N., Ma, Y., Kisha, T., Bett, K. E., McGee, R. J., & Kumar, S. (2021). Genetic diversity and GWAS of agronomic traits using an ICARDA lentil (*Lens culinaris* Medik.) Reference Plus collection. *Plant Genetic Resources: Characterization and Utilization*, *19*(4), 279–288. https://doi.org/10.1017/S147926212100006X

Rawat, V., Abdelsamad, A., Pietzenuk, B., Seymour, D. K., Koenig, D., Weigel, D., Pecinka, A., & Schneeberger, K. (2015). Improving the annotation of *Arabidopsis lyrata* using RNA-seq data. *PLOS ONE*, *10*(9), e0137391. https://doi.org/10.1371/journal.pone.0137391

Reisch, C., Lehmair, T. A., Pagel, E., & Poschlod, P. (2021). Drivers of genetic diversity in plant populations differ between semi-natural grassland types. *Biodiversity and Conservation*, *30*(12), 3549–3561. https://doi.org/10.1007/s10531-021-02260-1

Rodrigues, V. L., Dolde, U., Sun, B., Blaakmeer, A., Straub, D., Eguen, T., Botterweg-Paredes, E., Hong, S., Graeff, M., Li, M.-W., Gendron, J. M., & Wenkel, S. (2021). A microProtein repressor complex in the shoot meristem controls the transition to flowering. *Plant Physiology*, *187*(1), 187–202. https://doi.org/10.1093/plphys/kiab235

Roux, F., & Frachon, L. (2022). A genome-wide association study in *Arabidopsis thaliana* to decipher the adaptive genetics of quantitative disease resistance in a native heterogeneous environment. *PLOS ONE*, *17*(10), e0274561. https://doi.org/10.1371/journal.pone.0274561

Schneider, C. A., Rasband, W. S., & Eliceiri, K. W. (2012). NIH image to ImageJ: 25 years of image analysis. *Nature Methods*, *9*(7), 671–675. https://doi.org/10.1038/nmeth.2089

Schneider, J. C., Suzanne, H., & Somerville, C. R. (1995). Chilling-sensitive mutants of Arabidopsis. *Plant Molecular Biology Reporter*, *13*(1), 11–17. https://doi.org/10.1007/BF02668388

Shen, Y., Conde E Silva, N., Audonnet, L., Servet, C., Wei, W., & Zhou, D.-X. (2014). Over-expression of histone H3K4 demethylase gene *JMJ15* enhances salt tolerance in Arabidopsis. *Frontiers in Plant Science*, *5*. https://doi.org/10.3389/fpls.2014.00290

Sinapidou, E., Williams, K., Nott, L., Bahkt, S., Tör, M., Crute, I., Bittner-Eddy, P., & Beynon, J. (2004). Two TIR:NB:LRR genes are required to specify resistance to *Peronospora parasitica* isolate Cala2 in *Arabidopsis*. *The Plant Journal*, *38*(6), 898–909. https://doi.org/10.1111/j.1365-313X.2004.02099.x

Spichtig, M., & Kawecki, T. J. (2004). The maintenance (or not) of polygenic variation by soft selection in heterogeneous environments. *The American Naturalist*, *164*(1), 70–84. https://doi.org/10.1086/421335

Takeno, K. (2016). Stress-induced flowering: The third category of flowering response. *Journal of Experimental Botany*, *67*(17), 4925–4934. https://doi.org/10.1093/jxb/erw272

Temesgen, T., Zigale, S., & Tamirat, B. (2021). Multi environments and genetic-environmental interaction (GxE) in plant breeding and its challenges: A review article. *International Journal of Research Studies in Agricultural Sciences*, *7*(4). https://doi.org/10.20431/2454-6224.0704002

Thoen, M. P. M., Davila Olivas, N. H., Kloth, K. J., Coolen, S., Huang, P., Aarts, M. G. M., Bac-Molenaar, J. A., Bakker, J., Bouwmeester, H. J., Broekgaarden, C., Bucher, J., Busscher-Lange, J., Cheng, X., Fradin, E. F., Jongsma, M. A., Julkowska, M. M., Keurentjes, J. J. B., Ligterink, W., Pieterse, C. M. J., … Dicke, M. (2017). Genetic architecture of plant stress resistance: Multi-trait genome-wide association mapping. *New Phytologist*, *213*(3), 1346–1362. https://doi.org/10.1111/nph.14220

Valdisser, P. A. M. R., Müller, B. S. F., De Almeida Filho, J. E., Morais Júnior, O. P., Guimarães, C. M., Borba, T. C. O., De Souza, I. P., Zucchi, M. I., Neves, L. G., Coelho, A. S. G., Brondani, C., & Vianello, R. P. (2020). Genome-wide association studies detect multiple QTLs for productivity in mesoamerican diversity panel of common bean under drought stress. *Frontiers in Plant Science*, *11*, 574674. https://doi.org/10.3389/fpls.2020.574674

Van'T Hof, A. E., Edmonds, N., Dalíková, M., Marec, F., & Saccheri, I. J. (2011). Industrial melanism in British peppered moths has a singular and recent mutational origin. *Science*, *332*(6032), 958–960. https://doi.org/10.1126/science.1203043

Vermeulen, P. J. (2015). On selection for flowering time plasticity in response to density. *New Phytologist*, *205*(1), 429–439. https://doi.org/10.1111/nph.12984

Verslues, P. E., Lasky, J. R., Juenger, T. E., Liu, T.-W., & Kumar, M. N. (2014). Genome-wide association mapping combined with reverse genetics identifies new effectors of low water potential-induced proline accumulation in Arabidopsis. *Plant Physiology*, *164*(1), 144–159. https://doi.org/10.1104/pp.113.224014

Viechtbauer, W. (2010). Conducting meta-analyses in *R* with the **metafor** package. *Journal of Statistical Software*, *36*(3). https://doi.org/10.18637/jss.v036.i03

Wang, X., Li, Q., Zhang, Y., Pan, M., Wang, R., Sun, Y., An, L., Liu, X., Yu, F., & Qi, Y. (2022). *VAR2*/*AtFtsH2* and *EVR2*/*BCM1*/*CBD1* synergistically regulate the accumulation of PSII reaction centre D1 protein during de-etiolation in Arabidopsis. *Plant, Cell & Environment*, *45*(8), 2395–2409. https://doi.org/10.1111/pce.14368

Willi, Y., & Määttänen, K. (2010). Evolutionary dynamics of mating system shifts in Arabidopsis lyrata: Mating system shifts in A. lyrata. *Journal of Evolutionary Biology*, *23*(10), 2123–2131. https://doi.org/10.1111/j.1420-9101.2010.02073.x

Willi, Y., & Määttänen, K. (2011). The relative importance of factors determining genetic drift: Mating system, spatial genetic structure, habitat and census size in *Arabidopsis lyrata*. *New Phytologist*, *189*(4), 1200–1209. https://doi.org/10.1111/j.1469-8137.2010.03569.x

Willi, Y., Van Buskirk, J., & Hoffmann, A. A. (2006). Limits to the adaptive potential of small populations. *Annual Review of Ecology, Evolution, and Systematics*, *37*(1), 433–458. https://doi.org/10.1146/annurev.ecolsys.37.091305.110145

Wos, G., & Willi, Y. (2018). Genetic differentiation in life history traits and thermal stress performance across a heterogeneous dune landscape in *Arabidopsis lyrata*. *Annals of Botany*, *122*(3), 473–484. https://doi.org/10.1093/aob/mcy090

Wright, S. (1969). *Evolution and the genetics of populations: The theory of gene frequencies.* (2nd ed.). The University of Chicago Press.

Yang, B., Stamm, G., Bürstenbinder, K., & Voiniciuc, C. (2022). Microtubule-associated IQD9 orchestrates cellulose patterning in seed mucilage. *New Phytologist*, *235*(3), 1096–1110. https://doi.org/10.1111/nph.18188

Yang, B., Voiniciuc, C., Fu, L., Dieluweit, S., Klose, H., & Usadel, B. (2019). *TRM 4* is essential for cellulose deposition in Arabidopsis seed mucilage by maintaining cortical microtubule organization and interacting with *CESA 3*. *New Phytologist*, *221*(2), 881–895. https://doi.org/10.1111/nph.15442

Yang, H., Mo, H., Fan, D., Cao, Y., Cui, S., & Ma, L. (2012). Overexpression of a histone H3K4 demethylase, *JMJ15*, accelerates flowering time in Arabidopsis. *Plant Cell Reports*, *31*(7), 1297–1308. https://doi.org/10.1007/s00299-012-1249-5

Yeaman, S., & Whitlock, M. C. (2011). The genetic architecture of adaptation under migration-selection balance: The genetic architecture of local adaptation. *Evolution*, *65*(7), 1897–1911. https://doi.org/10.1111/j.1558-5646.2011.01269.x

Zhou, X., & Stephens, M. (2012). Genome-wide efficient mixed-model analysis for association studies. *Nature Genetics*, *44*(7), 821–824. https://doi.org/10.1038/ng.2310

Zhou, X., & Stephens, M. (2014). Efficient multivariate linear mixed model algorithms for genome-wide association studies. *Nature Methods*, *11*(4), 407–409. https://doi.org/10.1038/nmeth.2848

Figure 1

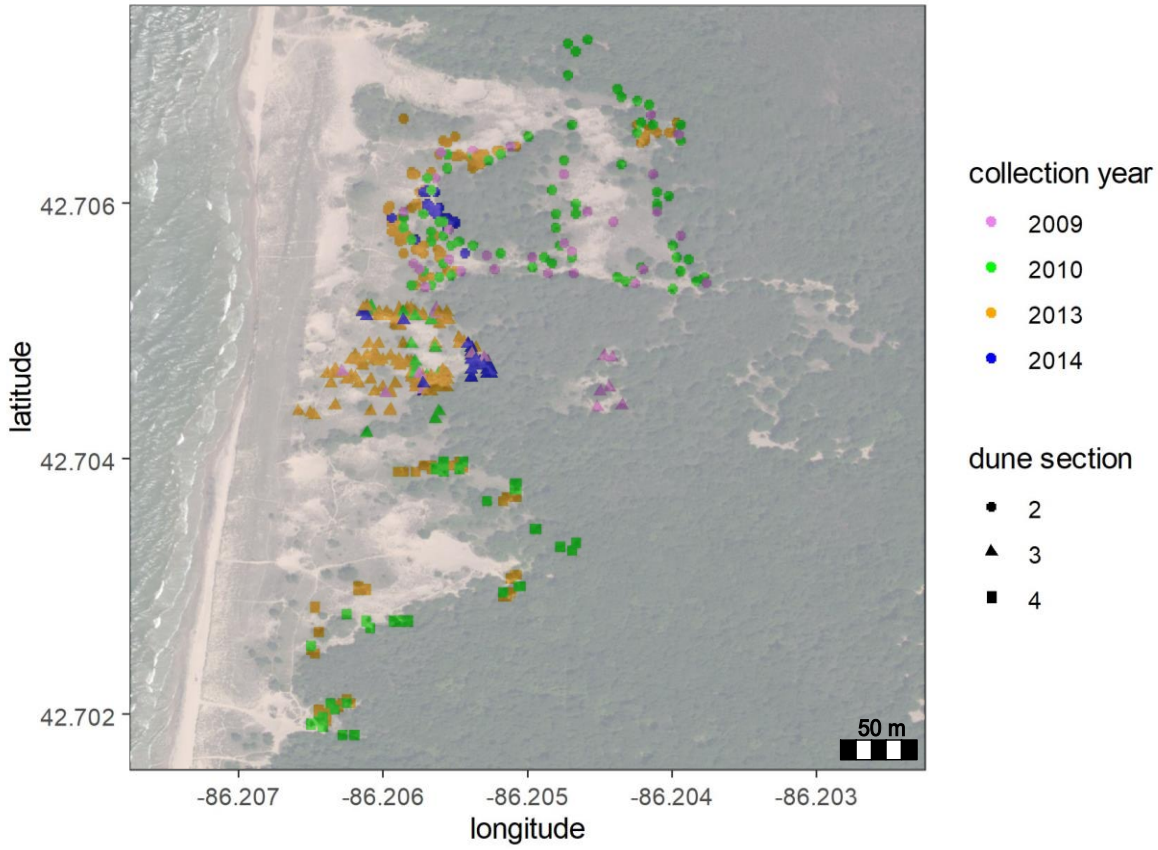

Figure 1: Distribution of *Arabidopsis lyrata* collected at Saugatuck Dunes State Park, MI, USA, on the shore of Lake Michigan. Colours indicate sampling year and shapes the dune section. [Source of satellite image 2023: Google Maps, 2023; **permission has to be required yet**].

Figure 2

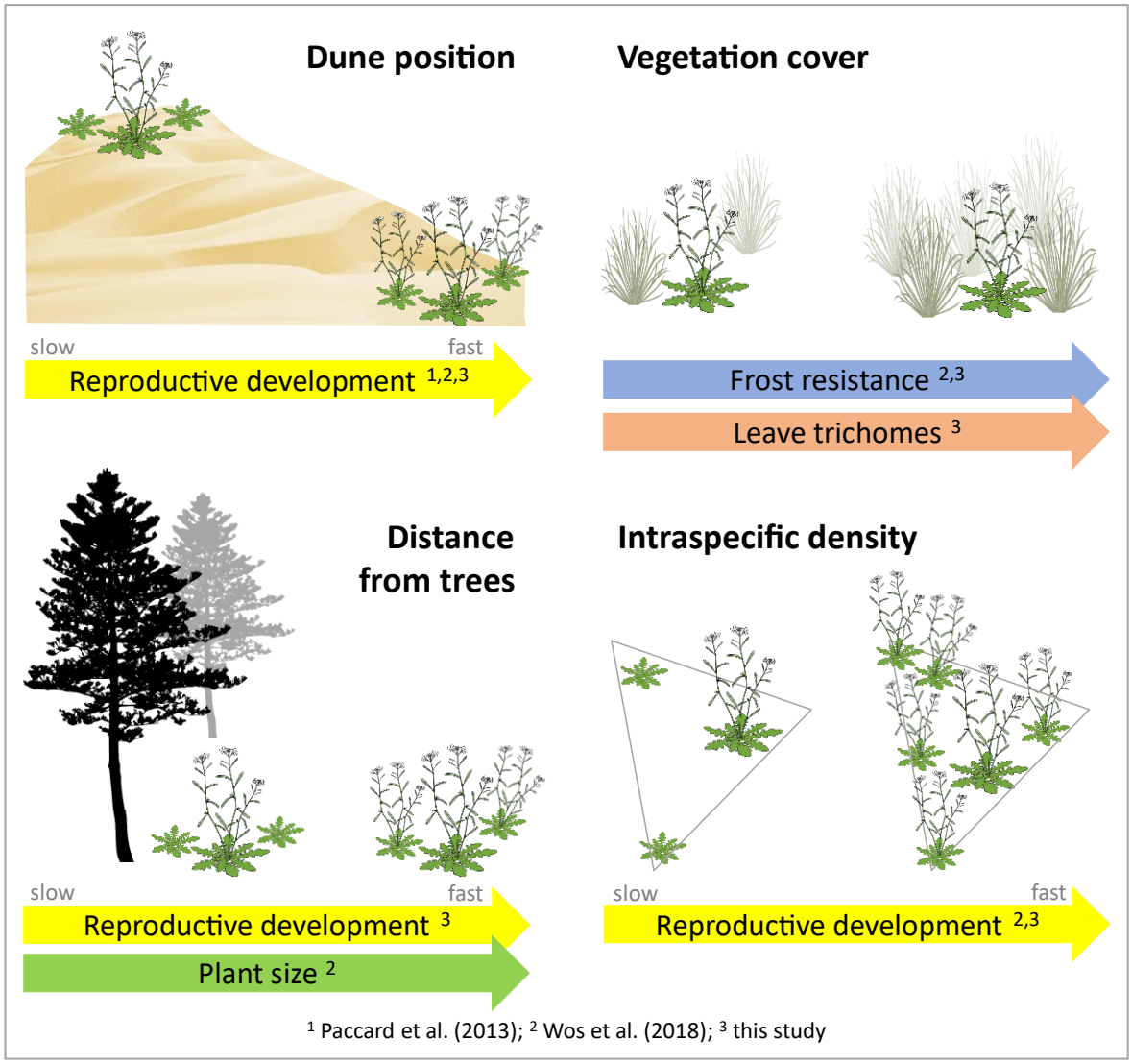

Figure 2: Significant relationships found between environmental variables (bold) and phenotypic traits (arrows) of *Arabidopsis lyrata* in the dune landscape of Saugatuck, MI, USA. Superscripts indicate which trait correlation was found in previous studies and the current study (only overall significant environment-trait pairs are shown here).

Figure 3

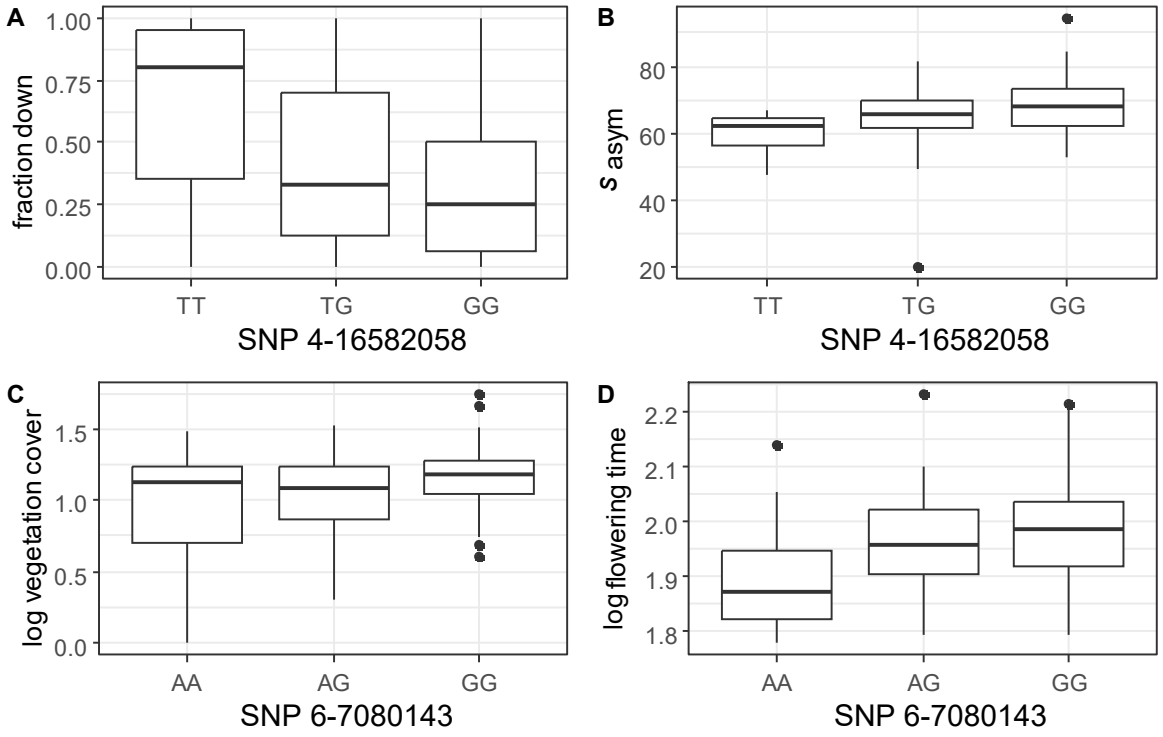

Figure 3: Correlation between trait and allelic state at a SNP of the candidate genes *JMJ15* (A, B) and *SDG40* (C, D) for the fraction down from dune top (A), asymptotic size (B), log-transformed vegetation cover (C), and log-transformed time to flowering (D), respectively.

Figure 4

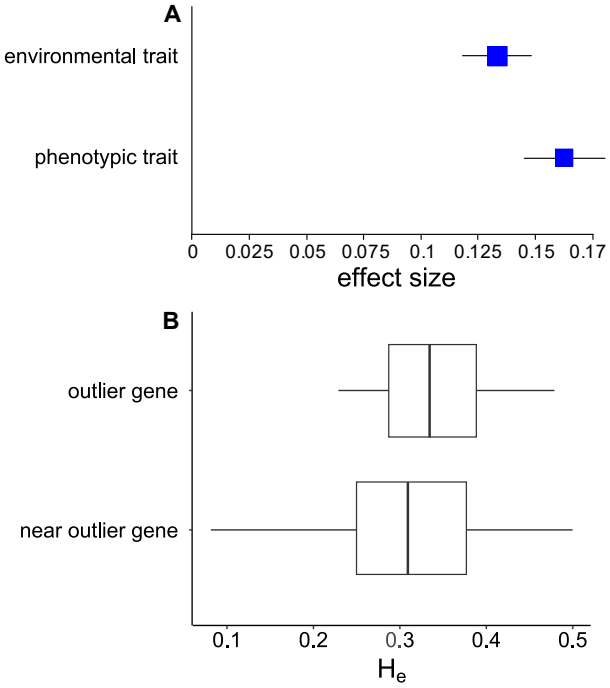

Figure 4: A - Effect size and 95% confidence intervals for the dominance deviation of the expected trait value of mid-homozygous SNP-haplotypes for environmental or phenotypic traits with significant associations. Only SNPs of outlier genes are considered. **B** - Expected heterozygosity (H_e) per gene. Outlier genes were those that had at least 2 outlier SNPs with MAF > 0.1 both in in the association with environmental or phenotypic traits. Adjacent genes were two randomly picked genes 50k bp up- and down-stream of the respective outlier gene.

Figure 5

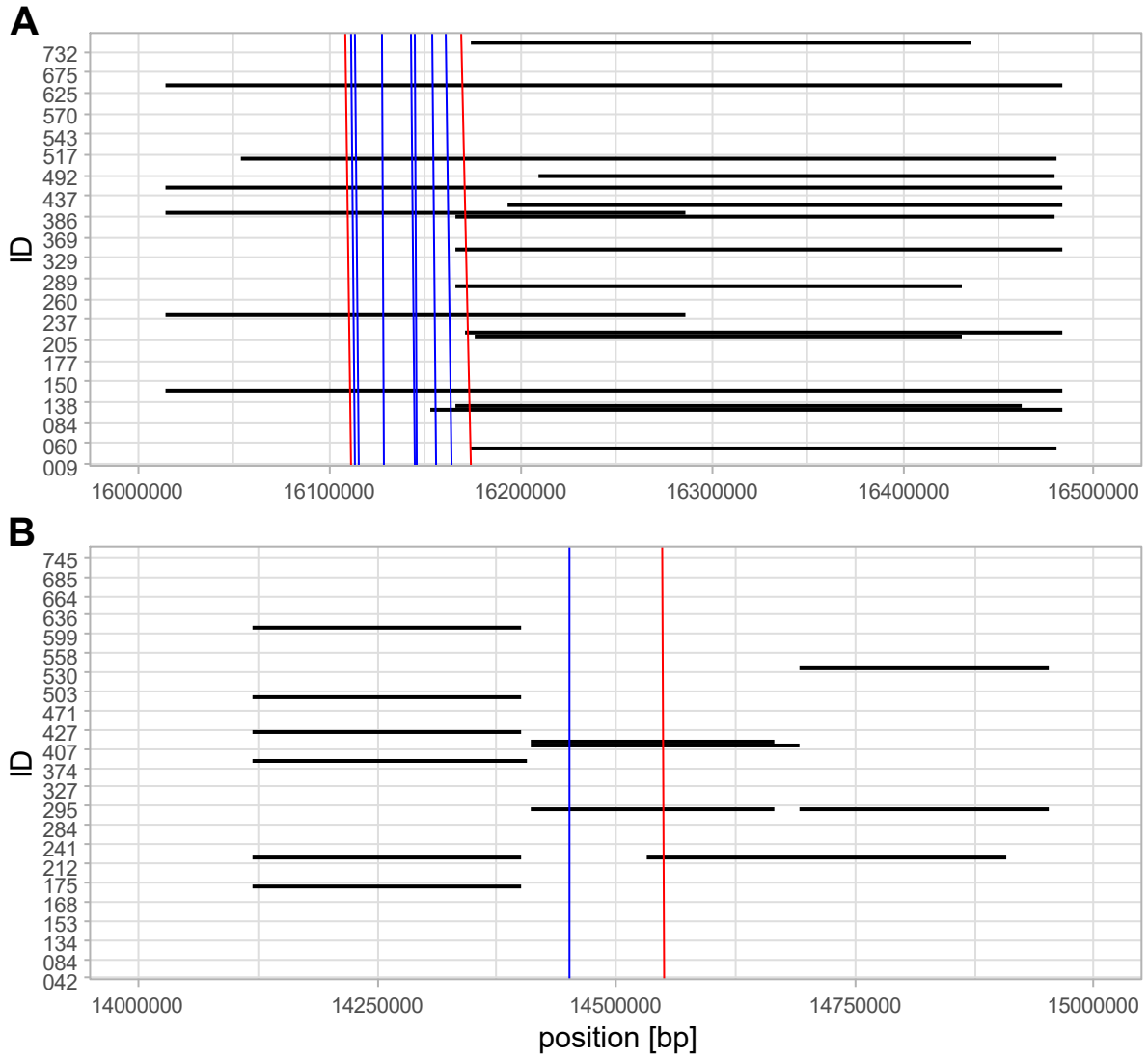

Figure 5: Distribution of runs of homozygosity, ROHs (black) and the position of outlier genes (red and blue) along chromosome 2 (A) and chromosome 4 (B) for each specimen. Candidate genes with physiological function are marked in red, all others in blue. ROH was calculated for 570 individuals of *A. lyrata*.

Table 1

Table 1: Relationship between environmental variables - dune position, vegetation cover, distance from trees, and intraspecific density and each of ten phenotypic variables - time till germination (t_{ger}), bolting (t_{bol}) and flowering (t_{flo}), asymptotic size (s_{asym}), time till half growth (x_{mid}), maximum growth rate (r_{max}), heat and frost resistance, leave trichomes and leave shape. N – number of samples. R^2 – model fit. F statistics (or χ^2 for binary dependent variables) and significant p-values of type-3 testing are indicated: *** $p < 0.001$, ** $p < 0.01$, * $p < 0.05$, $^{\bullet}$ $p < 0.1$.

	t_{ger}	t_{bol}	t_{flo}	s_{asym}	x_{mid}	r_{max}	res_{heat}	res_{frost}	*Leave trichomes*	*Leave shape*
N	561	555	542	560	560	560	557	558	560	559
R^2	0.114	0.092	0.116	0.104	0.083	0.081	0.072	0.070	-	-
	F	*F*	*F*	*F*	*F*	*F*	*F*	*F*	χ^2	χ^2
Dune position (*fD*)	0.120	0.640	**5.050** *	0.090	0.050	0.380	0.000	0.500	1.729	3.044 $^{\bullet}$
Vegetation cover (*BB*)	0.800	0.780	3.560 $^{\bullet}$	0.130	0.540	0.600	0.230	**4.630** *	**10.591** **	0.041
Distance from trees (*dC*)	2.040	3.410 $^{\bullet}$	**4.650** *	1.170	0.370	0.780	0.210	0.880	0.151	0.035
Intraspecific density (*dAlyr*)	3.330 $^{\bullet}$	**6.960** **	**5.630** *	0.000	0.290	0.020	0.300	0.380	3.295 $^{\bullet}$	2.119
Section (*s*)	0.250	2.470 $^{\bullet}$	1.020	2.260	0.340	0.550	0.030	**3.160**	**8.093** *	3.883
Year (*y*)	1.460	0.930	1.320	**3.470** *	1.160	1.090	0.370	0.550	**9.006** *	2.184
*fD*s*y*	1.710 $^{\bullet}$	0.530	0.880	1.450	0.630	**2.180** *	1.390	0.440	**16.518** *	8.653
*BB*s*y*	1.300	1.530	**2.100** *	1.270	0.520	0.290	1.070	1.820 $^{\bullet}$	5.607	2.070
*dC*s*y*	1.070	1.770 $^{\bullet}$	**2.800** **	1.240	0.570	1.230	0.400	0.370	9.402	0.648
*dAlyr*s*y*	**2.680** **	1.220	1.460	0.570	0.660	0.740	0.690	0.880	4.108	3.855

Table 2

Table 2: Environment-phenotypic associations that motivated GWAS analysis. Indicated are sections (e.g., *S2*) and years (e.g., '*09*) used for the analysis and the resulting number of samples per association (*# indv.*). Lastly, the number of overlapping outlier SNPs found for a pair of environmental and phenotypic traits (*overlap*). Abbreviations used for traits are written out in the legend of Table 1. Second columns (sign. rel.) indicates environment-trait pairs that showed a significant relationship between the respective environmental and phenotypic trait. Environment-trait pairs without significant relationship were added because of significant section-year influences or strong estimates within specific year-section combinations.

	Sign. rel.	*S2_09*	*S2_10*	*S2_13*	*S2_14*	*S3_09*	*S3_10*	*S3_13*	*S3_14*	*S4_10*	*S4_13*	*# Indv.*	*Overlap*
Dune position - t_{flo}	x	x	x	x	x			x	x	x	x	515	66
Dune position - s_{asym}			x			x	x			x		143	46
Dune position - *leave shape*		x			x			x	x	x	x	353	53
Vegetation cover - t_{flo}					x				x	x	x	149	224
Vegetation cover - res_{frost}	x				x	x	x		x	x	x	188	35
Vegetation cover - *leave trichomes*	x	x	x	x	x			x				393	196
Distance from trees - t_{flo}	x					x	x		x	x	x	161	176
Distance from trees - s_{asym}		x		x	x	x			x	x		263	121
Intraspecific density - t_{bol}	x	x			x	x	x	x		x	x	345	68
Intraspecific density - t_{flo}	x				x	x	x	x		x	x	297	73

Table 3

Table 3: Overview of candidate genes with known physiological function. Outlier SNPs: number of overlapping SNPs between the two associated variables and a MAF > 0.1. G-E association: genome-environment associations for *A. thaliana* found in Ferrero-Serrano and Assmann (2019). References to first descriptions of respective gene and their described function or proposed function within *tair* (Berardini et al., 2015) are given.

Gene	Association	Length [bp]	Outlier SNPs	AT gene	Gene name	Function	G-E association	References
AL6G18180	s_{asym} - *fD*	1813	4	*AT5G07840*	*PIA1*	ankyrin repeat family protein	IGBP DIS soil pH	-
AL4G30890	s_{asym} - *fD*	3590	2	*AT2G34880*	*JMJ15, PKDM7C*	involved in speeding up of floral transition & enhances stress tolerance (temperature & salt)	OMI Ozone summer, CHELSA BIO4	Cattaneo *et al.* (2019); Cui *et al.* (2021); Shen *et al.* (2014, 2014); Yang *et al.* (2012)
AL3G38380	t_{flo} - *BB*	7873	36	*AT3G23640*	*HGL1*	involved in the FERONIA (FER) signalling pathway	AVHRR landcover Woodland, ISRIC WISE Soil pH	Smith *et al.* (2004); Choi *et al.* (2022)
AL6G28290	t_{flo} - *BB*	2254	5	*AT5G17240*	*SDG40*	methyltransferase that regulates FLC though SDG40 to modulate flowering time	unknown	Nasim *et al.* (2021)
AL4G25980	t_{flo} - *BB*	2904	3	*AT2G30950*	*FTSH2, VAR2*	functions in thylakoid membrane biogenesis and repair of PSII	IGBP DIS soil pH	Chen *et al.* (2000); Liu *et al.* (2010); Martínez-Zapater (1993); Wang *et al.* (2022)
AL6G49560	t_{flo} - *BB*	3114	3	*AT4G03350*	*EVE1*	ubiquitin family protein involved in inflorescence stem development	AVHRR Vegetation condition index summer	Hwang *et al.* (2011)
AL2G34060	*leave trichomes - BB*	4977	13	*AT1G74160*	*LNG3, TRM4*	influence seed mucilage synthesis & might regulate leave length	CHELSA BIO9, CRU vapor pressure spring & summer	Lee *et al.* (2018); Yang *et al.* (2019, 2022)
AL2G32570	*leave trichomes - BB*	3827	2	*AT4G09360*	-	pseudogene involved in disease recognition & resistance	AVHRR Smoothed Brightness Temperature Summer & spring, WorldClim v2 Tmin summer	Meyers *et al.* (2003); Sinapidou *et al.* (2004)
AL2G33880	*leave trichomes - BB*	2724	3	*AT1G74030*	*ENO1*	encodes the plastid-localized phosphoenolpyruvate enolase	CHELSA BIO9, BIO6 & BIO11	Andriotis *et al.* (2010); Prabhakar *et al.* (2010, 2009)
AL1G44750	t_{bol} - *dAlyr*	2601	2	*AT1G30690*	*PATL4*	involved in plant responses to oxidative stress	WorldClim v2 Precipitation spring	Melicher *et al.* (2023); Tejos *et al.* (2017)
AL7G33510	t_{flo} - *dAlyr*	2451	3	*AT4G20380*	*CHS4, LSD1*	involved in responses to different stressors & cell death under cold conditions	WorldClim v2 BIO14 & BIO17	Schneider *et al.* (1995); Huang *et al.* (2010); Bernacki *et al.* (2019); Bernacki *et al.* (2019)
AL7G33490	t_{flo} - *dAlyr*	5172	2	*AT4G20400*	*JMJ14, PKDM7B*	involved in repressing of floral transition & thermosensory response	WorldClim v2 BIO2	Lu *et al.* (2010); Li *et al.*, (2011); Cattaneo *et al.* (2019); Cui *et al.* (2021); Rodrigues *et al.* (2021)

Chapter 2: **Evolutionary potential under heat and drought stress at the southern range edge of North American *Arabidopsis lyrata***

Jessica Heblack, Judith R. Schepers, and Yvonne Willi

Department of Environmental Sciences, University of Basel, 4056 Basel, Switzerland

Running title: Evolutionary potential under climate change

No. figures: 3

No. tables: 1

Supplementary: 5 figures, 8 tables, 2 methods

Published at the Journal of Evolutionary Biology (JEB), Volume 37, Issue 5, May 2024, Pages 555–565, https://doi.org/10.1093/jeb/voae045.

Abstract

The warm edges of species' distributions are vulnerable under global warming. Evidence is the recent range retraction from there found in many species. It is unclear why populations cannot easily adapt to warmer, drier, or combined hot and dry conditions and locally persist. Here, we assessed the ability to adapt to these stressors in the temperate species *Arabidopsis lyrata*. We grew plants from replicate seed families of a central population with high genetic diversity under a temperature and precipitation regime typical of the low-latitude margin or under hotter and/or drier conditions within naturally occurring amplitudes. We then estimated genetic variance-covariance (G-) matrices of traits depicting growth and allocation as well as selection vectors to compare the predicted adaptation potential under the different climate-stress regimes. We found that the sum of genetic variances and genetic correlations were not significantly different under stress as compared to benign conditions. But under drought and heat-drought, the predicted ability to adapt was severely constrained due to strong selection and selection pointing in a direction with less multivariate genetic variation. The much-reduced ability to adapt to dry and hot-dry conditions is likely to reduce the persistence of populations at the low-latitude margin of the species' distribution and contributes to the local extinction of the species under further warming.

Keywords: adaptation, climatic gradient, evolutionary potential, genetic variation, G-matrix, range edge, trade-offs

Introduction

Species' distribution limits often reflect endpoints of the ecological niche of a species, with the latter defined as the ranges of abiotic factors, availability of resources and the abundance of interacting species that enable long-term persistence (Hargreaves et al., 2014; Paquette & Hargreaves, 2021). However, for many species, climate alone is a good predictor of where a species reaches its geographical or elevational limit (Lee-Yaw et al., 2016; Patsiou et al., 2021), suggesting that failing climate adaptation at range limits plays a major role in determining distributions. Constrained climate adaptation at range limits is also indicated by the many examples of species that have shifted their distributions under recent climate warming, with expansions at the cold margins and retractions from the warm margins (Chen et al., 2011; Lenoir et al., 2020; Rumpf et al., 2018). In parallel, macroevolutionary studies have revealed that adaptation to climate is evolutionarily constrained, particularly adaptation to heat (Bennett et al., 2021; Liu et al., 2020). Still, the causes of constraint are unknown. Here, we focus on the genetic architecture of growth traits under selection and its role in constraining climate adaptation at warm range limits, as species seem mostly unable to adapt there (Parmesan, 2006).

Evolutionary theory has come up with several hypotheses as to why adaptation to changing conditions can fail at range limits (Sexton et al., 2009). These include steepening environmental gradients, too little or too much dispersal, small population size, and, linked with low dispersal and small population size, low genetic variation (Holt, 2003; Kirkpatrick & Barton, 1997; Polechová, 2018; Polechová & Barton, 2015). An aspect that has received relatively less attention is the nature of genetic variation. There may be ample genetic variation for traits under selection when evaluated individually, though genetic variation may still be constraining if selection acts on several traits and these are tied in genetic correlations antagonistic to the direction of selection (Blows & Hoffmann, 2005; Hansen et al., 2019;

Lande, 1979). Within a population, genetic correlations antagonistic to the direction of selection, or genetic trade-offs, may be the result either of physical linkage or antagonistic pleiotropy (Falconer & Mackay, 1996, p. 312). Evolutionary trade-offs can be detected within populations if genotypes differ enough in regard to the expression of traits involved in the trade-off, often under stressful conditions (Stearns, 1992) or across habitat types (Falconer & Mackay, 1996, pages 321-324). For the latter scenario, genotypes that are favoured in one habitat are less favoured in another habitat (Fry, 2003), thus preventing niche expansion of specialized organisms (Holt & Gaines, 1992) and the evolution of favourable traits at distribution margins (Hoffmann & Blows, 1994; Roff et al., 2002).

Genetic variance-covariance (G-) matrices are useful for disentangling correlations among multiple traits, for estimating genetic integration and for assessing constraints on recent or future multivariate evolution (Arnold, 1992; Lande, 1979). Genetic variances of specific traits are the elements on the main diagonal axis, whereas genetic covariances are the off-diagonal elements of G. G-matrices of different populations or revealed under different environmental conditions can be compared with each other and in regard to how easily they can contribute to a selection response (Roff & Fairbairn, 2012). An important estimate of G capturing genetic correlations in one value is the effective number of dimensions (Kirkpatrick, 2009). If genetic correlations are absent, this number equals the number of traits included in the matrix. The other extreme is when all genetic variation aligns along one axis, with the effective number of dimensions being 1. Angles between G or its components/eigenvectors and other vectors can predict the constraining nature of genetic correlations more specifically. A first such angle involves the vector of population divergence to assess the adaptability in a likely direction of selection (Schluter, 1996). A second involves a selection vector to predict the immediate response to selection (Blows & Hoffmann, 2005).

So far, few studies have assessed the role that genetic trade-offs may play in constraining

adaptive evolution at range margins and/or under climate change on a microevolutionary scale (Willi & Van Buskirk, 2022). Paccard et al. (2016) compared the G-matrices of populations of *Arabidopsis lyrata* of a latitudinal gradient and found that populations at range limits had reduced genetic variances, but genetic covariances were such that they constrained evolution less than those of more centrally located populations. Sheth and Angert (2016) imposed artificial selection on scarlet monkeyflowers (*Mimulus cardinalis*) from replicate populations of the latitudinal range, either for early or late flowering. They detected correlated responses in early flowering lines, namely higher specific leaf area (SLA) and leaf nitrogen content. But population divergence across latitude did not follow the pattern of correlations, suggesting that past evolution had gone in the direction of less multivariate genetic variation. Etterson & Shaw (2001) performed a quantitative genetics crossing experiment with three populations of *Chamaecrista fasciculata* from a latitudinal gradient, estimated G-matrices at the three sites of origin, and predicted responses to selection based on single traits or G. The predicted multivariate responses were mostly reduced compared to predicted univariate responses due to genetic correlations antagonistic to the direction of selection.

The traits included in the estimation of G needs special consideration. Sessile organisms, such as herbaceous plants, seem to respond to environmental stress either by a strategy of escape or tolerance (e.g., Kooyers, 2015; Puijalon et al., 2011; Upadhyay, 2019). Under stress, growth and development may be accelerated to finish an important life-history phase before the effect of stress becomes too severe, a strategy of escape. Alternatively, growth and development may be slowed down in favour of expressing protective traits. Sartori et al. (2019) showed in *A. thaliana* that an acceleration of phenology is related to lower precipitation and higher temperature along the species' range from high to low latitudes, indicating escape from stress under low-latitude conditions. For our study organism, *Arabidopsis lyrata* ssp. *lyrata*, of the many traits that were previously tested for latitudinal clinal variation, only plant size,

reproductive development and thermal resistance were found to vary. Plants of low-latitude areas grew to smaller size under benign temperatures, had a slower transition to flowering, higher thermal tolerance and higher heat resistance, indicating a strategy of slow development and tolerance/protection at low latitudes (Paccard et al., 2014; Wos & Willi, 2015). Hence, adjustments on the continuum of fast versus slow growth or development may be key for coping with stress (Sartori et al., 2019), and aspects of growth and development are therefore good candidate traits in investigations on G in the context of low-latitude/warm range limits.

In this study, we compared G-matrices of one large outcrossing population of North American *Arabidopsis lyrata* ssp. *lyrata* (*A. lyrata* in short) grown under experimental temperature and precipitation similar to those at the low-latitude range margin. In climatised glasshouse chambers, we simulated average temperature and precipitation, or extreme conditions, i.e., increased temperature or decreased precipitation, or both types of stressors combined, as they can occur in spring to summer at the southern range edge. Environmental niche modelling had revealed that the distribution of the species in south and north is restricted by climate, and the major climatic factor associated with range limits was mean minimum temperature in early spring (Lee-Yaw et al., 2018; Sánchez-Castro et al., 2024). Apart from warmer temperature, we chose drier conditions, as low precipitation during the growing season may reduce the transpiration capacity of plants, which is their typical way of coping with heat (Irvine et al., 1998). We focused on traits of growth and allocation based on previous findings that indicated the importance of growth progression and allocation in coping with stress. To achieve solid estimates on genetic correlations, we worked with one population only, but we included many replicate families. For the same reason, we chose a population of the southerly-centre of distribution with high genetic variation, including in expressed traits. Populations of the southern range limit generally harbour low genomic variation and genetic variation for expressed traits (Paccard et al., 2016; Willi et al., 2018), making the detection of trade-offs

difficult. We addressed the following questions: (1) Do genetic variances of traits differ under benign and climate-stress conditions? (2) Are there multivariate genetic constraints? (3) How well can *A. lyrata* respond to selection and adapt under heat, drought, or combined heat-drought?

MATERIAL AND METHODS

2.1. Seed material and propagation

Arabidopsis lyrata subsp. *lyrata* occurs in temperate eastern and mid-western North America, on sand dunes or rocky outcrops with some natural disturbance. It is a short-lived perennial that produces basal rosettes out of which inflorescences grow in late spring/early summer. We selected a population from the south-centre of the *A. lyrata* distribution, at Saugatuck Dunes State Park, Michigan, US (42.70° N, 86.20° W), with high genomic variation and a history of little genetic drift despite some postglacial range expansion (Willi et al., 2018). Furthermore, the population was found to harbour genetic variation in plant size and reproductive development under control conditions and in frost resistance, with traits being associated with environmental gradients of the dune landscape: position on the dune, distance from the canopy, vegetation cover and intraspecific density (Paccard et al., 2013; Wos & Willi, 2018). The same three traits were confirmed as being variable among populations across the latitudinal distribution of the species (Paccard et al., 2014; Wos & Willi, 2015).

Seeds of >600 maternal plants were collected between 2007 and 2014 in the field. We assumed that over the 7 years, there had been little change in allele frequencies as the species is common over a large surface area, with a large census size. Seeds of maternal plants were grown in separate pots in a glasshouse and thinned to one plant per pot (conditions in Table S1). Plants were cross-pollinated in pairs, with a preference for pairing within one of several habitat aspects, e.g., both plants from dune tops (Methods S1). The intention was to keep some

of the potentially existent adaptive variants linked to a habitat aspect at a higher frequency in some offspring genotypes. The design resulted in 271 successful cross pairs or 'families', of which 120 were randomly selected for offspring raising. Crosses were performed reciprocally, but cross direction was not included in the statistical models. Additionally, the crossing design included three families each from two northern and two southern populations. These were used later for comparing within-population variation of the Saugatuck population with within-species, latitudinal trait variation (Table S2, Fig. S1). One pair of northern/southern populations came from the eastern ancestral cluster of *A. lyrata* and one, together with the Saugatuck population, from the western ancestral cluster (Willi et al., 2018). The obtained seeds were stored in paper bags at 4°C with silica beads to reduce moisture.

2.2 Experimental setup

We designed a 2x2 factorial stress experiment with average or extreme temperatures and average or low precipitation occurring in the two populations at the southern range limit (Table S1). Low-temperature conditions (*Control* and *Dry*) were close to average temperature in late spring/early summer, with the corresponding experimental conditions of: 18°C at night, 22°C during the day and 25°C for the daily 1-h heat peak (Fig. 1a; climate data at the two southern edge sites in Schepers et al., 2024). High-temperature conditions (*Hot* and *Hot&Dry*) resembled the summer climate, with 23°C at night, 27°C during the day and 30°C for the daily 1-h heat peak. Experimental temperatures during night-time were not as low as those at the two southern sites. The baseline for watering (*Control* and *Hot*) was about average precipitation in late spring/early summer, 100 mm per month. Low watering (*Dry* and *Hot&Dry*) was chosen close to precipitation during the driest month, 60 mm per month. Precipitation amounts were broken down to watering the pots every second day, which was set to either 8.4 ml or 5 ml per pot. Because some mortality was observed early on, we increased watering after two weeks by

~20% to 10 ml or 6 ml.

Five replicate plants per family were grown in each of the four treatment combinations (in short: treatments), split over 5 blocks. Seeds were sown in pots (1 per pot, pot diameter/depth: 4/5 cm) of 54-multipot-trays filled with a mixture of 1:2 of peat and sand (120 families x 4 environments x 5 replicate blocks = 2400 pots, plus 3 families x 4 marginal populations x 4 environments x 3 replicates = 144 pots). Pots were watered to saturation and covered with mesh nets, and seeds were stratified at 4°C in dark climate cabinets for 12 days (ClimeCab 1400, KÄLTE 3000 AG, Landquart, Switzerland). Trays were then moved to the glasshouse for germination and kept moist by spraying from above and keeping the mesh nets until ~75% of seeds had germinated (for 7 days). After 3 weeks, when ~80% of the plants had reached the 4-leaf-stage, the stress experiment started. The experiment involved four glasshouse chambers, two with the low-temperature regime and two with the high-temperature regime. Within each of these, five blocks of multiport trays were maintained, with multiport trays allocated to either baseline- or low-watering. To reduce effects of glasshouse chamber and position within block, blocks and trays within blocks were randomly repositioned across the two glasshouse chambers of the same temperature regime twice a week. Plants received fertilizer every fourth week and some insecticide to combat thrips infestation. The stress experiment was terminated after 5 months for plants under the high-temperature regime and after 6 months for plants under the low-temperature regime.

2.2. Trait assessment

Seed germination was checked every day for the first two weeks. The starting size for the day of germination was set to 2 mm^2, representing about four times the mean seed size of *A. lyrata* (Willi, 2013). Growth was tracked by taking pictures of each tray twice a week (every 3-4 days) until at least bolting (Fig. 1b). At the same time, mortality was recorded. Camera setup, photo

box, and image analysis were based on descriptions by Exposito-Alonso et al. (2018) and were adapted to fit this study design. A detailed description and access to the image analysis script can be found in the Supporting Information (Methods S2).

Growth curve. Overrepresentation of late time points with size data occurred, and therefore, size values that were recorded after the four highest sizes of a plant were removed from the growth curve calculation. All remaining size measures of individual plants were used for fitting seven growth models: linear, exponential, power, two- and three-parametric logistic, Gompertz and von Bertalanffy, using the R package *minpack.lm* (Elzhov et al., 2022). Based on weighted AIC (AIC for each model and plant, and weighted relatively for each plant), the Gompertz model was overall the best but was only in third position for the *Hot&Dry* treatment (Table S3). For this reason, the next best model, the three-parameter logistic was chosen for trait extraction. For eleven plants (0.4%), this model could not be fitted, and asymptotic size was set to the mean of the four highest size values (no data for growth rate and time to half the asymptotic size). Model output for plant growth included the following three parameters: asymptotic size (s_{asym}, in mm^2), maximal growth rate (r_{max}) and time until half the asymptotic size and fastest growth was achieved (x_{mid}, in days).

Allocation traits. At the end of the experiment, all available plant material per pot was split into the following categories and weighted separately: green rosette tissue, dead rosette tissue, roots, and inflorescences. Soil particles were washed away, and saturated weight was measured. After 48 h of drying the material in an oven at 60°C, the dry weight was measured. We then calculated the specific leaf area (*SLA*; s_{asym} [mm^2] per green rosette dry matter [mg]), leaf dry matter content (*LDMC*; green rosette dry matter [mg] per green rosette saturated weight [g]), and root-shoot ratio (RS_{ratio}; dry weight of roots to dry weight of all aboveground biomass). Final sample sizes for all populations, growth traits and allocation traits are listed in Table S4.

2.3. G-matrices and their analysis

G-matrix. G-matrices were calculated with a focus on growth traits. A first reason for focusing on this set of traits was the modularity among growth and allocation traits (see Results), with considerable correlations within the two sets of traits but not between them. A second reason was that allocation estimates for the *Hot&Dry* treatment were few (n = 21-23), as many plants died after accelerated growth in this treatment, which precluded the comparison of G for these traits and treatment. For allocation traits and all traits combined, we ran the same set of analyses on G-matrices as for the growth traits, but by excluding the *Hot&Dry* treatment (results in the Supporting Information).

Around 1,800 growth data points per treatment were available: 120 families x 5 replicates x 3 growth traits. Trait estimates were first corrected for the effects of block, tray within block and position in the multi-pot tray for each treatment separately. The data points were then centred and rescaled across treatments, with a mean of 0 and variance of 1. We calculated G-matrices for each treatment combination using a Bayesian approach with *MCMCglmm* (Hadfield, 2010). The mixed-effects model was:

$$Y_{ijk} \sim \mu + F_{jk} + \varepsilon_{ijk},$$

where Y_{ijk} is an observation for plant i of family j on trait k, the intercept (μ) is a fixed effect, F_{jk} the random effect of family and ε_{ijk} the random residuals. Iterations were set to 200,000, with a burn-in of 5,000 and thinning of 50. Priors for G came from a restricted maximum likelihood model (*lme4*; Bates et al., 2014). The significance of family-level covariance and variance estimates was evaluated by comparing deviance information criterion values (DIC; generalization of the Akaike information criterion) of a) a model with a full G-matrix to b) one with a matrix with family-level variances only, and b) to c) one without variances or covariances on the family level (Paccard et al., 2016; Puentes et al., 2016). For further analyses and presentation, all obtained G-matrices were multiplied by 2 to approximate genetic

variances and covariances given the full-sib design.

Comparison of Gs. G-matrices of the four treatment combinations were compared by estimates of G-matrix geometry (Hansen & Houle, 2008; Kirkpatrick, 2009; Milocco & Salazar-Ciudad, 2022; Paccard et al., 2016). The first was the sum of the genetic variances across the traits, the trace of G (Kirkpatrick, 2009). The second was the effective number of dimensions (n_D), calculated as the sum of all eigenvalues of G divided by the first eigenvalue (eq. [2] in Kirkpatrick, 2009). The third measure was the angle between the dominant eigenvector of G, g_{max}, and the dominant eigenvector of the matrix of latitudinal trait divergence (D) among northern and southern populations, d_{max}. D matrices were established for the four environments in the same way as the G matrices, but with the input data of plant traits of the above-mentioned edge populations and including the random effect of southern position (north/south as 0/1). The fourth was the deviation of the predicted selection response from the endpoint of the selection vector, a measure of adaptive potential. We produced selection vectors using *longevity* (days of survival) as a fitness proxy. As with the three growth traits, *longevity* was first corrected for the effects of block, tray within block and position in the multi-pot tray within treatment, followed by dividing by the mean in that treatment. We used *blme* (Chung et al., 2013) to overcome singularity and the model (in blme format):

$$\frac{longevity}{mean\ longevity} \sim s_{\text{asym}} + r_{\text{max}} + x_{\text{mid}} + (1 \mid j),$$

with family, *j*, being the random factor. The obtained coefficients of the fixed effects of traits are the selection coefficients, which taken together build the selection vector (β) of the specific treatment (Hansen & Houle, 2008). The response to selection (Δz) can now be calculated by multiplying G with the selection vector (β) using the multivariate breeder's equation ($\Delta z = G*\beta$; Lande, 1979). Selection deviation is the distance of the endpoints between the selection vector and the predicted response to selection after one generation. As a fifth measure, we calculated evolvability (evo_{HH}) by the method of Hansen and Houle (2008, eq. [1]), which

incorporates the strength of selection (the length of the selection vector) and its orientation. More precisely, evo_{HH} is the projection of the predicted response to selection on the selection vector. All comparisons involving aspects of G were done based on the posterior distribution of 3,900 G-matrices per treatment, following the approach described in Aguirre et al. (2014). Testing was done based on 95% highest posterior density (HPD) intervals, and when HPD intervals were overlapping, a comparison of the region of practical equivalence (ROPE; Kruschke, 2018) followed. For this, the posterior distributions of the two treatments were divided. If the 95% HPD interval of the distribution of differences did not overlap with ROPE, i.e., a range between 0.9 and 1.1 (± 10%; Henry and Stinchcombe, 2023; Kruschke, 2018), then a difference between treatments was assumed to exist.

Heritability. We estimated broad-sense heritability (H^2) by analysis of variance on mean-centred data across treatments. H^2 was calculated as twice the variance explained by family (V_f) over the phenotypic variance ($V_z = V_f + V_{error}$). In a full sib design, $2V_f$ represents an upper-bound estimate of additive genetic variance (V_g), likely inflated by a fraction of dominance variance and variance due to common-environment/maternal effects that also contribute to V_f (Walsh & Chenoweth, 2017). However, maternal effects were shown to be insignificant beyond very early life stages in *A. lyrata* (Paccard et al., 2013), and empirical (Wolak & Keller, 2014) and theoretical results (Clo & Opedal, 2021) show that dominance variance is generally much lower than additive variance. To compare variance estimates among traits and treatments, we standardized them by the square of the trait mean of the specific environment as proposed by Houle (1992) – now I_g and I_e. Standardized genetic variance, I_g, is another measure of evolvability that, compared to heritability, estimates the response relative to the trait mean before selection (Houle, 1992). The standard error of H^2 was approximated based on sample sizes (Walsh & Chenoweth, 2017). All analysis were done in R v. 4.0.5 (R Core Team, 2021).

RESULTS

The four treatment combinations varied in stressfulness, indicated by the varying mean sizes the plants achieved. Plants had declining asymptotic sizes from *Control* (14.5 ± 0.3 cm^2) to *Hot* (12.4 ± 0.2 cm^2), *Dry* (10.8 ± 0.1 cm^2) and *Hot&Dry* (8.2 ± 0.2 cm^2; Table S5; Fig. S1). Correlation analysis among growth and allocation traits within treatments revealed a modular pattern (Table S6). Growth traits (s_{asym}, r_{max}, x_{mid}) were often highly correlated with each other, and allocation traits (*SLA*, *LDMC*, RS_{ratio}) were often highly correlated, but correlations between the two sets of traits were weak. This, and the low sample sizes for allocation traits in the *Hot&Dry* treatment (Table S4), motivated the focus on growth traits in further analyses.

We found that genetic co-/variances for growth traits were overall significant in all treatments. Models with covariances as compared to without covariances always had significantly lower DIC values, and models with variances only as compared to models without had lower DICs (Table 1). The comparison of the trace and dimensionality of treatment-specific G-matrices revealed little variation among the four environments. Neither the trace of Gs nor their dimensionality significantly differed between any of the four treatments; as 95% HPD intervals were highly overlapping (Fig. 2a, b). Dimensionality varied between averages of 1.3 and 1.6 for the three aspects of the logistic growth trajectory, indicating the presence of considerable correlations. The strongest correlations across treatments were revealed between maximal growth rate and time to the mid-point of growth (Tables S6, S7, Fig. S2). Plants either grew early (low x_{mid}) and had a high growth rate (r_{max}), or they grew late with a slow growth rate. In the *Hot&Dry* treatment, the two traits were associated with trade-offs with maximum size. Early and fast- growing plants reached small final size, while late and slow growing plants reached large asymptotic size.

The next five estimates related the direction of G with vectors of population divergence and selection. Two were angles, with higher angles (up to 180°) indicating stronger constraints.

The angle between g_{max} and d_{max} (dominant eigenvectors of G and the matrix of latitudinal trait divergence, D) was highest in the *Hot* and *Dry* treatments and lowest in the *Hot&Dry* treatment, with differences being significant (Fig. 2c; G-matrices in Table S7; D-matrices in Table S8). The result indicates good alignment between G and latitudinal trait divergence under combined stress. The angle between selection vector and the predicted response to selection based on G required the assessment of selection in each of the experimental environments. We found selection (vector length; $|\beta|$) to be strongest under *Hot&Dry* ($|\beta|$ = 0.136), considerably lower under *Dry* ($|\beta|$ = 0.058) and lowest under *Control* ($|\beta|$ = 0.011) and *Hot* ($|\beta|$ = 0.007; Fig. 3). The angle between the selection vector and the predicted response to selection revealed for the four treatment combinations decreased in the following order: *Dry* (close to 60°), *Hot&Dry*, *Control*, *Hot* (close to 20°) (Figs. 2d, 3). Similarly, the deviation between the endpoints of the selection vector and the predicted response significantly differed between treatments, with the distance decreasing from *Hot&Dry* and *Dry* to *Control* and *Hot* (Figs. 2e, 3). Somewhat in line, the projection of the selection response onto the selection vector (evo_{HH}) was lowest in the *Dry* treatment and significantly higher in the other three treatments (Figs. 2f, S3). This latter estimate indicated strongest constraints under *Dry*, followed by *Hot&Dry*.

Average broad-sense heritability deviated from the trace of G in predicting genetic variation across the four treatments. Heritability tended to be lower – across traits – in the *Control* (mean: 0.359, range: 0.278 - 0.440), the *Hot&Dry* treatment (0.370, 0.289 - 0.451) and the *Hot* treatment (0.477, 0.392 - 0.561), and higher in the *Dry* treatment (0.567, 0.481 - 0.653; Fig. S4). The maximal growth rate and the time to the mid-point of growth had heritabilities that were generally low across the four treatments (mean: 0.431 and 0.292, respectively; mean for asymptotic size: 0.606). Estimates of genetic and environmental variances as well as Houle's *I* varied across traits, with no consistent patterns across the four treatments (no systematic increase or decline with increasing stressfulness; Fig. S4).

G-matrices for allocation traits, as well as growth and allocation traits combined, revealed similar patterns as for growth traits. The three allocation traits had lower trace values, and differences among treatments were not significant (Fig. S5a). Furthermore, the dimensionality of G did not differ among treatments (Fig. S5b). The higher discrepancy between selection vector and selection response was pronounced under *Dry* (Fig. S5c). However, the mean was about four times smaller than for G-matrices with growth traits only. G-matrices including allocation and growth traits did not differ in trace or dimensionality among treatments, but the distance between selection vector and selection response was again pronounced under *Dry* (Fig. S5d-f). Despite the seemingly low correlation between growth and allocation traits, the dimensionality of G when all six traits were included was considerably lower than the sum of n_D of the two separate matrices with three traits.

DISCUSSION

There is no consensus on the causes of species' distribution limits when species have range limits that equal niche limits, as evolution should progress towards expanding the niche and the range if habitat is generally available (Sexton et al., 2009; Willi & Van Buskirk, 2019). Our study focused on the potential contribution of genetic correlations constraining adaptive responses to cope with extreme conditions at range limits. We picked conditions typical for the low-latitude range limit of *A. lyrata*, as numerous studies had shown that warm margins of species' distributions are places where constrained evolution becomes most evident under climate change (Clark et al., 2020; Parmesan, 2006). The population studied was from the southerly-centre of distribution with high genetic variation, which was assumed to make the detection of genetic correlations more likely. Furthermore, the population was reported to harbour genetic variation for traits that also vary along the latitudinal cline both in the eastern and western ancestral cluster of *A. lyrata* (Material and Methods, first paragraph). We found

support that heat stress imposes multivariate selection to which the specific population can respond to by adaptation. However, drought stress or the combination of heat and drought led to strong selection and in a direction away from high multivariate genetic variation, resulting in a high predicted lag of adaptation. We will discuss results in the light of aspects of G, the role of stress in affecting them, and what the results imply for low-latitude populations under climate warming. The focus is on traits of the growth trajectory.

Genetic variation and covariation in growth traits under climate stress

Across treatments, we found significant genetic variation in growth traits (Fig. 2a). Similarly, broad-sense heritabilities were considerable to high (range of means across environments: 0.260 - 0.799), with the lowest for the trait of time to fastest growth. However, the trace of G and average heritabilities did not vary concordantly. While the sum of genetic variances did not differ significantly across treatments (Fig. 2a), average heritability tended to be higher in the dry treatment (Fig. S4). Deviations were the result of environmental variances being relatively reduced under dry conditions. Furthermore, we found genetic covariances to be significant and important. They reduced the number of dimensions or sphericity of G by one half relative to no correlations, and there was little variation in this among treatments (Fig. 2b).

Environmental stress was hypothesized to either increase genetic variances or decrease them (Hoffmann & Merilä, 1999). Our results do not support a systematic increase or decrease of genetic variances or heritabilities under stress. The trace of G for growth and allocation traits did not significantly differ between treatments. Heritabilities across traits tended to be lowest in the benign and the most stressful environment. Furthermore, genetic, and environmental variances did not reveal a linear-like pattern with stressfulness (Fig. S4). Another way of depicting genetic variation for individual traits was suggested for fitness-relevant traits, the variance standardized by the square of the trait mean (Houle, 1992). In previous research, those

estimates were shown to increase consistently with the level of stress, including thermal stress (Willi et al., 2010, 2011). Here, the mean-standardized variances also did not reveal a linear-like pattern with stressfulness (Fig. S4), supporting inconsistent responses of genetic variation to stress.

Environmental stress has also been discussed to affect genetic correlations systematically. Empirical studies covering a wide range of taxa have documented that genetic correlations are ubiquitous, with the effective number of dimensions of G often being considerably lower than the number of traits studied (e.g., Chenoweth & Blows, 2008; Eroukhmanoff & Svensson, 2011; Kirkpatrick & Lofsvold, 1992; McGuigan & Blows, 2007; Mezey & Houle, 2005). In a previous study on *A. lyrata* populations of a latitudinal gradient, the dimensionality of Gs was relatively more reduced than shown here (Paccard et al., 2016), possibly because more traits were studied. Stearns (1992) argued that negative correlations between traits in regard to their fitness-implications, or trade-offs, might be expressed more likely under considerable stress. Our results and those of Paccard et al. (2016), who applied a dry treatment, suggest that genetic correlations are not necessarily altered by stress. We found no significant changes in the dimensionality of G despite dry and hot-dry conditions being most stressful (e.g., based on the effect on plant size).

Instead, our results and those of Paccard et al. (2016) point to increased divergence between the direction of G and the direction of selection under water stress (Fig. 2d, Fig. 3). Similar results were revealed in a meta-analysis by Wood and Brodie (2015). Despite only small differences in genetic correlations among environments, variation in the discrepancy (angle) between the direction of genetic correlations and the direction of selection was found to be considerable. The direction of multivariate genetic variation relative to the direction of selection plays a major role as genetic constrains may seriously limit adaptive evolution only if they are directed against selection (Agrawal & Stinchcombe, 2009; Conner, 2002).

Therefore, despite very similar G-matrices, the orientation of genetic constrains compared to selection as well as the strength of selection might be the most important factors for a species adaptive potential under differing selection regimes (Arnold et al., 2008; Phillips & Arnold, 1999).

Lastly, a reason for some consistency in the magnitude of genetic covariances in growth and allocation traits may be their generally high integration. There was one consistent and considerable genetic correlation among growth traits, namely between the time to the mid-point of growth and the maximal growth rate of the logistic growth model (Table S6, Fig. S2). Plants either grew early and fast, or they grew late and slowly. Furthermore, under combined stress, the two traits of time to the mid-point of growth and the maximal growth rate were tied in trade-offs with asymptotic size. Early-growing plants and plants that grew fast had a smaller final size, while late- and slow-growing plants achieved larger size. These results are in line with the slow-fast continuum suggested by Grime and Hunt (1975) and later extended by Stearns (1992, 1983), that organisms either grow fast, have a short lifecycle and are small, or the opposite. Support for the hypothesis is numerous (e.g., Oliveira et al., 2021; Salguero-Gómez, 2017; Sartori et al., 2019, 2022). Interestingly, a similar trade-off complex among the three growth traits was found in the latitudinal divergence matrices. To variable extents across treatments, time to the mid-point of growth and growth rate were negatively correlated, and, with the exception of one of these traits under heat, early and fast growth implied smaller final size (Table S8). Southern populations had generally smaller sizes within each of the two ancestral clusters, though the association with earlier and faster growth was not consistent (Table S5).

Predicted selection response under climate stress at the low-latitude range edge

Unlike genetic variances and genetic correlations, the predicted ability to adapt varied significantly among treatments, for growth traits, allocation traits and all traits combined. On

the one hand, selection was stronger both under drought and heat with drought as compared to benign or hot conditions. This strongly affected the deviation between ideal and predicted selection response (Fig. 2e; for allocation and all traits see Fig. S5c, f). Under both drought and heat with drought, the deviation was high. This pattern was also depicted by the estimate of evolvability (evo_{HH}), though only the estimate under drought was significantly lower. On the other hand, the genetic correlations were involved in lowering the ability to adapt. Though, and as discussed further up, what changed was that under drought and heat with drought, selection took a direction more antagonistic to the direction of highest multivariate genetic variation; the genetic correlations changed little (Figs. 2d, 3). Results confirm previous results by Lau et al. (2014) on *A. thaliana* that certain stressors and particularly combined stressors impose strong selection, and combined stress reduces the evolutionary potential along a phenotypic selection gradient. Furthermore they are in line with the constraining aspect of genetic correlations as found e.g., in the transplant experiment by Etterson and Shaw (2001). Covering gradients of temperature and water availability, they showed that genetic correlations antagonistic to the direction of selection decreased the evolutionary potential in a plant despite considerable genetic variances and heritabilities in the traits under selection.

If drought and combined heat with drought become more frequent at the low-latitude range limit of *Arabidopsis lyrata*, this will seriously impede population persistence. Niche-modelling indicated that temperature was a main driver of distribution limits in the south and north (Lee-Yaw et al., 2018; Sánchez-Castro et al., 2024). This suggests that the species occurs in areas with marginal temperature conditions at the range limit, which was confirmed in a transplant experiment with sites within and beyond the southern and northern range limits (Sánchez-Castro et al., 2024). With climate warming, drought will become an additional stressor. For the southern and eastern US, climate change has been associated not only with increasing temperature, but also with longer periods of drought (Easterling et al., 2017;

Schepers et al., 2024; Vose et al., 2017). For several accessions of the closely related *A. thaliana*, Vile et al. (2012) found that the fitness proxy of biomass production was mostly higher under heat than drought conditions, suggesting that drought is more of a stressor than heat. A meta-study on a variety of organisms revealed a more even picture, whereby at low latitudes, water availability is of similar importance for survival than temperature (Pearce-Higgins et al., 2015). Given that temperatures are marginal at the southern range limits for *A. lyrata* and drought phases are increasing, our results of low adaptation potential under these conditions suggest that populations at the low-latitude range limit are at risk of extinction.

Conclusions

Our study shows that drought and combined heat and drought – at magnitudes that may occur in nature at the low-latitude range limit of *Arabidopsis lyrata* – impose strong selection on traits related to the growth trajectory. At the same time, multivariate genetic variation for these traits is reduced due to some consistent genetic correlations. Correlations generally follow the continuum between slow and fast growth and become more constraining under drought and combined heat and drought because selection takes a direction more antagonistic to the direction of high multivariate genetic variation. When occurring together, strong selection and such constrained genetic variation led to a relatively low predicted selection response. If the future climate exposes low-latitude populations of *A. lyrata* to drought or heat with drought more frequently, populations may therefore fail to persist due to excessive deaths linked with selection.

Acknowledgements

We thank O. Bachmann, E. Belen, S. Ellenberger, C. Mattson, S. Riedl, F. Schlöth, and X. Quinter for help with raising plants and measuring them. K. Lucek and A. Narasimhan gave comments on an early draft of the manuscript. We were supported by the Swiss National Science Foundation (grant no. 310030_184763 to Y.W.).

Author contributions

JH, JS and YW designed the study. JH and JS performed the experiment. JH analysed and wrote the manuscript, with inputs by YW. JS contributed to manuscript preparation.

Competing interests

The authors have no competing interests to declare that are relevant to the content of this article.

Data availability

Data will be available on DRYAD: https://doi.org/10.5061/dryad.2rbnzs7sw. Image analysis script (Supplementary: Methods S2) is available under https://github.com/HeblackJ/automated_image_analysis.git.

References

Agrawal, A. F., & Stinchcombe, J. R. (2009). How much do genetic covariances alter the rate of adaptation? *Proceedings of the Royal Society B: Biological Sciences*, *276*(1659), 1183–1191. https://doi.org/10.1098/rspb.2008.1671

Arnold, S. J. (1992). Constraints on phenotypic evolution. *The American Naturalist*, *140*, S85–S107. https://doi.org/10.1086/285398

Arnold, S. J., Bürger, R., Hohenlohe, P. A., Ajie, B. C., & Jones, A. G. (2008). Understanding the evolution and stability of the G-matrix. *Evolution*, *62*(10), 2451–2461. https://doi.org/10.1111/j.1558-5646.2008.00472.x

Bates, D., Mächler, M., Bolker, B., & Walker, S. (2014). Fitting linear mixed-effects models using lme4. *arXiv:1406.5823 [Stat]*. http://arxiv.org/abs/1406.5823

Bennett, J. M., Sunday, J., Calosi, P., Villalobos, F., Martínez, B., Molina-Venegas, R., Araújo, M. B., Algar, A. C., Clusella-Trullas, S., Hawkins, B. A., Keith, S. A., Kühn, I., Rahbek, C., Rodríguez, L., Singer, A., Morales-Castilla, I., & Olalla-Tárraga, M. Á. (2021). The evolution of critical thermal limits of life on Earth. *Nature Communications*, *12*(1), 1198. https://doi.org/10.1038/s41467-021-21263-8

Blows, M. W., & Hoffmann, A. A. (2005). A reassessment of genetic limits to evolutionary change. *Ecology*, *86*(6), 1371–1384. https://doi.org/10.1890/04-1209

Chen, I.-C., Hill, J. K., Ohlemüller, R., Roy, D. B., & Thomas, C. D. (2011). Rapid range shifts of species associated with high levels of climate warming. *Science*, *333*(6045), 1024–1026. https://doi.org/10.1126/science.1206432

Chenoweth, S. F., & Blows, Mark. W. (2008). Q_{ST} meets the G matrix: The dimensionality of adaptive divergence in multiple correlated quantitative traits. *Evolution*, *62*(6), 1437–1449. https://doi.org/10.1111/j.1558-5646.2008.00374.x

Chung, Y., Rabe-Hesketh, S., Dorie, V., Gelman, A., & Liu, J. (2013). A nondegenerate penalized likelihood estimator for variance parameters in multilevel models. *Psychometrika*, *78*(4), 685–709. https://doi.org/10.1007/s11336-013-9328-2

Clark, J. S., Poore, A. G. B., Coleman, M. A., & Doblin, M. A. (2020). Local scale thermal environment and limited gene flow indicates vulnerability of warm edge populations in a habitat forming macroalga. *Frontiers in Marine Science*, *7*, 711. https://doi.org/10.3389/fmars.2020.00711

Clo, J., & Opedal, Ø. H. (2021). Genetics of quantitative traits with dominance under stabilizing and directional selection in partially selfing species. *Evolution*, *75*(8), 1920–1935. https://doi.org/10.1111/evo.14304

Conner, J. K. (2002). Genetic mechanisms of floral trait correlations in a natural population. *Nature*, *420*(6914), 407–410. https://doi.org/10.1038/nature01105

Easterling, D. R., Arnold, J. R., Knutson, T., Kunkel, K. E., LeGrande, A. N., Leung, L. R., Vose, R. S., Waliser, D. E., & Wehner, M. F. (2017). *Ch. 7: Precipitation change in the United States. Climate science special report: Fourth national climate assessment, Volume I*. U.S. Global Change Research Program. https://doi.org/10.7930/J0H993CC

Elzhov, T. V., Mullen, K. M., Spiess, A.-N., & Bolker, B. (2022). *minpack.lm: R Interface to the Levenberg-Marquardt nonlinear least-squares algorithm found in MINPACK, Plus support for bounds* (R package version 1.2-2) [Computer software]. https://CRAN.R-project.org/package=minpack.lm

Eroukhmanoff, F., & Svensson, E. I. (2011). Evolution and stability of the G-matrix during the colonization of a novel environment: G-matrix evolution. *Journal of Evolutionary Biology*, *24*(6), 1363–1373. https://doi.org/10.1111/j.1420-9101.2011.02270.x

Etterson, J. R., & Shaw, R. G. (2001). Constraint to adaptive evolution in response to global warming. *Science*, *294*(5540), 151–154. https://doi.org/10.1126/science.1063656

Exposito-Alonso, M., Vasseur, F., Ding, W., Wang, G., Burbano, H. A., & Weigel, D. (2018). Genomic basis and evolutionary potential for extreme drought adaptation in *Arabidopsis thaliana*. *Nature Ecology & Evolution*, *2*(2), 352–358. https://doi.org/10.1038/s41559-017-0423-0

Falconer, D. S., & Mackay, T. (1996). *Introduction to quantitative genetics* (4. ed., [16. print.]). Pearson, Prentice Hall.

Fry, J. D. (2003). Detecting ecological trade-offs using selection experiments. *Ecology*, *84*(7), 1672–1678. https://doi.org/10.1890/0012-9658(2003)084[1672:DETUSE]2.0.CO;2

Grime, J. P., & Hunt, R. (1975). Relative growth-rate: Its range and adaptive significance in a local flora. *The Journal of Ecology*, *63*(2), 393. https://doi.org/10.2307/2258728

Hadfield, J. D. (2010). MCMC methods for multi-response generalized linear mixed models: The MCMCglmm R package. *Journal of Statistical Software*, *33*(2), 22. https://doi.org/10.18637/jss.v033.i02

Hansen, T. F., & Houle, D. (2008). Measuring and comparing evolvability and constraint in multivariate characters. *Journal of Evolutionary Biology*, *21*(5), 1201–1219. https://doi.org/10.1111/j.1420-9101.2008.01573.x

Hansen, T. F., Solvin, T. M., & Pavlicev, M. (2019). Predicting evolutionary potential: A numerical test of evolvability measures. *Evolution*, *73*(4), 689–703. https://doi.org/10.1111/evo.13705

Hargreaves, A. L., Samis, K. E., & Eckert, C. G. (2014). Are species' range limits simply niche limits writ large? A review of transplant experiments beyond the range. *The American Naturalist*, *183*(2), 157–173. https://doi.org/10.1086/674525

Hoffmann, A. A., & Blows, M. W. (1994). Species borders: Ecological and evolutionary perspectives. *Trends in Ecology & Evolution*, *9*(6), 223–227. https://doi.org/10.1016/0169-5347(94)90248-8

Hoffmann, A. A., & Merilä, J. (1999). Heritable variation and evolution under favourable and unfavourable conditions. *Trends in Ecology & Evolution*, *14*(3), 96–101. https://doi.org/10.1016/S0169-5347(99)01595-5

Holt, R. D. (2003). On the evolutionary ecology of species' ranges. *Evolutionary Ecology Research*, *5*, 159–178.

Houle, D. (1992). Comparing evolvability and variability of quantitative traits. *Genetics*, *130*(1), 195–204. https://doi.org/10.1093/genetics/130.1.195

Irvine, J., Perks, M. P., Magnani, F., & Grace, J. (1998). The response of *Pinus sylvestris* to drought: Stomatal control of transpiration and hydraulic conductance. *Tree Physiology*, *18*(6), 393–402. https://doi.org/10.1093/treephys/18.6.393

Kirkpatrick, M. (2009). Patterns of quantitative genetic variation in multiple dimensions. *Genetica*, *136*(2), 271–284. https://doi.org/10.1007/s10709-008-9302-6

Kirkpatrick, M., & Barton, N. H. (1997). Evolution of a species' range. *The American Naturalist*, *150*(1), 1–23. https://doi.org/10.1086/286054

Kirkpatrick, M., & Lofsvold, D. (1992). Measuring selection and constraint in the evolution of growth. *Evolution*, *46*(4), 954. https://doi.org/10.2307/2409749

Kooyers, N. J. (2015). The evolution of drought escape and avoidance in natural herbaceous populations. *Plant Science*, *234*, 155–162. https://doi.org/10.1016/j.plantsci.2015.02.012

Kruschke, J. K. (2018). Rejecting or accepting parameter values in Bayesian estimation. *Advances in Methods and Practices in Psychological Science*, *1*(2), 270–280. https://doi.org/10.1177/2515245918771304

Lande, R. (1979). *Quantitative Genetic Analysis of Multivariate Evolution, Applied to Brain: Body Size Allometry*. 16.

Lau, J. A., Shaw, R. G., Reich, P. B., & Tiffin, P. (2014). Indirect effects drive evolutionary responses to global change. *New Phytologist*, *201*(1), 335–343. https://doi.org/10.1111/nph.12490

Lee-Yaw, J. A., Fracassetti, M., & Willi, Y. (2018). Environmental marginality and geographic range limits: A case study with *Arabidopsis lyrata* ssp. *lyrata*. *Ecography*, *41*(4), 622–634. https://doi.org/10.1111/ecog.02869

Lee-Yaw, J. A., Kharouba, H. M., Bontrager, M., Mahony, C., Csergő, A. M., Noreen, A. M. E., Li, Q., Schuster, R., & Angert, A. L. (2016). A synthesis of transplant experiments and ecological niche models suggests that range limits are often niche limits. *Ecology Letters*, *19*(6), 710–722. https://doi.org/10.1111/ele.12604

Lenoir, J., Bertrand, R., Comte, L., Bourgeaud, L., Hattab, T., Murienne, J., & Grenouillet, G. (2020). Species better track climate warming in the oceans than on land. *Nature Ecology & Evolution*, *4*(8), 1044–1059. https://doi.org/10.1038/s41559-020-1198-2

Liu, H., Ye, Q., & Wiens, J. J. (2020). Climatic-niche evolution follows similar rules in plants and animals. *Nature Ecology & Evolution*, *4*(5), 753–763. https://doi.org/10.1038/s41559-020-1158-x

McGuigan, K., & Blows, M. W. (2007). The phenotypic and genetic covariance structure of drosophilid wings. *Evolution*, *61*(4), 902–911. https://doi.org/10.1111/j.1558-5646.2007.00078.x

Mezey, J. G., & Houle, D. (2005). The dimensionality of genetic variation for wing shape in *Drosophila melanogaster*. *Evolution*, *59*(5), 1027–1038. https://doi.org/10.1111/j.0014-3820.2005.tb01041.x

Milocco, L., & Salazar-Ciudad, I. (2022). Evolution of the *G* matrix under nonlinear genotype-phenotype maps. *The American Naturalist*, *199*(3), 420–435. https://doi.org/10.1086/717814

Oliveira, R. S., Eller, C. B., Barros, F. D. V., Hirota, M., Brum, M., & Bittencourt, P. (2021). Linking plant hydraulics and the fast–slow continuum to understand resilience to drought in tropical ecosystems. *New Phytologist*, *230*(3), 904–923. https://doi.org/10.1111/nph.17266

Paccard, A., Fruleux, A., & Willi, Y. (2014). Latitudinal trait variation and responses to drought in *Arabidopsis lyrata*. *Oecologia*, *175*(2), 577–587. https://doi.org/10.1007/s00442-014-2932-8

Paccard, A., Van Buskirk, J., & Willi, Y. (2016). Quantitative genetic architecture at latitudinal range boundaries: Reduced variation but higher trait independence. *The American Naturalist*, *187*(5), 667–677. https://doi.org/10.1086/685643

Paccard, A., Vance, M., & Willi, Y. (2013). *Weak impact of finescale landscape heterogeneity on evolutionary potential in Arabidopsis lyrata*. 10.

Paquette, A., & Hargreaves, A. L. (2021). Biotic interactions are more often important at species' warm versus cool range edges. *Ecology Letters*, *24*(11), 2427–2438. https://doi.org/10.1111/ele.13864

Parmesan, C. (2006). Ecological and evolutionary responses to recent climate change. *Annual Review of Ecology, Evolution, and Systematics*, *37*(1), 637–669. https://doi.org/10.1146/annurev.ecolsys.37.091305.110100

Patsiou, T., Walden, N., & Willi, Y. (2021). What drives species' distributions along elevational gradients? Macroecological and -evolutionary insights from Brassicaceae of the central Alps. *Global Ecology and Biogeography*, *30*(5), 1030–1042. https://doi.org/10.1111/geb.13280

Pearce-Higgins, J. W., Ockendon, N., Baker, D. J., Carr, J., White, E. C., Almond, R. E. A., Amano, T., Bertram, E., Bradbury, R. B., Bradley, C., Butchart, S. H. M., Doswald, N., Foden, W., Gill, D. J. C., Green, R. E., Sutherland, W. J., & Tanner, E. V. J. (2015). Geographical variation in species' population responses to changes in temperature and precipitation. *Proceedings of the Royal Society B: Biological Sciences*, *282*(1818), 20151561. https://doi.org/10.1098/rspb.2015.1561

Phillips, P. C., & Arnold, S. J. (1999). Hierarchical comparison of genetic variance-covariance matrices. I. using the Flury hierarchy. *Evolution*, *53*(5), 1506–1515. https://doi.org/10.1111/j.1558-5646.1999.tb05414.x

Polechová, J. (2018). Is the sky the limit? On the expansion threshold of a species' range. *PloS Biology*, *16*(6). https://doi.org/10.1371/journal.pbio.2005372

Polechová, J., & Barton, N. H. (2015). Limits to adaptation along environmental gradients. *Proceedings of the National Academy of Sciences*, *112*(20), 6401–6406. https://doi.org/10.1073/pnas.1421515112

Puentes, A., Granath, G., & Ågren, J. (2016). Similarity in G matrix structure among natural populations of *Arabidopsis lyrata*: G matrix structure in populations of *A. lyrata*. *Evolution*, *70*(10), 2370–2386. https://doi.org/10.1111/evo.13034

Puijalon, S., Bouma, T. J., Douady, C. J., Van Groenendael, J., Anten, N. P. R., Martel, E., & Bornette, G. (2011). Plant resistance to mechanical stress: Evidence of an avoidance–tolerance trade-off. *New Phytologist*, *191*(4), 1141–1149. https://doi.org/10.1111/j.1469-8137.2011.03763.x

Roff, D. A., & Fairbairn, D. J. (2012). The evolution of trade-offs under directional and correlational selection: Selection on a trade-off. *Evolution*, *66*(8), 2461–2474. https://doi.org/10.1111/j.1558-5646.2012.01634.x

Roff, D. A., Mostowy, S., & Fairbairn, D. J. (2002). The Evolution of trade-offs: Testing predictions on response to selection and environmental variation. *Evolution*, *56*(1), 84–95.

Rumpf, S. B., Hülber, K., Klonner, G., Moser, D., Schütz, M., Wessely, J., Willner, W., Zimmermann, N. E., & Dullinger, S. (2018). Range dynamics of mountain plants decrease with elevation. *Proceedings of the National Academy of Sciences*, *115*(8), 1848–1853. https://doi.org/10.1073/pnas.1713936115

Salguero-Gómez, R. (2017). Applications of the fast–slow continuum and reproductive strategy framework of plant life histories. *New Phytologist*, *213*(4), 1618–1624. https://doi.org/10.1111/nph.14289

Sánchez-Castro, D., Armbruster, G., & Willi, Y. (2022). Reduced pollinator service in small populations of *Arabidopsis lyrata* at its southern range limit. *Oecologia*, *200*(1–2), 107–117. https://doi.org/10.1007/s00442-022-05237-1

Sánchez-Castro, D., Perrier, A., Willi, Y., & Hampe, A. (2022). Reduced climate adaptation at range edges in North American *Arabidopsis lyrata*. *Global Ecology and Biogeography*, *31*(6), 1066–1077. https://doi.org/10.1111/geb.13483

Sartori, K., Vasseur, F., Violle, C., Baron, E., Gerard, M., Rowe, N., Ayala-Garay, O., Christophe, A., Jalón, L. G. D., Masclef, D., Harscouet, E., Granado, M. D. R., Chassagneux, A., Kazakou, E., & Vile, D. (2019). Leaf economics and slow-fast adaptation across the geographic range of *Arabidopsis thaliana*. *Scientific Reports*, *9*(1), 10758. https://doi.org/10.1038/s41598-019-46878-2

Sartori, K., Violle, C., Vile, D., Vasseur, F., De Villemereuil, P., Bresson, J., Gillespie, L., Fletcher, L. R., Sack, L., & Kazakou, E. (2022). Do leaf nitrogen resorption dynamics align with the slow-fast continuum? A test at the intraspecific level. *Functional Ecology*, *36*(5), 1315–1328. https://doi.org/10.1111/1365-2435.14029

Schluter, D. (1996). Adaptive radiation along genetic lines of least resistance. *Evolution*, *50*(5), 1766–1774. https://doi.org/10.1111/j.1558-5646.1996.tb03563.x

Sexton, J. P., McIntyre, P. J., Angert, A. L., & Rice, K. J. (2009). Evolution and ecology of species range limits. *Annual Review of Ecology, Evolution, and Systematics*, *40*(1), 415–436. https://doi.org/10.1146/annurev.ecolsys.110308.120317

Sheth, S. N., & Angert, A. L. (2016). Artificial selection reveals high genetic variation in phenology at the trailing edge of a species range. *The American Naturalist*, *187*(2), 182–193. https://doi.org/10.1086/684440

Stearns, S. C. (1983). The influence of size and phylogeny on patterns of covariation among life-history traits in the mammals. *Oikos*, *41*(2), 173. https://doi.org/10.2307/3544261

Stearns, S. C. (1992). *The evolution of life histories* (1st ed.). Oxford University Press.

Upadhyay, P. (2019). Climate change and adaptation strategies: A study of agriculture and livelihood adaptation by farmers in Bardiya District, Nepal. *Advances in Agriculture and Environmental Science: Open Access (AAEOA)*, *2*(1), 47–52. https://doi.org/10.30881/aaeoa.00022

Vile, D., Pervent, M., Belluau, M., Vasseur, F., Bresson, J., Muller, B., Granier, C., & Simonneau, T. (2012). Arabidopsis growth under prolonged high temperature and water deficit: Independent or interactive effects?: Plant responses to high temperature and water deficit. *Plant, Cell & Environment*, *35*(4), 702–718. https://doi.org/10.1111/j.1365-3040.2011.02445.x

Vose, R. S., Easterling, D. R., Kunkel, K. E., LeGrande, A. N., & Wehner, M. F. (2017). *Ch. 6: Temperature changes in the United States. Climate science special report: Fourth national climate assessment, Volume I*. U.S. Global Change Research Program. https://doi.org/10.7930/J0N29V45

Walsh, B., & Chenoweth, S. F. (2017). *Summer institute in statistical genetics—Module1: Principles of quantitative genetics*. https://cnsgenomics.com/data/teaching/SISG/module_1/Module01-Lecture-Notes.pdf

Willi, Y. (2013). The Battle of the sexes over seed size: Support for both kinship genomic imprinting and interlocus contest evolution. *The American Naturalist*, *181*(6), 787–798. https://doi.org/10.1086/670196

Willi, Y., Follador, R., Keller, N., Schwander, Y., & McDonald, B. A. (2010). Heritability under benign and stressful conditions in the plant pathogenic fungus *Mycosphaerella graminicola*. *Evolutionary Ecology Research*, *12*, 761–768.

Willi, Y., Fracassetti, M., Zoller, S., & Van Buskirk, J. (2018). Accumulation of mutational load at the edges of a species range. *Molecular Biology and Evolution*, *35*(4), 781–791. https://doi.org/10.1093/molbev/msy003

Willi, Y., Frank, A., Heinzelmann, R., Kälin, A., Spalinger, L., & Ceresini, P. C. (2011). The adaptive potential of a plant pathogenic fungus, *Rhizoctonia solani* AG-3, under heat and fungicide stress. *Genetica*, *139*(7), 903–908. https://doi.org/10.1007/s10709-011-9594-9

Willi, Y., & Van Buskirk, J. (2019). A practical guide to the study of distribution limits. *The American Naturalist*, *193*(6), 773–785. https://doi.org/10.1086/703172

Wolak, M. E., & Keller, L. F. (2014). Dominance genetic variance and inbreeding in natural populations. In *Quantitative genetics in the wild*. Oxford University Press.

Wood, C. W., & Brodie, E. D. (2015). Environmental effects on the structure of the G-matrix: Environmental effects on genetic correlations. *Evolution*, *69*(11), 2927–2940. https://doi.org/10.1111/evo.12795

Wos, G., & Willi, Y. (2015). Temperature-stress resistance and tolerance along a latitudinal cline in North American *Arabidopsis lyrata*. *PLOS ONE*, *10*(6), e0131808. https://doi.org/10.1371/journal.pone.0131808

Wos, G., & Willi, Y. (2018). Genetic differentiation in life history traits and thermal stress performance across a heterogeneous dune landscape in *Arabidopsis lyrata*. *Annals of Botany*, *122*(3), 473–484. https://doi.org/10.1093/aob/mcy090

Figure 1

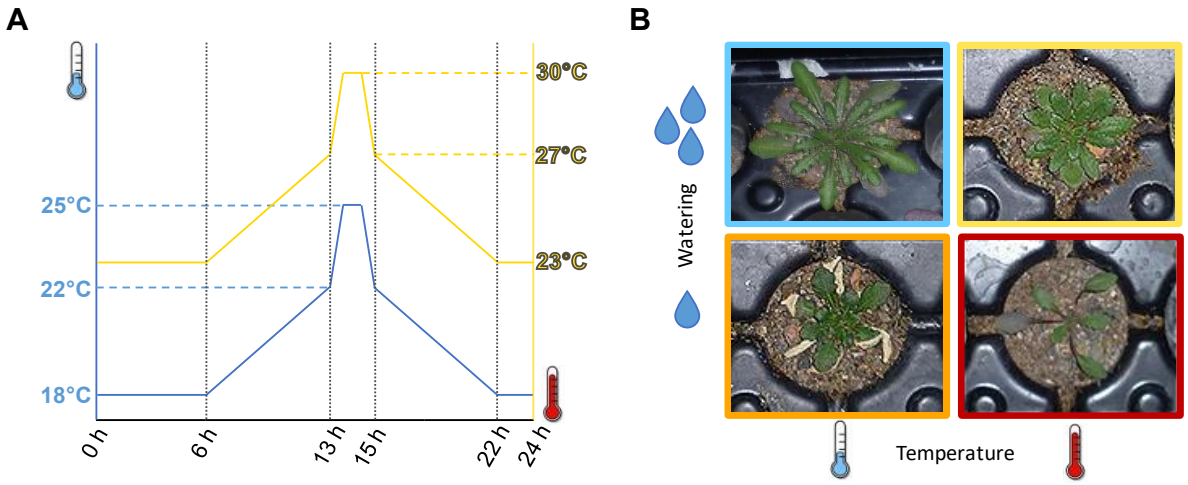

Figure 1: Climate stress experiment with *Arabidopsis lyrata* in the glasshouse. **a)** The two temperature treatments were: benign (left axis) and high temperature (right axis). Daily temperature profiles included an amplitude of 7 K per day. **b)** Differences in performance among plants of the same seed family in the respective treatment combinations (from top left to bottom right) - *Control* (benign temperature and watering), *Hot* (high temperature), *Dry* (low watering) & *Hot&Dry* (high temperature and low watering). Colours indicate the respective treatments.

Figure 2

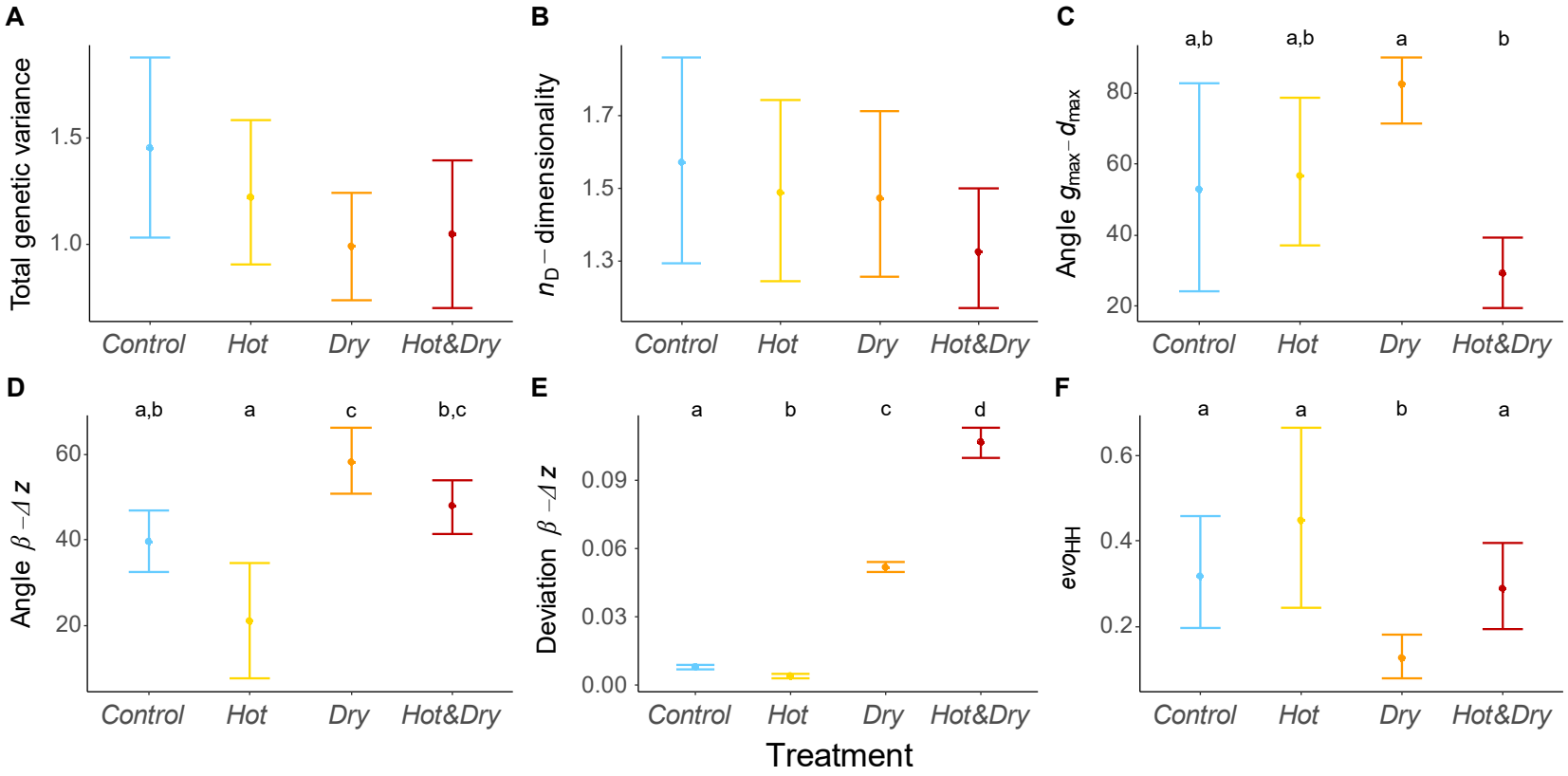

Figure 2: Comparison of geometric aspects of genetic variance-covariance (G-) matrices estimated under benign and stress conditions. **a)** Total genetic variance, trace of G - v_t. **b)** Number of dimensions - n_D. **c)** Change in the angle between g_{max}, the dominant eigenvector of G, and d_{max}, the dominant eigenvector of the matrix of latitudinal population divergence. **d)** Angle and **e)** deviation distance (*Dev*) between selection vector (β) and selection response (Δz). **f)** Hansen and Houle's measure of evolvability (evo_{HH}). The colours represent the respective treatments: *Control*, *Dry*, *Hot*, *Hot&Dry*. Dots indicate the predicted model estimates and bars the 95% HPD intervals. Letters above the bars indicate differences between treatments based on ROPE (Region of Practical Equivalence).

Figure 3

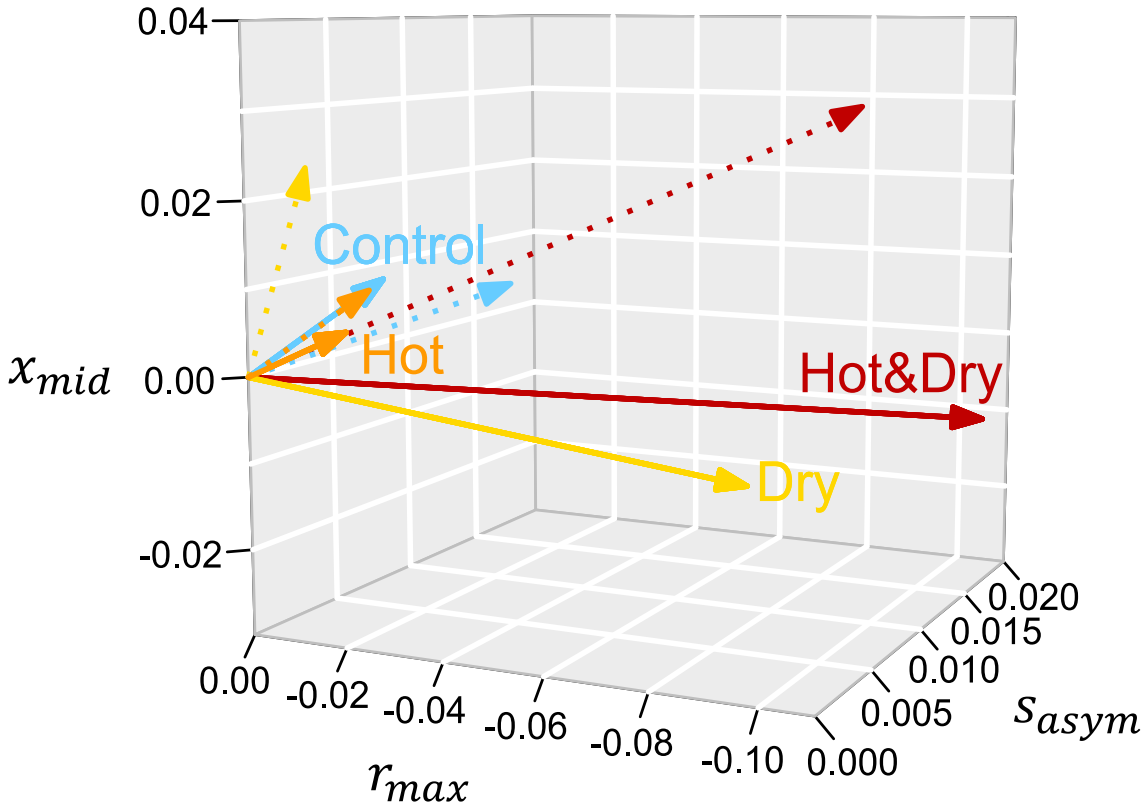

Figure 3: Direction and strength of viability selection (β, solid lines) and predicted selection response after three generations (Δz, dotted lines) for each treatment along the three aspects of logistic growth (size – s_{asym}, growth rate – r_{max}, time to half size – x_{mid}).

Table 1

Table 1: DIC values for G-matrices that include both co- and variances on the family level (*DIC* (co)variances), variances only (*DIC* variances) or no family effects (*DIC* null) for each treatment. Models with smaller DIC are better supported – those with variances and covariances on the family level as compared to variances only, and those with variances as compared to none.

	DIC (co)variances	*DIC* variances	*DIC* null
Control	4391.379	4440.294	4556.135
Dry	2951.876	2982.765	3410.213
Hot	3722.478	3785.262	4039.161
Hot&Dry	3846.137	3875.810	4001.464

Chapter 3: **Associated genes of fitness traits under different environmental conditions in *Arabidopsis lyrata***

Jessica Heblack, Judith R. Schepers and Yvonne Willi

Department of Environmental Sciences, University of Basel, 4056 Basel, Switzerland

Running title: Associated genes of differing environments

No. figures: 6

No. tables: 2

Supplementary: 3 figures, 2 tables

Draft for Environmental and Experimental Botany

Abstract

Facing the challenges posed by accelerating climate change, organisms at the warm edges of species' distributions experience stressful conditions, leading to reductions and extinctions. If sufficient genetic diversity is available species tend to adapt to these pressuring condition. The study aims to uncover the traits and genes under selection at these warm edges, where temperature and precipitation directly affect organism performance. The evolutionary potential of species to changing environmental conditions is explored through a genome-wide association study (GWAS). The research employs a 2x2 factorial stress experiment in a controlled greenhouse and a natural-selection experiment along the southern range edge. Family effects are examined, revealing significant genetic differences in performance traits within the greenhouse but limited family effects in the natural experiment. The study identifies outlier genes associated with various traits, indicating the genetic complexity of stress responses. However, the low overlap between treatments raises questions about the universality of genetic adaptations. The varying responses along different transects highlight the intricate interplay of genes and environmental factors. The study contributes insights into climate adaptation, emphasizing the need for comprehensive approaches in understanding genetic responses to environmental stress.

Keywords: environmental stress, genetic diversity, fitness traits, genome-wide association study (GWAS), natural selection, climate change adaptation

Introduction

Ecosystems as well as a considerable fraction of the species living in them face growing challenges due to accelerating climate change (Elsen et al., 2022; Parmesan, 2006). Organism at the warm edges of species' distributions are particularly facing increasing stressful conditions that are often outside of their niches with temperatures that are either too high, precipitation that is too little or both together (Dore, 2005). Indeed, population size reductions and extinctions at the warmer ends of species' distributions were shown to be frequent, affecting e.g., 60% of plant species in the Alps (Rumpf et al., 2019), or even stronger in marine ecosystems (Fredston-Hermann et al., 2020; Pinsky et al., 2019). Extinction can be counteracted by adaptation, allowing to cope with the novel conditions. Although, adaptive evolutionary responses require the necessary genetic variation, plastic responses may initially also mediate adaptation (Matesanz et al., 2010; Oostra et al., 2018). However, plastic responses are apparently not enough given the withdrawal of species from the warm edges (Oostra et al., 2018). So far, little is known about the traits and genes under selection at warm edges of distribution, in particular when temperature or a shortage of precipitation affects the performance of organisms directly.

The evolutionary potential of species in response to changing environmental conditions is a dynamic and complex process. Adaptation is mainly determined by selection and genetic diversity segregating in a population, but is also affected by de-novo mutations (Fournier-Level et al., 2011; Horton et al., 2012). A further aspect is the architecture of traits under selection. For instance, lifetime performance is often seen as a trait with a complex, polygenic genetic basis, where many traits contribute to overall lifetime performance and variation in their genetic underpinning correlated with each other (Michaels & Amasino, 1999). Genetic variation with a predictable response to selection at a particular locus may therefore be very low. In line, there is good support that traits such as lifetime performance have very limited

genetic variation (Mackay et al., 2012). However, under stressful environmental conditions, a small fraction of individuals may have the genetic disposition to do well, leading to some heritability on which selection can act (Jones, 1987). Recent studies elucidate the importance of understanding the genetic underpinnings of adaptive evolution and have revealed specific genetic regions associated with adaptation in various taxa. In stickleback fish, genomic regions controlling armor plate traits were identified as crucial for adapting to predation pressures in different lake environments (Colosimo et al., 2005). Similarly, in the peppered moth (*Biston betularia*), specific genomic regions were linked to color polymorphism, allowing adaptation to changing industrial landscapes (Van'T Hof et al., 2011). In *A. thaliana* differences in the expression level of flowering locus C (FLC) could be related to adaptations to specific climates and habitats (Brachi et al., 2010; Wilczek et al., 2009).

One commonly used approach in revealing the genetic underpinning of environmental adaptation are genome-wide association studies (GWAS), to find genomic regions involved in adaptation to the respective environmental conditions (De Villemereuil et al., 2016; Sork, 2017). In the common bean, GWAS revealed specific genomic regions linked to heat tolerance, shedding light on the genetic basis of adaptation to rising temperatures (López-Hernández & Cortés, 2019). Similarly, in *A. thaliana* genes related to abscisic acid (ABA) signaling could be detected via GWAS analysis in response to drought adaptation (Atwell et al., 2010). GWAS results can further be used in niche modelling studies to better predict the influence of changing environmental conditions in the future and the respective adaptive potential of the species (Bay & Palumbi, 2014; Capblancq et al., 2020). Additionally, results can further help to maintain lines of best climate adaptability that can be used in agriculture or for assisted gene flow between populations under threat (e.g., Aitken & Whitlock, 2013; Yuan et al., 2019). However, quantifying selection in the wild is much more complex and GWAS results from wild type individuals might be ideally compared to results found within greenhouse experimental

conditions (Selby & Willis, 2018; Wang et al., 2018).

Here, we study the genetic backbone of the performance of *Arabidopsis lyrata* at the southern range edge. We want to investigate the traits and genes involved in adapting to environmental conditions at the southern species distribution with a focus on the predictability of selection. A previous greenhouse stress experiment with 120 *Arabidopsis lyrata* families revealed that fitness related traits and growth traits show strong differences in the performance under drought and heat stress (Schepers et al., 2024; Heblack et al., in review). In a 2x2 factorial design trade-offs between growth traits related to the slow-fast continuum of plants were found to strongly reduce the evolvability of the species under drought as well as combined heat and drought conditions. Taking advantage of this greenhouse dataset, we compare genes and gene ontology (GO) terms of fitness related traits, on a family level, of different environments. Secondly, we performed a common garden experiment at two transects along the southern range edge of the species in the USA and assessed different performance traits. Like in the greenhouse experiment, we investigated genes and GO terms of different range edge positions and tested for parallelism by comparing the two independent transects. Our study includes fitness traits known to be involved in the adaptation to climate differences such as longevity, biomass, growth measures, and seedling establishment (Leinonen et al., 2009), shedding light on both short-term stress responses and long-term adaptive strategies. By including families from different ecotypes within one highly diverse population, which captured the latitudinal clinal variation observed in the species distribution (Paccard et al., 2014; Wos & Willi, 2015), we increase the possibility to detect different genomic regions of climate adaptation. We seek to identify the traits and genomic regions crucial for climate adaptation in *Arabidopsis lyrata*, shedding light on the intricate interplay between genetics and environmental stress responses. Additionally, we focus on assessing the predictability of selection based on parallelism observed in the field experiments.

Methods

Seed propagation and crossing

Seeds of individual plants were collected at Saugatuck Dunes States Park, MI, USA, in 2007, 2009, 2010, 2013, and 2014, and stored individually in paper bags in the dark at 4°C. In winter 2019/20 one plant of each of 617 field-collected seed families was raised in the greenhouse and a new generation of seeds propagated by mostly reciprocal cross-pollination in unique pairs. Hand-pollination was performed to produce at least six fruits per plant pair. This resulted in 271 parental families with at least ~60 seeds. Seeds were stored in individual paper bags at 4°C in the dark and with silica beads to reduce humidity. For a detailed summary of the growing conditions and crossing design see (Heblack et al. submitted). These seeds were used in the greenhouse stress experiment as well as in the selection experiment at the southern range edge of *A. lyrata* in the USA.

DNA extraction and SNP calling

The parental plants were genotyped to later perform a genome-wide association study (GWAS). During growth, two leaves per plant were collected in individual Eppendorf tubes for DNA extraction and stored at -20°C until further processing. DNA was extracted using a DNeasy Plant Mini Kit (Qiagen, Hilden, Germany) and sequenced on a NovaSeq 6000 (Illumina, San Diego, USA). Single-nucleotide polymorphisms (SNPs) were obtained by filtering along these main settings: allowing a minimum read depth per individual of four, a minor allele frequency of 5% (MAF), keeping only biallelic sites, and removing indels. The full pipeline is described in Heblack et al. (submitted). After filtering 747’538 SNPs were retained.

Stress experiment in greenhouse

A 2x2 factorial stress experiment was performed in 2020/21 in the greenhouse of the Botanical Institute in Basel, Switzerland. The two axes of manipulation were temperature and watering. For temperature, we used averages experienced by plants at the southern range edge of the North American *Arabidopsis lyrata* in spring or summer. The low-temperature regime was - night: 18°C; day: 22°C; 1-hour heat peak at noon: 25°C, the high-temperature regime was - night: 23°C; day: 27°C; peak: 30°. For precipitation, we mirrored mean precipitation in late spring or early summer (100 mm per month) or low watering imitating precipitation during the driest month (65 mm per month). Due to increasing mortality after two weeks, watering amounts had to be increased by ~20%, resulting in 120 mm and 72 mm respectively. Watering was applied every second day to each pot, meaning 10 ml or 6 ml of water. More details on the experiment can be found in (Heblack et al., in review; Schepers et al., 2024).

In each of the four treatment combinations, called *control*, *dry*, *hot*, and *hot&dry*, 120 randomly chosen families were sown, with five replicate pots/plants per family (120 families x 5 replicates x 4 treatments = 2'400 plants). Plants were exposed to treatments when ~80% of the plants had reached the 4-leave-stage. The experiment was spread over four greenhouse chambers, two with the control-temperature regime and two with the higher temperatures. Across the pairs of greenhouses, five spatial blocks were set up, either two or three per greenhouse. The spatial blocks contained plants of the two watering regimes, sub-blocked in small unites of equally watered pots (assembled in 28 multipot trays). To reduce spatial effects, blocks and trays within blocks were randomized twice a week within and between the climate chambers with the respective same treatment. Fertilizer was applied every fourth weeks and later some insecticide to reduce a thrips infestation. The experiment was terminated after 5 months for the high temperature regime and after 6 months for the benign temperatures.

For each plant, the following performance traits were assessed: germination (checked daily), flowering (checked every second day), and mortality (checked twice a week). During

peak growth, between germination and bolting at the latest, plants were photographed twice a week to measure growth. Images were automatically analyzed by a custom Python image analysis script described in Heblack et al. (in review). Obtained size measures were then fitted to seven growth models and the best model, based on weighted AIC over all treatments, was chosen: the three-parameter logistic growth model. Using this model, the asymptotic size (s_{asym} [mm^2]), time till half size (x_{mid} [d]) and maximal growth rate (r_{max}) for each plant was calculated.

Stress experiment at the southern range edge

A natural-selection experiment along the southern range edge of *A. lyrata* was conducted from autumn 2021 to spring 2023. The experiment included six sites split over two transects crossing the species range, one in Virginia (northern) and one in North Carolina (southern). Sites along the transects were within the range, at the range edge and outside the range edge (Figure 1, Table S1). Apart from their position, they were selected based on average suitability as suggested by ecological niche modelling done for the species (Lee-Yaw et al., 2018). The northern transect covered an aerial distance of ~320 km, the southern one of ~360 km arial distance.

At each location, the experimental sites were open, sunny, and not fertilized patches of 5 x 6 m. All vegetation and the topsoil layer within a patch were removed and eight blocks of 2.7 x 0.6 m were excavated. Walkways and edges of blocks were covered by weed barriers, to prevent competition with local plants. Each site consists of eight blocks fitting nine 38-multipot-trays. Depending on animal pressure of surrounding landscape sites were either fenced by chicken wire (50 cm height) or a mesh fence (2m height). Trays as well as blocks were filled at all sites with the same well-watered 2:1 peat-sand-mixture to correct for effects by differing underground soil. All sites were prepared first before sowing of the seeds was done

within 14 days for all sites. 266 seed families with 8 replicates per site were sown in October 2021 (12’768 seeds in total). Sowing was done in two sowing schemes per site so that half of the replicates per family were sown in the outer areas and the other half in the inner areas of a tray, reducing pot-position effects. For the first month, seeds were sprayed from above once per day and additionally covered by plastic tunnels for two weeks to reduce evaporation. From week two to four plants were covered by mesh tunnels to prevent predation and night frosts. After one month watering stopped and additional covering was removed, to expose plants to natural conditions until their harvest in April 2023.

The following performance traits were assessed: Germination was checked daily for the first month and then, together with survival, weekly. When the first snowfall occurred, plants were visited only every second week until spring. Analysis focused on the trait of seed establishment, which depicted whether a seed sown in autumn led to an alive plant until flowering. As this fraction was relatively low in some gardens, we did not consider any later performance estimate.

Statistical analysis

Phenotypic variables of the two stress experiments were first checked for normal distribution and transformed if necessary and corrected for possible pot, tray, or block influences. Fitness traits of the stress experiment were longevity and dry weight of the inflorescence stem (biomass). Biomass values for *control* had to be square root-transformed and $\log_{10}$-transformed for *dry*. Biomass data for *hot* and *hot&dry* had too few entries for a family-effect analysis. Biomass data of the USA experiment, dry weight of the inflorescence stem, had to be log10-transformed as well as longevity for the sites north and south edge and north inside. Previous greenhouse results stress experimental trade-offs between the growth traits maximal growth rate and time till half growth for the treatments *control*, *dry*, and *hot*. For the *hot&dry* treatment

a trade-off between all three growth traits could be detected (Heblack et al., in review). Therefore, the PC1 scores of the mentioned trade-offs were also included as an additional trait. With linear models traits were checked for plant family effects (*lmer*; Bates et al., 2014) and performance traits with sufficient family effect were used in GWAS.

GWAS was performed on the family frequencies of reference alleles, with the values of 0, 0.25, 0.5, 0.75 and 1. The dependent variable was the family mean of performance traits. Outlier SNPs were determined by two approaches: Hidden-Markov-Model and simple p-value threshold. The Hidden-Markov-Model was run with the *HiddenMarkov* (Harte, 2021) package and a state change likelihood of 0.00001 and 0.99999 respectively. For the simple p-value threshold differing cutoff values of p were chosen: 0.001, 0.0005, and 0.0001. On average 939 outlier SNPs per trait could be found with the HMM method and 777 outlier SNPs with a $p < 0.001$ threshold (Table S2). The $-\log_{10}(p)$ threshold for HMM was on average at 2.56 which corresponds to a $p < 0.003$. The HMM approach therefore being a bit more conservative.

In the next step, the *A. lyrata* v2 reference genome (Hu et al., 2011) was used to identify the genes underlying putative outlier SNP as well as their outlier SNP density. For pre-filtering genes were allowed to have more than one or more than two outlier SNPs. Outlier genes were then defined as having > 2 HMM outlier SNPs or a p-value threshold of $p < 0.001$ with > 1 outlier SNP per gene. Detected outlier genes of both methods were then merged and compared between treatments and sites.

Additionally, to gain insights into the functionality of found genes, a GO enrichment analysis was conducted using the R package *Snp2go* (Szkiba et al., 2014) implementing a False Discovery Rate (FDR) approach. FDR uses the SNP outlier and non-outlier set to test for clustering of SNPs along the genome, dependent of genome coverage, and relative to clustering of similarly annotated genes determined by FDR. A significance threshold of 0.05 was chosen. Lastly, *Revigo* v1.8.1 (Supek et al., 2011) was used to reveal functional clustering of GO terms

within each trait and treatment or site to obtain a tree map. Within the two selection experiments the respective family effect traits and their outlier genes and GO terms were compared.

Results

Significant family effects in the greenhouse experiment were found for longevity for both the *hot* and *hot* & *dry* treatment but not *control* or *dry*, when for biomass only the *control* treatment showed a significant effect (Table 1). For the three growth traits, all treatments showed significant effects (Table 1). Conversely, none of the traits measured in the field showed significant family effects. For seed establishment of the northern transect the results suggested some potential family trends, with more successful seed establishment for some families. Seed establishment was therefore included in the GWAS.

Final outlier genes were defined as the overlap between both detection thresholds, i.e. genes with more than two HMM outlier SNPs and genes with more than two SNPs at a statistical threshold of $p < 0.001$. This resulted in 29'583 outlier SNPs across all traits (3.96% of all SNPs) overlapping with 2'425 genes. Maximum number of genes detected in a trait ranged from 47 genes in r_{max} of the *hot* treatment to 167 for the PC1 scores of x_{mid} and r_{max} for the *hot&dry* treatment (see Table 2 for a full list SNPs, genes, and GO terms).

In the stress experiment in the greenhouse, hardly found any genes that overlap between the different treatments were found (Figure 2, 3). However, differences among traits and some treatments occurred, with the percentage always relative to the number of outlier genes within the respective trait over all treatments. Asymptotic size (s_{asym}) showed the only overlap between three treatments (3% of all genes = 9 genes) and the most two treatment overlaps (10% = 29 genes). It was followed by x_{mid} with 4.2% (14 genes), r_{max} with 3.6% (11 genes), and longevity with 3.5% (12 genes) two-treatment overlap. Beyond all growth traits the *hot&dry* treatment had the highest number of unique candidate genes (31% = 88 genes) but the lowest for

longevity (17% = 57 genes), where *control* was the most unique (33% = 111 genes). Otherwise, *control*, *dry* and *hot* ranged around 20% for their unique candidate genes. Due to detected trade-offs between growth traits in a previous study the overlap between growth traits was further investigated (Figure 4). For *dry* and *hot* no overlap between asymptotic size and the other two growth traits could be detected. *Control* shows a very strong overlap between x_{mid} and r_{max} of 13 genes. *Hot&Dry* reveals two genes being shared between all three growth traits. PC1 of x_{mid} and r_{max} revealed a stronger consistency between *control* and *dry* (1.9% = 7 genes) whereas the other treatments only overlapped by one to three SNPs (0.3% - 0.8%). Unique genes for *hot&dry* showed the overall maxima with 43% (161 genes), whereas *control* and *dry* ranged at 20% (~73 genes) and *hot* was the lowest with 14% (52 genes) (Figure S1).

Winter survival between the different transects and positions along the transect in the USA stress experiment were also compared (Figure 5, 6). Within the northern transect specific sites performed as expected with range edge being between the inside and outside sites and having overlap with both (0.4% to 0.8% = 1-2 genes; Figure 5). The southern transect behaved differently with having one gene (0.4%) being present at all positions, which shows a function during translation initiation (Berardini et al., 2015). Interestingly the outside position was intermediate and possesses overlap with the inside (0.4% = 1 gene) as well as the range edge site (0.75% = 2 genes). Both transects had ~30% of the candidate genes unique for each position. As climatic conditions at the same position of a transect should be comparable, based on suitability analysis, the expectation was to find a high overlap between the same position along to two transects. However, only one (0.5%; inside), two (1.2%; range edge), and even no candidate gene overlap for the outside sites were detected (Figure 6).

The GO enrichment analysis revealed 884 enriched GO terms and the overlap was comparable to the putative outlier genes (Figures 2-6). Different overlap occurred especially for the growth traits in the greenhouse experiment (Figure 4) and within the southern transect

in the natural selection experiment (Figure 5). Tree map analysis for enriched GO terms of longevity in the greenhouse revealed major functional grouping related to metabolic processes in the *control* and *dry* treatment (Figure S2). The *hot* treatment showed more adaptations in the direction of signalling pathways whereas *hot&dry* favoured functions related to vasculature development as well as water transport (Figure S3).

Discussion

The understanding of genetic adaptation mechanisms, especially in species of environmentally sensitive regions is of crucial importance. Studies, such as Rumpf et al. (2019) and Wiens (2016), highlight that especially populations of the warmer range edge of a species distribution are prone to extinction. Here, we aimed to identify the genetic underpinning of performance traits in *Arabidopsis lyrata*, focusing specifically on adaptation at its southern range edge combining both a greenhouse and an outdoor experiment.

Our findings shed light on the genes likely associated with differences in performance at the southern range edge. Especially for the greenhouse stress experiment, family effects as a proxy for heritable components of adaptation, were quite strong and could explain up to 40% of observed phenotypic variance. However, contrasting results emerge from the natural stress experiment along the southern range edge. Despite similar conditions than in the greenhouse, we found almost no family effect and if so, the explained variance was very limited (<1%). This discrepancy may be due to the inherent complexity of the natural environment imposing additional selection pressures that were not mirrored by the greenhouse experiment, as Karitter et al. (2023) recently also showed on genotypes of *Leontodon hispidus* in differing growth facilities (climate chamber, greenhouse, and common garden). Despite the low survival in the natural selection experiment, the number of outlier genes associated with the measured traits underscores the genetic complexity of stress responses (Selby & Willis, 2018; Wang et al.,

2018). Yet, the limited overlap between treatments raises questions about the universality of genetic adaptations.

The limited overlap between outlier genes for different environments in the greenhouse experiment (Figure 2, 3) is in accordance to another 2x2 factorial stress experiment with maize that found almost the same pattern of only a few overlapping genes in traits related to flowering time and grain yield (Yuan et al., 2019). Here, the authors suggested that this could be due to multiple small effect loci distributed along the genome. This is confirmed by experiments done on the same *A. lyrata* population as used in this study, respective to its environmental origin, with a few small effect SNPs directly influencing flowering related genes (Heblack et al., **landscape genetics**). Therefore, multiple small effect size markers are likely controlling for the different traits that we assessed, which makes predictions related to multi-environment adaptation as well as selection difficult.

Similar patterns, as observed in the greenhouse experiment, could also be found in the natural selection experiment in den United States (Figure 5). Results from our natural stress experiment align with context-dependent responses, revealing different genetic reactions along the northern and southern transect. Additionally to the idea of small effect size loci the complex nature of natural environments opens two other explanations for the low gene overlap: first, different environmental pressures, also considering the intricate interplay of factors influencing adaptation (Aitken & Whitlock, 2013; Ghalambor, 2006), are likely acting along the two transects. Another explanation could be, that different genes are used to respond to similar environmental pressures. However, GO term comparison did not reveal more similar GO terms, which suggests different functional pathways. Differences in gene expression as well as epigenetic makeovers, e.g., methylation or non-coding RNA regulation, could also explain the observed differences in associated genes between the transects but also within the greenhouse experiment.

Further, we want to highlight that we found possible genetic backbones for trade-off in growth traits of the greenhouse experiment (Heblack et al., in review). Indeed, growth traits known to be in a trade-off show a relative high overlap of genes, indicating a similar involvement of genes (Figure 4). Additionally, asymptotic size seems to be genetically maintained quite differently, as growth speed related traits under benign and single stress environments show almost no gene overlap. Just under *hot&dry* conditions plants seem to shift away from their specific gene expression and tend to go to higher multi gene expression to survive especially harsh conditions. Confirmation for this comes from rice studies, where it could be shown that drought response genes are activated based on the duration and strength of the applied stress (Hadiarto & Tran, 2011). This further highlights the complexity of understanding genetics in multi-environmental studies.

Lastly, the predictability of selection at the southern range edge poses a challenge. Despite the replicate of two transects with similar environmental conditions and contrary to our expectation of parallelism between similar transects, we saw strong differences between the transects and the respective transect positions (Figure 6). Genetic pathways as well as different traits are favoured between the transect as genes as well as GO term overlaps were strongly different from each other. The limited overlap in putative outlier genes between the same positions along the two transects underscores the influence of additional, possibly site-specific, factors. Recent studies have highlighted the intricate interplay of genes and gene networks in response to environmental stress, emphasizing the need for a nuanced understanding of functional clustering (Ament-Velásquez et al., 2022; Sork, 2017; Walden et al., 2020). We should also take into account that our assessed performance trait, seed establishment, might be a complex, polygenic trait. Additionally, many traits might contribute to our performance measure, e.g., size at winter onset or frost resistance, and variation in their genetic underpinnings may result in the observed strong differences between the same sites of

the two transects. Hence, work on the specific functions of genes involved are needed to explain the observed differences.

Conclusion

Our study contributes insights to the genetic basis of climate adaptation in *Arabidopsis lyrata*. The methodological integration of controlled experiments and field studies offers a nuanced understanding of genetic responses. However, the context-dependency of genetic adaptations demands careful consideration, urging researchers to account for the correlations of stressors and environmental conditions. Future studies should build upon these findings, integrating a broader range of environmental variables and expanding comparative analyses to enhance our understanding of adaptive evolution in face of climate change (Aitken & Whitlock, 2013; Exposito-Alonso, 2023; Waldvogel et al., 2020). Also, further microclimate studies at each site are needed to assess whether differences in the gene involvement could be explained by the differing environmental pressures occurring at the specific sites, especially between the same transect positions.

Acknowledgements

Collection permits were granted by the Michigan Department of Natural Resources. We thank all the institutions allowing us to run our experiment on their property and all provided help, namely Brooks Saville at Kentland Farm, Sara Childs, Tom Craven and his crew at Duke Forest, Carole Goodwillie, John Gill, Brian Tew, and the whole facility team at ECU, Jeffrey Derr and Rob Holz at the Hampton Roads research station, the Virginia Department of Conservation and Recreation as well as Charlie Whalen and his team at York River State Park and finally David Marsh, Nicole Poulin, and Bill Hamilton at Washington & Lee University. A big thank you also to all the helpers and students maintaining and controlling our experiment for 1.5 years, with your hard work we would not have gathered as much data as we have: Aleks H., Marisa F., Nadia S., Christy C., Marleigh M., Adam N., Steven H., Jordan B., Ni'Dajah B., Josh G., Jensen R., and Tanner H. Additional thanks to Elias Trachsel for valuable help during the experimental setup in the US as well as Olivier Bachmann and Susanna Riedl for their help in the lab and greenhouse. Lastly, we thank the team of the D-BSSE in Basel for the sequencing service, and the sciCORE facility at the University Basel for providing computational resources. We were supported by the Swiss National Science Foundation (grant no. 310030_184763 to Y.W.).

Data Accessibility

Data will be available on DRYAD. Genomic data will be stored on …

Author Contributions

Conceived and designed the experiments: JH, JS, YW. Performed experiment: JH, JS. Analysed the data: JH Wrote the paper: JH, YW, with inputs of JS.

Benefit-Sharing statement

Benefits from this research accrue from the sharing of our data and results on public databases as described above.

References

Aitken, S. N., & Whitlock, M. C. (2013). Assisted gene flow to facilitate local adaptation to climate change. *Annual Review of Ecology, Evolution, and Systematics*, *44*(1), 367–388. https://doi.org/10.1146/annurev-ecolsys-110512-135747

Ament-Velásquez, S. L., Gilchrist, C., Rêgo, A., Bendixsen, D. P., Brice, C., Grosse-Sommer, J. M., Rafati, N., & Stelkens, R. (2022). The dynamics of adaptation to stress from standing genetic variation and de novo mutations. *Molecular Biology and Evolution*, *39*(11), msac242. https://doi.org/10.1093/molbev/msac242

Atwell, S., Huang, Y. S., Vilhjálmsson, B. J., Willems, G., Horton, M., Li, Y., Meng, D., Platt, A., Tarone, A. M., Hu, T. T., Jiang, R., Muliyati, N. W., Zhang, X., Amer, M. A., Baxter, I., Brachi, B., Chory, J., Dean, C., Debieu, M., … Nordborg, M. (2010). Genome-wide association study of 107 phenotypes in Arabidopsis thaliana inbred lines. *Nature*, *465*(7298), 627–631. https://doi.org/10.1038/nature08800

Bates, D., Mächler, M., Bolker, B., & Walker, S. (2014). Fitting linear mixed-effects models using lme4. *arXiv:1406.5823 [Stat]*. http://arxiv.org/abs/1406.5823

Bay, R. A., & Palumbi, S. R. (2014). Multilocus adaptation associated with heat resistance in reef-building corals. *Current Biology*, *24*(24), 2952–2956. https://doi.org/10.1016/j.cub.2014.10.044

Berardini, T. Z., Reiser, L., Li, D., Mezheritsky, Y., Muller, R., Strait, E., & Huala, E. (2015). The arabidopsis information resource: Making and mining the "gold standard" annotated reference plant genome: Tair: Making and Mining the "Gold Standard" Plant Genome. *Genesis*, *53*(8), 474–485. https://doi.org/10.1002/dvg.22877

Brachi, B., Faure, N., Horton, M., Flahauw, E., Vazquez, A., Nordborg, M., Bergelson, J., Cuguen, J., & Roux, F. (2010). Linkage and association mapping of *Arabidopsis thaliana* flowering time in nature. *PLoS Genetics*, *6*(5), e1000940. https://doi.org/10.1371/journal.pgen.1000940

Capblancq, T., Fitzpatrick, M. C., Bay, R. A., Exposito-Alonso, M., & Keller, S. R. (2020). Genomic prediction of (mal)adaptation across current and future climatic landscapes. *Annual Review of Ecology, Evolution, and Systematics*, *51*(1), 245–269. https://doi.org/10.1146/annurev-ecolsys-020720-042553

Colosimo, P. F., Hosemann, K. E., Balabhadra, S., Villarreal, G., Dickson, M., Grimwood, J., Schmutz, J., Myers, R. M., Schluter, D., & Kingsley, D. M. (2005). Widespread parallel evolution in sticklebacks by repeated fixation of ectodysplasin alleles. *Science*, *307*(5717), 1928–1933. https://doi.org/10.1126/science.1107239

De Villemereuil, P., Gaggiotti, O. E., Mouterde, M., & Till-Bottraud, I. (2016). Common garden experiments in the genomic era: New perspectives and opportunities. *Heredity*, *116*(3), 249–254. https://doi.org/10.1038/hdy.2015.93

Dore, M. H. I. (2005). Climate change and changes in global precipitation patterns: What do we know? *Environment International*, *31*(8), 1167–1181. https://doi.org/10.1016/j.envint.2005.03.004

Elsen, P. R., Saxon, E. C., Simmons, B. A., Ward, M., Williams, B. A., Grantham, H. S., Kark, S., Levin, N., Perez-Hammerle, K., Reside, A. E., & Watson, J. E. M. (2022). Accelerated shifts in terrestrial life zones under rapid climate change. *Global Change Biology*, *28*(3), 918–935. https://doi.org/10.1111/gcb.15962

Exposito-Alonso, M. (2023). Understanding local plant extinctions before it is too late: Bridging evolutionary genomics with global ecology. *New Phytologist*, *237*(6), 2005–2011. https://doi.org/10.1111/nph.18718

Fournier-Level, A., Korte, A., Cooper, M. D., Nordborg, M., Schmitt, J., & Wilczek, A. M. (2011). A map of local adaptation in *Arabidopsis thaliana*. *Science*, *334*(6052), 86–89. https://doi.org/10.1126/science.1209271

Fredston-Hermann, A., Selden, R., Pinsky, M., Gaines, S. D., & Halpern, B. S. (2020). Cold range edges of marine fishes track climate change better than warm edges. *Global Change Biology*, *26*(5), 2908–2922. https://doi.org/10.1111/gcb.15035

Ghalambor, C. K. (2006). Are mountain passes higher in the tropics? Janzen's hypothesis revisited. *Integrative and Comparative Biology*, *46*(1), 5–17. https://doi.org/10.1093/icb/icj003

Hadiarto, T., & Tran, L.-S. P. (2011). Progress studies of drought-responsive genes in rice. *Plant Cell Reports*, *30*(3), 297–310. https://doi.org/10.1007/s00299-010-0956-z

Harte, D. (2021). *HiddenMarkov: Hidden Markov Models* (R package version 1.8-13) [Computer software]. Statitcs Research Associates. https://www.statsresearch.co.nz/dsh/sslib/

Horton, M. W., Hancock, A. M., Huang, Y. S., Toomajian, C., Atwell, S., Auton, A., Muliyati, N. W., Platt, A., Sperone, F. G., Vilhjálmsson, B. J., Nordborg, M., Borevitz, J. O., & Bergelson, J. (2012). Genome-wide patterns of genetic variation in worldwide Arabidopsis thaliana accessions from the RegMap panel. *Nature Genetics*, *44*(2), 212–216. https://doi.org/10.1038/ng.1042

Hu, T. T., Pattyn, P., Bakker, E. G., Cao, J., Cheng, J.-F., Clark, R. M., Fahlgren, N., Fawcett, J. A., Grimwood, J., Gundlach, H., Haberer, G., Hollister, J. D., Ossowski, S., Ottilar, R. P., Salamov, A. A., Schneeberger, K., Spannagl, M., Wang, X., Yang, L., … Guo, Y.-L. (2011). The *Arabidopsis lyrata* genome sequence

and the basis of rapid genome size change. *Nature Genetics*, *43*(5), 476–481. https://doi.org/10.1038/ng.807

Karitter, P., March-Salas, M., Ensslin, A., Rauschkolb, R., Godefroid, S., Poorter, H., & Scheepens, J. F. (2023). *Garden, greenhouse or climate chamber? Experimental conditions influence whether genetic differences are phenotypically expressed* [Preprint]. Ecology. https://doi.org/10.1101/2023.12.06.570376

Leinonen, P. H., Sandring, S., Quilot, B., Clauss, M. J., Mitchell-Olds, T., Agren, J., & Savolainen, O. (2009). Local adaptation in European populations of *Arabidopsis lyrata* (Brassicaceae). *American Journal of Botany*, *96*(6), 1129–1137. https://doi.org/10.3732/ajb.0800080

López-Hernández, F., & Cortés, A. J. (2019). Last-generation genome–environment associations reveal the genetic basis of heat tolerance in common bean (*Phaseolus vulgaris* L.). *Frontiers in Genetics*, *10*, 954. https://doi.org/10.3389/fgene.2019.00954

Mackay, T. F. C., Richards, S., Stone, E. A., Barbadilla, A., Ayroles, J. F., Zhu, D., Casillas, S., Han, Y., Magwire, M. M., Cridland, J. M., Richardson, M. F., Anholt, R. R. H., Barrón, M., Bess, C., Blankenburg, K. P., Carbone, M. A., Castellano, D., Chaboub, L., Duncan, L., … Gibbs, R. A. (2012). The *Drosophila melanogaster* genetic reference panel. *Nature*, *482*(7384), 173–178. https://doi.org/10.1038/nature10811

Matesanz, S., Gianoli, E., & Valladares, F. (2010). Global change and the evolution of phenotypic plasticity in plants. *Annals of the New York Academy of Sciences*, *1206*(1), 35–55. https://doi.org/10.1111/j.1749-6632.2010.05704.x

Michaels, S. D., & Amasino, R. M. (1999). *FLOWERING LOCUS C* encodes a novel MADS domain protein that acts as a repressor of flowering. *The Plant Cell*, *11*(5), 949–956. https://doi.org/10.1105/tpc.11.5.949

Oostra, V., Saastamoinen, M., Zwaan, B. J., & Wheat, C. W. (2018). Strong phenotypic plasticity limits potential for evolutionary responses to climate change. *Nature Communications*, *9*(1), 1005. https://doi.org/10.1038/s41467-018-03384-9

Paccard, A., Fruleux, A., & Willi, Y. (2014). Latitudinal trait variation and responses to drought in *Arabidopsis lyrata*. *Oecologia*, *175*(2), 577–587. https://doi.org/10.1007/s00442-014-2932-8

Parmesan, C. (2006). Ecological and evolutionary responses to recent climate change. *Annual Review of Ecology, Evolution, and Systematics*, *37*(1), 637–669. https://doi.org/10.1146/annurev.ecolsys.37.091305.110100

Pinsky, M. L., Eikeset, A. M., McCauley, D. J., Payne, J. L., & Sunday, J. M. (2019). Greater vulnerability to warming of marine versus terrestrial ectotherms. *Nature*, *569*(7754), 108–111. https://doi.org/10.1038/s41586-019-1132-4

Rumpf, S. B., Hülber, K., Wessely, J., Willner, W., Moser, D., Gattringer, A., Klonner, G., Zimmermann, N. E., & Dullinger, S. (2019). Extinction debts and colonization credits of non-forest plants in the European Alps. *Nature Communications*, *10*(1), 4293. https://doi.org/10.1038/s41467-019-12343-x

Schepers, J. R., Heblack, J., & Willi, Y. (2024). Negative interaction effect of heat and drought stress at the warm end of species distribution. *Oecologia*. https://doi.org/10.1007/s00442-023-05497-5

Selby, J. P., & Willis, J. H. (2018). Major QTL controls adaptation to serpentine soils in *Mimulus guttatus*. *Molecular Ecology*, *27*(24), 5073–5087. https://doi.org/10.1111/mec.14922

Sork, V. L. (2017). Genomic studies of local adaptation in natural plant populations. *Journal of Heredity*, *109*(1), 3–15. https://doi.org/10.1093/jhered/esx091

Supek, F., Bošnjak, M., Škunca, N., & Šmuc, T. (2011). REVIGO summarizes and visualizes long lists of gene ontology terms. *PLoS ONE*, *6*(7), e21800. https://doi.org/10.1371/journal.pone.0021800

Szkiba, D., Kapun, M., von Haeseler, A., & Gallach, M. (2014). SNP2GO: Functional analysis of genome-wide association studies. *Genetics*, *197*(1), 285–289. https://doi.org/10.1534/genetics.113.160341

Van'T Hof, A. E., Edmonds, N., Dalíková, M., Marec, F., & Saccheri, I. J. (2011). Industrial melanism in British peppered moths has a singular and recent mutational origin. *Science*, *332*(6032), 958–960. https://doi.org/10.1126/science.1203043

Walden, N., Lucek, K., & Willi, Y. (2020). Lineage-specific adaptation to climate involves flowering time in North American *Arabidopsis lyrata*. *Molecular Ecology*, *29*(8), 1436–1451. https://doi.org/10.1111/mec.15338

Waldvogel, A.-M., Feldmeyer, B., Rolshausen, G., Exposito-Alonso, M., Rellstab, C., Kofler, R., Mock, T., Schmid, K., Schmitt, I., Bataillon, T., Savolainen, O., Bergland, A., Flatt, T., Guillaume, F., & Pfenninger, M. (2020). Evolutionary genomics can improve prediction of species' responses to climate change. *Evolution Letters*, *4*(1), 4–18. https://doi.org/10.1002/evl3.154

Wang, J., Ding, J., Tan, B., Robinson, K. M., Michelson, I. H., Johansson, A., Nystedt, B., Scofield, D. G., Nilsson, O., Jansson, S., Street, N. R., & Ingvarsson, P. K. (2018). A major locus controls local adaptation and adaptive life history variation in a perennial plant. *Genome Biology*, *19*(1), 72. https://doi.org/10.1186/s13059-018-1444-y

Wiens, J. J. (2016). Climate-related local extinctions are already widespread among plant and animal species. *PLOS Biology*, *14*(12), e2001104. https://doi.org/10.1371/journal.pbio.2001104

Wilczek, A. M., Roe, J. L., Knapp, M. C., Cooper, M. D., Lopez-Gallego, C., Martin, L. J., Muir, C. D., Sim, S., Walker, A., Anderson, J., Egan, J. F., Moyers, B. T., Petipas, R., Giakountis, A., Charbit, E., Coupland, G., Welch, S. M., & Schmitt, J. (2009). Effects of genetic perturbation on seasonal life history plasticity. *Science*, *323*(5916), 930–934. https://doi.org/10.1126/science.1165826

Wos, G., & Willi, Y. (2015). Temperature-stress resistance and tolerance along a latitudinal cline in North American *Arabidopsis lyrata*. *PLOS ONE*, *10*(6), e0131808. https://doi.org/10.1371/journal.pone.0131808

Yuan, Y., Cairns, J. E., Babu, R., Gowda, M., Makumbi, D., Magorokosho, C., Zhang, A., Liu, Y., Wang, N., Hao, Z., San Vicente, F., Olsen, M. S., Prasanna, B. M., Lu, Y., & Zhang, X. (2019). Genome-wide association mapping and genomic prediction analyses reveal the genetic architecture of grain yield and flowering time under drought and heat stress conditions in maize. *Frontiers in Plant Science*, *9*, 1919. https://doi.org/10.3389/fpls.2018.01919

Figure 1

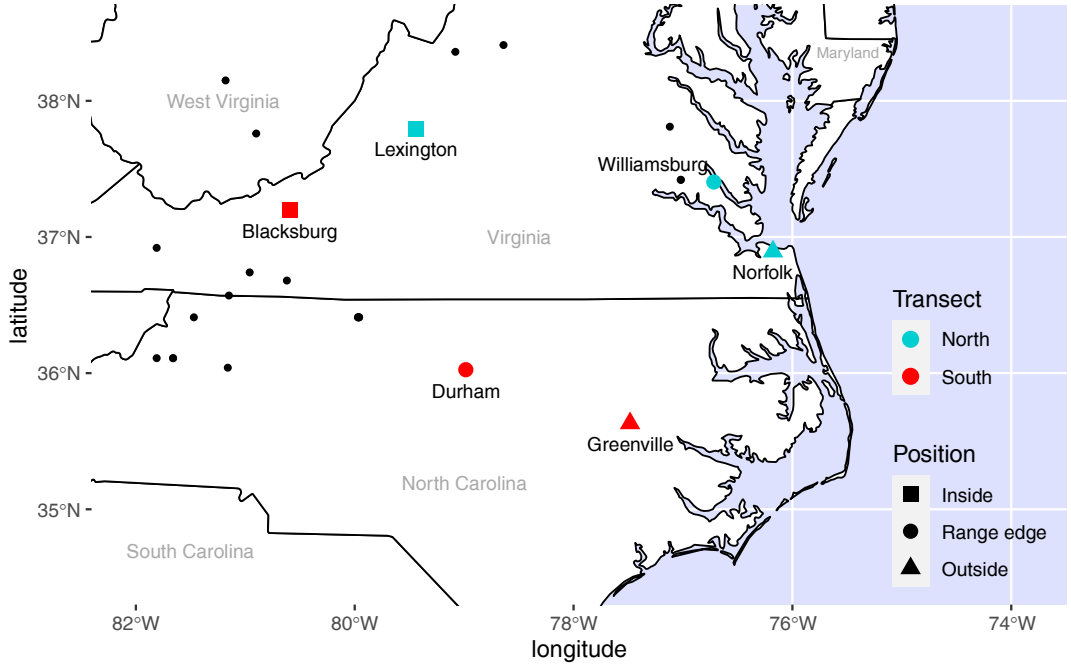

Figure 1: Map with the sites of the selection experiment at the southern range edge of *Arabidopsis lyrata* in the USA (blue and red) and species occurrences (black dots). Colours of the symbols indicate the two transects (north versus south) and the shape of symbols their position relative to the southern range edge of *A. lyrata*.

Figure 2

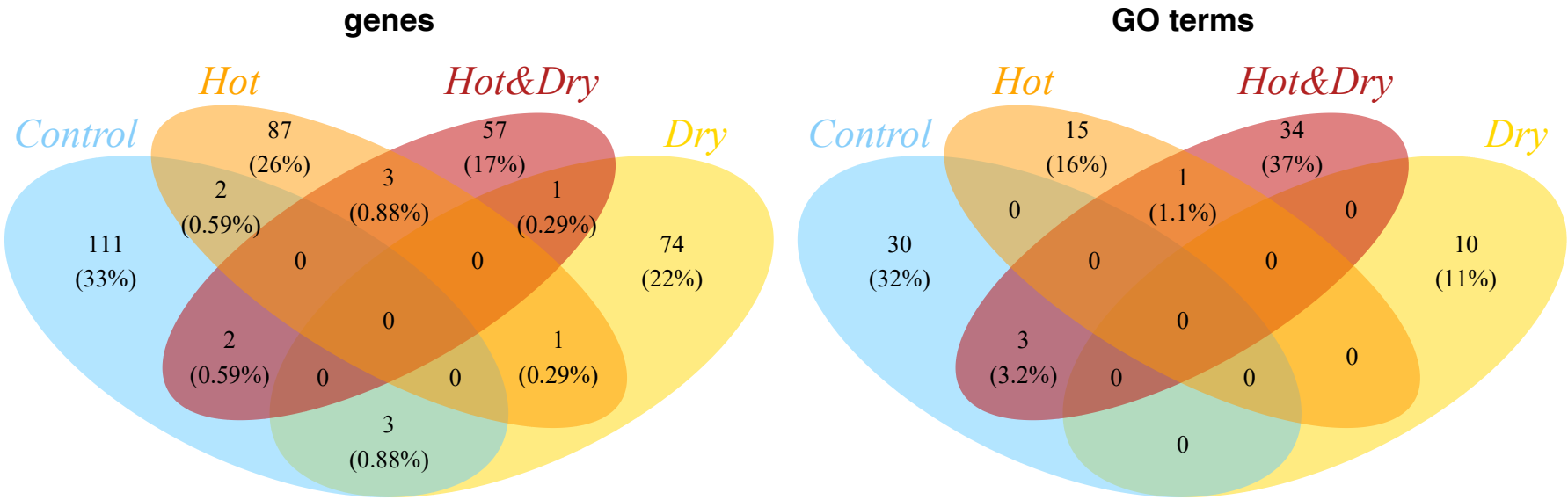

Figure 2: Overlap in outlier genes and enriched GO terms linked to the performance trait longevity among the four treatments in the stress experiment conducted in the greenhouse. Colours of ellipses indicate the treatments: control in blue, dry in yellow, hot in orange, and hot with dry in red, with mixtures of these colours for outlier genes that overlapped. Percentages are relative to all outlier genes found for a trait.

Figure 3

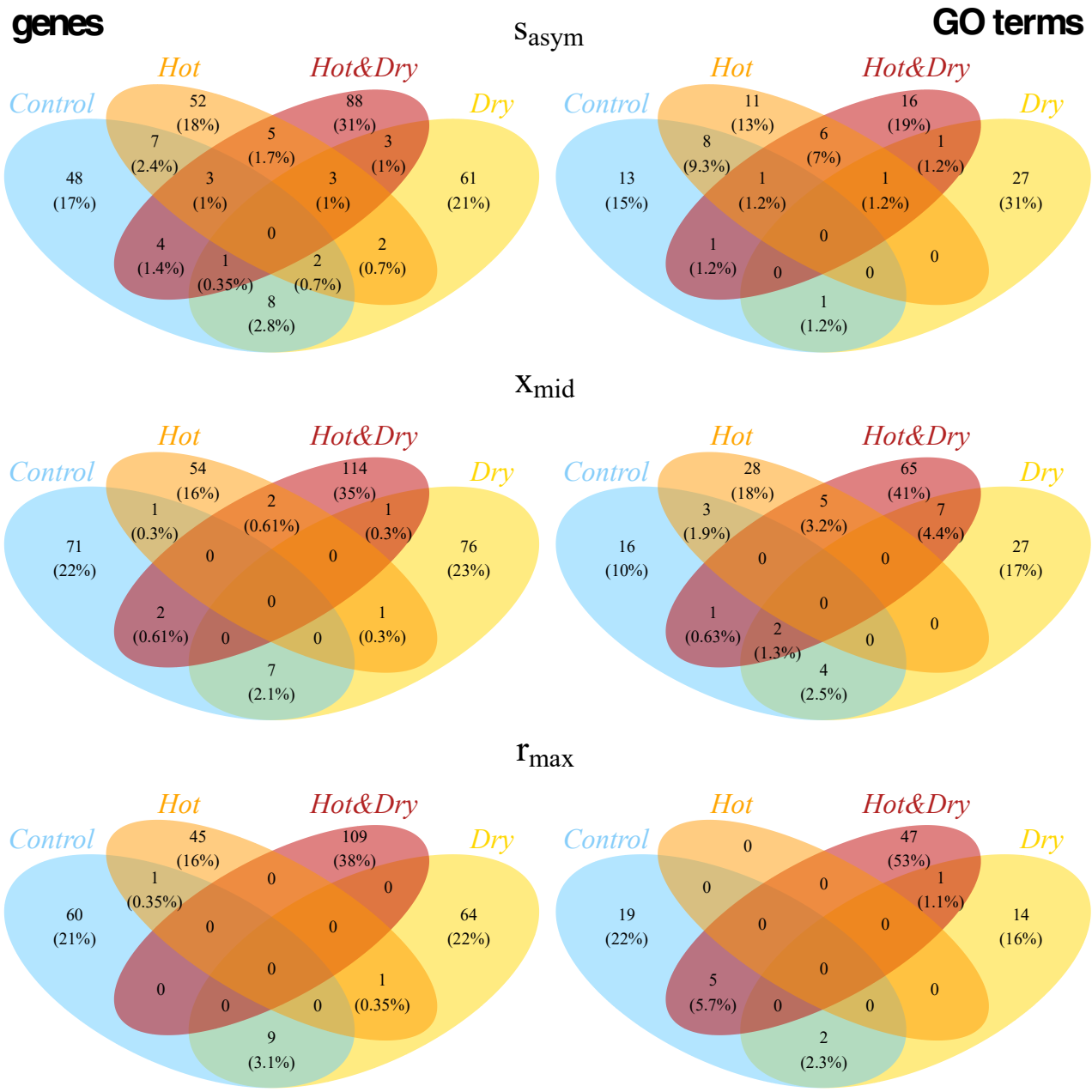

Figure 3: Overlap in outlier genes and enriched GO terms linked to performance traits among the four treatments in the stress experiment conducted in the greenhouse. The three performance traits were: asymptotic size (s_{asym}), time till half size (x_{mid}), and maximum growth rate (r_{max}). Colours of ellipses indicate the treatments: control in blue, dry in yellow, hot in orange, and hot with dry in red, with mixtures of these colours for outlier genes that overlapped. Percentages are relative to all outlier genes found for a trait.

Figure 4

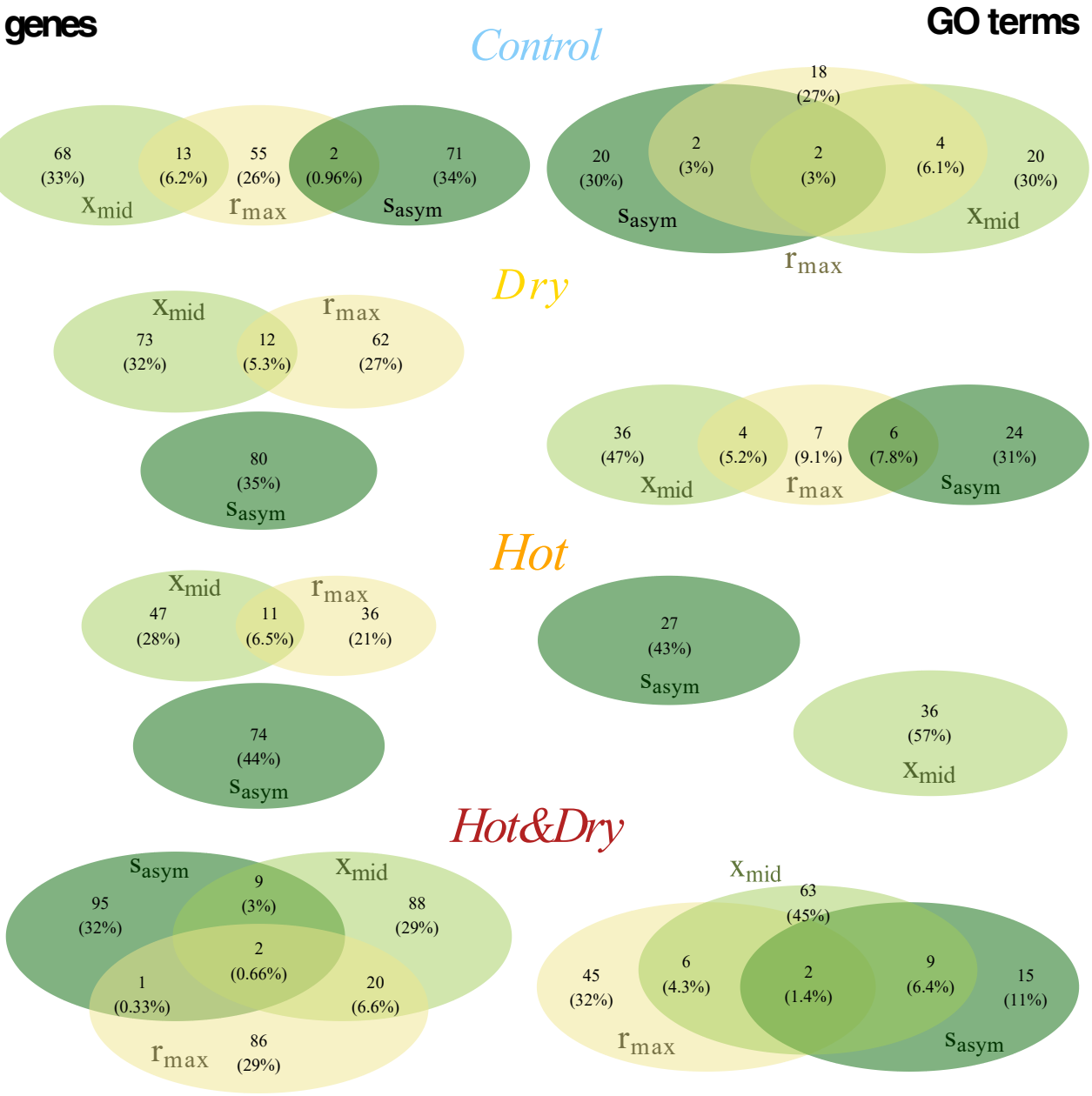

Figure 4: Overlap in outlier genes and enriched GO terms linked to performance traits among the three growth traits: asymptotic size (s_{asym}), time till half size (x_{mid}), and maximum growth rate (r_{max}) for the four treatments within the glasshouse stress experiment. Shades of green of ellipses indicate the growth trait: s_{asym} in dark green, x_{mid} in light green, and r_{max} in yellow, with mixtures of these colours for outlier genes that overlapped. Percentages are relative to all outlier genes found for a trait.

Figure 5

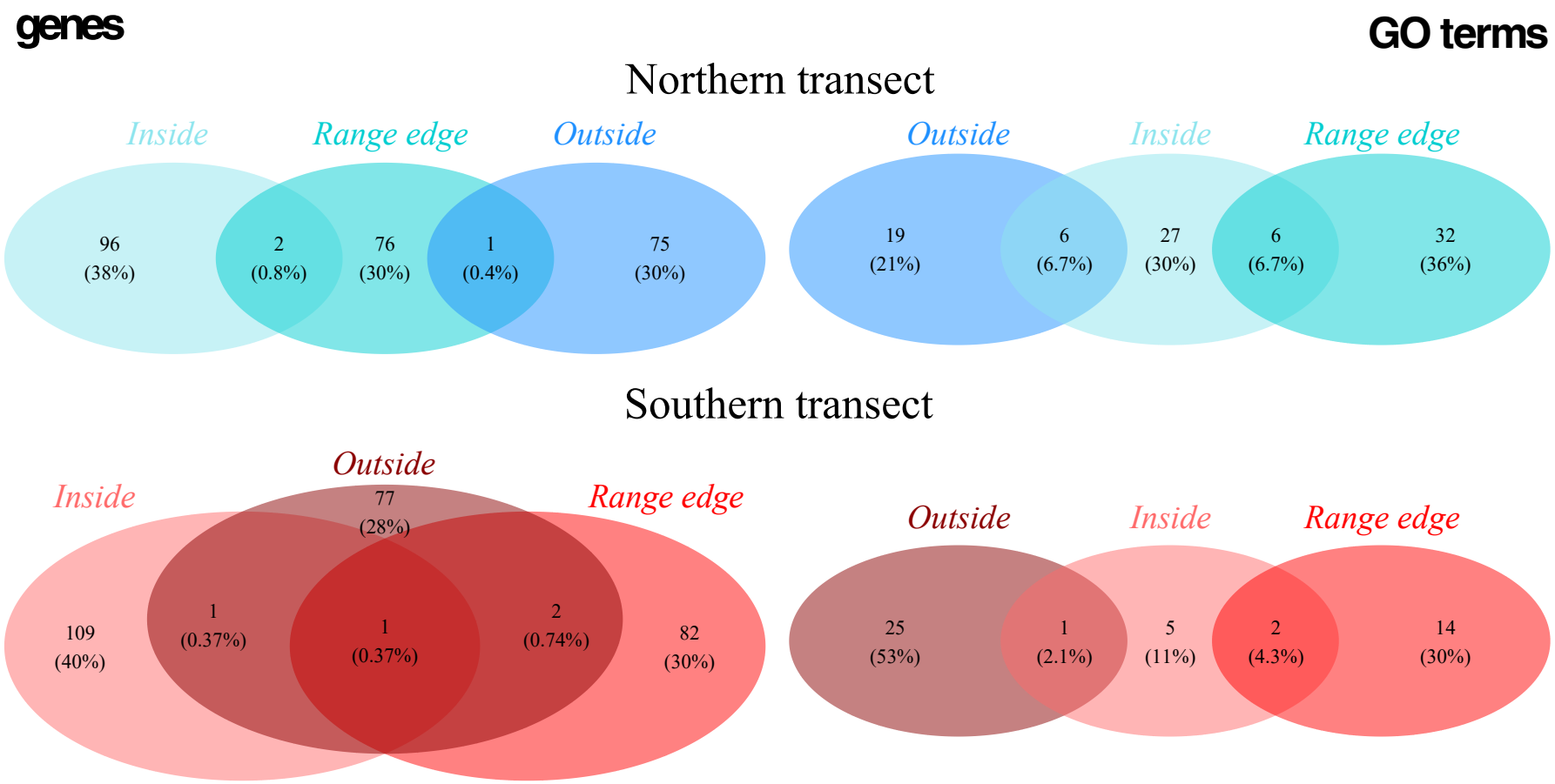

Figure 5: Overlap in outlier genes and enriched GO terms linked to seed establishment between the transects in the natural stress experiment conducted in the USA. Comparisons within the transects of the northern transect on the top row (blue) and southern transect in the bottom row (red). Percentages are relative to all outlier genes found for a trait.

Figure 6

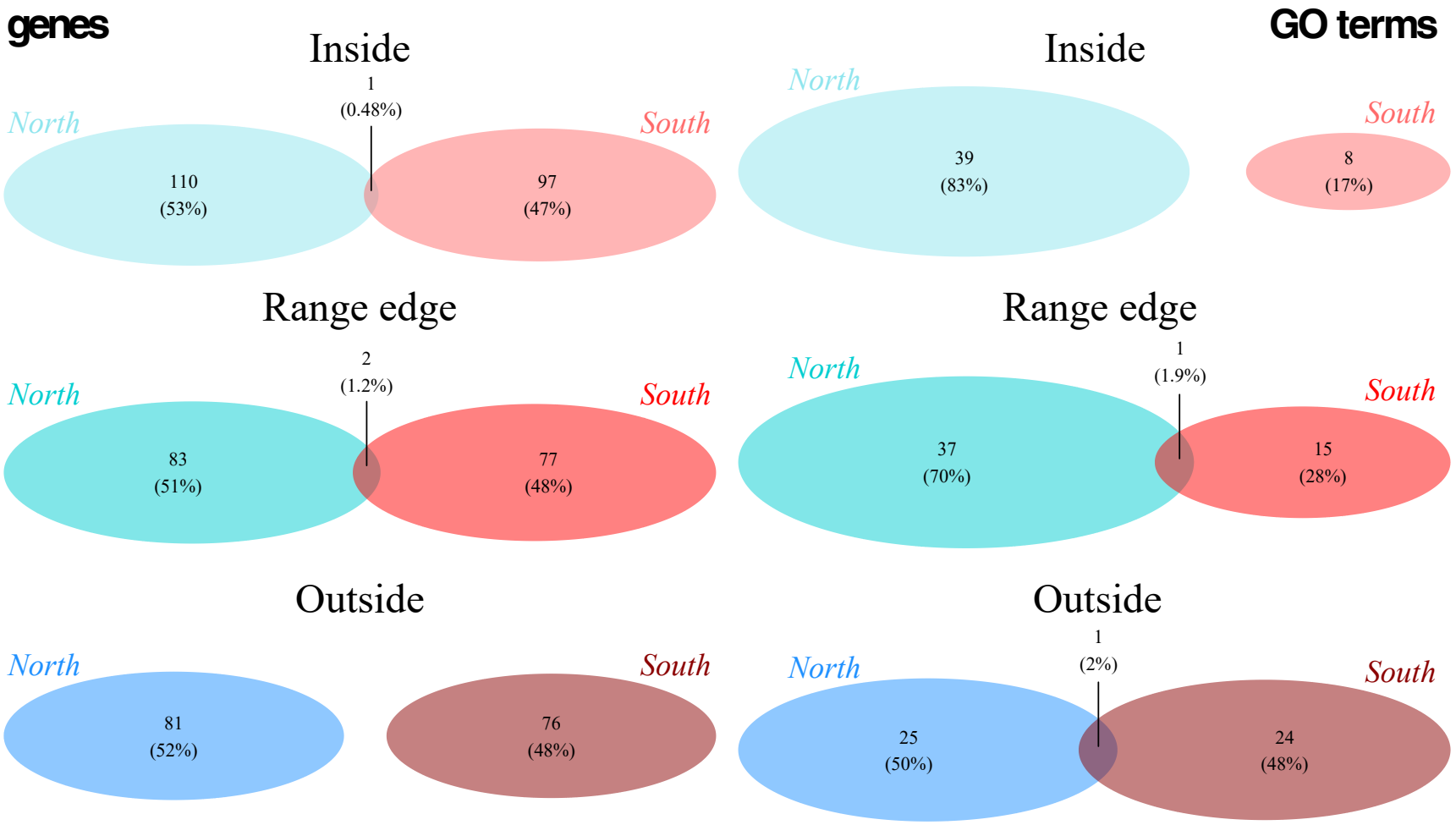

Figure 6: Overlap in outlier genes and enriched GO terms linked to seed establishment among the transect positions in the natural stress experiment conducted in the USA. Colours of ellipses indicate the transects: north in blue, and south in red. Percentages are relative to all outlier genes found for a trait.

Table 1: The effect of family on performance traits assessed in the glasshouse experiment (top) and in the selection experiment (bottom). The five traits assessed in the greenhouse experiment were longevity, biomass, and the three aspects of the growth trajectory, asymptotic size, the time till half growth and the maximal growth rate. The three traits considered in the selection experiment were longevity, biomass and whether a seed sown in autumn produced an established plant in spring. n – Number of analysed individuals. Significant effects are indicated in bold. R^2 – variance explained.

	Trait	Longevity			Biomass			a_{sym}			x_{mid}			r_{max}		
Treatment		n	p(F)	R^2	n	p(F)	R^2	n	p(F)	R^2	n	p(F)	R^2	n	p(F)	R^2
Control		480	0.257	0.018	168	**0.028**	0.126	475	**< 0.001**	0.193	451	**< 0.001**	0.145	468	**< 0.001**	0.211
Dry		480	*0.074*	0.043	42	0.425	0.033	468	**< 0.001**	0.404	466	**< 0.001**	0.152	446	**< 0.001**	0.313
Hot		479	**0.035**	0.054				474	**< 0.001**	0.336	455	**< 0.001**	0.163	460	**< 0.001**	0.228
Hot&Dry		476	**< 0.001**	0.171				468	**< 0.001**	0.289	465	**< 0.001**	0.142	469	**< 0.001**	0.132
	Trait	Longevity			Biomass			Seed establishment								
Site		n	p(F)	R^2	n	p(F)	R^2	n	p(F)	R^2						
North inside		474	0.214	0.001	474	0.667	0.002	2359	0.115	< 0.001						
North range edge		1116	0.686	< 0.001	1116	0.898	< 0.001	2331	0.141	< 0.001						
North outside		1586	0.163	< 0.001	1586	0.197	< 0.001	2344	0.191	< 0.001						
South inside		324	0.445	0.002	324	0.544	0.002	2376	0.350	< 0.001						
South range edge		1195	0.917	< 0.001	1195	0.925	< 0.001	2352	0.832	< 0.001						
South outside		719	0.865	0.001	719	0.993	0.001	2357	0.509	< 0.001						

Table 2: Number of outlier SNPs, outlier genes, and GO terms detected using the both approaches: Hidden-Markov-Models (HMM) with > 2 outlier SNPs per gene or a p cut-off value < 0.001 with > 1 outlier SNPs per gene. The upper part of the table is on performance traits measured in the stress experiment in the greenhouse, with the four treatments of *control*, *dry*, *hot*, and *hot&dry*. The lower part of the table reports on performance (whether a seed sown in autumn led to an established plant in spring) estimated in the selection experiment at the southern range edge of *Arabidopsis lyrata*.

	Treatment / site	HMM			Type
		SNPs	Genes	GO terms	
Longevity	*Control*	1567	118	33	Stress experiment in greenhouse
	Dry	826	79	10	
	Hot	1030	93	16	
	Hot&Dry	819	63	38	
Biomass	*Control*	1182	69	47	
s_{asym}	*Control*	572	73	24	
	Dry	868	80	30	
	Hot	870	74	27	
	Hot&Dry	1335	107	26	
x_{mid}	*Control*	1145	81	26	
	Dry	1184	85	40	
	Hot	703	58	36	
	Hot&Dry	1389	119	80	
r_{max}	*Control*	927	70	26	
	Dry	903	74	17	
	Hot	509	47	0	
	Hot&Dry	1164	109	53	
PC1 x_{mid} r_{max}	*Control*	1162	82	26	
	Dry	1172	83	41	
	Hot	695	57	35	
	Hot&Dry	1468	167	62	
PC1 s_{asym} x_{mid} r_{max}	*Hot&Dry*	1336	107	26	
seed establishment	*Lexington*	850	98	39	Selection experiment
	Williamsburg	1108	79	41	
	Norfolk	1123	76	31	
	Blacksburg	1260	111	10	
	Durham	1345	85	18	
	Greenville	1072	81	26	

Synthesis and conclusions

My thesis aimed to identify traits, and genes under selection in response to environmental changes across *Arabidopsis lyrata's* southern distribution range. Along with identifying factors that could contribute to southern distributions range limits. Here, I will synthesize the key findings of each chapter and discuss their implications for understanding the climate adaptations of plant populations at the warm end of a species distribution.

In Chapter 1, I investigated the mechanisms that maintain genetic diversity in a dynamic dune landscape, with multiple ecotypes possibly favouring local adaptation. I performed a genome-wide-association study (GWAS) with environmental variables and phenotypic traits showing signs of local adaptation. I found multiple outlier genes with slightly increased diversity compared to less associated genes, indicating a diversification effect of local adaptation, despite a homogenizing effect of dispersal activity in the population. Outlier genes showed additive effects of mid-homozygous SNP haplotype divergence, but effect sizes and putative effects were small, implying the involvement of a few small effect loci. Gene functions were mainly related to reproductive development, especially regulating flowering related processes, resulting in strong adaptation to the local environment. The results highlight the role of landscape features, and climate in driving genetic differentiation and emphasize the importance of considering the landscape context in understanding the genetic basis of adaptation.

Chapter 2 addressed genetic constraints on traits of adaptation across different environmental conditions and the resulting effects on the evolutionary potential of the species. I performed a 2x2 factorial stress experiment (control, drought, heat, and heat and drought combined) with conditions mimicking those at the southern range edge of distribution. Phenotypic performance differences revealed reduced survival under multi-stress conditions that was stronger than expected by a purely additive effect of heat and drought (see

supplementary paper Schepers, Heblack &Willi (2024), *Oecologia*). This synergistic effect might be explained by genetic constraints. However, the genetic variance-covariance matrices (G-matrices) of growth and allocation traits revealed no clear pattern between environments. Nonetheless, significant genetic correlations between different growth traits were detected, which might limit multivariate genetic variation. In single-stress environments, we evidenced trade-offs between time to fastest growth and the speed of growth. Additionally, we found a supplementary genetic trade-off involving time to fastest growth and speed of growth with maximum size in the multi-stress environment, following the direction of the slow-fast continuum. Plants growing early and fast being small, and late-slow growing plants being tall. Following the direction of the slow-fast continuum was found to be antagonistic to the selection vector, especially under drought and multi-stress conditions, thus strongly limiting the ability to effectively adapt to southern range edge conditions. These findings confirm the importance of genetic constraints in adaptation to novel or changing environmental conditions.

In chapter 3, I explored more extensively the genomic basis of differences in performance at the southern range edge, by studying selection at the southern range edge of the species distribution in the USA. Plant families of *A. lyrata* were grown at three different positions along the species range edge: within, at the edge, and beyond the range, with two replicate transects. I assessed seedling establishment in the first spring after sowing and used this, as well as fitness traits from the greenhouse experiment, to explore genetic responses to different environmental pressures. I found much stronger family effects in the greenhouse experiment than in the natural selection experiment. Especially for the greenhouse experiment, the observed family effects explain a high fraction of the observed variance, highlighting the complexity of natural environments by increased genome-environment associations. At the gene level, I generally observed low gene overlap between treatment and sites of the same phenotypic trait, indicating different genomic pathways of trait expression. Interestingly, I

found a much stronger gene overlap between growth traits known to be involved in genetic and phenotypic trade-offs, indicating that different growth traits might be integrated, resulting in genetic constraints for such traits. Lastly, there were few gene overlaps among transects as well as among transect positions, against an idea of parallelism among the transects. A possible reason could be, that seedling establishment might be a good performance trait, but could also include multiple other traits important for persistence, e.g., size at winter onset, frost resistance, and so on. These different underlying traits then result in strong differences in associated genes found among sites. Additionally, stronger differences in microclimate influences then expected also need to be considered. Taken together this study confirms the complexity of genes involved in expressing fitness traits and the challenges it imposes for predicting selection at the southern range edge.

Concluding remarks

Overall, my results confirm the complexity of genetic processes shaping a species' adaptive potential. I showed that enough genetic variability is available at range edges to adapt, but the multi-dimensionality of the environment may facilitate genetic constraints. However, as traits seem to be genetically coded via multiple genetic pathways as well as small effect size loci, sufficient adaptation could still be possible. However, the extent to which a plant species can effectively adapt to new conditions, considering the underlying mechanisms and constraints mentioned above, remains uncertain and should be tested through experiments focusing on real-time evolutionary processes.

Despite that the results in the greenhouse experiment confirmed that my study population harbours the same phenotypic diversity as southern range edge populations, it would be intriguing to perform similar genetic analysis with a wider range of plant families from the southern range edge. Additionally, the genetic examination of individuals performing

particularly well outside the range edge would help to better understand the traits selected for as well as to detect the genes underlying adaptive potential at the southern range edge. A microclimate study analysing the climatic conditions responsible for the state change of plants (e.g., climatic conditions necessary for a shift from dormancy to germination) over the southern range edge is ongoing and might reveal specific environmental factors that can be related in a more in depth GWAS study.

Supporting Information – Chapter I

Figure S1

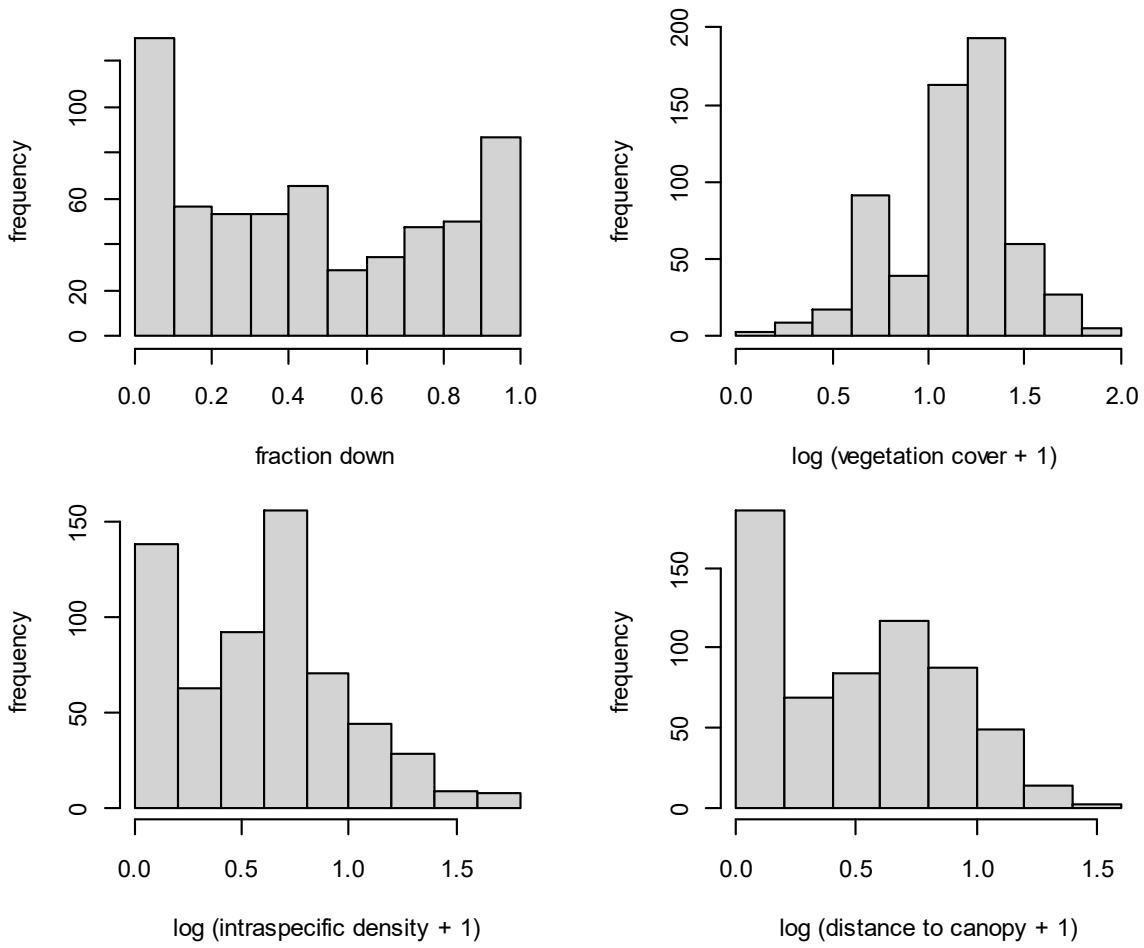

Figure S1: Frequency distribution of the environmental variables. **Top left**) dune position as fraction down of the dune (0 = dune top, 1 = dune bottom). **Top right**) vegetation cover (log-transformed). **Bottom left**) intraspecific density (log-transformed). **Bottom right**) distance to canopy (log-transformed).

Figure S2

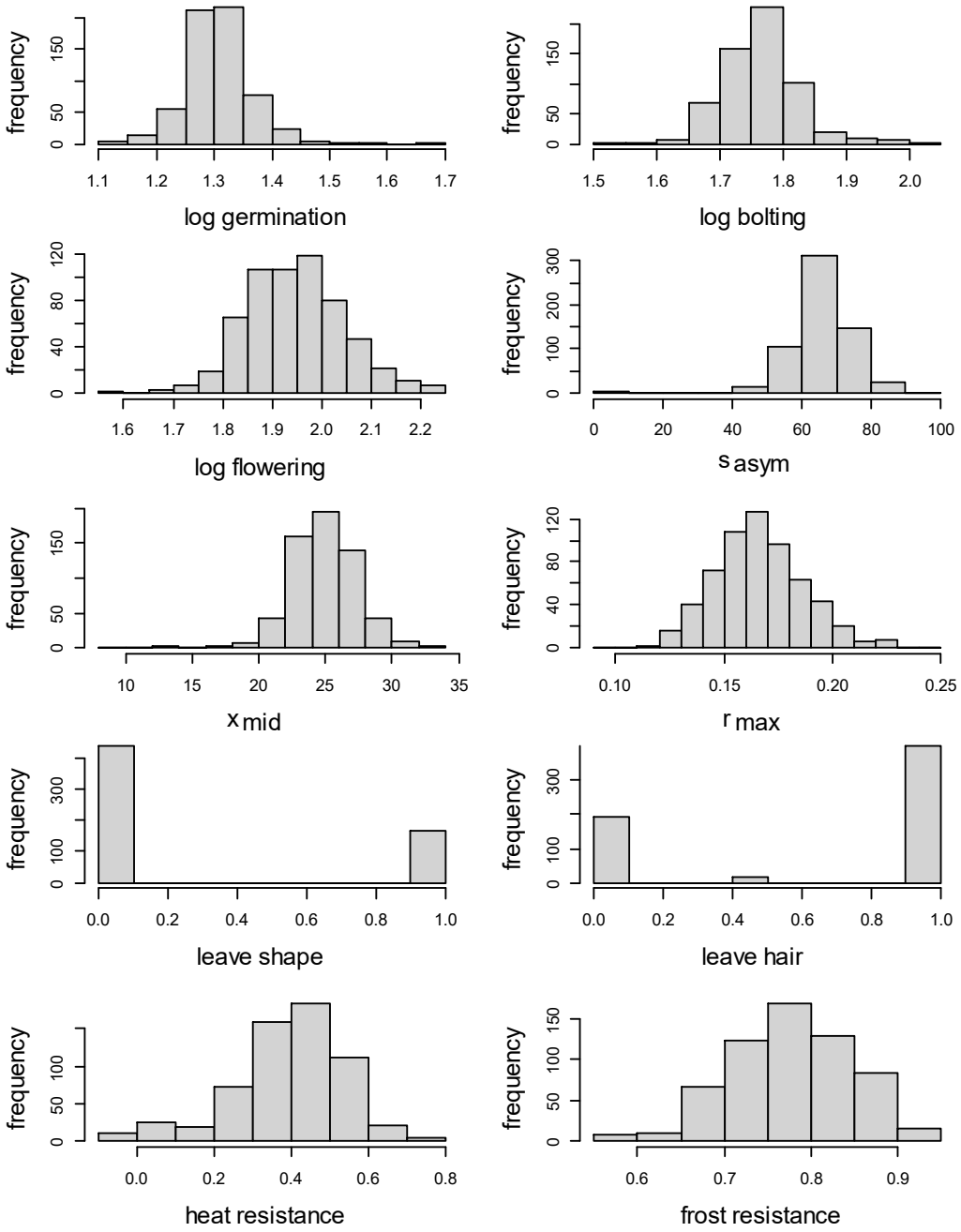

Figure S2: Frequency distribution of the phenotypic variables after applying any necessary data transformation.

Figure S3

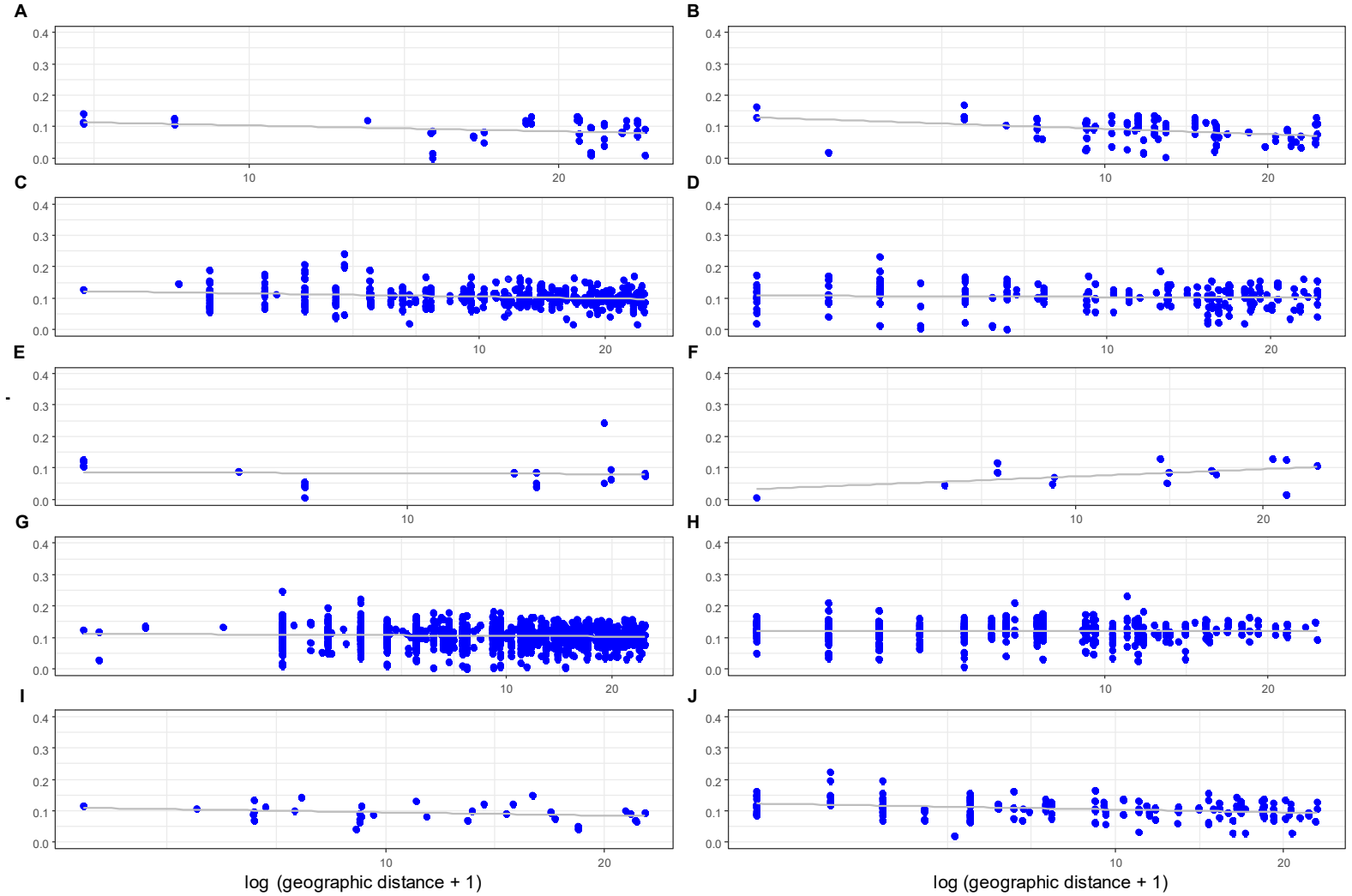

Figure S3: KING kinship related to geographic distance (log_{10}) for section 2 in a) 2009, b) 2010, c) 2013, d) 2014, and section 3 in e) 2009, f) 2010, g) 2013, h) 2014, and section 4 in i) 2010, and j) 2013.

Figure S4

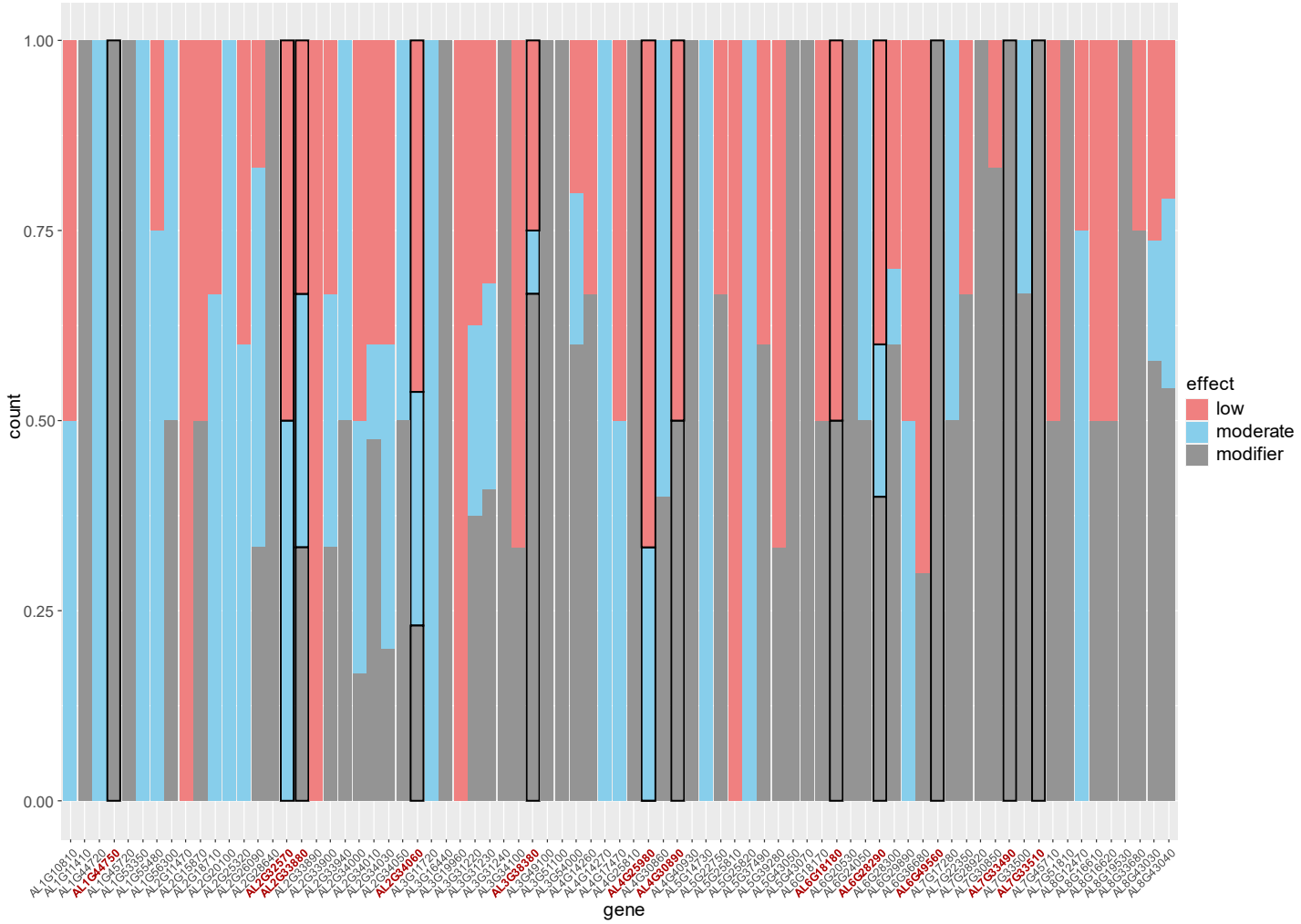

Figure S4: Mapping of putative effects of outlier SNPs in outlier genes. Colours indicate SNP effect: red for low, blue for moderate, and grey modifier. Candidate genes are highlighted in red and respective bars in black.

Figure S5

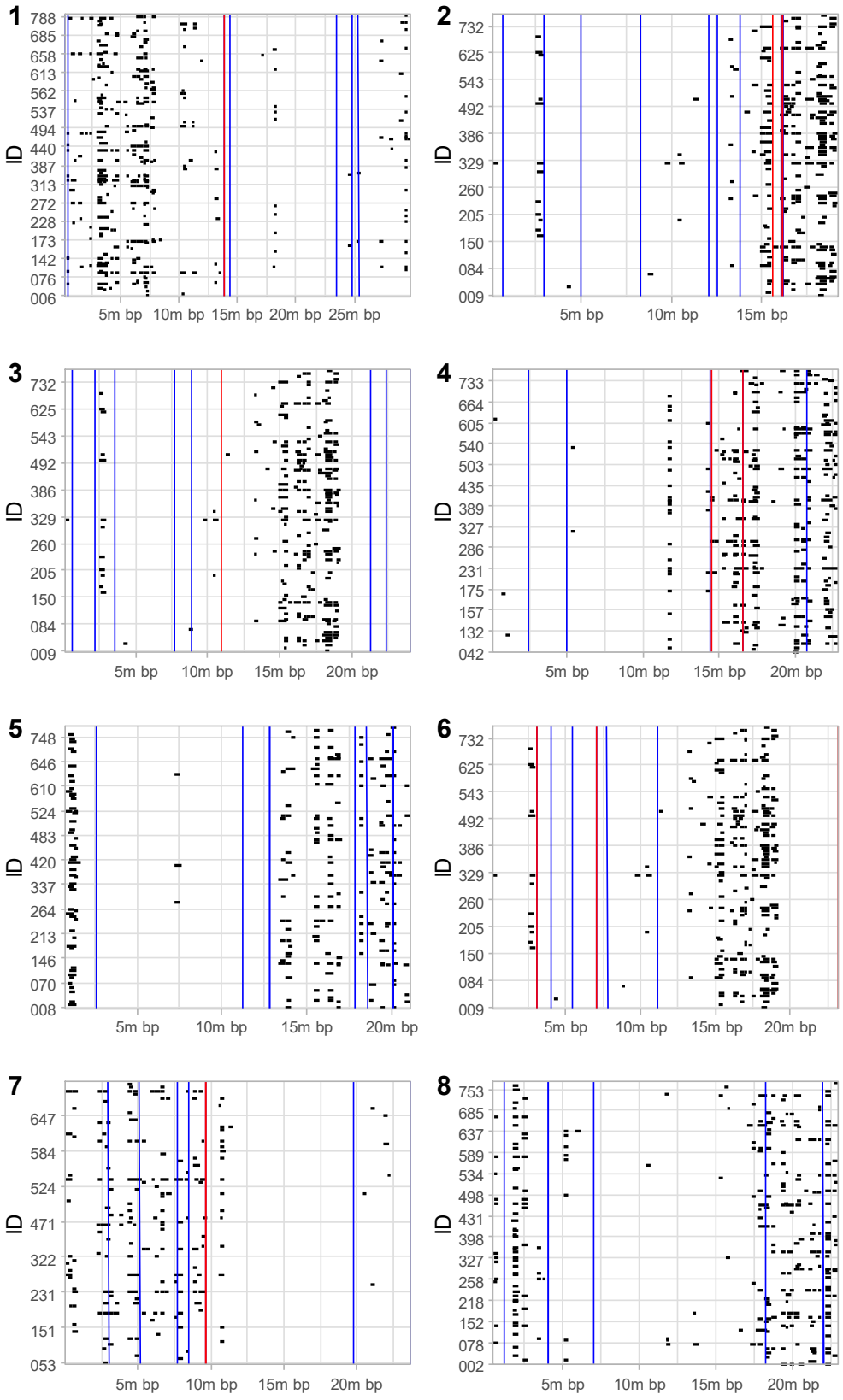

Figure S5: Distribution of runs of homozygosity (ROHs; black) for single individuals along the *A. lyrata* chromosome 1 to 8. Location of outlier genes are highlighted in blue and functional candidate genes in red.

Table S1: *PLINK* settings for calculating ROHs. Default settings and settings used in this study.

Setting	Default	Used
Homozyg-snp	100	40
Homozyg-kb	1000	250
Homozyg-density [kb/SNP]	50	1000
Homozyg-gap [kb]	1000	-
Homozyg-window-kb	5000	-
Homozyg-window-snp	50	40
Homozyg-window-het	1	-
Homozyg-window-missing	5	3
Homozyg-window-threshold	0.05	-

Table S2: Pearson correlation matrix among environmental variables (top) and among phenotypic traits (bottom). Corelation coefficients in lower and p-values in upper half. Red and blue indicate positive and negative significant correlations, respectively. Asterisks indicate significant levels: *** $p < 0.001$, ** $p < 0.01$, * $p < 0.05$, $^{\cdot}$ $p < 0.1$.

Environmental traits

Corr \ p	Dune position	Vegetation cover	Distance from trees	Intraspecific density
Dune position	-	0.000	0.000	0.005
Vegetation cover	0.144 ***	-	0.000	0.005
Distance from trees	-0.256 ***	0.193 ***	-	0.031
Intraspecific density	0.087 **	-0.069 **	-0.105 *	-

Phenotypic traits

Corr \ p	t_{ger}	t_{bol}	t_{flo}	s_{asym}	x_{mid}	r_{max}	res_{heat}	res_{frost}	*Leave trichomes*	*Leave shape*
t_{ger}	-	0.000	0.043	0.000	0.001	0.090	0.716	0.203	0.729	0.612
t_{bol}	-0.175 ***	-	0.000	0.016	0.506	0.195	0.677	0.153	0.023	0.702
t_{flo}	-0.121 *	0.763 ***	-	0.098	0.496	0.222	0.995	0.987	0.021	0.158
s_{asym}	-0.304 ***	-0.092 *	-0.044	-	0.008	0.000	0.748	0.518	0.838	0.000
x_{mid}	-0.606 ***	0.154	0.151	0.519 **	-	0.009	0.769	0.569	0.806	0.855
r_{max}	0.137 $^{\cdot}$	-0.042	-0.072	-0.182 ***	-0.475 **	-	0.800	0.011	0.267	0.644
res_{heat}	0.014	-0.006	-0.012	0.000	-0.019	0.075	-	0.726	0.705	0.773
res_{frost}	0.057	0.077	0.008	-0.039	-0.046	0.099 *	0.003	-	0.439	0.406
Leave trichomes	-0.021	-0.074 *	-0.093 *	0.015	-0.015	0.038	-0.021	-0.022	-	0.891
Leave shape	-0.008	0.005	0.059	0.168 ***	0.037	-0.038	0.015	0.045	0.003	-

Table S3: Test for spatial autocorrelation for all environmental variables.

	Moran's I	*p*
Dune position	-0.017	< 0.0001
Vegetation cover	-0.022	< 0.0001
Distance from trees	-0.038	< 0.0001
Intraspecific density	-0.042	< 0.0001

Table S4: Relationship between environmental variables - dune position, vegetation cover, distance from trees, and intraspecific density and each of ten phenotypical variables - time till germination (t_{ger}), bolting (t_{bol}) and flowering (t_{flo}), asymptotic size (s_{asym}), time till half growth (x_{mid}), maximum growth rate (r_{max}), heat and frost resistance, leave trichomes and leave shape. Estimates in red are positive and significant. Estimates in blue are negative and significant. Asterisks indicate significant levels: *** $p < 0.001$, ** $p < 0.01$, * $p < 0.05$, $^{\cdot}$ $p < 0.1$.

			t_{ger}	t_{bol}	t_{flo}	s_{asym}	x_{mid}	r_{max}	res_{heat}	res_{frost}	*Leave trichomes*	*Leave shape*
			est. (p)	est. (p)	est. (p)	est. (p)	est. (p)	est. (p)	est. (p)	est. (p)	est. (p)	est. (p)
Dune position			0.023	-0.001	-0.012	4.976	-0.262	0.008	-0.074	0.018	-0.482	0.602 $^{\cdot}$
Vegetation cover			-0.005	0.072 $^{\cdot}$	**0.159** **	-1.979	-0.217	-0.003	-0.030	0.023	**1.507*****	0.086
Distance from trees			0.025	-0.018	-0.035	-7.564 $^{\cdot}$	-1.055	-0.002	-0.060	0.010	0.154	-0.073
Intraspecific density			-0.004	-0.028	-0.107 $^{\cdot}$	7.553	1.374	-0.007	0.131	0.015	-0.667 $^{\cdot}$	-0.452
Estimate deviations are from section 4 in sampling year 2013												
Dune position	2	‘09	-0.029	-0.006	-0.043	-2.802	-0.188	0.009	0.071	0.005	**-3.714*****	-0.106
	2	‘10	-0.027	-0.020	-0.023	-6.634	-0.792	0.020	0.099	-0.016	0.810	-0.591
	2	‘13	-0.035	-0.028	-0.010	-0.855	1.100	-0.013	0.036	-0.035	0.928 $^{\cdot}$	-0.599
	2	‘14	**-0.078** *	0.002	-0.077	-1.627	1.689	-0.004	0.212 $^{\cdot}$	-0.055	-	-
	3	‘09	0.045	0.035	0.041	-8.300	-1.198	-0.001	0.088	-0.031	-1.361	-2.614 $^{\cdot}$
	3	‘10	-0.066	0.031	0.007	-11.823	1.388	-0.035 $^{\cdot}$	0.071	-0.050	-1.432	-0.825
	3	‘13	-0.014	-0.003	0.021	-4.071	0.654	-0.015	-0.040	-0.010	0.634	0.145
	3	‘14	-0.088 $^{\cdot}$	-0.063	-0.110	0.538	0.295	-0.004	0.205	-0.068	-	-
	4	‘10	0.030	-0.028	-0.093	**-18.759****	-1.375	-0.014	-0.017	-0.012	-	-
	4	‘13	-	-	-	-	-	-	-	-	-	-
Vegetation cover	2	‘09	-0.015	**-0.111** *	**-0.213** **	7.054	1.626	0.004	-0.087	-0.049	-0.092	-0.819
	2	‘10	0.011	-0.074	**-0.168** *	-2.027	0.682	0.006	0.118	-0.045	-0.599	0.352
	2	‘13	0.001	-0.053	**-0.132** *	3.627	0.965	0.010	0.051	-0.045	-0.744	0.172
	2	‘14	-0.022	-0.036	-0.053	11.080	1.659	0.012	-0.033	-0.001	-	-
	3	‘09	-0.050	-0.087 $^{\cdot}$	**-0.156** *	1.358	1.607	0.001	0.006	-0.006	-1.897 $^{\cdot}$	0.305
	3	‘10	0.050	-0.068	-0.140	-13.453	-3.553	0.011	0.119	0.132	0.220	-0.411
	3	‘13	-0.014	**-0.109****	**-0.206** **	1.987	0.912	0.001	0.088	-0.037	0.169	-0.439
	3	‘14	0.033	-0.052	-0.096	-0.042	0.651	0.000	0.018	0.079	-	-
	4	‘10	-0.048	-0.010	-0.024	3.638	1.798	0.015	0.173	0.063	-	-
	4	‘13	-	-	-	-	-	-	-	-	-	-
Distance from trees	2	‘09	-0.067 $^{\cdot}$	0.012	0.048	10.379 $^{\cdot}$	1.945	0.006	0.139	-0.015	**-2.619** *	0.258
	2	‘10	-0.062 $^{\cdot}$	0.013	0.045	7.169	0.527	0.021	0.030	-0.014	1.130	-0.049
	2	‘13	-0.039	0.002	0.029	**13.269** *	2.445	-0.008	0.054	-0.013	0.323	0.275
	2	‘14	-0.007	0.014	0.001	**19.347** **	2.372	-0.005	0.116	-0.034	-	-
	3	‘09	**-0.092** *	**-0.110** *	**-0.207** **	11.586 $^{\cdot}$	2.947	-0.006	0.037	-0.034	-2.164	-0.551
	3	‘10	-0.074	-0.027	-0.065	3.156	1.452	-0.002	-0.016	-0.112	1.907	0.629
	3	‘13	-0.027	0.025	0.067	7.487	1.419	0.003	0.020	-0.004	-0.228	0.038
	3	‘14	-0.026	-0.027	-0.046	12.639 $^{\cdot}$	1.168	-0.013	-0.029	-0.049	-	-
	4	‘10	-0.026	0.025	0.002	11.040	-0.218	-0.015	0.099	0.031	-	-
	4	‘13	-	-	-	-	-	-	-	-	-	-
Intraspecific density	2	‘09	-0.052	0.003	0.118 $^{\cdot}$	-4.796	-0.176	0.005	-0.086	-0.046	1.639	-0.565
	2	‘10	-0.001	0.011	0.080	-7.130	-1.456	0.010	-0.152	-0.002	0.718	0.329
	2	‘13	-0.006	0.029	0.107 $^{\cdot}$	-6.431	-1.259	0.008	-0.129	-0.044	0.258	-0.308
	2	‘14	**0.181*****	-0.015	0.089	-13.729	-3.541	0.001	-0.307 $^{\cdot}$	0.039	-	-
	3	‘09	-0.025	-0.068	-0.039	-7.868	-1.476	0.007	-0.157	-0.062	0.883	1.290
	3	‘10	0.002	-0.012	0.061	-7.459	-1.796	0.023	-0.109	-0.053	-1.109	0.331
	3	‘13	0.003	-0.001	0.065	-9.587 $^{\cdot}$	-1.829	-0.001	-0.118	-0.010	0.226	-0.200
	3	‘14	0.048	0.057	0.154 $^{\cdot}$	-7.946	-1.319	0.009	-0.224 $^{\cdot}$	-0.027	-	-
	4	‘10	0.053	0.004	0.042	-9.583	-3.254 $^{\cdot}$	0.014	-0.162	-0.018	-	-
	4	‘13	-	-	-	-	-	-	-	-	-	-

Table S5: Linear regression analysis of kinship distance on geographic distance for each year-section combination. Significant slopes are indicated in bold.

Section	Year	Slope	R^2	F	df	p
2	2009	-0.075	0.037	1.761	19	0.200
2	2010	-0.122	0.266	8.255	19	**0.010**
2	2013	-0.011	-0.227	0.076	4	0.796
2	2014	-0.009	-0.002	0.684	199	0.409
3	2009	0.308	-0.010	0.828	16	0.376
3	2010	0.074	0.118	2.739	12	0.124
3	2013	-0.002	-0.250	0.000	4	0.985
3	2014	-0.006	-0.086	0.054	11	0.821
4	2010	-0.041	0.103	3.076	17	0.097
4	2013	-0.028	0.059	9.252	130	**0.003**

Table S6: Comparison of slopes of kinship-dispersal relationship of different year-section combinations. Upper half-matrix shows *p* values. Lower half-matrix shows differences in slopes. Blue fields indicate significant slope differences (negative).

Est \ *p*	S2_09	S2_10	S2_13	S2_14	S3_09	S3_10	S3_13	S3_14	S4_10	S4_13
S2_09	-	0.439	**0.006**	**0.001**	0.975	**0.002**	**0.000**	**0.000**	0.174	**0.008**
S2_10	-0.101	-	0.501	0.100	1.000	0.101	**0.016**	**0.032**	0.988	0.615
S2_13	-0.152	-0.051	-	0.830	0.703	0.497	**0.032**	0.284	1.000	1.000
S2_14	-0.174	-0.073	-0.022	-	0.380	0.805	1.000	1.000	1.000	0.928
S3_09	-0.070	0.031	0.082	0.104	-	0.114	0.243	0.276	0.943	0.736
S3_10	-0.259	-0.159	-0.108	-0.085	-0.190	-	0.866	0.862	0.748	0.513
S3_13	-0.182	-0.081	-0.030	-0.008	-0.112	0.078	-	1.000	0.997	0.334
S3_14	-0.180	-0.080	-0.029	-0.006	-0.111	0.079	0.001	-	0.998	0.607
S4_10	-0.148	-0.047	0.004	0.026	-0.078	0.112	0.034	0.033	-	1.000
S4_13	-0.151	-0.051	0.001	0.023	-0.082	0.108	0.030	0.029	-0.003	-

Table S7: Annotation of all outlier SNPs in outlier genes with MAF > 0.1. Genes are sorted along their respective chromosome and in ascending chromosome number. Last three columns indicate the putative effect of all outlier SNPs.

Gene	No. outlier SNPs	3' prime UTR	5' prime UTR	Missense	Intron	Splice region & intron	Upstream gene	Synonymous	Downstream gene	Splice region & synonymous	Missense & splice region	Low	Moderate	Modifier
AL1G10810	2	-	-	1	-	-	-	1	-	-	-	1	1	-
AL1G11410	2	-	-	-	-	-	2	-	-	-	-	-	-	2
AL1G44720	2	-	-	1	-	-	-	-	-	-	1	-	2	-
AL1G44750	2	-	-	-	-	-	2	-	-	-	-	-	-	2
AL1G45720	2	-	-	-	-	-	2	-	-	-	-	-	-	2
AL1G53350	2	-	-	2	-	-	-	-	-	-	-	-	2	-
AL1G55480	4	-	-	3	-	-	-	1	-	-	-	1	3	-
AL1G56300	2	-	-	1	-	-	-	-	1	-	-	-	1	1
AL2G11470	2	-	-	-	-	-	-	2	-	-	-	2	-	-
AL2G15870	4	-	-	-	-	1	2	1	-	-	-	2	-	2
AL2G18710	3	-	-	2	-	-	-	1	-	-	-	1	2	-
AL2G20100	2	-	-	2	-	-	-	-	-	-	-	-	2	-
AL2G25320	5	-	-	3	-	-	-	2	-	-	-	2	3	-
AL2G26090	6	-	-	3	-	-	-	-	2	1	-	1	3	2
AL2G28640	2	-	-	-	-	-	2	-	-	-	-	-	-	2
AL2G32570	2	-	-	1	-	-	-	1	-	-	-	1	1	-
AL2G33880	3	-	-	1	-	-	1	1	-	-	-	1	1	1
AL2G33890	2	-	-	-	-	-	-	2	-	-	-	2	-	-
AL2G33900	3	-	-	1	-	-	1	1	-	-	-	1	1	1
AL2G33940	2	1	-	1	-	-	-	-	-	-	-	-	1	1
AL2G34000	12	-	-	4	-	-	-	6	2	-	-	6	4	2
AL2G34010	40	-	-	5	-	-	6	16	13	-	-	16	5	19
AL2G34030	5	1	-	2	-	-	-	2	-	-	-	2	2	1
AL2G34050	2	-	-	1	-	-	-	-	1	-	-	-	1	1
AL2G34060	13	1	-	4	2	-	-	6	-	-	-	6	4	3
AL3G11720	3	-	-	3	-	-	-	-	-	-	-	-	3	-
AL3G16440	4	-	-	-	4	-	-	-	-	-	-	-	-	4
AL3G19960	2	-	-	-	-	-	-	2	-	-	-	2	-	-
AL3G31220	8	-	-	2	-	-	3	3	-	-	-	3	2	3
AL3G31230	22	-	-	5	-	1	-	6	9	-	1	7	6	9
AL3G31240	2	-	-	-	-	-	2	-	-	-	-	-	-	2
AL3G34100	3	-	-	-	-	1	1	1	-	-	-	2	-	1
AL3G38380	36	-	1	3	-	4	21	5	2	-	-	9	3	24
AL3G49100	3	3	-	-	-	-	-	-	-	-	-	-	-	3
AL3G51100	3	-	-	-	-	-	3	-	-	-	-	-	-	3
AL3G54000	5	-	-	1	-	-	3	1	-	-	-	1	1	3
AL4G14260	3	-	1	-	-	-	-	1	1	-	-	1	-	2

Gene	No. outlier SNPs	3' prime UTR	5' prime UTR	Missense	Intron	Splice region & intron	Upstream gene	Synonymous	Downstream gene	Splice region & synonymous	Missense & splice region	Low	Moderate	Modifier
AL4G14270	2	-	-	2	-	-	-	-	-	-	-	-	2	-
AL4G17470	2	-	-	1	-	-	-	1	-	-	-	1	1	-
AL4G25810	2	2	-	-	-	-	-	-	-	-	-	-	-	2
AL4G25980	3	-	-	1	-	-	-	2	-	-	-	2	1	-
AL4G30860	5	-	-	3	-	-	2	-	-	-	-	-	3	2
AL4G30890	2	-	-	-	-	-	-	1	1	-	-	1	-	1
AL4G40930	2	-	-	-	-	-	2	-	-	-	-	-	-	2
AL5G14730	2	-	-	2	-	-	-	-	-	-	-	-	2	-
AL5G22750	6	-	-	-	4	-	-	2	-	-	-	2	-	4
AL5G25810	2	-	-	-	-	-	-	2	-	-	-	2	-	-
AL5G25820	3	-	-	3	-	-	-	-	-	-	-	-	3	-
AL5G37490	5	-	-	-	-	2	3	-	-	-	-	2	-	3
AL5G39280	3	-	-	-	1	-	-	2	-	-	-	2	-	1
AL5G43050	2	-	-	-	-	-	2	-	-	-	-	-	-	2
AL5G43070	2	-	-	-	-	-	2	-	-	-	-	-	-	2
AL6G18170	2	-	-	-	-	-	1	1	-	-	-	1	-	1
AL6G18180	4	-	-	-	-	1	2	1	-	-	-	2	-	2
AL6G20530	2	-	-	-	-	-	2	-	-	-	-	-	-	2
AL6G24050	2	-	-	1	-	-	1	-	-	-	-	-	1	1
AL6G28290	5	-	-	1	-	-	-	2	2	-	-	2	1	2
AL6G28300	10	-	-	1	-	1	-	2	6	-	-	3	1	6
AL6G29890	2	-	-	-	-	-	-	1	-	-	1	1	1	-
AL6G36680	10	-	-	-	-	-	-	7	3	-	-	7	-	3
AL6G49560	3	-	-	-	-	-	3	-	-	-	-	-	-	3
AL7G17280	2	-	-	1	-	-	1	-	-	-	-	-	1	1
AL7G22350	6	-	-	-	2	-	-	2	2	-	-	2	-	4
AL7G28920	2	-	-	-	-	-	2	-	-	-	-	-	-	2
AL7G30850	6	-	-	-	-	1	-	-	5	-	-	1	-	5
AL7G33490	2	-	-	-	-	-	1	-	1	-	-	-	-	2
AL7G33500	3	1	-	1	-	-	1	-	-	-	-	-	1	2
AL7G33510	3	-	-	-	-	-	3	-	-	-	-	-	-	3
AL7G45710	2	-	-	-	-	-	-	1	1	-	-	1	-	1
AL7G51810	3	-	-	-	3	-	-	-	-	-	-	-	-	3
AL8G12470	4	-	-	3	-	-	-	1	-	-	-	1	3	-
AL8G16610	2	-	-	-	-	-	-	1	1	-	-	1	-	1
AL8G16620	2	-	-	-	-	-	-	1	1	-	-	1	-	1
AL8G19530	4	-	-	-	-	-	4	-	-	-	-	-	-	4
AL8G33680	4	-	-	-	3	-	-	1	-	-	-	1	-	3
AL8G43030	19	-	-	3	-	1	4	4	7	-	-	5	3	11

Table S8

Table S8: Fixed effects model for the deviation from the expected mid-homozygous haplotype of environmental and phenotypic traits respectively. H^2 – total variability.

	AIC	H^2	Effect size	SE	Z	*p (Z)*
Environmental traits	-597.14	0.31	0.133	0.008	17.478	< 0.001
Phenotypic traits	-447.02	0.34	0.163	0.009	18.072	< 0.001

Figure S9

Table S9: Overview of outlier SNPs ($p < 0.005$) between the environmental and phenotypic trait of each environment-trait pair association in the GWAS analysis and all outlier genes (outlier SNPs > 1) with their *A. thaliana* homolog, gene name, and respective function.

Assoc	CHR	BP	Af_env	Af_phen	p (env)	p (phen)	Gene	AT homolog	Gene name	Function
Dune position - t_{flo}	1	14450203	0.179	0.178	0.00490	0.00384	NA			
Dune position - t_{flo}	1	16477669	0.118	0.116	0.00084	0.00076	NA			
Dune position - t_{flo}	1	21776932	0.201	0.197	0.00300	0.00194	NA			
Dune position - t_{flo}	1	4183963	0.347	0.347	0.00398	0.00266	AL1G21520			
Dune position - t_{flo}	2	10838940	0.177	0.177	0.00215	0.00420	AL2G23890			
Dune position - t_{flo}	2	10958368	0.233	0.234	0.00472	0.00401	AL2G24050			
Dune position - t_{flo}	2	16600155	0.166	0.167	0.00114	0.00487	AL2G35130			
Dune position - t_{flo}	2	16895779	0.245	0.244	0.00031	0.00298	NA			
Dune position - t_{flo}	2	17400386	0.472	0.473	0.00051	0.00124	AL2G37060			
Dune position - t_{flo}	2	4962728	0.105	0.104	0.00152	0.00098	AL2G18710			
Dune position - t_{flo}	2	4962761	0.091	0.089	0.00117	0.00035	AL2G18710			
Dune position - t_{flo}	2	4962763	0.093	0.091	0.00130	0.00017	AL2G18710			
Dune position - t_{flo}	2	4962770	0.091	0.089	0.00103	0.00008	AL2G18710	unknown		
Dune position - t_{flo}	2	4962772	0.093	0.091	0.00183	0.00027	AL2G18710			
Dune position - t_{flo}	2	4962782	0.11	0.108	0.00446	0.00012	AL2G18710			
Dune position - t_{flo}	2	4962793	0.11	0.108	0.00126	0.00017	AL2G18710			
Dune position - t_{flo}	3	10407243	0.513	0.507	0.00456	0.00340	AL3G37470			
Dune position - t_{flo}	3	2405011	0.176	0.177	0.00294	0.00172	AL3G16880			
Dune position - t_{flo}	3	2581374	0.114	0.115	0.00035	0.00363	AL3G17380			

Dune position - t_{flo}	3	3301854	0.613	0.608	0.00083	0.00447	AL3G19270			
Dune position - t_{flo}	4	10012128	0.078	0.076	0.00466	0.00464	NA			
Dune position - t_{flo}	4	11193326	0.178	0.175	0.00235	0.00173	NA			
Dune position - t_{flo}	4	11228485	0.177	0.175	0.00444	0.00188	NA			
Dune position - t_{flo}	4	11410651	0.136	0.135	0.00338	0.00355	AL4G21230			
Dune position - t_{flo}	4	11999242	0.08	0.077	0.00311	0.00491	AL4G21960			
Dune position - t_{flo}	4	12376590	0.077	0.075	0.00130	0.00350	NA			
Dune position - t_{flo}	4	15315543	0.119	0.12	0.00119	0.00088	AL4G27780			
Dune position - t_{flo}	4	19280722	0.899	0.898	0.00187	0.00088	AL4G37190			
Dune position - t_{flo}	4	20738763	0.182	0.182	0.00368	0.00310	AL4G40930	AT2G42470	-	TRAF-like family protein
Dune position - t_{flo}	4	20739049	0.19	0.189	0.00428	0.00462	AL4G40930			
Dune position - t_{flo}	4	6306469	0.112	0.11	0.00173	0.00462	NA			
Dune position - t_{flo}	4	6309181	0.12	0.117	0.00077	0.00343	NA			
Dune position - t_{flo}	5	10518074	0.069	0.068	0.00472	0.00311	AL5G21920			
Dune position - t_{flo}	5	13718193	0.199	0.198	0.00467	0.00104	NA			
Dune position - t_{flo}	5	2816507	0.213	0.211	0.00431	0.00206	NA			
Dune position - t_{flo}	5	4711590	0.188	0.189	0.00472	0.00386	NA			
Dune position - t_{flo}	6	3031566	0.498	0.5	0.00214	0.00004	AL6G18120			
Dune position - t_{flo}	6	3885953	0.207	0.209	0.00351	0.00116	NA			
Dune position - t_{flo}	6	3955763	0.053	0.052	0.00169	0.00370	NA			
Dune position - t_{flo}	6	3955764	0.053	0.052	0.00165	0.00354	NA			
Dune position - t_{flo}	6	3955862	0.252	0.253	0.00398	0.00030	NA			
Dune position - t_{flo}	6	3955945	0.053	0.051	0.00357	0.00379	NA			
Dune position - t_{flo}	6	3984802	0.62	0.621	0.00256	0.00007	AL6G20530			

Dune position - t_{flo}	6	4069652	0.722	0.722	0.00040	0.00209	AL6G20680			
Dune position - t_{flo}	6	4661560	0.193	0.191	0.00007	0.00412	AL6G22270			
Dune position - t_{flo}	6	4674285	0.242	0.241	0.00035	0.00425	AL6G22280			
Dune position - t_{flo}	6	5448487	0.145	0.147	0.00011	0.00177	AL6G24120			
Dune position - t_{flo}	6	5539190	0.055	0.054	0.00462	0.00473	AL6G24330			
Dune position - t_{flo}	6	752068	0.239	0.239	0.00079	0.00385	AL6G12050			
Dune position - t_{flo}	7	13096565	0.127	0.125	0.00330	0.00118	NA			
Dune position - t_{flo}	7	13218007	0.114	0.113	0.00162	0.00219	NA			
Dune position - t_{flo}	7	17741488	0.149	0.147	0.00141	0.00260	NA			
Dune position - t_{flo}	7	17741619	0.165	0.164	0.00335	0.00491	NA			
Dune position - t_{flo}	7	18844256	0.224	0.221	0.00324	0.00004	NA			
Dune position - t_{flo}	7	21211633	0.154	0.154	0.00012	0.00360	AL7G47340			
Dune position - t_{flo}	7	5742403	0.117	0.118	0.00034	0.00424	AL7G24040			
Dune position - t_{flo}	7	6689546	0.245	0.24	0.00162	0.00159	AL7G26570			
Dune position - t_{flo}	7	8223932	0.845	0.844	0.00214	0.00484	AL7G30270			
Dune position - t_{flo}	8	12021213	0.731	0.735	0.00378	0.00352	NA			
Dune position - t_{flo}	8	13370748	0.447	0.448	0.00140	0.00282	NA			
Dune position - t_{flo}	8	14653004	0.628	0.631	0.00337	0.00347	NA			
Dune position - t_{flo}	8	15126612	0.1	0.096	0.00416	0.00045	AL8G26860			
Dune position - t_{flo}	8	1514493	0.153	0.153	0.00236	0.00157	AL8G13000			
Dune position - t_{flo}	8	15147290	0.078	0.078	0.00008	0.00010	NA			
Dune position - t_{flo}	8	15151394	0.066	0.066	0.00088	0.00086	NA			
Dune position - t_{flo}	8	6430110	0.103	0.103	0.00180	0.00116	NA			
Assoc	**CHR**	**BP**	**Af_env**	**Af_phen**	**p (env)**	**p (phen)**	**Gene**	**AT homolog**	**Gene name**	**Function**

Dune position - s_{asym}	1	28830645	0.172	0.172	0.00228	0.00220	AL1G62560			
Dune position - s_{asym}	1	3368306	0.175	0.175	0.00043	0.00261	NA			
Dune position - s_{asym}	1	3369173	0.17	0.17	0.00003	0.00368	AL1G19310			
Dune position - s_{asym}	1	9847516	0.061	0.061	0.00215	0.00090	NA			
Dune position - s_{asym}	2	2110850	0.343	0.343	0.00067	0.00054	NA			
Dune position - s_{asym}	2	9411112	0.413	0.413	0.00440	0.00323	NA			
Dune position - s_{asym}	2	9411118	0.438	0.438	0.00286	0.00017	NA			
Dune position - s_{asym}	3	927675	0.109	0.109	0.00108	0.00141	AL3G12720			
Dune position - s_{asym}	4	11406958	0.174	0.174	0.00335	0.00294	AL4G21220			
Dune position - s_{asym}	4	16574296	0.171	0.171	0.00104	0.00410	AL4G30860	AT1G30620	HSR8, MUR4, UXE1	Catalyzes 4-epimerization of UDP-D-Xylose to UDP-L-Arabinose in vitro, the nucleotide sugar used by glycosyltransferases in the arabinosylation of cell wall polysaccharides and wall-resident proteoglycans.
Dune position - s_{asym}	4	16574326	0.165	0.165	0.00106	0.00426	AL4G30860			
Dune position - s_{asym}	4	16574405	0.18	0.18	0.00089	0.00123	AL4G30860			
Dune position - s_{asym}	4	16574644	0.167	0.167	0.00036	0.00358	AL4G30860			
Dune position - s_{asym}	4	16574686	0.196	0.196	0.00009	0.00480	AL4G30860			
Dune position - s_{asym}	4	16582058	0.685	0.685	0.00050	0.00289	AL4G30890	AT2G34880	JMJ15, PKDM7C	JMJ15 - novel H3K4 demethylase that regulates genes involved in flowering and stress response.
Dune position - s_{asym}	4	16582151	0.692	0.692	0.00113	0.00461	AL4G30890			
Dune position - s_{asym}	4	6233788	0.229	0.229	0.00134	0.00015	NA			
Dune position - s_{asym}	4	7004840	0.066	0.066	0.00407	0.00118	NA			
Dune position - s_{asym}	4	961659	0.036	0.036	0.00096	0.00387	AL4G11960			
Dune position - s_{asym}	5	11643253	0.122	0.122	0.00026	0.00066	NA			
Dune position - s_{asym}	5	11643609	0.133	0.133	0.00027	0.00134	NA			
Dune position - s_{asym}	5	11643766	0.136	0.136	0.00024	0.00148	NA			
Dune position - s_{asym}	5	11643812	0.112	0.112	0.00091	0.00379	NA			
Dune position - s_{asym}	5	17226496	0.489	0.489	0.00068	0.00405	AL5G35980			

Dune position - s_{asym}	5	5102948	0.121	0.121	0.00163	0.00062	NA			
Dune position - s_{asym}	5	5459440	0.394	0.394	0.00096	0.00396	NA			
Dune position - s_{asym}	6	11661922	0.446	0.446	0.00237	0.00144	NA			
Dune position - s_{asym}	6	19081853	0.209	0.209	0.00478	0.00422	NA			
Dune position - s_{asym}	6	20299210	0.106	0.106	0.00499	0.00439	NA			
Dune position - s_{asym}	6	24494947	0.504	0.504	0.00062	0.00453	AL6G52260			
Dune position - s_{asym}	6	3056651	0.737	0.737	0.00498	0.00183	AL6G18170	AT5G07830	GUS2	Protein that is extensively modified posttranslationally. Involved in cell elongation.
Dune position - s_{asym}	6	3057392	0.775	0.775	0.00370	0.00353	AL6G18170			
Dune position - s_{asym}	6	3058982	0.737	0.737	0.00353	0.00067	AL6G18180	AT5G07840	PIA1	Ankyrin repeat family protein
Dune position - s_{asym}	6	3059319	0.741	0.741	0.00332	0.00125	AL6G18180			
Dune position - s_{asym}	6	3059426	0.745	0.745	0.00450	0.00070	AL6G18180			
Dune position - s_{asym}	6	3059442	0.741	0.741	0.00356	0.00232	AL6G18180			
Dune position - s_{asym}	6	5150579	0.058	0.058	0.00378	0.00476	AL6G23480	AT5G12920	-	Transducin/WD40 repeat-like superfamily protein
Dune position - s_{asym}	6	5150609	0.058	0.058	0.00378	0.00477	AL6G23480			
Dune position - s_{asym}	6	5419821	0.432	0.432	0.00170	0.00206	AL6G24050	AT5G13430	RISP	Rieske FeS protein.Ubiquinol-cytochrome C reductase iron-sulfur subunit
Dune position - s_{asym}	6	5420607	0.429	0.429	0.00019	0.00082	AL6G24050			
Dune position - s_{asym}	7	12610043	0.206	0.206	0.00142	0.00474	AL7G39420			
Dune position - s_{asym}	7	23712655	0.241	0.241	0.00228	0.00429	AL7G51810			
Dune position - s_{asym}	7	23712700	0.105	0.105	0.00074	0.00110	AL7G51810	unknown		
Dune position - s_{asym}	7	23712888	0.119	0.119	0.00103	0.00079	AL7G51810			
Dune position - s_{asym}	8	13798321	0.165	0.165	0.00431	0.00237	AL8G24270			
Dune position - s_{asym}	8	17029393	0.214	0.214	0.00416	0.00187	AL8G30920			
Assoc	**CHR**	**BP**	**Af_env**	**Af_phen**	**p (env)**	**p (phen)**	**Gene**	**AT homolog**	**Gene name**	**Function**
Dune position - *leave shape*	1	28974788	0.501	0.501	0.00024	0.00053	AL1G62860			

Dune position - *leave shape*	1	30656326	0.331	0.331	0.00352	0.00331	NA			
Dune position - *leave shape*	1	31282945	0.179	0.179	0.00126	0.00093	NA			
Dune position - *leave shape*	1	31283177	0.17	0.17	0.00301	0.00314	NA			
Dune position - *leave shape*	1	5963612	0.16	0.16	0.00310	0.00438	AL1G26020			
Dune position - *leave shape*	1	6209923	0.138	0.138	0.00298	0.00014	AL1G26670			
Dune position - *leave shape*	1	7746956	0.268	0.268	0.00240	0.00415	AL1G30880			
Dune position - *leave shape*	1	7910667	0.128	0.128	0.00188	0.00397	AL1G31240			
Dune position - *leave shape*	1	8013153	0.242	0.242	0.00286	0.00338	AL1G31490			
Dune position - *leave shape*	1	9502970	0.165	0.165	0.00341	0.00222	NA			
Dune position - *leave shape*	2	17340739	0.058	0.058	0.00345	0.00085	AL2G36950			
Dune position - *leave shape*	2	1790383	0.923	0.923	0.00310	0.00093	AL2G13540			
Dune position - *leave shape*	2	1808076	0.05	0.05	0.00369	0.00141	AL2G13580			
Dune position - *leave shape*	2	2431668	0.037	0.037	0.00145	0.00016	AL2G14750			
Dune position - *leave shape*	3	1789069	0.058	0.058	0.00139	0.00429	AL3G15320			
Dune position - *leave shape*	3	21250864	0.438	0.438	0.00320	0.00216	NA			
Dune position - *leave shape*	3	21251806	0.433	0.433	0.00050	0.00376	AL3G49100	AT4G38920	AVA-P3, VHA-C3	vacuolar-type H[+]-ATPase C3
Dune position - *leave shape*	3	21251813	0.437	0.437	0.00088	0.00448	AL3G49100			
Dune position - *leave shape*	3	21251838	0.434	0.434	0.00125	0.00211	AL3G49100			
Dune position - *leave shape*	3	22302481	0.528	0.528	0.00497	0.00382	AL3G50910			
Dune position - *leave shape*	4	16121100	0.826	0.826	0.00088	0.00216	NA			
Dune position - *leave shape*	4	16121197	0.161	0.161	0.00287	0.00383	AL4G29880			
Dune position - *leave shape*	4	18263830	0.185	0.185	0.00359	0.00498	AL4G34690			
Dune position - *leave shape*	4	21790783	0.063	0.063	0.00081	0.00419	NA			
Dune position - *leave shape*	4	6283153	0.073	0.073	0.00139	0.00430	AL4G18940			

Dune position - *leave shape*	4	9860567	0.059	0.059	0.00304	0.00433	NA			
Dune position - *leave shape*	4	9946187	0.162	0.162	0.00228	0.00189	AL4G19710			
Dune position - *leave shape*	5	13315050	0.179	0.179	0.00334	0.00050	NA			
Dune position - *leave shape*	5	19377689	0.756	0.756	0.00069	0.00411	AL5G41460			
Dune position - *leave shape*	5	2635116	0.371	0.371	0.00012	0.00174	AL5G14730	AT3G26050	-	TPX2 (targeting protein for Xklp2) protein family
Dune position - *leave shape*	5	2636965	0.318	0.318	0.00001	0.00286	AL5G14730			
Dune position - *leave shape*	5	2638955	0.283	0.283	0.00454	0.00283	AL5G14740			
Dune position - *leave shape*	5	3698078	0.094	0.094	0.00030	0.00016	NA			
Dune position - *leave shape*	5	3698114	0.102	0.102	0.00033	0.00018	NA			
Dune position - *leave shape*	5	3698364	0.102	0.102	0.00161	0.00029	NA			
Dune position - *leave shape*	5	3698753	0.101	0.101	0.00030	0.00040	NA			
Dune position - *leave shape*	5	4224543	0.137	0.137	0.00462	0.00180	AL5G17490			
Dune position - *leave shape*	5	437340	0.362	0.362	0.00043	0.00022	NA			
Dune position - *leave shape*	5	5997724	0.156	0.156	0.00223	0.00287	NA			
Dune position - *leave shape*	6	10350236	0.101	0.101	0.00274	0.00377	AL6G35420			
Dune position - *leave shape*	6	11566549	0.058	0.058	0.00055	0.00382	AL6G37570			
Dune position - *leave shape*	6	4989448	0.12	0.12	0.00076	0.00162	AL6G23090			
Dune position - *leave shape*	6	4990716	0.087	0.087	0.00377	0.00087	NA			
Dune position - *leave shape*	6	4998937	0.1	0.1	0.00276	0.00176	NA			
Dune position - *leave shape*	6	912339	0.22	0.22	0.00280	0.00439	AL6G12560			
Dune position - *leave shape*	6	9866415	0.15	0.15	0.00178	0.00199	AL6G34340			
Dune position - *leave shape*	7	11755384	0.059	0.059	0.00002	0.00315	AL7G37820			
Dune position - *leave shape*	7	11937431	0.119	0.119	0.00078	0.00149	AL7G38100			
Dune position - *leave shape*	7	12257819	0.106	0.106	0.00245	0.00458	AL7G38810			

Dune position - *leave shape*	7	13827077	0.086	0.086	0.00028	0.00327	NA			
Dune position - *leave shape*	7	24472333	0.472	0.472	0.00097	0.00173	NA			
Dune position - *leave shape*	7	9430900	0.366	0.366	0.00192	0.00266	AL7G32910			
Dune position - *leave shape*	8	1471331	0.409	0.409	0.00204	0.00496	NA			
Assoc	**CHR**	**BP**	**Af_env**	**Af_phen**	**p (env)**	**p (phen)**	**Gene**	**AT homolog**	**Gene name**	**Function**
Vegetation cover - t_{flo}	1	1170414	0.092	0.09	0.00088	0.00471	NA			
Vegetation cover - t_{flo}	1	1170507	0.087	0.085	0.00192	0.00416	NA			
Vegetation cover - t_{flo}	1	1170520	0.088	0.086	0.00216	0.00310	NA			
Vegetation cover - t_{flo}	1	1171253	0.091	0.088	0.00108	0.00235	AL1G13400			
Vegetation cover - t_{flo}	1	14300521	0.068	0.069	0.00015	0.00347	AL1G45710	AT5G45390	CLPP4, NCLPP4	One of several nuclear-encoded ClpPs (caseinolytic protease).
Vegetation cover - t_{flo}	1	14300528	0.069	0.07	0.00017	0.00357	AL1G45710			
Vegetation cover - t_{flo}	1	14300775	0.084	0.082	0.00000	0.00235	AL1G45710			
Vegetation cover - t_{flo}	1	14302596	0.914	0.917	0.00000	0.00187	AL1G45720	AT5G45400	RPA1C, RPA70C	Replication factor-A protein 1-like protein
Vegetation cover - t_{flo}	1	14302601	0.914	0.916	0.00000	0.00227	AL1G45720			
Vegetation cover - t_{flo}	1	1561920	0.082	0.083	0.00369	0.00097	AL1G14360	AT1G04650	FLIP	Forms a complex with FIGL1 regulates meiotic crossover formation via RAD51 and DMC1
Vegetation cover - t_{flo}	1	1564686	0.082	0.083	0.00279	0.00267	AL1G14360			
Vegetation cover - t_{flo}	1	17696549	0.069	0.07	0.00092	0.00082	AL1G50800			
Vegetation cover - t_{flo}	1	23492867	0.449	0.449	0.00002	0.00419	AL1G53350	AT4G16143	IMPA2	Protein interacts with Agrobacterium proteins VirD2 and VirE2.
Vegetation cover - t_{flo}	1	23492916	0.449	0.449	0.00006	0.00288	AL1G53350			
Vegetation cover - t_{flo}	1	24847364	0.259	0.262	0.00007	0.00329	AL1G55480	AT1G48760	AP-3DELTA	Encodes the putative delta subunit of the AP(adaptor protein)-3 complex and plays a role in vacuolar function.
Vegetation cover - t_{flo}	1	24847370	0.257	0.26	0.00010	0.00192	AL1G55480			
Vegetation cover - t_{flo}	1	24848650	0.266	0.269	0.00007	0.00140	AL1G55480			
Vegetation cover - t_{flo}	1	24849196	0.262	0.266	0.00004	0.00246	AL1G55480			
Vegetation cover - t_{flo}	1	24990111	0.233	0.236	0.00000	0.00478	AL1G55730			

Vegetation cover - t_{flo}	1	24994606	0.552	0.553	0.00060	0.00115	NA			
Vegetation cover - t_{flo}	1	24999254	0.482	0.482	0.00054	0.00205	NA			
Vegetation cover - t_{flo}	1	24999287	0.462	0.462	0.00034	0.00323	NA			
Vegetation cover - t_{flo}	1	25001478	0.271	0.275	0.00000	0.00498	AL1G55740			
Vegetation cover - t_{flo}	1	25005342	0.284	0.288	0.00000	0.00204	AL1G55750			
Vegetation cover - t_{flo}	1	25345243	0.201	0.197	0.00085	0.00304	AL1G56300	AT1G49340	ATPI4K ALPHA	Encodes a phosphatidylinositol 4-kinase that is expressed in inflorescences and shoots.
Vegetation cover - t_{flo}	1	25345893	0.219	0.215	0.00017	0.00044	AL1G56300			
Vegetation cover - t_{flo}	1	25409833	0.299	0.296	0.00028	0.00426	AL1G56430			
Vegetation cover - t_{flo}	1	25442918	0.07	0.071	0.00137	0.00140	NA			
Vegetation cover - t_{flo}	1	25771370	0.055	0.056	0.00404	0.00466	AL1G57010			
Vegetation cover - t_{flo}	1	25806755	0.088	0.089	0.00028	0.00396	NA			
Vegetation cover - t_{flo}	1	29070561	0.698	0.694	0.00133	0.00173	AL1G63040			
Vegetation cover - t_{flo}	1	30900724	0.684	0.683	0.00002	0.00061	AL1G65130			
Vegetation cover - t_{flo}	1	31069937	0.345	0.346	0.00407	0.00247	NA			
Vegetation cover - t_{flo}	1	31070420	0.347	0.35	0.00403	0.00398	NA			
Vegetation cover - t_{flo}	1	31082471	0.342	0.345	0.00249	0.00365	NA			
Vegetation cover - t_{flo}	1	31084820	0.344	0.345	0.00349	0.00421	NA			
Vegetation cover - t_{flo}	1	32084682	0.406	0.405	0.00084	0.00150	AL1G65870			
Vegetation cover - t_{flo}	1	481396	0.843	0.844	0.00376	0.00107	AL1G11410	AT1G01110	IQD18	Member of IQ67 (CaM binding) domain containing family.
Vegetation cover - t_{flo}	1	481410	0.845	0.846	0.00294	0.00062	AL1G11410			
Vegetation cover - t_{flo}	2	12493144	0.078	0.076	0.00068	0.00485	AL2G26040			
Vegetation cover - t_{flo}	2	1304829	0.211	0.21	0.00235	0.00164	NA			
Vegetation cover - t_{flo}	2	13174535	0.101	0.102	0.00001	0.00334	AL2G27410			
Vegetation cover - t_{flo}	2	14216962	0.236	0.236	0.00086	0.00369	AL2G29370			

Vegetation cover - t_{flo}	2	15018040	0.882	0.88	0.00415	0.00398	AL2G31290			
Vegetation cover - t_{flo}	2	15019613	0.884	0.882	0.00267	0.00470	AL2G31300			
Vegetation cover - t_{flo}	2	15021461	0.889	0.887	0.00064	0.00458	AL2G31320			
Vegetation cover - t_{flo}	2	15588132	0.084	0.082	0.00398	0.00052	AL2G32540			
Vegetation cover - t_{flo}	2	4482725	0.07	0.071	0.00138	0.00053	AL2G18100			
Vegetation cover - t_{flo}	2	7764845	0.386	0.388	0.00157	0.00039	AL2G19540			
Vegetation cover - t_{flo}	2	8252103	0.156	0.155	0.00279	0.00205	AL2G20060			
Vegetation cover - t_{flo}	2	8306647	0.493	0.493	0.00409	0.00258	AL2G20100	AT1G04640	LIP2	Lipoyltransferase, located in mitochondria but not found in chloroplasts
Vegetation cover - t_{flo}	2	8306655	0.497	0.497	0.00058	0.00326	AL2G20100			
Vegetation cover - t_{flo}	3	10640307	0.297	0.294	0.00303	0.00292	NA			
Vegetation cover - t_{flo}	3	10933233	0.197	0.198	0.00370	0.00390	AL3G38380	AT3G23640	HGL1	Protein which interacts with Feronia; likely involved in FER-mediated intracellular signaling pathways that are essential in plant growth and development, and possibly plant immunity.
Vegetation cover - t_{flo}	3	10933337	0.207	0.207	0.00131	0.00337	AL3G38380			
Vegetation cover - t_{flo}	3	10933438	0.217	0.219	0.00175	0.00483	AL3G38380			
Vegetation cover - t_{flo}	3	10933478	0.21	0.212	0.00058	0.00349	AL3G38380			
Vegetation cover - t_{flo}	3	10933713	0.206	0.208	0.00214	0.00416	AL3G38380			
Vegetation cover - t_{flo}	3	10933931	0.207	0.209	0.00111	0.00189	AL3G38380			
Vegetation cover - t_{flo}	3	10933970	0.208	0.21	0.00170	0.00226	AL3G38380			
Vegetation cover - t_{flo}	3	10934063	0.202	0.201	0.00110	0.00340	AL3G38380			
Vegetation cover - t_{flo}	3	10934083	0.209	0.208	0.00087	0.00361	AL3G38380			
Vegetation cover - t_{flo}	3	10934109	0.206	0.206	0.00080	0.00459	AL3G38380			
Vegetation cover - t_{flo}	3	10934137	0.202	0.201	0.00154	0.00390	AL3G38380			
Vegetation cover - t_{flo}	3	10934148	0.202	0.201	0.00153	0.00439	AL3G38380			
Vegetation cover - t_{flo}	3	10934163	0.207	0.207	0.00082	0.00220	AL3G38380			
Vegetation cover - t_{flo}	3	10934165	0.207	0.207	0.00082	0.00220	AL3G38380			

Vegetation cover - t_{flo}	3	10934179	0.194	0.193	0.00127	0.00417	AL3G38380			
Vegetation cover - t_{flo}	3	10934406	0.214	0.214	0.00151	0.00371	AL3G38380			
Vegetation cover - t_{flo}	3	10934416	0.212	0.214	0.00148	0.00371	AL3G38380			
Vegetation cover - t_{flo}	3	10934443	0.21	0.212	0.00115	0.00411	AL3G38380			
Vegetation cover - t_{flo}	3	10934446	0.21	0.212	0.00115	0.00411	AL3G38380			
Vegetation cover - t_{flo}	3	10934450	0.21	0.212	0.00115	0.00411	AL3G38380			
Vegetation cover - t_{flo}	3	10934488	0.209	0.212	0.00117	0.00411	AL3G38380			
Vegetation cover - t_{flo}	3	10934805	0.207	0.21	0.00183	0.00316	AL3G38380			
Vegetation cover - t_{flo}	3	10934856	0.208	0.21	0.00203	0.00419	AL3G38380			
Vegetation cover - t_{flo}	3	10935515	0.212	0.211	0.00455	0.00419	AL3G38380			
Vegetation cover - t_{flo}	3	10935517	0.212	0.211	0.00455	0.00419	AL3G38380			
Vegetation cover - t_{flo}	3	10936028	0.218	0.218	0.00130	0.00487	AL3G38380			
Vegetation cover - t_{flo}	3	10936699	0.217	0.218	0.00271	0.00446	AL3G38380			
Vegetation cover - t_{flo}	3	10937221	0.206	0.206	0.00307	0.00323	AL3G38380			
Vegetation cover - t_{flo}	3	10937739	0.212	0.212	0.00130	0.00488	AL3G38380			
Vegetation cover - t_{flo}	3	10937770	0.21	0.21	0.00171	0.00478	AL3G38380			
Vegetation cover - t_{flo}	3	10937776	0.21	0.21	0.00141	0.00247	AL3G38380			
Vegetation cover - t_{flo}	3	10937778	0.212	0.211	0.00188	0.00301	AL3G38380			
Vegetation cover - t_{flo}	3	10937779	0.212	0.211	0.00188	0.00301	AL3G38380			
Vegetation cover - t_{flo}	3	10938130	0.212	0.212	0.00289	0.00309	AL3G38380			
Vegetation cover - t_{flo}	3	10938516	0.212	0.212	0.00328	0.00471	AL3G38380			
Vegetation cover - t_{flo}	3	10939315	0.205	0.205	0.00415	0.00415	AL3G38380			
Vegetation cover - t_{flo}	3	11875039	0.487	0.493	0.00283	0.00206	NA			
Vegetation cover - t_{flo}	3	12789405	0.066	0.067	0.00186	0.00139	NA			

Vegetation cover - t_{flo}	3	12797212	0.074	0.075	0.00044	0.00033	NA			
Vegetation cover - t_{flo}	3	12797340	0.07	0.071	0.00041	0.00049	NA			
Vegetation cover - t_{flo}	3	12798614	0.068	0.069	0.00077	0.00080	NA			
Vegetation cover - t_{flo}	3	12801277	0.07	0.071	0.00141	0.00084	NA			
Vegetation cover - t_{flo}	3	14565544	0.051	0.051	0.00393	0.00416	AL3G43610			
Vegetation cover - t_{flo}	3	4415328	0.171	0.17	0.00380	0.00169	AL3G22540			
Vegetation cover - t_{flo}	3	4693484	0.153	0.155	0.00396	0.00196	NA			
Vegetation cover - t_{flo}	3	6142576	0.416	0.415	0.00470	0.00072	AL3G27000			
Vegetation cover - t_{flo}	4	10103906	0.616	0.614	0.00479	0.00354	NA			
Vegetation cover - t_{flo}	4	10112645	0.393	0.395	0.00406	0.00290	NA			
Vegetation cover - t_{flo}	4	10726127	0.504	0.507	0.00318	0.00022	AL4G20540			
Vegetation cover - t_{flo}	4	10807978	0.527	0.531	0.00122	0.00259	NA			
Vegetation cover - t_{flo}	4	12039662	0.071	0.066	0.00090	0.00074	AL4G22030			
Vegetation cover - t_{flo}	4	12051377	0.161	0.156	0.00262	0.00274	AL4G22050			
Vegetation cover - t_{flo}	4	12278590	0.259	0.252	0.00004	0.00411	AL4G22350			
Vegetation cover - t_{flo}	4	12828805	0.158	0.161	0.00041	0.00184	NA			
Vegetation cover - t_{flo}	4	14264569	0.101	0.099	0.00391	0.00341	NA			
Vegetation cover - t_{flo}	4	14531092	0.101	0.103	0.00002	0.00403	NA			
Vegetation cover - t_{flo}	4	14547956	0.276	0.269	0.00010	0.00420	AL4G25980	AT2G30950	FTSH2, VAR2	Involved in the repair of PSII following damaged during photoinhibition. Forms a complex with VAR1. Mutants show a variegated phenotype.
Vegetation cover - t_{flo}	4	14548115	0.219	0.218	0.00250	0.00033	AL4G25980			
Vegetation cover - t_{flo}	4	14549794	0.296	0.286	0.00063	0.00355	AL4G25980			
Vegetation cover - t_{flo}	4	14555650	0.153	0.152	0.00000	0.00213	AL4G26000			
Vegetation cover - t_{flo}	4	14907848	0.127	0.129	0.00101	0.00258	NA			
Vegetation cover - t_{flo}	4	22157974	0.18	0.177	0.00463	0.00325	AL4G44680			

Vegetation cover - t_{flo}	4	6242328	0.185	0.184	0.00094	0.00167	NA			
Vegetation cover - t_{flo}	4	6242669	0.104	0.105	0.00119	0.00380	NA			
Vegetation cover - t_{flo}	4	6242864	0.111	0.112	0.00005	0.00338	NA			
Vegetation cover - t_{flo}	5	12576221	0.076	0.077	0.00334	0.00330	AL5G25190			
Vegetation cover - t_{flo}	5	13873382	0.166	0.168	0.00283	0.00212	AL5G27990			
Vegetation cover - t_{flo}	5	20853707	0.808	0.812	0.00109	0.00298	AL5G45360			
Vegetation cover - t_{flo}	5	3026470	0.372	0.371	0.00299	0.00400	AL5G15500			
Vegetation cover - t_{flo}	5	4779950	0.6	0.597	0.00244	0.00085	NA			
Vegetation cover - t_{flo}	5	4805990	0.541	0.545	0.00414	0.00195	AL5G18250			
Vegetation cover - t_{flo}	5	5999790	0.269	0.273	0.00005	0.00239	NA			
Vegetation cover - t_{flo}	6	13092795	0.091	0.089	0.00003	0.00382	NA			
Vegetation cover - t_{flo}	6	23209638	0.583	0.584	0.00084	0.00489	AL6G49560	AT4G03350 or AT4G02970	EVE1	Protein involved in the transition from the vegetative to the reproductive phase of growth.
Vegetation cover - t_{flo}	6	23209706	0.59	0.587	0.00098	0.00399	AL6G49560			
Vegetation cover - t_{flo}	6	23209712	0.599	0.596	0.00051	0.00441	AL6G49560		AT7SL-1	Signal recognition particle.
Vegetation cover - t_{flo}	6	23209837	0.599	0.597	0.00039	0.00465	NA			
Vegetation cover - t_{flo}	6	23209839	0.598	0.596	0.00040	0.00462	NA			
Vegetation cover - t_{flo}	6	23209885	0.591	0.589	0.00019	0.00160	NA			
Vegetation cover - t_{flo}	6	23209893	0.58	0.581	0.00013	0.00153	NA			
Vegetation cover - t_{flo}	6	23209895	0.573	0.574	0.00006	0.00046	NA			
Vegetation cover - t_{flo}	6	23209900	0.576	0.577	0.00009	0.00080	NA			
Vegetation cover - t_{flo}	6	23209906	0.577	0.577	0.00007	0.00109	NA			
Vegetation cover - t_{flo}	6	23210478	0.348	0.35	0.00121	0.00490	AL6G49570			
Vegetation cover - t_{flo}	6	2723043	0.649	0.648	0.00122	0.00330	NA			
Vegetation cover - t_{flo}	6	6985106	0.07	0.071	0.00329	0.00275	AL6G28020			

Vegetation cover - t_{flo}	6	7048796	0.101	0.099	0.00256	0.00242	AL6G28220	AT5G17170	ENH1	rubredoxin family protein
Vegetation cover - t_{flo}	6	7048823	0.103	0.098	0.00447	0.00357	AL6G28220			
Vegetation cover - t_{flo}	6	7079555	0.658	0.661	0.00404	0.00389	AL6G28290	AT5G17240	SDG40	NMD epigenetically regulates FLC though SDG40 to modulate flowering time.
Vegetation cover - t_{flo}	6	7079571	0.665	0.668	0.00293	0.00417	AL6G28290			
Vegetation cover - t_{flo}	6	7079648	0.663	0.666	0.00337	0.00450	AL6G28290			
Vegetation cover - t_{flo}	6	7080143	0.658	0.661	0.00359	0.00248	AL6G28290			
Vegetation cover - t_{flo}	6	7080562	0.666	0.668	0.00453	0.00315	AL6G28290			
Vegetation cover - t_{flo}	6	7081604	0.639	0.64	0.00078	0.00067	AL6G28300	AT5G17250	-	Alkaline-phosphatase-like family protein
Vegetation cover - t_{flo}	6	7082808	0.648	0.65	0.00213	0.00265	AL6G28300			
Vegetation cover - t_{flo}	6	7082949	0.661	0.663	0.00458	0.00235	AL6G28300			
Vegetation cover - t_{flo}	6	7083381	0.672	0.675	0.00336	0.00413	AL6G28300			
Vegetation cover - t_{flo}	6	7083449	0.656	0.658	0.00265	0.00168	AL6G28300			
Vegetation cover - t_{flo}	6	7083462	0.65	0.652	0.00262	0.00161	AL6G28300			
Vegetation cover - t_{flo}	6	7083514	0.66	0.662	0.00166	0.00177	AL6G28300			
Vegetation cover - t_{flo}	6	7083528	0.667	0.669	0.00377	0.00223	AL6G28300			
Vegetation cover - t_{flo}	6	7083913	0.651	0.653	0.00336	0.00233	AL6G28300			
Vegetation cover - t_{flo}	6	7084323	0.651	0.654	0.00224	0.00363	AL6G28300			
Vegetation cover - t_{flo}	6	7880278	0.19	0.192	0.00164	0.00184	NA			
Vegetation cover - t_{flo}	6	7880288	0.191	0.194	0.00094	0.00053	NA			
Vegetation cover - t_{flo}	7	10825524	0.339	0.34	0.00315	0.00399	NA			
Vegetation cover - t_{flo}	7	10825771	0.302	0.299	0.00326	0.00162	NA			
Vegetation cover - t_{flo}	7	10825772	0.305	0.303	0.00303	0.00045	NA			
Vegetation cover - t_{flo}	7	17680870	0.114	0.108	0.00222	0.00027	NA			
Vegetation cover - t_{flo}	7	17721608	0.116	0.111	0.00174	0.00193	AL7G43640			

Vegetation cover - t_{flo}	7	17723217	0.107	0.101	0.00026	0.00442	NA
Vegetation cover - t_{flo}	7	17732319	0.122	0.116	0.00086	0.00053	NA
Vegetation cover - t_{flo}	7	17738042	0.118	0.113	0.00153	0.00141	NA
Vegetation cover - t_{flo}	7	17739342	0.106	0.101	0.00105	0.00143	NA
Vegetation cover - t_{flo}	7	17740202	0.094	0.088	0.00090	0.00376	NA
Vegetation cover - t_{flo}	7	17748280	0.12	0.115	0.00111	0.00060	NA
Vegetation cover - t_{flo}	7	17749057	0.119	0.117	0.00063	0.00089	NA
Vegetation cover - t_{flo}	7	17754985	0.104	0.102	0.00108	0.00093	NA
Vegetation cover - t_{flo}	7	17756320	0.115	0.109	0.00107	0.00027	NA
Vegetation cover - t_{flo}	7	17767491	0.111	0.106	0.00040	0.00149	NA
Vegetation cover - t_{flo}	7	17769118	0.123	0.118	0.00111	0.00058	NA
Vegetation cover - t_{flo}	7	17770113	0.121	0.115	0.00170	0.00022	NA
Vegetation cover - t_{flo}	7	17770407	0.112	0.107	0.00161	0.00022	NA
Vegetation cover - t_{flo}	7	17775526	0.114	0.108	0.00254	0.00208	NA
Vegetation cover - t_{flo}	7	17779361	0.124	0.119	0.00107	0.00078	NA
Vegetation cover - t_{flo}	7	17780497	0.103	0.097	0.00034	0.00124	NA
Vegetation cover - t_{flo}	7	17820750	0.305	0.303	0.00356	0.00063	NA
Vegetation cover - t_{flo}	7	17822008	0.119	0.117	0.00093	0.00039	NA
Vegetation cover - t_{flo}	7	17822099	0.321	0.318	0.00251	0.00069	NA
Vegetation cover - t_{flo}	7	17822190	0.122	0.117	0.00129	0.00053	NA
Vegetation cover - t_{flo}	7	17824311	0.318	0.316	0.00477	0.00039	NA
Vegetation cover - t_{flo}	7	17829435	0.32	0.317	0.00305	0.00100	NA
Vegetation cover - t_{flo}	7	17841297	0.121	0.115	0.00087	0.00070	AL7G43760
Vegetation cover - t_{flo}	7	17867374	0.125	0.12	0.00101	0.00046	NA

Vegetation cover - t_{flo}	7	17891646	0.114	0.111	0.00442	0.00080	AL7G43810			
Vegetation cover - t_{flo}	7	18893770	0.142	0.141	0.00132	0.00147	NA			
Vegetation cover - t_{flo}	7	20667653	0.158	0.153	0.00285	0.00447	AL7G46590			
Vegetation cover - t_{flo}	7	21362763	0.103	0.105	0.00031	0.00096	AL7G47650			
Vegetation cover - t_{flo}	7	21745840	0.115	0.113	0.00309	0.00316	AL7G48360			
Vegetation cover - t_{flo}	7	22574040	0.241	0.241	0.00365	0.00406	NA			
Vegetation cover - t_{flo}	7	22861541	0.622	0.624	0.00469	0.00020	NA			
Vegetation cover - t_{flo}	7	22861671	0.618	0.62	0.00129	0.00009	NA			
Vegetation cover - t_{flo}	7	22861987	0.615	0.616	0.00446	0.00025	NA			
Vegetation cover - t_{flo}	7	22862288	0.542	0.542	0.00391	0.00248	NA			
Vegetation cover - t_{flo}	7	22862446	0.613	0.615	0.00298	0.00026	NA			
Vegetation cover - t_{flo}	7	22863039	0.61	0.612	0.00308	0.00013	NA			
Vegetation cover - t_{flo}	7	22863075	0.589	0.59	0.00321	0.00071	NA			
Vegetation cover - t_{flo}	7	22866388	0.559	0.559	0.00483	0.00054	NA			
Vegetation cover - t_{flo}	7	22869338	0.661	0.66	0.00336	0.00167	NA			
Vegetation cover - t_{flo}	7	2564039	0.442	0.441	0.00233	0.00374	AL7G16240			
Vegetation cover - t_{flo}	7	5095004	0.136	0.138	0.00193	0.00173	AL7G22350	AT4G29900	ACA10, CIF1	one of the type IIB calcium pump isoforms. encodes an autoinhibited Ca(2+)-ATPase that contains an N-terminal calmodulin binding autoinhibitory domain.ACA8 and ACA10, as well as ACA4 and ACA11, are critical in maintaining low resting cytosol Ca2+ level (DOI:10.1093/plphys/kiad047)
Vegetation cover - t_{flo}	7	5095847	0.139	0.141	0.00076	0.00181	AL7G22350			
Vegetation cover - t_{flo}	7	5097245	0.134	0.136	0.00091	0.00183	AL7G22350			
Vegetation cover - t_{flo}	7	5097554	0.127	0.128	0.00270	0.00363	AL7G22350			
Vegetation cover - t_{flo}	7	5097935	0.132	0.134	0.00096	0.00169	AL7G22350			
Vegetation cover - t_{flo}	7	5098056	0.14	0.142	0.00224	0.00208	AL7G22350			
Vegetation cover - t_{flo}	7	5109706	0.233	0.229	0.00278	0.00098	AL7G22390			
Vegetation cover - t_{flo}	7	5110117	0.755	0.759	0.00255	0.00299	NA			

Vegetation cover - t_{flo}	7	9757463	0.282	0.283	0.00082	0.00046	NA			
Vegetation cover - t_{flo}	7	9757616	0.282	0.283	0.00165	0.00043	NA			
Vegetation cover - t_{flo}	7	9757618	0.28	0.281	0.00180	0.00039	NA			
Vegetation cover - t_{flo}	7	9757638	0.272	0.272	0.00048	0.00029	NA			
Vegetation cover - t_{flo}	7	9757648	0.29	0.291	0.00224	0.00124	NA			
Vegetation cover - t_{flo}	7	9757731	0.288	0.288	0.00131	0.00102	NA			
Vegetation cover - t_{flo}	7	9757736	0.344	0.345	0.00104	0.00327	NA			
Vegetation cover - t_{flo}	7	9773299	0.276	0.277	0.00038	0.00447	AL7G33710			
Vegetation cover - t_{flo}	8	13370746	0.198	0.197	0.00331	0.00057	NA			
Vegetation cover - t_{flo}	8	18266496	0.359	0.361	0.00491	0.00437	NA			
Vegetation cover - t_{flo}	8	4599245	0.051	0.051	0.00219	0.00381	NA			
Vegetation cover - t_{flo}	8	7059454	0.51	0.51	0.00251	0.00384	NA			
Vegetation cover - t_{flo}	8	725074	0.321	0.323	0.00217	0.00479	AL8G11560			
Assoc	**CHR**	**BP**	**Af_env**	**Af_phen**	**p (env)**	**p (phen)**	**Gene**	**AT homolog**	**Gene name**	**Function**
Vegetation cover - res_{frost}	1	16066580	0.093	0.093	0.00069	0.00012	NA			
Vegetation cover - res_{frost}	1	32128542	0.245	0.245	0.00140	0.00400	AL1G65920			
Vegetation cover - res_{frost}	2	689512	0.051	0.051	0.00397	0.00228	NA			
Vegetation cover - res_{frost}	2	928708	0.315	0.315	0.00305	0.00084	AL2G11870			
Vegetation cover - res_{frost}	2	981484	0.218	0.218	0.00012	0.00059	NA			
Vegetation cover - res_{frost}	3	11215777	0.148	0.148	0.00159	0.00029	NA			
Vegetation cover - res_{frost}	3	12263466	0.358	0.358	0.00442	0.00152	AL3G40540			
Vegetation cover - res_{frost}	3	17677471	0.309	0.309	0.00399	0.00025	NA			
Vegetation cover - res_{frost}	3	19965805	0.132	0.132	0.00336	0.00460	NA			
Vegetation cover - res_{frost}	3	20435773	0.194	0.194	0.00383	0.00181	NA			

Vegetation cover - res_{frost}	3	23781889	0.08	0.08	0.00319	0.00240	NA			
Vegetation cover - res_{frost}	3	24063849	0.386	0.386	0.00301	0.00228	AL3G54000	AT2G20830	-	folic acid binding / transferase
Vegetation cover - res_{frost}	3	24064254	0.391	0.391	0.00431	0.00264	AL3G54000			
Vegetation cover - res_{frost}	3	24064314	0.393	0.393	0.00366	0.00241	AL3G54000			
Vegetation cover - res_{frost}	3	24064486	0.391	0.391	0.00235	0.00130	AL3G54000			
Vegetation cover - res_{frost}	3	24064494	0.392	0.392	0.00470	0.00271	AL3G54000			
Vegetation cover - res_{frost}	3	8285408	0.069	0.069	0.00466	0.00454	AL3G32600			
Vegetation cover - res_{frost}	4	1306072	0.069	0.069	0.00010	0.00330	NA			
Vegetation cover - res_{frost}	5	14124929	0.125	0.125	0.00217	0.00144	AL5G28560			
Vegetation cover - res_{frost}	5	18524850	0.374	0.374	0.00460	0.00387	AL5G39280	AT3G57660	NRPA1	Encodes a subunit of RNA polymerase I (aka RNA polymerase A). The mRNA is cell-to-cell mobile.
Vegetation cover - res_{frost}	5	18525496	0.322	0.322	0.00007	0.00123	AL5G39280			
Vegetation cover - res_{frost}	5	18525511	0.327	0.327	0.00028	0.00493	AL5G39280			
Vegetation cover - res_{frost}	5	5455526	0.242	0.242	0.00366	0.00062	NA			
Vegetation cover - res_{frost}	5	5806912	0.394	0.394	0.00185	0.00280	NA			
Vegetation cover - res_{frost}	6	17950315	0.061	0.061	0.00230	0.00494	NA			
Vegetation cover - res_{frost}	6	6075680	0.261	0.261	0.00015	0.00347	AL6G25740			
Vegetation cover - res_{frost}	6	9340872	0.142	0.142	0.00143	0.00276	NA			
Vegetation cover - res_{frost}	6	9348617	0.147	0.147	0.00035	0.00445	NA			
Vegetation cover - res_{frost}	7	12302399	0.086	0.086	0.00351	0.00212	NA			
Vegetation cover - res_{frost}	7	14125186	0.257	0.257	0.00141	0.00393	AL7G41830			
Vegetation cover - res_{frost}	7	18771854	0.053	0.053	0.00035	0.00091	AL7G44700			
Vegetation cover - res_{frost}	7	19466678	0.082	0.082	0.00369	0.00385	NA			
Vegetation cover - res_{frost}	7	22475100	0.233	0.233	0.00160	0.00001	AL7G49700			
Vegetation cover - res_{frost}	7	22890705	0.121	0.121	0.00123	0.00437	NA			

Assoc	CHR	BP	Af_env	Af_phen	p (env)	p (phen)	Gene	AT homolog	Gene name	Function
Vegetation cover - *res*$_{frost}$	8	5767367	0.06	0.06	0.00246	0.00191	NA			
Vegetation cover - *leave trichomes*	1	12259581	0.516	0.516	0.00280	0.00460	NA			
Vegetation cover - *leave trichomes*	1	14873897	0.254	0.254	0.00047	0.00023	AL1G46690			
Vegetation cover - *leave trichomes*	1	32041351	0.299	0.299	0.00018	0.00248	NA			
Vegetation cover - *leave trichomes*	1	32043593	0.42	0.42	0.00285	0.00025	NA			
Vegetation cover - *leave trichomes*	1	6013823	0.078	0.078	0.00017	0.00270	NA			
Vegetation cover - *leave trichomes*	1	8819695	0.09	0.09	0.00313	0.00417	AL1G33580			
Vegetation cover - *leave trichomes*	2	12516935	0.456	0.456	0.00000	0.00005	AL2G26090	AT1G78960	LUP2	Encodes a multifunctional 2-3-oxidosqualene (OS)-triterpene cyclase that can cyclize OS into lupeol, alpha- and beta-amyrin.
Vegetation cover - *leave trichomes*	2	12516943	0.458	0.458	0.00001	0.00002	AL2G26090			
Vegetation cover - *leave trichomes*	2	12517195	0.426	0.426	0.00128	0.00023	AL2G26090			
Vegetation cover - *leave trichomes*	2	12517234	0.424	0.424	0.00102	0.00011	AL2G26090			
Vegetation cover - *leave trichomes*	2	12517269	0.513	0.513	0.00243	0.00077	AL2G26090			
Vegetation cover - *leave trichomes*	2	12517905	0.453	0.453	0.00206	0.00130	AL2G26090			
Vegetation cover - *leave trichomes*	2	13776669	0.327	0.327	0.00412	0.00061	AL2G28640	AT1G69520	-	S-adenosyl-L-methionine-dependent methyltransferases superfamily protein
Vegetation cover - *leave trichomes*	2	13776670	0.325	0.325	0.00403	0.00047	AL2G28640			
Vegetation cover - *leave trichomes*	2	14333008	0.108	0.108	0.00434	0.00221	NA			
Vegetation cover - *leave trichomes*	2	15594464	0.146	0.146	0.00135	0.00159	AL2G32570	AT4G09360	-	NB-ARC domain-containing disease resistance protein
Vegetation cover - *leave trichomes*	2	15596858	0.157	0.157	0.00404	0.00400	AL2G32570			
Vegetation cover - *leave trichomes*	2	15761842	0.067	0.067	0.00148	0.00175	NA			
Vegetation cover - *leave trichomes*	2	15788254	0.087	0.087	0.00425	0.00490	AL2G33140			
Vegetation cover - *leave trichomes*	2	16011780	0.092	0.092	0.00136	0.00474	AL2G33620			
Vegetation cover - *leave trichomes*	2	16108535	0.146	0.146	0.00134	0.00270	AL2G33880	AT1G74030	ENO1	Encodes the plastid-localized phosphoenol-pyruvate enolase. Mutant plants have abnormal trichomes, defects in fatty acid metabolism.
Vegetation cover - *leave trichomes*	2	16109744	0.147	0.147	0.00213	0.00464	AL2G33880			

Vegetation cover - *leave trichomes*	2	16110357	0.164	0.164	0.00119	0.00389	AL2G33880			
Vegetation cover - *leave trichomes*	2	16111638	0.144	0.144	0.00228	0.00367	AL2G33890	unknown		
Vegetation cover - *leave trichomes*	2	16111641	0.149	0.149	0.00135	0.00337	AL2G33890			
Vegetation cover - *leave trichomes*	2	16113139	0.139	0.139	0.00054	0.00217	NA			
Vegetation cover - *leave trichomes*	2	16113460	0.136	0.136	0.00065	0.00054	AL2G33900			
Vegetation cover - *leave trichomes*	2	16113634	0.137	0.137	0.00024	0.00219	AL2G33900	unknown		
Vegetation cover - *leave trichomes*	2	16113828	0.135	0.135	0.00062	0.00043	AL2G33900			
Vegetation cover - *leave trichomes*	2	16115633	0.138	0.138	0.00058	0.00268	NA			
Vegetation cover - *leave trichomes*	2	16115670	0.139	0.139	0.00038	0.00246	NA			
Vegetation cover - *leave trichomes*	2	16115684	0.139	0.139	0.00043	0.00154	NA			
Vegetation cover - *leave trichomes*	2	16115718	0.139	0.139	0.00058	0.00124	NA			
Vegetation cover - *leave trichomes*	2	16115778	0.134	0.134	0.00084	0.00230	NA			
Vegetation cover - *leave trichomes*	2	16115952	0.136	0.136	0.00051	0.00085	NA			
Vegetation cover - *leave trichomes*	2	16117116	0.125	0.125	0.00173	0.00101	NA			
Vegetation cover - *leave trichomes*	2	16117414	0.123	0.123	0.00034	0.00027	NA			
Vegetation cover - *leave trichomes*	2	16118101	0.134	0.134	0.00428	0.00406	NA			
Vegetation cover - *leave trichomes*	2	16118603	0.139	0.139	0.00102	0.00121	NA			
Vegetation cover - *leave trichomes*	2	16119404	0.132	0.132	0.00186	0.00433	NA			
Vegetation cover - *leave trichomes*	2	16119425	0.136	0.136	0.00060	0.00326	NA			
Vegetation cover - *leave trichomes*	2	16119474	0.134	0.134	0.00036	0.00265	NA			
Vegetation cover - *leave trichomes*	2	16119557	0.133	0.133	0.00073	0.00445	NA			
Vegetation cover - *leave trichomes*	2	16119789	0.131	0.131	0.00392	0.00374	NA			
Vegetation cover - *leave trichomes*	2	16119839	0.137	0.137	0.00083	0.00118	NA			
Vegetation cover - *leave trichomes*	2	16121713	0.157	0.157	0.00074	0.00053	AL2G33910			

Vegetation cover - *leave trichomes*	2	16122152	0.149	0.149	0.00081	0.00020	NA			
Vegetation cover - *leave trichomes*	2	16122249	0.153	0.153	0.00046	0.00008	NA			
Vegetation cover - *leave trichomes*	2	16127218	0.165	0.165	0.00039	0.00028	AL2G33940	AT1G74050 AT1G74060	EL6X EL6Y	Ribosomal protein L6 family protein
Vegetation cover - *leave trichomes*	2	16127638	0.178	0.178	0.00024	0.00034	AL2G33940			
Vegetation cover - *leave trichomes*	2	16128986	0.162	0.162	0.00037	0.00007	NA			
Vegetation cover - *leave trichomes*	2	16143551	0.162	0.162	0.00345	0.00076	AL2G34000	AT1G74090	ATSOT18, ATST5B	encodes a desulfoglucosinolate sulfotransferase, involved in the final step of glucosinolate core structure biosynthesis. Has a broad-substrate specificity with preference with methionine-derived desulfoglucosinolates.
Vegetation cover - *leave trichomes*	2	16143645	0.164	0.164	0.00256	0.00050	AL2G34000			
Vegetation cover - *leave trichomes*	2	16143857	0.157	0.157	0.00101	0.00015	AL2G34000			
Vegetation cover - *leave trichomes*	2	16143885	0.164	0.164	0.00172	0.00011	AL2G34000			
Vegetation cover - *leave trichomes*	2	16143902	0.163	0.163	0.00183	0.00010	AL2G34000			
Vegetation cover - *leave trichomes*	2	16143905	0.161	0.161	0.00183	0.00019	AL2G34000			
Vegetation cover - *leave trichomes*	2	16143923	0.161	0.161	0.00283	0.00012	AL2G34000			
Vegetation cover - *leave trichomes*	2	16143957	0.166	0.166	0.00437	0.00029	AL2G34000			
Vegetation cover - *leave trichomes*	2	16143959	0.163	0.163	0.00189	0.00012	AL2G34000			
Vegetation cover - *leave trichomes*	2	16144185	0.158	0.158	0.00232	0.00395	AL2G34000			
Vegetation cover - *leave trichomes*	2	16144260	0.163	0.163	0.00253	0.00069	AL2G34000			
Vegetation cover - *leave trichomes*	2	16144307	0.164	0.164	0.00388	0.00088	AL2G34000			
Vegetation cover - *leave trichomes*	2	16144390	0.164	0.164	0.00324	0.00028	NA			
Vegetation cover - *leave trichomes*	2	16144409	0.16	0.16	0.00143	0.00059	NA			
Vegetation cover - *leave trichomes*	2	16144421	0.162	0.162	0.00238	0.00070	AL2G34010	AT1G74100	ATSOT16, SOT16	encodes a desulfoglucosinolate sulfotransferase, involved in the final step of glucosinolate core structure biosynthesis. Has a broad-substrate specificity with different desulfoglucosinolates, the best substrate is indole-3-methyl-dsGS, followed by benzyl-dsGS. Expression was induced by wounding, jasmonate and ethylene stimulates.
Vegetation cover - *leave trichomes*	2	16144425	0.16	0.16	0.00279	0.00135	AL2G34010			
Vegetation cover - *leave trichomes*	2	16144444	0.159	0.159	0.00150	0.00030	AL2G34010			
Vegetation cover - *leave trichomes*	2	16144446	0.16	0.16	0.00178	0.00053	AL2G34010			
Vegetation cover - *leave trichomes*	2	16144451	0.161	0.161	0.00175	0.00054	AL2G34010			

Vegetation cover - *leave trichomes*	2	16144490	0.162	0.162	0.00059	0.00026	AL2G34010			
Vegetation cover - *leave trichomes*	2	16144537	0.161	0.161	0.00189	0.00007	AL2G34010			
Vegetation cover - *leave trichomes*	2	16144538	0.162	0.162	0.00170	0.00012	AL2G34010			
Vegetation cover - *leave trichomes*	2	16144547	0.161	0.161	0.00149	0.00026	AL2G34010			
Vegetation cover - *leave trichomes*	2	16144571	0.164	0.164	0.00123	0.00020	AL2G34010			
Vegetation cover - *leave trichomes*	2	16144578	0.162	0.162	0.00237	0.00033	AL2G34010			
Vegetation cover - *leave trichomes*	2	16144581	0.163	0.163	0.00130	0.00034	AL2G34010			
Vegetation cover - *leave trichomes*	2	16144596	0.164	0.164	0.00126	0.00034	AL2G34010			
Vegetation cover - *leave trichomes*	2	16144646	0.164	0.164	0.00187	0.00014	AL2G34010			
Vegetation cover - *leave trichomes*	2	16144654	0.162	0.162	0.00172	0.00014	AL2G34010			
Vegetation cover - *leave trichomes*	2	16144693	0.16	0.16	0.00274	0.00047	AL2G34010			
Vegetation cover - *leave trichomes*	2	16144717	0.162	0.162	0.00235	0.00019	AL2G34010			
Vegetation cover - *leave trichomes*	2	16144744	0.161	0.161	0.00136	0.00008	AL2G34010			
Vegetation cover - *leave trichomes*	2	16144747	0.162	0.162	0.00132	0.00027	AL2G34010			
Vegetation cover - *leave trichomes*	2	16144884	0.144	0.144	0.00136	0.00046	AL2G34010			
Vegetation cover - *leave trichomes*	2	16145092	0.144	0.144	0.00117	0.00044	AL2G34010			
Vegetation cover - *leave trichomes*	2	16145236	0.145	0.145	0.00093	0.00038	AL2G34010			
Vegetation cover - *leave trichomes*	2	16145271	0.148	0.148	0.00159	0.00034	AL2G34010			
Vegetation cover - *leave trichomes*	2	16145287	0.146	0.146	0.00277	0.00052	AL2G34010			
Vegetation cover - *leave trichomes*	2	16145296	0.146	0.146	0.00288	0.00058	AL2G34010			
Vegetation cover - *leave trichomes*	2	16145349	0.143	0.143	0.00385	0.00156	AL2G34010			
Vegetation cover - *leave trichomes*	2	16145350	0.143	0.143	0.00385	0.00156	AL2G34010			
Vegetation cover - *leave trichomes*	2	16145353	0.144	0.144	0.00379	0.00121	AL2G34010			
Vegetation cover - *leave trichomes*	2	16145374	0.144	0.144	0.00292	0.00206	AL2G34010			

Vegetation cover - *leave trichomes*	2	16145518	0.143	0.143	0.00267	0.00167	AL2G34010			
Vegetation cover - *leave trichomes*	2	16145524	0.144	0.144	0.00270	0.00127	AL2G34010			
Vegetation cover - *leave trichomes*	2	16145566	0.147	0.147	0.00284	0.00083	AL2G34010			
Vegetation cover - *leave trichomes*	2	16145572	0.146	0.146	0.00150	0.00046	AL2G34010			
Vegetation cover - *leave trichomes*	2	16145599	0.143	0.143	0.00190	0.00032	AL2G34010			
Vegetation cover - *leave trichomes*	2	16145684	0.147	0.147	0.00329	0.00031	AL2G34010			
Vegetation cover - *leave trichomes*	2	16145690	0.146	0.146	0.00277	0.00020	AL2G34010			
Vegetation cover - *leave trichomes*	2	16145695	0.145	0.145	0.00299	0.00042	AL2G34010			
Vegetation cover - *leave trichomes*	2	16145696	0.146	0.146	0.00243	0.00048	AL2G34010			
Vegetation cover - *leave trichomes*	2	16145705	0.147	0.147	0.00209	0.00028	AL2G34010			
Vegetation cover - *leave trichomes*	2	16145710	0.147	0.147	0.00169	0.00028	AL2G34010			
Vegetation cover - *leave trichomes*	2	16145748	0.148	0.148	0.00177	0.00114	NA			
Vegetation cover - *leave trichomes*	2	16148422	0.162	0.162	0.00056	0.00083	AL2G34020			
Vegetation cover - *leave trichomes*	2	16148869	0.159	0.159	0.00129	0.00113	NA			
Vegetation cover - *leave trichomes*	2	16148870	0.156	0.156	0.00144	0.00190	NA			
Vegetation cover - *leave trichomes*	2	16148871	0.156	0.156	0.00180	0.00142	NA			
Vegetation cover - *leave trichomes*	2	16150517	0.163	0.163	0.00095	0.00162	NA			
Vegetation cover - *leave trichomes*	2	16151419	0.154	0.154	0.00064	0.00027	NA			
Vegetation cover - *leave trichomes*	2	16151612	0.161	0.161	0.00097	0.00117	NA			
Vegetation cover - *leave trichomes*	2	16151642	0.206	0.206	0.00014	0.00174	NA			
Vegetation cover - *leave trichomes*	2	16152120	0.157	0.157	0.00419	0.00193	NA			
Vegetation cover - *leave trichomes*	2	16152172	0.164	0.164	0.00121	0.00044	NA			
Vegetation cover - *leave trichomes*	2	16152553	0.159	0.159	0.00109	0.00059	NA			
Vegetation cover - *leave trichomes*	2	16152561	0.159	0.159	0.00099	0.00098	NA			

Vegetation cover - *leave trichomes*	2	16152732	0.16	0.16	0.00104	0.00139	NA			
Vegetation cover - *leave trichomes*	2	16152894	0.147	0.147	0.00112	0.00066	NA			
Vegetation cover - *leave trichomes*	2	16153083	0.157	0.157	0.00117	0.00098	NA			
Vegetation cover - *leave trichomes*	2	16153319	0.159	0.159	0.00191	0.00070	NA			
Vegetation cover - *leave trichomes*	2	16153607	0.16	0.16	0.00249	0.00069	NA			
Vegetation cover - *leave trichomes*	2	16153935	0.16	0.16	0.00157	0.00065	AL2G34030	AT1G74120	MTERF15	Encodes a mitochondrial transcription termination factor mTERF15. Required for mitochondrial nad2 intron 3 splicing and functional complex I activity
Vegetation cover - *leave trichomes*	2	16154236	0.159	0.159	0.00082	0.00471	AL2G34030			
Vegetation cover - *leave trichomes*	2	16154395	0.159	0.159	0.00079	0.00059	AL2G34030			
Vegetation cover - *leave trichomes*	2	16154727	0.163	0.163	0.00150	0.00061	AL2G34030			
Vegetation cover - *leave trichomes*	2	16154912	0.158	0.158	0.00133	0.00041	AL2G34030			
Vegetation cover - *leave trichomes*	2	16155959	0.157	0.157	0.00182	0.00037	NA			
Vegetation cover - *leave trichomes*	2	16158207	0.158	0.158	0.00198	0.00084	AL2G34040			
Vegetation cover - *leave trichomes*	2	16160893	0.208	0.208	0.00005	0.00338	AL2G34050	AT1G74150	-	Galactose oxidase/kelch repeat superfamily protein
Vegetation cover - *leave trichomes*	2	16161267	0.175	0.175	0.00318	0.00172	AL2G34050			
Vegetation cover - *leave trichomes*	2	16165562	0.158	0.158	0.00415	0.00151	NA			
Vegetation cover - *leave trichomes*	2	16166013	0.155	0.155	0.00402	0.00113	NA			
Vegetation cover - *leave trichomes*	2	16171284	0.169	0.169	0.00183	0.00366	AL2G34060	AT1G74160	LNG3, TRM4	Member of a small gene family in Arabidopsis. Quadruple mutants in this family display defects in cell elongation.
Vegetation cover - *leave trichomes*	2	16171497	0.164	0.164	0.00206	0.00472	AL2G34060			
Vegetation cover - *leave trichomes*	2	16171800	0.161	0.161	0.00410	0.00499	AL2G34060			
Vegetation cover - *leave trichomes*	2	16171953	0.159	0.159	0.00128	0.00221	AL2G34060			
Vegetation cover - *leave trichomes*	2	16172007	0.157	0.157	0.00329	0.00164	AL2G34060			
Vegetation cover - *leave trichomes*	2	16172663	0.157	0.157	0.00231	0.00198	AL2G34060			
Vegetation cover - *leave trichomes*	2	16172749	0.164	0.164	0.00165	0.00187	AL2G34060			
Vegetation cover - *leave trichomes*	2	16172834	0.159	0.159	0.00110	0.00347	AL2G34060			

Vegetation cover - *leave trichomes*	2	16173567	0.157	0.157	0.00104	0.00154	AL2G34060			
Vegetation cover - *leave trichomes*	2	16173601	0.155	0.155	0.00143	0.00261	AL2G34060			
Vegetation cover - *leave trichomes*	2	16173605	0.155	0.155	0.00120	0.00261	AL2G34060			
Vegetation cover - *leave trichomes*	2	16173608	0.155	0.155	0.00119	0.00325	AL2G34060			
Vegetation cover - *leave trichomes*	2	16173762	0.161	0.161	0.00323	0.00075	AL2G34060			
Vegetation cover - *leave trichomes*	2	16174110	0.161	0.161	0.00290	0.00355	NA			
Vegetation cover - *leave trichomes*	2	16174134	0.158	0.158	0.00374	0.00340	NA			
Vegetation cover - *leave trichomes*	2	16174322	0.16	0.16	0.00192	0.00349	NA			
Vegetation cover - *leave trichomes*	2	16174332	0.158	0.158	0.00237	0.00242	NA			
Vegetation cover - *leave trichomes*	2	16174369	0.161	0.161	0.00230	0.00285	NA			
Vegetation cover - *leave trichomes*	2	16174386	0.157	0.157	0.00216	0.00403	NA			
Vegetation cover - *leave trichomes*	2	16174387	0.159	0.159	0.00201	0.00287	NA			
Vegetation cover - *leave trichomes*	2	16174439	0.159	0.159	0.00391	0.00356	NA			
Vegetation cover - *leave trichomes*	2	2984057	0.171	0.171	0.00420	0.00175	AL2G15870			
Vegetation cover - *leave trichomes*	2	2984138	0.204	0.204	0.00286	0.00329	AL2G15870	AT1G60710	ATB2	Encodes ATB2.
Vegetation cover - *leave trichomes*	2	2984161	0.205	0.205	0.00239	0.00229	AL2G15870			
Vegetation cover - *leave trichomes*	2	2984204	0.209	0.209	0.00276	0.00207	AL2G15870			
Vegetation cover - *leave trichomes*	2	3108848	0.651	0.651	0.00171	0.00326	AL2G16110			
Vegetation cover - *leave trichomes*	2	7467153	0.316	0.316	0.00135	0.00104	NA			
Vegetation cover - *leave trichomes*	2	7467184	0.295	0.295	0.00034	0.00004	NA			
Vegetation cover - *leave trichomes*	2	7467225	0.28	0.28	0.00332	0.00496	NA			
Vegetation cover - *leave trichomes*	2	7467240	0.281	0.281	0.00155	0.00060	NA			
Vegetation cover - *leave trichomes*	3	11729261	0.548	0.548	0.00477	0.00251	AL3G39830			
Vegetation cover - *leave trichomes*	3	3537009	0.182	0.182	0.00252	0.00193	AL3G19960		-	ARM repeat superfamily protein

Vegetation cover - *leave trichomes*	3	3537021	0.179	0.179	0.00492	0.00313	AL3G19960	AT3G08947 AT3G08943		
Vegetation cover - *leave trichomes*	3	597513	0.403	0.403	0.00470	0.00228	AL3G11720	AT4G16080	ATDOA8	hypothetical protein (DUF295)
Vegetation cover - *leave trichomes*	3	597518	0.406	0.406	0.00357	0.00200	AL3G11720			
Vegetation cover - *leave trichomes*	3	597522	0.408	0.408	0.00135	0.00359	AL3G11720			
Vegetation cover - *leave trichomes*	4	16666897	0.09	0.09	0.00098	0.00122	AL4G31110			
Vegetation cover - *leave trichomes*	4	16700779	0.11	0.11	0.00285	0.00008	AL4G31180			
Vegetation cover - *leave trichomes*	4	21743948	0.08	0.08	0.00183	0.00347	NA			
Vegetation cover - *leave trichomes*	4	2420766	0.356	0.356	0.00098	0.00323	AL4G14260	AT2G24140	MRF7	MyoB myosin receptor which specifically localises to the Golgi membrane and affects its movement.
Vegetation cover - *leave trichomes*	4	2420901	0.393	0.393	0.00381	0.00284	AL4G14260			
Vegetation cover - *leave trichomes*	4	2420967	0.385	0.385	0.00102	0.00497	AL4G14260			
Vegetation cover - *leave trichomes*	4	2424365	0.339	0.339	0.00353	0.00450	AL4G14270	AT2G24150	HHP3	heptahelical transmembrane protein HHP3
Vegetation cover - *leave trichomes*	4	2424380	0.336	0.336	0.00382	0.00186	AL4G14270			
Vegetation cover - *leave trichomes*	4	4981864	0.1	0.1	0.00407	0.00216	AL4G17470	AT2G25790	SKM1	Leucine-rich receptor-like protein kinase family protein
Vegetation cover - *leave trichomes*	4	4982787	0.1	0.1	0.00457	0.00285	AL4G17470			
Vegetation cover - *leave trichomes*	4	4982900	0.099	0.099	0.00306	0.00304	AL4G17470			
Vegetation cover - *leave trichomes*	5	11033197	0.145	0.145	0.00202	0.00062	NA			
Vegetation cover - *leave trichomes*	5	18405608	0.22	0.22	0.00325	0.00077	AL5G38990			
Vegetation cover - *leave trichomes*	6	10688683	0.068	0.068	0.00457	0.00442	AL6G36050			
Vegetation cover - *leave trichomes*	6	10702907	0.098	0.098	0.00401	0.00063	AL6G36080			
Vegetation cover - *leave trichomes*	6	3668283	0.119	0.119	0.00392	0.00097	AL6G19580			
Vegetation cover - *leave trichomes*	6	3902267	0.863	0.863	0.00331	0.00061	AL6G20290			
Vegetation cover - *leave trichomes*	6	9718035	0.132	0.132	0.00077	0.00488	NA			
Vegetation cover - *leave trichomes*	7	1450604	0.058	0.058	0.00193	0.00431	AL7G13670			
Vegetation cover - *leave trichomes*	7	23099276	0.078	0.078	0.00106	0.00481	NA			

Vegetation cover - *leave trichomes*	7	2955099	0.141	0.141	0.00294	0.00143	AL7G17280	AT4G34110	PAB2	Putative poly-A binding protein. M.Expressed in stele, root meristem and post-fertilization ovules.
Vegetation cover - *leave trichomes*	7	2955174	0.14	0.14	0.00232	0.00404	AL7G17280			
Vegetation cover - *leave trichomes*	8	12771649	0.043	0.043	0.00424	0.00152	NA			
Vegetation cover - *leave trichomes*	8	18046864	0.066	0.066	0.00457	0.00441	NA			
Vegetation cover - *leave trichomes*	8	20004726	0.268	0.268	0.00170	0.00124	AL8G38100			
Vegetation cover - *leave trichomes*	8	6479040	0.491	0.491	0.00072	0.00170	AL8G18950			
Assoc	**CHR**	**BP**	**Af_env**	**Af_phen**	**p (env)**	**p (phen)**	**Gene**	**AT homolog**	**Gene name**	**Function**
Distance from trees - t_{flo}	1	14684424	0.056	0.057	0.00049	0.00453	AL1G46370	AT1G32230	RIMB1, ATP8, CEO1	Encodes a protein belonging to the (ADP-ribosyl)transferase domain-containing subfamily of WWE protein-protein interaction domain protein family. Superoxide radicals are necessary and sufficient to propagate cell death or lesion formation in rcd1 mutants. Without stress treatment, RCD1 is localized in the nucleus. Under high salt or oxidative stress, RCD1 is found not only in the nucleus but also in the cytoplasm.
Distance from trees - t_{flo}	1	14684774	0.057	0.058	0.00059	0.00383	AL1G46370			
Distance from trees - t_{flo}	1	14684814	0.051	0.052	0.00067	0.00437	AL1G46370			
Distance from trees - t_{flo}	1	14684949	0.051	0.052	0.00133	0.00362	AL1G46370			
Distance from trees - t_{flo}	1	14684954	0.051	0.052	0.00133	0.00402	AL1G46370			
Distance from trees - t_{flo}	1	14685126	0.057	0.058	0.00035	0.00465	AL1G46370			
Distance from trees - t_{flo}	1	14685211	0.056	0.057	0.00046	0.00419	AL1G46370			
Distance from trees - t_{flo}	1	14685213	0.056	0.057	0.00046	0.00419	AL1G46370			
Distance from trees - t_{flo}	1	14685219	0.056	0.057	0.00046	0.00419	AL1G46370			
Distance from trees - t_{flo}	1	14845233	0.069	0.071	0.00061	0.00419	AL1G46670	AT1G32440	PKP3	Encodes a chloroplast pyruvate kinase beta subunit. Involved in seed oil biosynthesis.
Distance from trees - t_{flo}	1	14846589	0.073	0.075	0.00039	0.00293	AL1G46670			
Distance from trees - t_{flo}	1	14926327	0.064	0.065	0.00004	0.00439	AL1G46800	AT1G32550	FDC2	Encodes FdC2, a ferredoxin protein capable of alternative electron partitioning at PSI.
Distance from trees - t_{flo}	1	14926328	0.064	0.065	0.00004	0.00439	AL1G46800			
Distance from trees - t_{flo}	1	23322037	0.031	0.032	0.00045	0.00218	NA			
Distance from trees - t_{flo}	1	268095	0.687	0.684	0.00295	0.00365	AL1G10810	AT1G01580	FRD1, FRO2	Encodes the a reductase responsible for reduction of iron at the root surface.
Distance from trees - t_{flo}	1	270001	0.678	0.677	0.00236	0.00123	AL1G10810			
Distance from trees - t_{flo}	1	27471412	0.313	0.317	0.00110	0.00463	NA			

Distance from trees - t_{flo}	1	27471926	0.529	0.526	0.00215	0.00018	NA			
Distance from trees - t_{flo}	1	27472149	0.301	0.307	0.00082	0.00475	NA			
Distance from trees - t_{flo}	1	27472527	0.317	0.324	0.00032	0.00474	NA			
Distance from trees - t_{flo}	1	29421181	0.226	0.224	0.00385	0.00333	AL1G63690			
Distance from trees - t_{flo}	1	30381050	0.031	0.032	0.00403	0.00155	NA			
Distance from trees - t_{flo}	1	31066134	0.237	0.235	0.00013	0.00220	NA			
Distance from trees - t_{flo}	1	31066135	0.234	0.232	0.00300	0.00256	NA			
Distance from trees - t_{flo}	1	31066152	0.224	0.222	0.00029	0.00209	NA			
Distance from trees - t_{flo}	1	31528759	0.155	0.158	0.00244	0.00067	NA			
Distance from trees - t_{flo}	1	32830224	0.295	0.297	0.00018	0.00388	NA			
Distance from trees - t_{flo}	1	8124066	0.144	0.146	0.00463	0.00227	NA			
Distance from trees - t_{flo}	2	11751190	0.095	0.09	0.00253	0.00385	AL2G24850			
Distance from trees - t_{flo}	2	12041610	0.322	0.321	0.00175	0.00053	AL2G25320	AT1G67000	-	Protein kinase superfamily protein
Distance from trees - t_{flo}	2	12041613	0.325	0.325	0.00171	0.00074	AL2G25320			
Distance from trees - t_{flo}	2	12041710	0.326	0.326	0.00152	0.00189	AL2G25320			
Distance from trees - t_{flo}	2	12041721	0.326	0.326	0.00330	0.00068	AL2G25320			
Distance from trees - t_{flo}	2	12041740	0.326	0.326	0.00152	0.00189	AL2G25320			
Distance from trees - t_{flo}	2	12071713	0.448	0.45	0.00214	0.00108	NA			
Distance from trees - t_{flo}	2	12071725	0.448	0.451	0.00192	0.00052	NA			
Distance from trees - t_{flo}	2	15194796	0.197	0.201	0.00433	0.00001	AL2G31670			
Distance from trees - t_{flo}	2	16535025	0.506	0.51	0.00378	0.00249	AL2G34940			
Distance from trees - t_{flo}	2	17862426	0.447	0.453	0.00154	0.00368	AL2G38140			
Distance from trees - t_{flo}	2	3145544	0.611	0.614	0.00445	0.00352	NA			
Distance from trees - t_{flo}	2	3881680	0.139	0.138	0.00033	0.00406	AL2G17420			

Distance from trees - t_{flo}	2	7556463	0.726	0.721	0.00182	0.00409	NA			
Distance from trees - t_{flo}	3	1779268	0.167	0.17	0.00459	0.00150	AL3G15300			
Distance from trees - t_{flo}	3	7240251	0.261	0.253	0.00370	0.00116	AL3G29920			
Distance from trees - t_{flo}	3	7263391	0.422	0.424	0.00058	0.00051	NA			
Distance from trees - t_{flo}	3	7263456	0.534	0.532	0.00370	0.00317	NA			
Distance from trees - t_{flo}	3	8386329	0.05	0.051	0.00017	0.00072	AL3G32830	AT3G19420	PTEN2	Encodes a phosphatase with low in vitro tyrosine phosphatase activity.
Distance from trees - t_{flo}	3	8387958	0.05	0.051	0.00017	0.00063	AL3G32830			
Distance from trees - t_{flo}	4	10011377	0.512	0.506	0.00064	0.00455	NA			
Distance from trees - t_{flo}	4	10011432	0.531	0.525	0.00371	0.00207	NA			
Distance from trees - t_{flo}	4	10022138	0.438	0.437	0.00428	0.00479	NA			
Distance from trees - t_{flo}	4	10022255	0.406	0.404	0.00097	0.00351	NA			
Distance from trees - t_{flo}	4	13157194	0.416	0.418	0.00455	0.00393	NA			
Distance from trees - t_{flo}	4	13812773	0.097	0.095	0.00159	0.00442	NA			
Distance from trees - t_{flo}	4	14451845	0.308	0.301	0.00216	0.00037	AL4G25810	AT2G30860	GSTF9	Encodes glutathione transferase belonging to the phi class of GSTs.
Distance from trees - t_{flo}	4	14451849	0.301	0.294	0.00077	0.00009	AL4G25810			
Distance from trees - t_{flo}	4	16649071	0.13	0.132	0.00043	0.00474	AL4G31090			
Distance from trees - t_{flo}	4	17963750	0.119	0.118	0.00301	0.00085	AL4G33910			
Distance from trees - t_{flo}	4	211873	0.593	0.588	0.00412	0.00141	AL4G10360			
Distance from trees - t_{flo}	5	12696192	0.088	0.09	0.00109	0.00027	AL5G25440			
Distance from trees - t_{flo}	5	12720457	0.099	0.098	0.00290	0.00064	AL5G25490	AT3G46600	-	GRAS family transcription factor
Distance from trees - t_{flo}	5	12720723	0.903	0.905	0.00414	0.00085	AL5G25490			
Distance from trees - t_{flo}	5	12824835	0.323	0.319	0.00366	0.00452	AL5G25810	AT3G46790	CRR2	The protein is involved the intergenic processing of chloroplast RNA between rps7 and ndhB.
Distance from trees - t_{flo}	5	12824880	0.315	0.312	0.00335	0.00342	AL5G25810			
Distance from trees - t_{flo}	5	12829737	0.282	0.281	0.00359	0.00027	AL5G25820	AT3G46810	-	Cysteine/Histidine-rich C1 domain family protein

Distance from trees - t_{flo}	5	12829742	0.282	0.281	0.00359	0.00027	AL5G25820			
Distance from trees - t_{flo}	5	12829745	0.282	0.281	0.00359	0.00027	AL5G25820			
Distance from trees - t_{flo}	5	12900032	0.209	0.21	0.00220	0.00475	AL5G26050			
Distance from trees - t_{flo}	5	14378760	0.062	0.064	0.00078	0.00320	AL5G28970	AT3G49240	EMB1796, NUWA	Encodes NUWA, an imprinted gene that controls mitochondrial function in early seed development.
Distance from trees - t_{flo}	5	14378898	0.063	0.065	0.00110	0.00296	AL5G28970			
Distance from trees - t_{flo}	5	1772881	0.396	0.394	0.00376	0.00062	NA			
Distance from trees - t_{flo}	5	1772995	0.429	0.427	0.00319	0.00389	NA			
Distance from trees - t_{flo}	5	1774546	0.444	0.443	0.00273	0.00202	NA			
Distance from trees - t_{flo}	5	17841024	0.58	0.578	0.00218	0.00148	AL5G37490	AT3G56170	CAN1, CA-2+	Encodes a calcium-dependent nuclease with similarity to staphylococcal nuclease.
Distance from trees - t_{flo}	5	17841028	0.589	0.584	0.00451	0.00136	AL5G37490			
Distance from trees - t_{flo}	5	17841032	0.577	0.576	0.00313	0.00211	AL5G37490			
Distance from trees - t_{flo}	5	17841033	0.579	0.577	0.00126	0.00082	AL5G37490			
Distance from trees - t_{flo}	5	17841402	0.587	0.586	0.00395	0.00444	AL5G37490			
Distance from trees - t_{flo}	5	17901088	0.544	0.541	0.00030	0.00300	AL5G37680			
Distance from trees - t_{flo}	5	20031599	0.184	0.184	0.00491	0.00381	AL5G43050	AT3G60740	EMB133, TTn1	Encodes tubulin-folding cofactor D.
Distance from trees - t_{flo}	5	20033833	0.168	0.17	0.00135	0.00154	AL5G43050			
Distance from trees - t_{flo}	5	20035941	0.18	0.181	0.00259	0.00500	AL5G43060			
Distance from trees - t_{flo}	5	20040026	0.172	0.172	0.00322	0.00209	AL5G43070	AT3G60770	US15Z	Ribosomal protein S13/S15
Distance from trees - t_{flo}	5	20040072	0.166	0.166	0.00031	0.00435	AL5G43070			
Distance from trees - t_{flo}	5	3202935	0.314	0.313	0.00294	0.00136	NA			
Distance from trees - t_{flo}	5	3202938	0.311	0.31	0.00253	0.00259	NA			
Distance from trees - t_{flo}	5	7585668	0.072	0.067	0.00112	0.00172	NA			
Distance from trees - t_{flo}	6	18135572	0.398	0.402	0.00311	0.00136	NA			
Distance from trees - t_{flo}	6	24426610	0.082	0.083	0.00030	0.00375	NA			

Distance from trees - t_{flo}	6	4068040	0.304	0.303	0.00364	0.00055	AL6G20680			
Distance from trees - t_{flo}	6	7763958	0.146	0.143	0.00215	0.00407	AL6G29890	AT5G18620	CHR17	Double mutation in CHR17 and CHR11 results in the loss of the evenly spaced nucleosome pattern.
Distance from trees - t_{flo}	6	7763989	0.144	0.141	0.00116	0.00404	AL6G29890			
Distance from trees - t_{flo}	6	8067058	0.092	0.091	0.00008	0.00121	AL6G30580			
Distance from trees - t_{flo}	6	8074611	0.097	0.096	0.00191	0.00053	NA			
Distance from trees - t_{flo}	6	8095251	0.075	0.076	0.00049	0.00020	NA			
Distance from trees - t_{flo}	6	8111617	0.436	0.441	0.00256	0.00327	AL6G30670			
Distance from trees - t_{flo}	6	910700	0.079	0.077	0.00270	0.00340	AL6G12560	AT5G03250	-	Phototropic-responsive NPH3 family protein
Distance from trees - t_{flo}	6	912503	0.073	0.071	0.00464	0.00355	AL6G12560			
Distance from trees - t_{flo}	6	912506	0.073	0.071	0.00464	0.00368	AL6G12560			
Distance from trees - t_{flo}	6	912554	0.073	0.071	0.00464	0.00423	AL6G12560			
Distance from trees - t_{flo}	6	913127	0.079	0.077	0.00184	0.00467	AL6G12570	AT5G03260	LAC11	LAC11 is a putative laccase, a member of laccase family of genes (17 members in Arabidopsis).
Distance from trees - t_{flo}	6	914641	0.078	0.08	0.00056	0.00413	AL6G12570			
Distance from trees - t_{flo}	7	13314680	0.142	0.141	0.00429	0.00000	AL7G40650			
Distance from trees - t_{flo}	7	17614659	0.09	0.085	0.00371	0.00039	NA			
Distance from trees - t_{flo}	7	18869462	0.058	0.056	0.00032	0.00387	AL7G44810			
Distance from trees - t_{flo}	7	19836914	0.728	0.722	0.00400	0.00107	AL7G45710	AT4G00930	CIP4.1	Encodes COP1-interacting protein CIP4.1.
Distance from trees - t_{flo}	7	19837422	0.733	0.728	0.00248	0.00076	AL7G45710			
Distance from trees - t_{flo}	7	20596672	0.796	0.795	0.00028	0.00015	NA			
Distance from trees - t_{flo}	7	5901876	0.053	0.047	0.00390	0.00358	AL7G24580			
Distance from trees - t_{flo}	7	7505310	0.222	0.226	0.00091	0.00434	AL7G28580			
Distance from trees - t_{flo}	7	8716197	0.082	0.083	0.00173	0.00184	AL7G31340	AT4G22280	-	F-box/RNI-like superfamily protein
Distance from trees - t_{flo}	7	8716319	0.071	0.072	0.00068	0.00087	AL7G31340			
Distance from trees - t_{flo}	8	16761705	0.087	0.089	0.00141	0.00082	NA			

Distance from trees - t_{flo}	8	18245391	0.315	0.316	0.00467	0.00162	AL8G33680	AT5G57655	-	xylose isomerase family protein
Distance from trees - t_{flo}	8	18245394	0.315	0.316	0.00467	0.00162	AL8G33680			
Distance from trees - t_{flo}	8	18245778	0.329	0.332	0.00499	0.00295	AL8G33680			
Distance from trees - t_{flo}	8	18245945	0.275	0.28	0.00448	0.00251	AL8G33680			
Distance from trees - t_{flo}	8	21949767	0.443	0.442	0.00126	0.00118	AL8G43030	AT5G65450	UBP17	Encodes a ubiquitin-specific protease.The mRNA is cell-to-cell mobile.
Distance from trees - t_{flo}	8	21949800	0.436	0.435	0.00118	0.00123	AL8G43030			
Distance from trees - t_{flo}	8	21950417	0.432	0.431	0.00092	0.00107	AL8G43030			
Distance from trees - t_{flo}	8	21950580	0.252	0.255	0.00370	0.00025	AL8G43030			
Distance from trees - t_{flo}	8	21950636	0.219	0.222	0.00160	0.00008	AL8G43030			
Distance from trees - t_{flo}	8	21950643	0.248	0.252	0.00335	0.00027	AL8G43030			
Distance from trees - t_{flo}	8	21950696	0.245	0.247	0.00126	0.00015	AL8G43030			
Distance from trees - t_{flo}	8	21950700	0.24	0.242	0.00166	0.00026	AL8G43030			
Distance from trees - t_{flo}	8	21950748	0.247	0.25	0.00074	0.00019	AL8G43030			
Distance from trees - t_{flo}	8	21950839	0.252	0.253	0.00145	0.00010	AL8G43030			
Distance from trees - t_{flo}	8	21950841	0.255	0.256	0.00152	0.00015	AL8G43030			
Distance from trees - t_{flo}	8	21950852	0.255	0.256	0.00152	0.00015	AL8G43030			
Distance from trees - t_{flo}	8	21951151	0.25	0.252	0.00049	0.00008	AL8G43030			
Distance from trees - t_{flo}	8	21951348	0.247	0.248	0.00233	0.00011	AL8G43030			
Distance from trees - t_{flo}	8	21951468	0.247	0.248	0.00485	0.00021	AL8G43030			
Distance from trees - t_{flo}	8	21951563	0.248	0.25	0.00472	0.00080	AL8G43030			
Distance from trees - t_{flo}	8	21951901	0.25	0.252	0.00237	0.00035	AL8G43030			
Distance from trees - t_{flo}	8	21952027	0.245	0.247	0.00162	0.00009	AL8G43030			
Distance from trees - t_{flo}	8	21952034	0.252	0.252	0.00039	0.00013	AL8G43030			
Distance from trees - t_{flo}	8	21952111	0.247	0.248	0.00105	0.00002	AL8G43040	AT5G65460	KAC2, KCA2	

Distance from trees - t_{flo}	8	21952537	0.242	0.244	0.00079	0.00048	AL8G43040			Kinesin that binds cyclin-dependent kinase CDKA;1 as homodimer or as heterodimer with KCA1
Distance from trees - t_{flo}	8	21952839	0.248	0.252	0.00248	0.00011	AL8G43040			
Distance from trees - t_{flo}	8	21952878	0.259	0.261	0.00153	0.00013	AL8G43040			
Distance from trees - t_{flo}	8	21952972	0.248	0.25	0.00121	0.00010	AL8G43040			
Distance from trees - t_{flo}	8	21952974	0.248	0.25	0.00121	0.00010	AL8G43040			
Distance from trees - t_{flo}	8	21953095	0.255	0.258	0.00148	0.00016	AL8G43040			
Distance from trees - t_{flo}	8	21953352	0.253	0.255	0.00053	0.00008	AL8G43040			
Distance from trees - t_{flo}	8	21953463	0.252	0.253	0.00116	0.00015	AL8G43040			
Distance from trees - t_{flo}	8	21953554	0.253	0.255	0.00173	0.00017	AL8G43040			
Distance from trees - t_{flo}	8	21953773	0.253	0.258	0.00422	0.00014	AL8G43040			
Distance from trees - t_{flo}	8	21954069	0.253	0.255	0.00121	0.00029	AL8G43040			
Distance from trees - t_{flo}	8	21954945	0.247	0.248	0.00093	0.00003	AL8G43040			
Distance from trees - t_{flo}	8	21955029	0.245	0.247	0.00272	0.00040	AL8G43040			
Distance from trees - t_{flo}	8	21955227	0.248	0.25	0.00246	0.00040	AL8G43040			
Distance from trees - t_{flo}	8	21955358	0.247	0.248	0.00050	0.00019	AL8G43040			
Distance from trees - t_{flo}	8	21956298	0.739	0.737	0.00142	0.00205	AL8G43040			
Distance from trees - t_{flo}	8	21956920	0.248	0.25	0.00427	0.00009	AL8G43040			
Distance from trees - t_{flo}	8	21957336	0.252	0.253	0.00101	0.00005	AL8G43040			
Distance from trees - t_{flo}	8	21957607	0.247	0.247	0.00147	0.00007	AL8G43040			
Distance from trees - t_{flo}	8	21957871	0.253	0.255	0.00207	0.00039	AL8G43040			
Distance from trees - t_{flo}	8	21957938	0.25	0.252	0.00110	0.00065	AL8G43040			
Distance from trees - t_{flo}	8	21957998	0.248	0.25	0.00074	0.00015	AL8G43040			
Distance from trees - t_{flo}	8	21958059	0.25	0.252	0.00145	0.00008	AL8G43040			
Distance from trees - t_{flo}	8	2373073	0.545	0.545	0.00141	0.00160	NA			

Distance from trees - t_{flo}	8	4113233	0.927	0.926	0.00354	0.00238	AL8G16610	AT5G43710	ATEGEM2, MNS4	Glycosyl hydrolase family 47 protein
Distance from trees - t_{flo}	8	4114711	0.927	0.926	0.00453	0.00296	AL8G16610			
Distance from trees - t_{flo}	8	4116800	0.917	0.916	0.00041	0.00366	AL8G16620	AT5G43700	IAA4	Auxin inducible protein similar to transcription factors.
Distance from trees - t_{flo}	8	4116870	0.919	0.918	0.00061	0.00419	AL8G16620			
Distance from trees - t_{flo}	8	4325276	0.031	0.032	0.00090	0.00392	NA			
Distance from trees - t_{flo}	8	4326173	0.025	0.025	0.00478	0.00250	NA			
Distance from trees - t_{flo}	8	4383324	0.341	0.344	0.00376	0.00208	NA			
Distance from trees - t_{flo}	8	6509332	0.097	0.092	0.00454	0.00321	AL8G18990			
Distance from trees - t_{flo}	8	6771061	0.522	0.519	0.00237	0.00072	NA			
Distance from trees - t_{flo}	8	7063446	0.25	0.248	0.00380	0.00280	AL8G19530			
Distance from trees - t_{flo}	8	7063463	0.299	0.299	0.00400	0.00174	AL8G19530	unknown		
Distance from trees - t_{flo}	8	7063487	0.339	0.335	0.00217	0.00005	AL8G19530			
Distance from trees - t_{flo}	8	7063492	0.356	0.354	0.00255	0.00006	AL8G19530			
Distance from trees - t_{flo}	8	7332921	0.352	0.349	0.00036	0.00316	AL8G19600			
Distance from trees - t_{flo}	8	7351365	0.303	0.303	0.00385	0.00071	AL8G19630			
Assoc	**CHR**	**BP**	**Af_env**	**Af_phen**	**p (env)**	**p (phen)**	**Gene**	**AT homolog**	**Gene name**	**Function**
Distance from trees - s_{asym}	1	10853171	0.315	0.315	0.00345	0.00238	AL1G38300			
Distance from trees - s_{asym}	1	13175237	0.449	0.449	0.00398	0.00208	AL1G43740			
Distance from trees - s_{asym}	1	28414465	0.133	0.133	0.00444	0.00406	AL1G61700			
Distance from trees - s_{asym}	1	28606267	0.091	0.091	0.00302	0.00039	AL1G62130			
Distance from trees - s_{asym}	1	9465280	0.072	0.072	0.00110	0.00371	AL1G35040			
Distance from trees - s_{asym}	1	9506966	0.342	0.342	0.00133	0.00181	AL1G35140			
Distance from trees - s_{asym}	1	9676081	0.083	0.083	0.00418	0.00234	AL1G35490			
Distance from trees - s_{asym}	1	9838286	0.32	0.32	0.00336	0.00174	AL1G35890			

Distance from trees - s_{asym}	2	14860154	0.056	0.056	0.00080	0.00467	AL2G30910			
Distance from trees - s_{asym}	2	15990800	0.213	0.213	0.00349	0.00439	AL2G33570			
Distance from trees - s_{asym}	2	17872478	0.355	0.355	0.00041	0.00232	AL2G38170			
Distance from trees - s_{asym}	2	2123922	0.188	0.188	0.00265	0.00109	NA			
Distance from trees - s_{asym}	2	2460232	0.855	0.855	0.00140	0.00475	AL2G14800			
Distance from trees - s_{asym}	2	2480342	0.115	0.115	0.00109	0.00387	AL2G14860			
Distance from trees - s_{asym}	2	717573	0.479	0.479	0.00235	0.00234	AL2G11470	AT2G42470	-	TRAF-like family protein
Distance from trees - s_{asym}	2	717678	0.482	0.482	0.00313	0.00248	AL2G11470			
Distance from trees - s_{asym}	2	7628317	0.185	0.185	0.00352	0.00174	NA			
Distance from trees - s_{asym}	3	21992347	0.175	0.175	0.00063	0.00363	NA			
Distance from trees - s_{asym}	3	21992365	0.179	0.179	0.00042	0.00443	NA			
Distance from trees - s_{asym}	3	2404217	0.457	0.457	0.00490	0.00450	AL3G16880			
Distance from trees - s_{asym}	3	689519	0.083	0.083	0.00177	0.00452	AL3G11990			
Distance from trees - s_{asym}	3	718229	0.087	0.087	0.00100	0.00124	NA			
Distance from trees - s_{asym}	3	718231	0.087	0.087	0.00100	0.00124	NA			
Distance from trees - s_{asym}	3	744232	0.084	0.084	0.00435	0.00375	AL3G12210			
Distance from trees - s_{asym}	3	7712979	0.216	0.216	0.00053	0.00307	AL3G31210			
Distance from trees - s_{asym}	3	7719638	0.219	0.219	0.00122	0.00341	AL3G31220	AT3G18060	-	transducin family protein / WD-40 repeat family protein
Distance from trees - s_{asym}	3	7720441	0.217	0.217	0.00009	0.00418	AL3G31220			
Distance from trees - s_{asym}	3	7720747	0.223	0.223	0.00056	0.00397	AL3G31220			
Distance from trees - s_{asym}	3	7720788	0.225	0.225	0.00065	0.00294	AL3G31220			
Distance from trees - s_{asym}	3	7720796	0.227	0.227	0.00110	0.00345	AL3G31220			
Distance from trees - s_{asym}	3	7720910	0.218	0.218	0.00172	0.00226	AL3G31220			
Distance from trees - s_{asym}	3	7720928	0.219	0.219	0.00127	0.00234	AL3G31220			

Distance from trees - s_{asym}	3	7721006	0.217	0.217	0.00026	0.00277	AL3G31220			
Distance from trees - s_{asym}	3	7721958	0.229	0.229	0.00158	0.00305	AL3G31230	AT3G18070	BGLU43	beta glucosidase 43
Distance from trees - s_{asym}	3	7722004	0.215	0.215	0.00155	0.00292	AL3G31230			
Distance from trees - s_{asym}	3	7722284	0.22	0.22	0.00060	0.00302	AL3G31230			
Distance from trees - s_{asym}	3	7722397	0.217	0.217	0.00040	0.00237	AL3G31230			
Distance from trees - s_{asym}	3	7722759	0.202	0.202	0.00288	0.00192	AL3G31230			
Distance from trees - s_{asym}	3	7722890	0.218	0.218	0.00078	0.00439	AL3G31230			
Distance from trees - s_{asym}	3	7722892	0.219	0.219	0.00025	0.00289	AL3G31230			
Distance from trees - s_{asym}	3	7722973	0.219	0.219	0.00020	0.00443	AL3G31230			
Distance from trees - s_{asym}	3	7722975	0.219	0.219	0.00015	0.00425	AL3G31230			
Distance from trees - s_{asym}	3	7723030	0.215	0.215	0.00053	0.00211	AL3G31230			
Distance from trees - s_{asym}	3	7723048	0.215	0.215	0.00162	0.00144	AL3G31230			
Distance from trees - s_{asym}	3	7723072	0.209	0.209	0.00148	0.00171	AL3G31230			
Distance from trees - s_{asym}	3	7723079	0.21	0.21	0.00302	0.00130	AL3G31230			
Distance from trees - s_{asym}	3	7723093	0.215	0.215	0.00389	0.00242	AL3G31230			
Distance from trees - s_{asym}	3	7723097	0.215	0.215	0.00329	0.00323	AL3G31230			
Distance from trees - s_{asym}	3	7723106	0.219	0.219	0.00056	0.00411	AL3G31230			
Distance from trees - s_{asym}	3	7723114	0.222	0.222	0.00073	0.00364	AL3G31230			
Distance from trees - s_{asym}	3	7723186	0.222	0.222	0.00095	0.00161	AL3G31230			
Distance from trees - s_{asym}	3	7723201	0.224	0.224	0.00051	0.00242	AL3G31230			
Distance from trees - s_{asym}	3	7723247	0.22	0.22	0.00111	0.00347	AL3G31230			
Distance from trees - s_{asym}	3	7723890	0.217	0.217	0.00090	0.00421	AL3G31230			
Distance from trees - s_{asym}	3	7724124	0.219	0.219	0.00113	0.00499	AL3G31230			
Distance from trees - s_{asym}	3	7729220	0.231	0.231	0.00049	0.00476	AL3G31240	AT3G18080	BGLU44	B-S glucosidase 44

Distance from trees - s_{asym}	3	7729245	0.233	0.233	0.00107	0.00265	AL3G31240			
Distance from trees - s_{asym}	4	10023259	0.052	0.052	0.00423	0.00102	NA			
Distance from trees - s_{asym}	4	10023291	0.058	0.058	0.00079	0.00075	NA			
Distance from trees - s_{asym}	4	20007922	0.151	0.151	0.00078	0.00301	NA			
Distance from trees - s_{asym}	4	20008045	0.156	0.156	0.00112	0.00194	NA			
Distance from trees - s_{asym}	4	6170562	0.053	0.053	0.00170	0.00298	NA			
Distance from trees - s_{asym}	5	11217376	0.155	0.155	0.00133	0.00407	NA			
Distance from trees - s_{asym}	5	11222383	0.142	0.142	0.00236	0.00302	NA			
Distance from trees - s_{asym}	5	11228788	0.638	0.638	0.00154	0.00382	AL5G22750	AT3G44610	AGC1-12	Kinase involved in the first positive phototropism and gravitropism. Critical component for both hypocotyl phototropism and gravitropism, control tropic responses mainly through regulation of PIN-mediated auxin transport by protein phosphorylation.
Distance from trees - s_{asym}	5	11228803	0.643	0.643	0.00040	0.00145	AL5G22750			
Distance from trees - s_{asym}	5	11228825	0.643	0.643	0.00110	0.00189	AL5G22750			
Distance from trees - s_{asym}	5	11228828	0.641	0.641	0.00098	0.00157	AL5G22750			
Distance from trees - s_{asym}	5	11228856	0.643	0.643	0.00033	0.00151	AL5G22750			
Distance from trees - s_{asym}	5	11228889	0.644	0.644	0.00087	0.00055	AL5G22750			
Distance from trees - s_{asym}	5	15796322	0.64	0.64	0.00487	0.00363	AL5G32280			
Distance from trees - s_{asym}	5	17255371	0.15	0.15	0.00440	0.00125	AL5G36070			
Distance from trees - s_{asym}	5	19646802	0.097	0.097	0.00331	0.00409	AL5G42230			
Distance from trees - s_{asym}	5	2627050	0.198	0.198	0.00095	0.00307	AL5G14700			
Distance from trees - s_{asym}	5	4406203	0.665	0.665	0.00240	0.00439	AL5G17730			
Distance from trees - s_{asym}	5	4703257	0.217	0.217	0.00441	0.00382	NA			
Distance from trees - s_{asym}	5	4709864	0.21	0.21	0.00237	0.00229	NA			
Distance from trees - s_{asym}	5	4709928	0.214	0.214	0.00181	0.00187	NA			
Distance from trees - s_{asym}	5	4709933	0.213	0.213	0.00151	0.00153	NA			
Distance from trees - s_{asym}	5	4709953	0.218	0.218	0.00303	0.00447	NA			

Distance from trees - s_{asym}	5	4710174	0.212	0.212	0.00297	0.00498	NA			
Distance from trees - s_{asym}	5	4711490	0.21	0.21	0.00212	0.00289	NA			
Distance from trees - s_{asym}	5	4711552	0.216	0.216	0.00318	0.00423	NA			
Distance from trees - s_{asym}	5	4711597	0.214	0.214	0.00427	0.00436	NA			
Distance from trees - s_{asym}	5	4712254	0.212	0.212	0.00454	0.00231	NA			
Distance from trees - s_{asym}	5	4712690	0.216	0.216	0.00263	0.00413	NA			
Distance from trees - s_{asym}	5	4729940	0.177	0.177	0.00139	0.00038	AL5G18190			
Distance from trees - s_{asym}	5	4739161	0.227	0.227	0.00303	0.00159	NA			
Distance from trees - s_{asym}	5	5454287	0.145	0.145	0.00276	0.00242	NA			
Distance from trees - s_{asym}	6	11055844	0.165	0.165	0.00124	0.00338	NA			
Distance from trees - s_{asym}	6	11089566	0.573	0.573	0.00064	0.00346	AL6G36680	AT5G25050	-	Major facilitator superfamily protein
Distance from trees - s_{asym}	6	11089768	0.477	0.477	0.00205	0.00121	AL6G36680			
Distance from trees - s_{asym}	6	11089841	0.471	0.471	0.00462	0.00085	AL6G36680			
Distance from trees - s_{asym}	6	11089847	0.471	0.471	0.00158	0.00120	AL6G36680			
Distance from trees - s_{asym}	6	11089996	0.475	0.475	0.00440	0.00094	AL6G36680			
Distance from trees - s_{asym}	6	11090126	0.474	0.474	0.00346	0.00057	AL6G36680			
Distance from trees - s_{asym}	6	11090144	0.477	0.477	0.00229	0.00040	AL6G36680			
Distance from trees - s_{asym}	6	11090154	0.477	0.477	0.00305	0.00082	AL6G36680			
Distance from trees - s_{asym}	6	11090198	0.471	0.471	0.00478	0.00220	AL6G36680			
Distance from trees - s_{asym}	6	11090366	0.477	0.477	0.00265	0.00065	AL6G36680			
Distance from trees - s_{asym}	6	11153266	0.183	0.183	0.00181	0.00073	NA			
Distance from trees - s_{asym}	6	12181500	0.165	0.165	0.00043	0.00487	NA			
Distance from trees - s_{asym}	6	12183158	0.169	0.169	0.00344	0.00209	NA			
Distance from trees - s_{asym}	6	12190633	0.307	0.307	0.00190	0.00157	NA			

Distance from trees - s_{asym}	6	12191114	0.406	0.406	0.00284	0.00500	NA			
Distance from trees - s_{asym}	6	12191845	0.27	0.27	0.00183	0.00072	NA			
Distance from trees - s_{asym}	6	12500796	0.805	0.805	0.00049	0.00301	NA			
Distance from trees - s_{asym}	6	23102456	0.184	0.184	0.00130	0.00473	NA			
Distance from trees - s_{asym}	6	23104199	0.165	0.165	0.00044	0.00434	NA			
Distance from trees - s_{asym}	6	23899322	0.264	0.264	0.00058	0.00188	AL6G51090			
Distance from trees - s_{asym}	6	23956839	0.074	0.074	0.00236	0.00296	NA			
Distance from trees - s_{asym}	7	23441270	0.314	0.314	0.00495	0.00434	AL7G51360			
Distance from trees - s_{asym}	7	3532546	0.293	0.293	0.00078	0.00162	AL7G18760			
Distance from trees - s_{asym}	7	7653883	0.253	0.253	0.00459	0.00445	AL7G28920	AT4G22970	AESP1, RSW4	Separase - protease required for release of sister chromatid cohesion during meiosis and mitosis.
Distance from trees - s_{asym}	7	7654107	0.245	0.245	0.00430	0.00390	AL7G28920			
Distance from trees - s_{asym}	8	10517390	0.099	0.099	0.00429	0.00357	NA			
Distance from trees - s_{asym}	8	12085504	0.342	0.342	0.00233	0.00466	NA			
Distance from trees - s_{asym}	8	12377765	0.714	0.714	0.00489	0.00218	AL8G22230			
Distance from trees - s_{asym}	8	15275646	0.261	0.261	0.00237	0.00469	AL8G27230			
Distance from trees - s_{asym}	8	18429827	0.76	0.76	0.00309	0.00496	AL8G34150			
Distance from trees - s_{asym}	8	4647855	0.156	0.156	0.00177	0.00215	AL8G17320			
Assoc	**CHR**	**BP**	**Af_env**	**Af_phen**	**p (env)**	**p (phen)**	**Gene**	**AT homolog**	**Gene name**	**Function**
Intraspecific density - t_{bol}	1	13811088	0.155	0.155	0.00301	0.00393	AL1G44720	AT1G30660	TWINKY	A truncated version of Twinkle that retains only the DNA primase domain.
Intraspecific density - t_{bol}	1	13811104	0.156	0.155	0.00409	0.00328	AL1G44720			
Intraspecific density - t_{bol}	1	13821035	0.59	0.591	0.00003	0.00364	AL1G44750	AT1G30690	PATL4	Affects plant responses to oxidative stress by effects on stomatal closure.
Intraspecific density - t_{bol}	1	13821036	0.592	0.592	0.00003	0.00384	AL1G44750			
Intraspecific density - t_{bol}	1	13869642	0.056	0.056	0.00203	0.00257	NA			
Intraspecific density - t_{bol}	1	17574026	0.157	0.157	0.00468	0.00337	NA			

Intraspecific density - t_{bol}	1	3407634	0.885	0.886	0.00204	0.00336	AL1G19390			
Intraspecific density - t_{bol}	2	19077466	0.348	0.347	0.00141	0.00330	AL2G41140			
Intraspecific density - t_{bol}	2	3496369	0.281	0.283	0.00302	0.00241	NA			
Intraspecific density - t_{bol}	3	1313051	0.308	0.308	0.00205	0.00302	AL3G13880			
Intraspecific density - t_{bol}	3	13798895	0.082	0.083	0.00069	0.00420	NA			
Intraspecific density - t_{bol}	3	14084605	0.341	0.342	0.00304	0.00008	NA			
Intraspecific density - t_{bol}	3	14084739	0.278	0.278	0.00397	0.00406	NA			
Intraspecific density - t_{bol}	3	14838829	0.178	0.179	0.00458	0.00474	AL3G43970			
Intraspecific density - t_{bol}	3	2216493	0.646	0.644	0.00485	0.00315	AL3G16440	AT3G05740	RECQI1	RECQ helicase l1
Intraspecific density - t_{bol}	3	2216927	0.651	0.648	0.00445	0.00377	AL3G16440			
Intraspecific density - t_{bol}	3	2216988	0.651	0.649	0.00435	0.00373	AL3G16440			
Intraspecific density - t_{bol}	3	2217232	0.65	0.648	0.00383	0.00471	AL3G16440			
Intraspecific density - t_{bol}	3	2790791	0.16	0.159	0.00367	0.00155	AL3G17760			
Intraspecific density - t_{bol}	4	14148371	0.225	0.225	0.00108	0.00315	AL4G25230			
Intraspecific density - t_{bol}	4	14407305	0.558	0.558	0.00351	0.00476	NA			
Intraspecific density - t_{bol}	4	14410011	0.591	0.591	0.00149	0.00309	NA			
Intraspecific density - t_{bol}	4	15140031	0.089	0.088	0.00066	0.00117	AL4G27390	AT2G31470	DOR	DOR (Drought tolerance Repressor) - abscisic acid-induced stomatal closure under drought stress.
Intraspecific density - t_{bol}	4	15140053	0.088	0.087	0.00230	0.00499	AL4G27390			
Intraspecific density - t_{bol}	4	18704609	0.107	0.107	0.00036	0.00403	AL4G35790			
Intraspecific density - t_{bol}	5	10611402	0.122	0.123	0.00055	0.00486	NA			
Intraspecific density - t_{bol}	5	15943625	0.202	0.202	0.00425	0.00241	AL5G32650			
Intraspecific density - t_{bol}	5	2363131	0.033	0.033	0.00028	0.00057	NA			
Intraspecific density - t_{bol}	6	1262700	0.219	0.219	0.00248	0.00086	AL6G13550			
Intraspecific density - t_{bol}	6	13836632	0.27	0.271	0.00308	0.00008	NA			

Intraspecific density - t_{bol}	6	13836642	0.269	0.269	0.00155	0.00007	NA			
Intraspecific density - t_{bol}	6	13837086	0.336	0.336	0.00440	0.00451	NA			
Intraspecific density - t_{bol}	6	13837619	0.284	0.284	0.00126	0.00177	NA			
Intraspecific density - t_{bol}	6	13838777	0.265	0.267	0.00450	0.00476	NA			
Intraspecific density - t_{bol}	6	17359200	0.289	0.289	0.00118	0.00481	NA			
Intraspecific density - t_{bol}	6	17359222	0.29	0.29	0.00250	0.00180	NA			
Intraspecific density - t_{bol}	6	17359480	0.306	0.307	0.00131	0.00445	NA			
Intraspecific density - t_{bol}	6	17359547	0.312	0.312	0.00454	0.00489	NA			
Intraspecific density - t_{bol}	6	17359584	0.305	0.306	0.00430	0.00372	NA			
Intraspecific density - t_{bol}	6	22901898	0.111	0.112	0.00368	0.00208	NA			
Intraspecific density - t_{bol}	6	2930349	0.217	0.217	0.00067	0.00145	AL6G17820			
Intraspecific density - t_{bol}	6	3981402	0.115	0.115	0.00003	0.00002	AL6G20520			
Intraspecific density - t_{bol}	6	3982203	0.162	0.161	0.00129	0.00009	AL6G20530	AT5G10080	-	Eukaryotic aspartyl protease family protein
Intraspecific density - t_{bol}	6	3982204	0.16	0.16	0.00093	0.00008	AL6G20530			
Intraspecific density - t_{bol}	6	4418017	0.563	0.563	0.00145	0.00225	NA			
Intraspecific density - t_{bol}	7	10307927	0.334	0.336	0.00137	0.00103	NA			
Intraspecific density - t_{bol}	7	18188640	0.422	0.423	0.00432	0.00329	AL7G44170			
Intraspecific density - t_{bol}	7	18227475	0.263	0.265	0.00128	0.00195	NA			
Intraspecific density - t_{bol}	7	18246258	0.481	0.482	0.00195	0.00331	NA			
Intraspecific density - t_{bol}	7	2629785	0.069	0.07	0.00243	0.00321	AL7G16420			
Intraspecific density - t_{bol}	7	2638731	0.071	0.072	0.00029	0.00241	NA			
Intraspecific density - t_{bol}	7	2638764	0.083	0.083	0.00193	0.00420	NA			
Intraspecific density - t_{bol}	7	9391539	0.145	0.146	0.00238	0.00034	AL7G32790			
Intraspecific density - t_{bol}	7	9664699	0.573	0.576	0.00127	0.00331	AL7G33510			

Intraspecific density - t_{bol}	7	9722598	0.303	0.301	0.00297	0.00498	AL7G33620			
Intraspecific density - t_{bol}	8	10163765	0.068	0.068	0.00141	0.00414	NA			
Intraspecific density - t_{bol}	8	10201638	0.066	0.066	0.00329	0.00386	NA			
Intraspecific density - t_{bol}	8	10201713	0.065	0.065	0.00288	0.00338	NA			
Intraspecific density - t_{bol}	8	10210512	0.073	0.074	0.00273	0.00481	NA			
Intraspecific density - t_{bol}	8	10780362	0.075	0.076	0.00353	0.00160	NA			
Intraspecific density - t_{bol}	8	1238273	0.172	0.173	0.00176	0.00305	AL8G12470	AT5G46040	-	Major facilitator superfamily protein
Intraspecific density - t_{bol}	8	1238886	0.178	0.179	0.00106	0.00087	AL8G12470			
Intraspecific density - t_{bol}	8	1239032	0.177	0.178	0.00018	0.00062	AL8G12470			
Intraspecific density - t_{bol}	8	1239053	0.179	0.18	0.00036	0.00081	AL8G12470			
Intraspecific density - t_{bol}	8	16226317	0.143	0.143	0.00490	0.00082	NA			
Intraspecific density - t_{bol}	8	20821895	0.083	0.083	0.00262	0.00057	AL8G40110			
Intraspecific density - t_{bol}	8	5791193	0.225	0.225	0.00130	0.00424	NA			
Intraspecific density - t_{bol}	8	9966646	0.13	0.129	0.00462	0.00438	NA			
Assoc	**CHR**	**BP**	**Af_env**	**Af_phen**	**p (env)**	**p (phen)**	**Gene**	**AT homolog**	**Gene name**	**Function**
Intraspecific density - t_{flo}	1	10524918	0.107	0.109	0.00084	0.00122	AL1G37600			
Intraspecific density - t_{flo}	1	12161071	0.451	0.449	0.00117	0.00486	NA			
Intraspecific density - t_{flo}	1	13774220	0.281	0.28	0.00320	0.00315	AL1G44680			
Intraspecific density - t_{flo}	1	21527164	0.106	0.109	0.00252	0.00419	NA			
Intraspecific density - t_{flo}	1	22225304	0.162	0.166	0.00314	0.00111	NA			
Intraspecific density - t_{flo}	1	22269731	0.18	0.184	0.00399	0.00319	NA			
Intraspecific density - t_{flo}	1	22271784	0.178	0.182	0.00259	0.00205	NA			
Intraspecific density - t_{flo}	1	22333954	0.135	0.135	0.00094	0.00154	AL1G51980			
Intraspecific density - t_{flo}	1	22337189	0.145	0.144	0.00036	0.00289	AL1G51990			

Intraspecific density - t_{flo}	1	22364953	0.136	0.136	0.00212	0.00204	NA			
Intraspecific density - t_{flo}	1	22365027	0.142	0.141	0.00050	0.00425	NA			
Intraspecific density - t_{flo}	1	30248990	0.274	0.279	0.00243	0.00150	NA			
Intraspecific density - t_{flo}	1	30510389	0.378	0.379	0.00365	0.00406	NA			
Intraspecific density - t_{flo}	1	459897	0.118	0.117	0.00382	0.00085	AL1G11350			
Intraspecific density - t_{flo}	1	6514078	0.076	0.078	0.00417	0.00172	AL1G27560			
Intraspecific density - t_{flo}	2	18076338	0.199	0.203	0.00063	0.00359	AL2G38590			
Intraspecific density - t_{flo}	2	8310035	0.351	0.35	0.00132	0.00431	AL2G20110			
Intraspecific density - t_{flo}	3	14084605	0.343	0.35	0.00016	0.00277	NA			
Intraspecific density - t_{flo}	3	22408231	0.087	0.088	0.00069	0.00282	AL3G51100	AT5G63030	GRXC1	Thioredoxin superfamily protein, redox sensor. Together with GRXC2 regenerates PRXIIB/C/D.
Intraspecific density - t_{flo}	3	22408362	0.185	0.188	0.00323	0.00296	AL3G51100			
Intraspecific density - t_{flo}	3	22408792	0.194	0.198	0.00421	0.00273	AL3G51100			
Intraspecific density - t_{flo}	3	22408895	0.174	0.177	0.00115	0.00265	AL3G51100			
Intraspecific density - t_{flo}	3	8898528	0.331	0.327	0.00202	0.00498	AL3G34100	AT3G20390	RIDA	Encodes a plastidial RidA (Reactive Intermediate Deaminase A) homolog
Intraspecific density - t_{flo}	3	8898773	0.655	0.659	0.00283	0.00402	AL3G34100			
Intraspecific density - t_{flo}	3	8898808	0.659	0.664	0.00287	0.00122	AL3G34100			
Intraspecific density - t_{flo}	4	10168513	0.055	0.055	0.00165	0.00083	NA			
Intraspecific density - t_{flo}	4	10173780	0.055	0.055	0.00166	0.00136	AL4G19870	unknown		
Intraspecific density - t_{flo}	4	10174074	0.053	0.054	0.00074	0.00049	AL4G19870			
Intraspecific density - t_{flo}	4	10176305	0.056	0.056	0.00117	0.00174	AL4G19870			
Intraspecific density - t_{flo}	4	10183212	0.057	0.057	0.00178	0.00092	AL4G19890	AT1G31150	-	K-box region protein (DUF1985)
Intraspecific density - t_{flo}	4	10183890	0.055	0.056	0.00093	0.00186	AL4G19890			
Intraspecific density - t_{flo}	4	14401715	0.093	0.095	0.00098	0.00310	NA			
Intraspecific density - t_{flo}	4	18695212	0.111	0.116	0.00189	0.00260	NA			

Intraspecific density - t_{flo}	4	19421167	0.503	0.495	0.00368	0.00374	AL4G37520			
Intraspecific density - t_{flo}	4	22484516	0.124	0.121	0.00251	0.00298	NA			
Intraspecific density - t_{flo}	5	17707333	0.3	0.3	0.00275	0.00228	AL5G37160			
Intraspecific density - t_{flo}	5	513494	0.135	0.137	0.00246	0.00411	NA			
Intraspecific density - t_{flo}	6	18712862	0.062	0.062	0.00434	0.00226	NA			
Intraspecific density - t_{flo}	6	20960962	0.668	0.671	0.00368	0.00130	AL6G45600			
Intraspecific density - t_{flo}	6	3981402	0.095	0.086	0.00219	0.00054	AL6G20520			
Intraspecific density - t_{flo}	7	8498176	0.199	0.199	0.00307	0.00051	AL7G30850	AT4G22740	-	glycine-rich protein
Intraspecific density - t_{flo}	7	8498457	0.205	0.206	0.00500	0.00017	AL7G30850			
Intraspecific density - t_{flo}	7	8498458	0.205	0.206	0.00500	0.00017	AL7G30850			
Intraspecific density - t_{flo}	7	8498469	0.205	0.206	0.00388	0.00029	AL7G30850			
Intraspecific density - t_{flo}	7	8498474	0.204	0.205	0.00483	0.00027	AL7G30850			
Intraspecific density - t_{flo}	7	8498504	0.205	0.206	0.00497	0.00032	AL7G30850			
Intraspecific density - t_{flo}	7	8500270	0.098	0.1	0.00481	0.00068	AL7G30860	AT5G46000	-	Mannose-binding lectin superfamily protein
Intraspecific density - t_{flo}	7	8500305	0.098	0.098	0.00442	0.00123	AL7G30860			
Intraspecific density - t_{flo}	7	8500323	0.096	0.096	0.00275	0.00086	AL7G30860			
Intraspecific density - t_{flo}	7	9450363	0.148	0.149	0.00253	0.00298	AL7G32950			
Intraspecific density - t_{flo}	7	9472681	0.134	0.135	0.00253	0.00428	NA			
Intraspecific density - t_{flo}	7	9479363	0.773	0.772	0.00074	0.00341	AL7G33030			
Intraspecific density - t_{flo}	7	9655717	0.603	0.616	0.00302	0.00001	AL7G33480			
Intraspecific density - t_{flo}	7	9657010	0.723	0.737	0.00481	0.00205	AL7G33490	AT4G20400	JMJ14	Encodes a histone H3K4 demethylase repressing floral transition.
Intraspecific density - t_{flo}	7	9661353	0.638	0.651	0.00431	0.00005	AL7G33490			
Intraspecific density - t_{flo}	7	9662939	0.321	0.313	0.00034	0.00004	AL7G33500	AT4G20390	CASPL1B2	Uncharacterized protein family (UPF0497)
Intraspecific density - t_{flo}	7	9662954	0.557	0.568	0.00001	0.00001	AL7G33500			

Intraspecific density - t_{flo}	7	9663446	0.364	0.356	0.00171	0.00087	AL7G33500			
Intraspecific density - t_{flo}	7	9664699	0.571	0.582	0.00009	0.00004	AL7G33510	AT4G20380	LSD1	LSD1 monitors a superoxide-dependent signal and negatively regulates a plant cell death pathway.
Intraspecific density - t_{flo}	7	9665238	0.622	0.634	0.00033	0.00091	AL7G33510			
Intraspecific density - t_{flo}	7	9665417	0.311	0.302	0.00389	0.00022	AL7G33510			
Intraspecific density - t_{flo}	7	9667612	0.574	0.583	0.00139	0.00000	NA			
Intraspecific density - t_{flo}	7	9670601	0.505	0.513	0.00014	0.00149	NA			
Intraspecific density - t_{flo}	7	9670643	0.509	0.516	0.00029	0.00153	NA			
Intraspecific density - t_{flo}	7	9670714	0.517	0.525	0.00179	0.00227	NA			
Intraspecific density - t_{flo}	7	9722598	0.308	0.299	0.00209	0.00358	AL7G33620			
Intraspecific density - t_{flo}	7	9726891	0.281	0.275	0.00481	0.00451	AL7G33630			
Intraspecific density - t_{flo}	8	12668064	0.049	0.049	0.00219	0.00227	NA			
Intraspecific density - t_{flo}	8	20821895	0.075	0.078	0.00002	0.00433	AL8G40110			
Intraspecific density - t_{flo}	8	2373086	0.531	0.532	0.00059	0.00410	NA			
Intraspecific density - t_{flo}	8	5632001	0.364	0.363	0.00261	0.00154	AL8G18110			
Intraspecific density - t_{flo}	8	691525	0.498	0.509	0.00317	0.00398	AL8G11500			
Intraspecific density - t_{flo}	8	7355156	0.081	0.082	0.00375	0.00290	AL8G19630			

Table S10

Table S 10: Contrast analysis for the deviation from the expected mid-homozygous haplotype. Each outlier SNP within a candidate gene for the associated environmental trait was tested. N - number of analysed individual genotypes. Standard error (SE) and model fit (R^2) for the respective linear model and the absolute deviation (|deviation|) as well as the direction of deviation.

SNP	gene	N	deviation	SE	R^2	|deviation|	direction
S_1_268095	AL1G10810	151	-0.068	0.129	0.038	0.068	negative
S_1_270001	AL1G10810	150	0.023	0.131	0.038	0.023	positive
S_1_481396	AL1G11410	140	-0.077	0.212	0.063	0.077	negative
S_1_481410	AL1G11410	142	-0.080	0.209	0.065	0.080	negative
S_1_13811088	AL1G44720	290	-0.505	0.238	0.025	0.505	negative
S_1_13811104	AL1G44720	286	-0.502	0.239	0.025	0.502	negative
S_1_13821035	AL1G44750	288	-0.011	0.128	0.021	0.011	negative
S_1_13821036	AL1G44750	289	-0.015	0.127	0.022	0.015	negative
S_1_14302596	AL1G45720	143	-0.212	0.284	0.100	0.212	negative
S_1_14302601	AL1G45720	142	-0.211	0.285	0.099	0.211	negative
S_1_23492916	AL1G53350	145	0.336	0.365	0.043	0.336	positive
S_1_24847364	AL1G55480	144	-0.073	0.145	0.109	0.073	negative
S_1_24847370	AL1G55480	143	-0.088	0.150	0.106	0.088	negative
S_1_24848650	AL1G55480	142	-0.087	0.150	0.108	0.087	negative
S_1_24849196	AL1G55480	144	-0.095	0.148	0.111	0.095	negative
S_1_25345243	AL1G56300	141	0.002	0.164	0.099	0.002	positive
S_1_25345893	AL1G56300	141	0.032	0.158	0.098	0.032	positive
S_2_717573	AL2G11470	237	-0.176	0.114	0.054	0.176	negative
S_2_717678	AL2G11470	235	-0.171	0.114	0.050	0.171	negative
S_2_2984057	AL2G15870	333	0.104	0.179	0.021	0.104	positive
S_2_2984138	AL2G15870	325	0.125	0.140	0.024	0.125	positive
S_2_2984161	AL2G15870	327	0.126	0.140	0.025	0.126	positive
S_2_2984204	AL2G15870	321	0.141	0.135	0.024	0.141	positive
S_2_8306647	AL2G20100	141	-0.135	0.137	0.051	0.135	negative
S_2_8306655	AL2G20100	143	-0.170	0.134	0.071	0.170	negative
S_2_12041710	AL2G25320	154	0.398	0.353	0.055	0.398	positive
S_2_12041721	AL2G25320	154	0.389	0.353	0.051	0.389	positive
S_2_12041740	AL2G25320	154	0.398	0.353	0.055	0.398	positive
S_2_12516935	AL2G26090	329	-0.192	0.095	0.069	0.192	negative
S_2_12516943	AL2G26090	325	-0.169	0.096	0.067	0.169	negative
S_2_12517195	AL2G26090	331	-0.048	0.098	0.019	0.048	negative
S_2_12517234	AL2G26090	329	-0.061	0.098	0.021	0.061	negative
S_2_12517269	AL2G26090	333	-0.070	0.096	0.019	0.070	negative
S_2_12517905	AL2G26090	326	0.005	0.098	0.018	0.005	positive
S_2_13776669	AL2G28640	326	-0.221	0.100	0.040	0.221	negative
S_2_13776670	AL2G28640	326	-0.221	0.100	0.040	0.221	negative
S_2_15594464	AL2G32570	322	0.193	0.171	0.017	0.193	positive

S_2_15596858	AL2G32570	322	0.057	0.164	0.008	0.057	positive
S_2_16108535	AL2G33880	325	-0.213	0.165	0.032	0.213	negative
S_2_16109744	AL2G33880	333	-0.234	0.163	0.031	0.234	negative
S_2_16110357	AL2G33880	326	-0.280	0.151	0.039	0.280	negative
S_2_16111638	AL2G33890	327	-0.304	0.175	0.035	0.304	negative
S_2_16111641	AL2G33890	330	-0.293	0.159	0.038	0.293	negative
S_2_16113460	AL2G33900	326	-0.307	0.174	0.043	0.307	negative
S_2_16113634	AL2G33900	329	-0.245	0.168	0.042	0.245	negative
S_2_16113828	AL2G33900	331	-0.312	0.172	0.043	0.312	negative
S_2_16127218	AL2G33940	330	-0.275	0.151	0.050	0.275	negative
S_2_16127638	AL2G33940	333	-0.222	0.143	0.048	0.222	negative
S_2_16143551	AL2G34000	332	-0.221	0.147	0.036	0.221	negative
S_2_16143645	AL2G34000	331	-0.209	0.147	0.037	0.209	negative
S_2_16143857	AL2G34000	329	-0.271	0.153	0.050	0.271	negative
S_2_16143885	AL2G34000	330	-0.234	0.149	0.042	0.234	negative
S_2_16143902	AL2G34000	329	-0.235	0.149	0.042	0.235	negative
S_2_16143905	AL2G34000	330	-0.230	0.149	0.043	0.230	negative
S_2_16143923	AL2G34000	331	-0.239	0.149	0.042	0.239	negative
S_2_16143957	AL2G34000	329	-0.228	0.146	0.036	0.228	negative
S_2_16143959	AL2G34000	328	-0.239	0.151	0.041	0.239	negative
S_2_16144185	AL2G34000	329	-0.186	0.149	0.039	0.186	negative
S_2_16144260	AL2G34000	329	-0.205	0.147	0.036	0.205	negative
S_2_16144307	AL2G34000	329	-0.208	0.146	0.035	0.208	negative
S_2_16144421	AL2G34010	326	-0.183	0.148	0.040	0.183	negative
S_2_16144425	AL2G34010	327	-0.186	0.148	0.040	0.186	negative
S_2_16144444	AL2G34010	324	-0.168	0.149	0.043	0.168	negative
S_2_16144446	AL2G34010	325	-0.141	0.147	0.040	0.141	negative
S_2_16144451	AL2G34010	328	-0.179	0.148	0.042	0.179	negative
S_2_16144490	AL2G34010	328	-0.161	0.148	0.042	0.161	negative
S_2_16144537	AL2G34010	328	-0.204	0.147	0.038	0.204	negative
S_2_16144538	AL2G34010	328	-0.203	0.147	0.038	0.203	negative
S_2_16144547	AL2G34010	325	-0.193	0.148	0.039	0.193	negative
S_2_16144571	AL2G34010	329	-0.182	0.147	0.040	0.182	negative
S_2_16144578	AL2G34010	326	-0.206	0.147	0.037	0.206	negative
S_2_16144581	AL2G34010	329	-0.182	0.147	0.039	0.182	negative
S_2_16144596	AL2G34010	330	-0.185	0.147	0.039	0.185	negative
S_2_16144646	AL2G34010	330	-0.218	0.149	0.042	0.218	negative
S_2_16144654	AL2G34010	332	-0.219	0.149	0.042	0.219	negative
S_2_16144693	AL2G34010	326	-0.202	0.154	0.039	0.202	negative
S_2_16144717	AL2G34010	328	-0.202	0.147	0.039	0.202	negative
S_2_16144744	AL2G34010	331	-0.213	0.150	0.042	0.213	negative
S_2_16144747	AL2G34010	332	-0.182	0.147	0.040	0.182	negative
S_2_16144884	AL2G34010	329	-0.057	0.159	0.028	0.057	negative
S_2_16145092	AL2G34010	333	-0.029	0.154	0.028	0.029	negative
S_2_16145236	AL2G34010	330	-0.002	0.152	0.029	0.002	negative

S_2_16145271	AL2G34010	327	-0.038	0.154	0.028	0.038	negative
S_2_16145287	AL2G34010	331	-0.052	0.154	0.025	0.052	negative
S_2_16145296	AL2G34010	332	-0.052	0.154	0.026	0.052	negative
S_2_16145349	AL2G34010	332	-0.062	0.155	0.023	0.062	negative
S_2_16145350	AL2G34010	332	-0.062	0.155	0.023	0.062	negative
S_2_16145353	AL2G34010	331	-0.061	0.155	0.024	0.061	negative
S_2_16145374	AL2G34010	330	-0.052	0.156	0.025	0.052	negative
S_2_16145518	AL2G34010	327	-0.049	0.157	0.026	0.049	negative
S_2_16145524	AL2G34010	330	-0.048	0.155	0.026	0.048	negative
S_2_16145566	AL2G34010	329	-0.057	0.154	0.025	0.057	negative
S_2_16145572	AL2G34010	332	-0.053	0.153	0.026	0.053	negative
S_2_16145599	AL2G34010	328	-0.079	0.158	0.026	0.079	negative
S_2_16145684	AL2G34010	329	-0.077	0.158	0.026	0.077	negative
S_2_16145690	AL2G34010	327	-0.068	0.159	0.027	0.068	negative
S_2_16145695	AL2G34010	328	-0.069	0.159	0.026	0.069	negative
S_2_16145696	AL2G34010	326	-0.063	0.159	0.027	0.063	negative
S_2_16145705	AL2G34010	324	-0.067	0.159	0.027	0.067	negative
S_2_16145710	AL2G34010	325	-0.065	0.159	0.028	0.065	negative
S_2_16153935	AL2G34030	325	-0.038	0.149	0.027	0.038	negative
S_2_16154236	AL2G34030	325	-0.060	0.147	0.031	0.060	negative
S_2_16154395	AL2G34030	331	-0.044	0.149	0.028	0.044	negative
S_2_16154727	AL2G34030	324	-0.055	0.149	0.027	0.055	negative
S_2_16154912	AL2G34030	331	-0.075	0.151	0.028	0.075	negative
S_2_16160893	AL2G34050	332	0.041	0.127	0.044	0.041	positive
S_2_16161267	AL2G34050	331	-0.047	0.144	0.020	0.047	negative
S_2_16171284	AL2G34060	335	-0.120	0.144	0.026	0.120	negative
S_2_16171497	AL2G34060	328	-0.074	0.146	0.025	0.074	negative
S_2_16171800	AL2G34060	330	-0.150	0.149	0.028	0.150	negative
S_2_16171953	AL2G34060	329	-0.175	0.151	0.032	0.175	negative
S_2_16172007	AL2G34060	326	-0.245	0.153	0.034	0.245	negative
S_2_16172663	AL2G34060	329	-0.164	0.152	0.030	0.164	negative
S_2_16172749	AL2G34060	328	-0.143	0.148	0.029	0.143	negative
S_2_16172834	AL2G34060	332	-0.191	0.150	0.034	0.191	negative
S_2_16173567	AL2G34060	333	-0.247	0.153	0.037	0.247	negative
S_2_16173601	AL2G34060	328	-0.245	0.154	0.036	0.245	negative
S_2_16173605	AL2G34060	325	-0.240	0.154	0.037	0.240	negative
S_2_16173608	AL2G34060	324	-0.241	0.155	0.037	0.241	negative
S_2_16173762	AL2G34060	328	-0.138	0.148	0.028	0.138	negative
S_3_2216493	AL3G16440	294	-0.023	0.136	0.010	0.023	negative
S_3_2216927	AL3G16440	289	-0.044	0.140	0.011	0.044	negative
S_3_2216988	AL3G16440	294	0.004	0.136	0.010	0.004	positive
S_3_2217232	AL3G16440	291	-0.050	0.140	0.011	0.050	negative
S_3_3537009	AL3G19960	324	0.201	0.144	0.041	0.201	positive
S_3_3537021	AL3G19960	323	0.182	0.146	0.035	0.182	positive
S_3_7719638	AL3G31220	240	0.086	0.161	0.046	0.086	positive

S_3_7720441	AL3G31220	238	0.200	0.156	0.068	0.200	positive
S_3_7720747	AL3G31220	240	0.189	0.157	0.062	0.189	positive
S_3_7720788	AL3G31220	235	0.195	0.159	0.062	0.195	positive
S_3_7720796	AL3G31220	238	0.224	0.155	0.060	0.224	positive
S_3_7720910	AL3G31220	238	0.227	0.161	0.057	0.227	positive
S_3_7720928	AL3G31220	239	0.113	0.154	0.053	0.113	positive
S_3_7721006	AL3G31220	235	0.194	0.156	0.065	0.194	positive
S_3_7721958	AL3G31230	235	0.181	0.158	0.060	0.181	positive
S_3_7722004	AL3G31230	233	0.230	0.163	0.058	0.230	positive
S_3_7722284	AL3G31230	231	0.201	0.161	0.060	0.201	positive
S_3_7722397	AL3G31230	238	0.169	0.162	0.065	0.169	positive
S_3_7722759	AL3G31230	235	0.143	0.167	0.044	0.143	positive
S_3_7722890	AL3G31230	239	0.149	0.157	0.054	0.149	positive
S_3_7722892	AL3G31230	238	0.192	0.159	0.061	0.192	positive
S_3_7722973	AL3G31230	234	0.188	0.162	0.070	0.188	positive
S_3_7722975	AL3G31230	237	0.182	0.161	0.070	0.182	positive
S_3_7723030	AL3G31230	234	0.202	0.161	0.061	0.202	positive
S_3_7723048	AL3G31230	232	0.232	0.165	0.052	0.232	positive
S_3_7723072	AL3G31230	237	0.239	0.163	0.055	0.239	positive
S_3_7723079	AL3G31230	237	0.228	0.163	0.051	0.228	positive
S_3_7723093	AL3G31230	234	0.188	0.163	0.044	0.188	positive
S_3_7723097	AL3G31230	235	0.190	0.163	0.044	0.190	positive
S_3_7723106	AL3G31230	239	0.170	0.157	0.059	0.170	positive
S_3_7723114	AL3G31230	239	0.164	0.157	0.058	0.164	positive
S_3_7723186	AL3G31230	237	0.150	0.158	0.053	0.150	positive
S_3_7723201	AL3G31230	237	0.175	0.157	0.060	0.175	positive
S_3_7723247	AL3G31230	236	0.131	0.158	0.049	0.131	positive
S_3_7723890	AL3G31230	235	0.275	0.160	0.067	0.275	positive
S_3_7724124	AL3G31230	234	0.114	0.160	0.055	0.114	positive
S_3_7729220	AL3G31240	234	0.157	0.154	0.065	0.157	positive
S_3_7729245	AL3G31240	234	0.181	0.151	0.060	0.181	positive
S_3_8898528	AL3G34100	254	0.132	0.148	0.028	0.132	positive
S_3_8898773	AL3G34100	251	0.136	0.151	0.026	0.136	positive
S_3_8898808	AL3G34100	251	0.166	0.146	0.026	0.166	positive
S_3_10933233	AL3G38380	142	-0.237	0.160	0.091	0.237	negative
S_3_10933337	AL3G38380	144	-0.189	0.153	0.100	0.189	negative
S_3_10933438	AL3G38380	142	-0.204	0.154	0.098	0.204	negative
S_3_10933478	AL3G38380	142	-0.177	0.156	0.103	0.177	negative
S_3_10933713	AL3G38380	140	-0.207	0.158	0.098	0.207	negative
S_3_10933931	AL3G38380	144	-0.182	0.138	0.131	0.182	negative
S_3_10933970	AL3G38380	141	-0.191	0.140	0.128	0.191	negative
S_3_10934063	AL3G38380	143	-0.193	0.157	0.096	0.193	negative
S_3_10934083	AL3G38380	143	-0.167	0.154	0.101	0.167	negative
S_3_10934109	AL3G38380	140	-0.146	0.157	0.104	0.146	negative
S_3_10934137	AL3G38380	143	-0.182	0.157	0.100	0.182	negative

S_3_10934148	AL3G38380	143	-0.182	0.157	0.100	0.182	negative
S_3_10934163	AL3G38380	144	-0.170	0.155	0.103	0.170	negative
S_3_10934165	AL3G38380	144	-0.170	0.155	0.103	0.170	negative
S_3_10934179	AL3G38380	144	-0.182	0.160	0.098	0.182	negative
S_3_10934406	AL3G38380	144	-0.191	0.153	0.098	0.191	negative
S_3_10934416	AL3G38380	143	-0.184	0.154	0.098	0.184	negative
S_3_10934443	AL3G38380	142	-0.165	0.155	0.101	0.165	negative
S_3_10934446	AL3G38380	142	-0.165	0.155	0.101	0.165	negative
S_3_10934450	AL3G38380	142	-0.165	0.155	0.101	0.165	negative
S_3_10934488	AL3G38380	143	-0.165	0.154	0.101	0.165	negative
S_3_10934805	AL3G38380	142	-0.221	0.155	0.099	0.221	negative
S_3_10934856	AL3G38380	141	-0.224	0.158	0.093	0.224	negative
S_3_10935515	AL3G38380	141	-0.144	0.152	0.081	0.144	negative
S_3_10935517	AL3G38380	141	-0.144	0.152	0.081	0.144	negative
S_3_10936028	AL3G38380	139	-0.198	0.139	0.135	0.198	negative
S_3_10936699	AL3G38380	140	-0.219	0.157	0.093	0.219	negative
S_3_10937221	AL3G38380	140	-0.234	0.159	0.091	0.234	negative
S_3_10937739	AL3G38380	143	-0.175	0.153	0.099	0.175	negative
S_3_10937770	AL3G38380	142	-0.192	0.154	0.098	0.192	negative
S_3_10937776	AL3G38380	142	-0.175	0.155	0.099	0.175	negative
S_3_10937778	AL3G38380	141	-0.195	0.156	0.095	0.195	negative
S_3_10937779	AL3G38380	141	-0.195	0.156	0.095	0.195	negative
S_3_10938130	AL3G38380	143	-0.215	0.154	0.092	0.215	negative
S_3_10938516	AL3G38380	143	-0.231	0.155	0.093	0.231	negative
S_3_10939315	AL3G38380	143	-0.234	0.155	0.093	0.234	negative
S_3_21251806	AL3G49100	297	0.055	0.113	0.036	0.055	positive
S_3_21251813	AL3G49100	299	0.074	0.112	0.031	0.074	positive
S_3_21251838	AL3G49100	297	0.053	0.113	0.028	0.053	positive
S_3_22408362	AL3G51100	259	0.141	0.297	0.021	0.141	positive
S_3_22408792	AL3G51100	260	0.221	0.208	0.023	0.221	positive
S_3_22408895	AL3G51100	257	0.037	0.336	0.026	0.037	positive
S_3_24063849	AL3G54000	174	0.087	0.152	0.032	0.087	positive
S_3_24064254	AL3G54000	177	0.091	0.148	0.027	0.091	positive
S_3_24064314	AL3G54000	176	0.095	0.148	0.027	0.095	positive
S_3_24064486	AL3G54000	176	0.046	0.148	0.030	0.046	positive
S_3_24064494	AL3G54000	179	0.088	0.146	0.026	0.088	positive
S_4_2420766	AL4G14260	324	-0.062	0.106	0.036	0.062	negative
S_4_2420901	AL4G14260	321	-0.083	0.103	0.026	0.083	negative
S_4_2420967	AL4G14260	321	-0.058	0.102	0.033	0.058	negative
S_4_2424365	AL4G14270	323	-0.082	0.108	0.037	0.082	negative
S_4_2424380	AL4G14270	321	-0.070	0.109	0.040	0.070	negative
S_4_4981864	AL4G17470	321	0.294	0.220	0.027	0.294	positive
S_4_4982787	AL4G17470	330	0.302	0.210	0.027	0.302	positive
S_4_14451845	AL4G25810	150	0.081	0.130	0.047	0.081	positive
S_4_14451849	AL4G25810	151	0.111	0.130	0.058	0.111	positive

S_4_14547956	AL4G25980	142	0.065	0.142	0.045	0.065	positive
S_4_14548115	AL4G25980	141	0.163	0.156	0.036	0.163	positive
S_4_14549794	AL4G25980	139	0.100	0.125	0.056	0.100	positive
S_4_16574296	AL4G30860	126	-0.278	0.253	0.091	0.278	negative
S_4_16574326	AL4G30860	125	-0.277	0.256	0.092	0.277	negative
S_4_16574405	AL4G30860	127	-0.095	0.240	0.076	0.095	negative
S_4_16574644	AL4G30860	127	-0.204	0.254	0.101	0.204	negative
S_4_16574686	AL4G30860	126	-0.254	0.230	0.139	0.254	negative
S_4_16582058	AL4G30890	125	-0.071	0.191	0.080	0.071	negative
S_4_16582151	AL4G30890	123	-0.064	0.192	0.069	0.064	negative
S_4_20738763	AL4G40930	448	-0.082	0.145	0.016	0.082	negative
S_4_20739049	AL4G40930	440	-0.061	0.145	0.015	0.061	negative
S_5_2635116	AL5G14730	301	0.098	0.117	0.058	0.098	positive
S_5_2636965	AL5G14730	301	0.152	0.126	0.063	0.152	positive
S_5_11228788	AL5G22750	232	-0.014	0.123	0.028	0.014	negative
S_5_11228803	AL5G22750	236	-0.016	0.124	0.033	0.016	negative
S_5_11228825	AL5G22750	239	-0.040	0.122	0.031	0.040	negative
S_5_11228828	AL5G22750	238	-0.045	0.123	0.032	0.045	negative
S_5_11228856	AL5G22750	239	-0.020	0.122	0.034	0.020	negative
S_5_11228889	AL5G22750	238	-0.020	0.122	0.031	0.020	negative
S_5_12720723	AL5G25490	148	0.469	0.363	0.047	0.469	positive
S_5_12824835	AL5G25810	151	-0.046	0.124	0.054	0.046	negative
S_5_12824880	AL5G25810	150	-0.042	0.127	0.052	0.042	negative
S_5_12829737	AL5G25820	149	-0.102	0.132	0.054	0.102	negative
S_5_12829742	AL5G25820	149	-0.102	0.132	0.054	0.102	negative
S_5_12829745	AL5G25820	149	-0.102	0.132	0.054	0.102	negative
S_5_17841024	AL5G37490	149	0.265	0.115	0.081	0.265	positive
S_5_17841028	AL5G37490	150	0.318	0.115	0.087	0.318	positive
S_5_17841032	AL5G37490	148	0.253	0.116	0.076	0.253	positive
S_5_17841033	AL5G37490	151	0.246	0.114	0.080	0.246	positive
S_5_17841402	AL5G37490	148	0.283	0.115	0.084	0.283	positive
S_5_20031599	AL5G43050	151	-0.343	0.164	0.110	0.343	negative
S_5_20033833	AL5G43050	148	-0.413	0.171	0.141	0.413	negative
S_5_20040026	AL5G43070	147	-0.339	0.167	0.112	0.339	negative
S_5_20040072	AL5G43070	147	-0.240	0.167	0.135	0.240	negative
S_6_3056651	AL6G18170	124	0.158	0.214	0.053	0.158	positive
S_6_3057392	AL6G18170	124	0.051	0.220	0.054	0.051	positive
S_6_3058982	AL6G18180	122	0.198	0.211	0.062	0.198	positive
S_6_3059319	AL6G18180	123	0.107	0.212	0.062	0.107	positive
S_6_3059426	AL6G18180	124	0.129	0.211	0.055	0.129	positive
S_6_3059442	AL6G18180	122	0.121	0.211	0.058	0.121	positive
S_6_3982203	AL6G20530	288	0.136	0.201	0.007	0.136	positive
S_6_3982204	AL6G20530	287	0.139	0.203	0.007	0.139	positive
S_6_5419821	AL6G24050	124	-0.239	0.173	0.080	0.239	negative
S_6_5420607	AL6G24050	125	-0.292	0.170	0.110	0.292	negative

S_6_7079555	AL6G28290	139	-0.185	0.131	0.056	0.185	negative
S_6_7079571	AL6G28290	139	-0.188	0.133	0.056	0.188	negative
S_6_7079648	AL6G28290	144	-0.175	0.130	0.055	0.175	negative
S_6_7080143	AL6G28290	139	-0.167	0.132	0.053	0.167	negative
S_6_7080562	AL6G28290	142	-0.180	0.131	0.053	0.180	negative
S_6_7081604	AL6G28300	145	-0.176	0.124	0.074	0.176	negative
S_6_7082808	AL6G28300	139	-0.188	0.129	0.063	0.188	negative
S_6_7082949	AL6G28300	143	-0.105	0.131	0.043	0.105	negative
S_6_7083381	AL6G28300	142	-0.155	0.132	0.060	0.155	negative
S_6_7083449	AL6G28300	141	-0.179	0.130	0.058	0.179	negative
S_6_7083462	AL6G28300	140	-0.178	0.129	0.058	0.178	negative
S_6_7083514	AL6G28300	141	-0.186	0.130	0.062	0.186	negative
S_6_7083528	AL6G28300	141	-0.177	0.132	0.053	0.177	negative
S_6_7083913	AL6G28300	143	-0.139	0.127	0.051	0.139	negative
S_6_7084323	AL6G28300	139	-0.122	0.130	0.055	0.122	negative
S_6_7763958	AL6G29890	150	-0.258	0.182	0.072	0.258	negative
S_6_7763989	AL6G29890	149	-0.237	0.184	0.074	0.237	negative
S_6_11089566	AL6G36680	241	-0.079	0.114	0.043	0.079	negative
S_6_11089768	AL6G36680	239	0.096	0.114	0.030	0.096	positive
S_6_11089841	AL6G36680	241	0.081	0.113	0.025	0.081	positive
S_6_11089847	AL6G36680	239	0.057	0.114	0.030	0.057	positive
S_6_11089996	AL6G36680	237	0.079	0.115	0.028	0.079	positive
S_6_11090126	AL6G36680	234	0.081	0.115	0.027	0.081	positive
S_6_11090144	AL6G36680	237	0.082	0.114	0.029	0.082	positive
S_6_11090154	AL6G36680	238	0.094	0.114	0.028	0.094	positive
S_6_11090198	AL6G36680	237	0.104	0.113	0.025	0.104	positive
S_6_11090366	AL6G36680	236	0.124	0.113	0.035	0.124	positive
S_6_23209638	AL6G49560	141	0.008	0.120	0.084	0.008	positive
S_6_23209706	AL6G49560	142	-0.009	0.121	0.079	0.009	negative
S_6_23209712	AL6G49560	139	-0.033	0.123	0.086	0.033	negative
S_7_2955099	AL7G17280	328	-0.071	0.170	0.026	0.071	negative
S_7_2955174	AL7G17280	323	-0.059	0.176	0.028	0.059	negative
S_7_5095004	AL7G22350	140	-0.005	0.215	0.074	0.005	negative
S_7_5095847	AL7G22350	141	0.007	0.215	0.079	0.007	positive
S_7_5097245	AL7G22350	142	0.004	0.216	0.078	0.004	positive
S_7_5097554	AL7G22350	143	-0.091	0.199	0.067	0.091	negative
S_7_5097935	AL7G22350	145	0.020	0.213	0.080	0.020	positive
S_7_5098056	AL7G22350	143	0.078	0.200	0.071	0.078	positive
S_7_7653883	AL7G28920	234	-0.137	0.144	0.048	0.137	negative
S_7_7654107	AL7G28920	235	-0.165	0.149	0.051	0.165	negative
S_7_8498176	AL7G30850	257	0.146	0.191	0.017	0.146	positive
S_7_8498457	AL7G30850	254	0.160	0.190	0.017	0.160	positive
S_7_8498458	AL7G30850	254	0.160	0.190	0.017	0.160	positive
S_7_8498469	AL7G30850	254	0.158	0.190	0.018	0.158	positive
S_7_8498474	AL7G30850	255	0.160	0.190	0.017	0.160	positive

S_7_8498504	AL7G30850	257	0.153	0.189	0.017	0.153	positive
S_7_9657010	AL7G33490	251	-0.076	0.164	0.028	0.076	negative
S_7_9661353	AL7G33490	248	0.090	0.140	0.032	0.090	positive
S_7_9662939	AL7G33500	256	-0.110	0.152	0.035	0.110	negative
S_7_9662954	AL7G33500	257	-0.009	0.130	0.049	0.009	negative
S_7_9663446	AL7G33500	255	-0.114	0.145	0.036	0.114	negative
S_7_9664699	AL7G33510	254	-0.152	0.139	0.043	0.152	negative
S_7_9665238	AL7G33510	253	-0.054	0.143	0.040	0.054	negative
S_7_9665417	AL7G33510	256	-0.066	0.155	0.022	0.066	negative
S_7_19836914	AL7G45710	149	-0.219	0.149	0.060	0.219	negative
S_7_19837422	AL7G45710	152	-0.221	0.148	0.062	0.221	negative
S_8_1238273	AL8G12470	295	-0.057	0.177	0.018	0.057	negative
S_8_1238886	AL8G12470	296	0.014	0.177	0.016	0.014	positive
S_8_1239032	AL8G12470	290	-0.061	0.174	0.023	0.061	negative
S_8_1239053	AL8G12470	292	0.000	0.180	0.017	0.000	positive
S_8_4113233	AL8G16610	151	-0.488	0.285	0.088	0.488	negative
S_8_4114711	AL8G16610	151	-0.494	0.288	0.084	0.494	negative
S_8_4116800	AL8G16620	150	-0.234	0.247	0.097	0.234	negative
S_8_4116870	AL8G16620	149	-0.476	0.281	0.110	0.476	negative
S_8_18245391	AL8G33680	150	-0.112	0.129	0.042	0.112	negative
S_8_18245394	AL8G33680	150	-0.112	0.129	0.042	0.112	negative
S_8_18245778	AL8G33680	151	-0.126	0.129	0.037	0.126	negative
S_8_18245945	AL8G33680	153	-0.226	0.145	0.052	0.226	negative
S_8_21949767	AL8G43030	150	-0.054	0.114	0.058	0.054	negative
S_8_21949800	AL8G43030	150	-0.073	0.115	0.060	0.073	negative
S_8_21950417	AL8G43030	148	0.002	0.113	0.058	0.002	positive
S_8_21950580	AL8G43030	147	-0.112	0.153	0.071	0.112	negative
S_8_21950636	AL8G43030	149	-0.079	0.149	0.076	0.079	negative
S_8_21950643	AL8G43030	149	-0.112	0.144	0.071	0.112	negative
S_8_21950696	AL8G43030	151	-0.094	0.153	0.080	0.094	negative
S_8_21950700	AL8G43030	150	-0.202	0.159	0.085	0.202	negative
S_8_21950748	AL8G43030	149	-0.054	0.147	0.079	0.054	negative
S_8_21950839	AL8G43030	150	-0.077	0.146	0.074	0.077	negative
S_8_21950841	AL8G43030	150	-0.084	0.146	0.073	0.084	negative
S_8_21950852	AL8G43030	150	-0.084	0.146	0.073	0.084	negative
S_8_21951151	AL8G43030	151	-0.124	0.153	0.086	0.124	negative
S_8_21951348	AL8G43030	153	-0.089	0.150	0.064	0.089	negative
S_8_21951468	AL8G43030	149	0.023	0.152	0.055	0.023	positive
S_8_21951563	AL8G43030	150	-0.127	0.154	0.066	0.127	negative
S_8_21951901	AL8G43030	149	-0.028	0.147	0.068	0.028	negative
S_8_21952027	AL8G43030	146	-0.091	0.149	0.071	0.091	negative
S_8_21952034	AL8G43030	147	-0.022	0.151	0.082	0.022	negative
S_8_21952111	AL8G43040	148	-0.032	0.151	0.077	0.032	negative
S_8_21952537	AL8G43040	150	-0.169	0.160	0.086	0.169	negative
S_8_21952839	AL8G43040	148	-0.084	0.149	0.070	0.084	negative

S_8_21952878	AL8G43040	151	-0.066	0.149	0.072	0.066	negative
S_8_21952972	AL8G43040	150	-0.070	0.155	0.078	0.070	negative
S_8_21952974	AL8G43040	150	-0.070	0.155	0.078	0.070	negative
S_8_21953095	AL8G43040	152	-0.090	0.145	0.073	0.090	negative
S_8_21953352	AL8G43040	151	-0.077	0.149	0.091	0.077	negative
S_8_21953463	AL8G43040	152	-0.056	0.149	0.075	0.056	negative
S_8_21953554	AL8G43040	153	-0.078	0.148	0.071	0.078	negative
S_8_21953773	AL8G43040	150	-0.101	0.151	0.060	0.101	negative
S_8_21954069	AL8G43040	149	-0.051	0.151	0.075	0.051	negative
S_8_21954945	AL8G43040	148	-0.048	0.149	0.081	0.048	negative
S_8_21955029	AL8G43040	148	-0.094	0.155	0.073	0.094	negative
S_8_21955227	AL8G43040	148	0.044	0.152	0.063	0.044	positive
S_8_21955358	AL8G43040	149	-0.117	0.153	0.090	0.117	negative
S_8_21956298	AL8G43040	150	-0.033	0.143	0.070	0.033	negative
S_8_21956920	AL8G43040	150	-0.121	0.156	0.067	0.121	negative
S_8_21957336	AL8G43040	150	-0.063	0.149	0.075	0.063	negative
S_8_21957607	AL8G43040	147	-0.091	0.139	0.084	0.091	negative
S_8_21957871	AL8G43040	149	-0.059	0.151	0.070	0.059	negative
S_8_21957938	AL8G43040	149	-0.080	0.155	0.079	0.080	negative
S_8_21957998	AL8G43040	149	-0.027	0.149	0.085	0.027	negative
S_8_21958059	AL8G43040	150	-0.061	0.149	0.075	0.061	negative

Table S11

Table S 11: Contrast analysis for the deviation from the expected mid-homozygous haplotype. Each outlier SNP within a candidate gene for the associated phenotypic trait was tested. N - number of analysed individual genotypes. Standard error (SE) and model fit (R^2) for the respective linear model and the absolute deviation (|deviation|) as well as the direction of deviation.

SNP	gene	N	deviation	SE	R2	|deviation|	direction
S_1_268095	AL1G10810	148	0.211	0.181	0.064	0.211	positive
S_1_270001	AL1G10810	148	0.291	0.181	0.077	0.291	positive
S_1_481396	AL1G11410	138	-0.107	0.299	0.062	0.107	negative
S_1_481410	AL1G11410	140	-0.119	0.301	0.066	0.119	negative
S_1_13811088	AL1G44720	289	0.109	0.251	0.030	0.109	positive
S_1_13811104	AL1G44720	285	0.117	0.253	0.032	0.117	positive
S_1_13821035	AL1G44750	287	-0.190	0.133	0.030	0.190	negative
S_1_13821036	AL1G44750	288	-0.196	0.133	0.030	0.196	negative
S_1_14302596	AL1G45720	141	-0.656	0.419	0.065	0.656	negative
S_1_14302601	AL1G45720	140	-0.650	0.419	0.063	0.650	negative
S_1_23492916	AL1G53350	143	0.272	0.519	0.056	0.272	positive
S_1_24847364	AL1G55480	142	0.045	0.214	0.060	0.045	positive
S_1_24847370	AL1G55480	141	0.103	0.220	0.068	0.103	positive
S_1_24848650	AL1G55480	140	0.085	0.220	0.071	0.085	positive
S_1_24849196	AL1G55480	142	0.101	0.218	0.066	0.101	positive
S_1_25345243	AL1G56300	139	0.202	0.245	0.059	0.202	positive
S_1_25345893	AL1G56300	139	0.137	0.234	0.082	0.137	positive
S_2_717573	AL2G11470	237	0.185	0.109	0.034	0.185	positive
S_2_717678	AL2G11470	235	0.233	0.111	0.036	0.233	positive
S_2_2984057	AL2G15870	333	0.269	0.205	0.039	0.269	positive
S_2_2984138	AL2G15870	325	0.247	0.157	0.040	0.247	positive
S_2_2984161	AL2G15870	327	0.255	0.157	0.042	0.255	positive
S_2_2984204	AL2G15870	321	0.233	0.159	0.039	0.233	positive
S_2_8306647	AL2G20100	139	-0.440	0.195	0.113	0.440	negative
S_2_8306655	AL2G20100	141	-0.353	0.194	0.093	0.353	negative
S_2_12041710	AL2G25320	151	0.192	0.500	0.046	0.192	positive
S_2_12041721	AL2G25320	151	0.165	0.498	0.055	0.165	positive
S_2_12041740	AL2G25320	151	0.192	0.500	0.046	0.192	positive
S_2_12516935	AL2G26090	329	0.088	0.110	0.061	0.088	positive
S_2_12516943	AL2G26090	325	0.094	0.110	0.069	0.094	positive
S_2_12517195	AL2G26090	331	-0.006	0.111	0.048	0.006	negative
S_2_12517234	AL2G26090	329	-0.061	0.111	0.055	0.061	negative
S_2_12517269	AL2G26090	333	-0.047	0.109	0.042	0.047	negative
S_2_12517905	AL2G26090	326	-0.138	0.111	0.038	0.138	negative
S_2_13776669	AL2G28640	326	-0.175	0.120	0.035	0.175	negative
S_2_13776670	AL2G28640	326	-0.175	0.120	0.035	0.175	negative
S_2_15594464	AL2G32570	322	-0.074	0.196	0.039	0.074	negative

S_2_15596858	AL2G32570	322	0.006	0.184	0.032	0.006	positive
S_2_16108535	AL2G33880	325	-0.183	0.189	0.026	0.183	negative
S_2_16109744	AL2G33880	333	-0.153	0.189	0.022	0.153	negative
S_2_16110357	AL2G33880	326	-0.094	0.175	0.024	0.094	negative
S_2_16111638	AL2G33890	327	-0.206	0.201	0.027	0.206	negative
S_2_16111641	AL2G33890	330	-0.108	0.183	0.025	0.108	negative
S_2_16113460	AL2G33900	326	-0.266	0.202	0.036	0.266	negative
S_2_16113634	AL2G33900	329	-0.293	0.195	0.031	0.293	negative
S_2_16113828	AL2G33900	331	-0.285	0.201	0.040	0.285	negative
S_2_16127218	AL2G33940	330	-0.090	0.175	0.034	0.090	negative
S_2_16127638	AL2G33940	333	-0.163	0.166	0.038	0.163	negative
S_2_16143551	AL2G34000	332	-0.226	0.170	0.038	0.226	negative
S_2_16143645	AL2G34000	331	-0.229	0.169	0.039	0.229	negative
S_2_16143857	AL2G34000	329	-0.173	0.177	0.046	0.173	negative
S_2_16143885	AL2G34000	330	-0.225	0.171	0.048	0.225	negative
S_2_16143902	AL2G34000	329	-0.232	0.172	0.048	0.232	negative
S_2_16143905	AL2G34000	330	-0.217	0.172	0.045	0.217	negative
S_2_16143923	AL2G34000	331	-0.218	0.172	0.045	0.218	negative
S_2_16143957	AL2G34000	329	-0.242	0.169	0.042	0.242	negative
S_2_16143959	AL2G34000	328	-0.219	0.172	0.046	0.219	negative
S_2_16144185	AL2G34000	329	-0.167	0.173	0.026	0.167	negative
S_2_16144260	AL2G34000	329	-0.214	0.169	0.037	0.214	negative
S_2_16144307	AL2G34000	329	-0.284	0.167	0.041	0.284	negative
S_2_16144421	AL2G34010	326	-0.237	0.170	0.040	0.237	negative
S_2_16144425	AL2G34010	327	-0.217	0.171	0.035	0.217	negative
S_2_16144444	AL2G34010	324	-0.267	0.170	0.045	0.267	negative
S_2_16144446	AL2G34010	325	-0.308	0.168	0.044	0.308	negative
S_2_16144451	AL2G34010	328	-0.235	0.170	0.039	0.235	negative
S_2_16144490	AL2G34010	328	-0.256	0.169	0.044	0.256	negative
S_2_16144537	AL2G34010	328	-0.284	0.168	0.053	0.284	negative
S_2_16144538	AL2G34010	328	-0.270	0.167	0.051	0.270	negative
S_2_16144547	AL2G34010	325	-0.243	0.168	0.046	0.243	negative
S_2_16144571	AL2G34010	329	-0.265	0.168	0.048	0.265	negative
S_2_16144578	AL2G34010	326	-0.251	0.169	0.046	0.251	negative
S_2_16144581	AL2G34010	329	-0.249	0.168	0.045	0.249	negative
S_2_16144596	AL2G34010	330	-0.257	0.169	0.045	0.257	negative
S_2_16144646	AL2G34010	330	-0.233	0.172	0.049	0.233	negative
S_2_16144654	AL2G34010	332	-0.231	0.172	0.048	0.231	negative
S_2_16144693	AL2G34010	326	-0.276	0.178	0.044	0.276	negative
S_2_16144717	AL2G34010	328	-0.289	0.170	0.048	0.289	negative
S_2_16144744	AL2G34010	331	-0.243	0.172	0.049	0.243	negative
S_2_16144747	AL2G34010	332	-0.263	0.169	0.044	0.263	negative
S_2_16144884	AL2G34010	329	-0.272	0.181	0.040	0.272	negative
S_2_16145092	AL2G34010	333	-0.344	0.176	0.046	0.344	negative
S_2_16145236	AL2G34010	330	-0.272	0.174	0.042	0.272	negative

S_2_16145271	AL2G34010	327	-0.339	0.175	0.048	0.339	negative
S_2_16145287	AL2G34010	331	-0.331	0.176	0.044	0.331	negative
S_2_16145296	AL2G34010	332	-0.327	0.176	0.043	0.327	negative
S_2_16145349	AL2G34010	332	-0.285	0.177	0.036	0.285	negative
S_2_16145350	AL2G34010	332	-0.285	0.177	0.036	0.285	negative
S_2_16145353	AL2G34010	331	-0.291	0.177	0.038	0.291	negative
S_2_16145374	AL2G34010	330	-0.271	0.177	0.034	0.271	negative
S_2_16145518	AL2G34010	327	-0.277	0.177	0.037	0.277	negative
S_2_16145524	AL2G34010	330	-0.280	0.176	0.038	0.280	negative
S_2_16145566	AL2G34010	329	-0.305	0.176	0.041	0.305	negative
S_2_16145572	AL2G34010	332	-0.317	0.175	0.042	0.317	negative
S_2_16145599	AL2G34010	328	-0.269	0.179	0.042	0.269	negative
S_2_16145684	AL2G34010	329	-0.283	0.179	0.045	0.283	negative
S_2_16145690	AL2G34010	327	-0.300	0.179	0.048	0.300	negative
S_2_16145695	AL2G34010	328	-0.280	0.180	0.043	0.280	negative
S_2_16145696	AL2G34010	326	-0.277	0.180	0.042	0.277	negative
S_2_16145705	AL2G34010	324	-0.296	0.179	0.047	0.296	negative
S_2_16145710	AL2G34010	325	-0.298	0.179	0.047	0.298	negative
S_2_16153935	AL2G34030	325	-0.223	0.171	0.037	0.223	negative
S_2_16154236	AL2G34030	325	-0.280	0.171	0.032	0.280	negative
S_2_16154395	AL2G34030	331	-0.210	0.170	0.035	0.210	negative
S_2_16154727	AL2G34030	324	-0.215	0.170	0.038	0.215	negative
S_2_16154912	AL2G34030	331	-0.175	0.173	0.037	0.175	negative
S_2_16160893	AL2G34050	332	-0.091	0.149	0.019	0.091	negative
S_2_16161267	AL2G34050	331	-0.215	0.164	0.032	0.215	negative
S_2_16171284	AL2G34060	335	-0.338	0.165	0.038	0.338	negative
S_2_16171497	AL2G34060	328	-0.384	0.166	0.039	0.384	negative
S_2_16171800	AL2G34060	330	-0.301	0.171	0.034	0.301	negative
S_2_16171953	AL2G34060	329	-0.262	0.173	0.035	0.262	negative
S_2_16172007	AL2G34060	326	-0.224	0.178	0.035	0.224	negative
S_2_16172663	AL2G34060	329	-0.260	0.172	0.037	0.260	negative
S_2_16172749	AL2G34060	328	-0.316	0.168	0.040	0.316	negative
S_2_16172834	AL2G34060	332	-0.248	0.173	0.032	0.248	negative
S_2_16173567	AL2G34060	333	-0.227	0.177	0.036	0.227	negative
S_2_16173601	AL2G34060	328	-0.210	0.178	0.033	0.210	negative
S_2_16173605	AL2G34060	325	-0.198	0.178	0.032	0.198	negative
S_2_16173608	AL2G34060	324	-0.197	0.178	0.031	0.197	negative
S_2_16173762	AL2G34060	328	-0.228	0.169	0.039	0.228	negative
S_3_2216493	AL3G16440	293	0.060	0.139	0.023	0.060	positive
S_3_2216927	AL3G16440	288	0.007	0.146	0.021	0.007	positive
S_3_2216988	AL3G16440	293	0.082	0.142	0.024	0.082	positive
S_3_2217232	AL3G16440	290	0.017	0.146	0.023	0.017	positive
S_3_3537009	AL3G19960	324	0.102	0.167	0.024	0.102	positive
S_3_3537021	AL3G19960	323	0.124	0.168	0.022	0.124	positive
S_3_7719638	AL3G31220	240	-0.055	0.164	0.023	0.055	negative

S_3_7720441	AL3G31220	238	-0.008	0.163	0.027	0.008	negative
S_3_7720747	AL3G31220	240	-0.059	0.162	0.021	0.059	negative
S_3_7720788	AL3G31220	235	-0.062	0.162	0.021	0.062	negative
S_3_7720796	AL3G31220	238	-0.058	0.158	0.023	0.058	negative
S_3_7720910	AL3G31220	238	-0.053	0.166	0.020	0.053	negative
S_3_7720928	AL3G31220	239	-0.057	0.163	0.019	0.057	negative
S_3_7721006	AL3G31220	235	-0.004	0.163	0.029	0.004	negative
S_3_7721958	AL3G31230	235	-0.067	0.162	0.021	0.067	negative
S_3_7722004	AL3G31230	233	-0.009	0.164	0.026	0.009	negative
S_3_7722284	AL3G31230	231	-0.092	0.160	0.028	0.092	negative
S_3_7722397	AL3G31230	238	-0.017	0.161	0.025	0.017	negative
S_3_7722759	AL3G31230	235	-0.010	0.169	0.025	0.010	negative
S_3_7722890	AL3G31230	239	-0.016	0.158	0.025	0.016	negative
S_3_7722892	AL3G31230	238	0.002	0.162	0.027	0.002	positive
S_3_7722973	AL3G31230	234	-0.040	0.163	0.022	0.040	negative
S_3_7722975	AL3G31230	237	-0.032	0.161	0.023	0.032	negative
S_3_7723030	AL3G31230	234	-0.022	0.160	0.023	0.022	negative
S_3_7723048	AL3G31230	232	0.032	0.163	0.029	0.032	positive
S_3_7723072	AL3G31230	237	-0.003	0.164	0.022	0.003	negative
S_3_7723079	AL3G31230	237	-0.018	0.163	0.020	0.018	negative
S_3_7723093	AL3G31230	234	-0.015	0.168	0.022	0.015	negative
S_3_7723097	AL3G31230	235	-0.018	0.168	0.021	0.018	negative
S_3_7723106	AL3G31230	239	-0.049	0.162	0.022	0.049	negative
S_3_7723114	AL3G31230	239	-0.053	0.162	0.022	0.053	negative
S_3_7723186	AL3G31230	237	-0.025	0.158	0.023	0.025	negative
S_3_7723201	AL3G31230	237	-0.021	0.158	0.024	0.021	negative
S_3_7723247	AL3G31230	236	-0.018	0.156	0.025	0.018	negative
S_3_7723890	AL3G31230	235	-0.085	0.163	0.026	0.085	negative
S_3_7724124	AL3G31230	234	-0.091	0.168	0.017	0.091	negative
S_3_7729220	AL3G31240	234	-0.106	0.163	0.016	0.106	negative
S_3_7729245	AL3G31240	234	-0.057	0.159	0.023	0.057	negative
S_3_8898528	AL3G34100	247	0.059	0.147	0.024	0.059	positive
S_3_8898773	AL3G34100	244	0.033	0.143	0.025	0.033	positive
S_3_8898808	AL3G34100	243	0.067	0.147	0.029	0.067	positive
S_3_10933233	AL3G38380	141	-0.268	0.227	0.068	0.268	negative
S_3_10933337	AL3G38380	142	-0.235	0.225	0.066	0.235	negative
S_3_10933438	AL3G38380	141	-0.291	0.218	0.070	0.291	negative
S_3_10933478	AL3G38380	141	-0.242	0.226	0.065	0.242	negative
S_3_10933713	AL3G38380	139	-0.249	0.228	0.064	0.249	negative
S_3_10933931	AL3G38380	143	-0.228	0.215	0.078	0.228	negative
S_3_10933970	AL3G38380	140	-0.205	0.215	0.078	0.205	negative
S_3_10934063	AL3G38380	141	-0.265	0.228	0.067	0.265	negative
S_3_10934083	AL3G38380	141	-0.272	0.225	0.066	0.272	negative
S_3_10934109	AL3G38380	138	-0.285	0.224	0.070	0.285	negative
S_3_10934137	AL3G38380	141	-0.251	0.230	0.064	0.251	negative

S_3_10934148	AL3G38380	141	-0.254	0.230	0.064	0.254	negative
S_3_10934163	AL3G38380	142	-0.230	0.221	0.073	0.230	negative
S_3_10934165	AL3G38380	142	-0.230	0.221	0.073	0.230	negative
S_3_10934179	AL3G38380	142	-0.289	0.228	0.066	0.289	negative
S_3_10934406	AL3G38380	142	-0.262	0.218	0.070	0.262	negative
S_3_10934416	AL3G38380	142	-0.262	0.218	0.070	0.262	negative
S_3_10934443	AL3G38380	141	-0.268	0.220	0.070	0.268	negative
S_3_10934446	AL3G38380	141	-0.268	0.220	0.070	0.268	negative
S_3_10934450	AL3G38380	141	-0.268	0.220	0.070	0.268	negative
S_3_10934488	AL3G38380	141	-0.268	0.220	0.070	0.268	negative
S_3_10934805	AL3G38380	140	-0.256	0.227	0.066	0.256	negative
S_3_10934856	AL3G38380	140	-0.261	0.228	0.064	0.261	negative
S_3_10935515	AL3G38380	139	-0.263	0.225	0.066	0.263	negative
S_3_10935517	AL3G38380	139	-0.263	0.225	0.066	0.263	negative
S_3_10936028	AL3G38380	137	-0.270	0.219	0.074	0.270	negative
S_3_10936699	AL3G38380	139	-0.280	0.222	0.070	0.280	negative
S_3_10937221	AL3G38380	138	-0.226	0.231	0.066	0.226	negative
S_3_10937739	AL3G38380	141	-0.276	0.224	0.065	0.276	negative
S_3_10937770	AL3G38380	140	-0.260	0.227	0.064	0.260	negative
S_3_10937776	AL3G38380	140	-0.233	0.226	0.069	0.233	negative
S_3_10937778	AL3G38380	139	-0.246	0.226	0.070	0.246	negative
S_3_10937779	AL3G38380	139	-0.246	0.226	0.070	0.246	negative
S_3_10938130	AL3G38380	141	-0.241	0.221	0.071	0.241	negative
S_3_10938516	AL3G38380	141	-0.268	0.221	0.069	0.268	negative
S_3_10939315	AL3G38380	141	-0.254	0.229	0.064	0.254	negative
S_3_21251806	AL3G49100	297	-0.035	0.121	0.020	0.035	negative
S_3_21251813	AL3G49100	299	-0.047	0.120	0.019	0.047	negative
S_3_21251838	AL3G49100	297	-0.029	0.121	0.022	0.029	negative
S_3_22408362	AL3G51100	251	0.188	0.283	0.019	0.188	positive
S_3_22408792	AL3G51100	252	0.072	0.199	0.019	0.072	positive
S_3_22408895	AL3G51100	249	0.400	0.320	0.023	0.400	positive
S_3_24063849	AL3G54000	174	0.050	0.165	0.067	0.050	positive
S_3_24064254	AL3G54000	177	0.013	0.162	0.067	0.013	positive
S_3_24064314	AL3G54000	176	-0.003	0.162	0.061	0.003	negative
S_3_24064486	AL3G54000	176	0.070	0.162	0.074	0.070	positive
S_3_24064494	AL3G54000	179	0.019	0.161	0.065	0.019	positive
S_4_2420766	AL4G14260	324	0.032	0.121	0.033	0.032	positive
S_4_2420901	AL4G14260	321	0.020	0.116	0.030	0.020	positive
S_4_2420967	AL4G14260	321	0.002	0.118	0.023	0.002	positive
S_4_2424365	AL4G14270	323	0.024	0.125	0.027	0.024	positive
S_4_2424380	AL4G14270	321	0.017	0.125	0.031	0.017	positive
S_4_4981864	AL4G17470	321	0.055	0.249	0.025	0.055	positive
S_4_4982787	AL4G17470	330	0.079	0.248	0.021	0.079	positive
S_4_14451845	AL4G25810	147	-0.117	0.183	0.089	0.117	negative
S_4_14451849	AL4G25810	148	-0.160	0.183	0.102	0.160	negative

S_4_14547956	AL4G25980	140	-0.068	0.204	0.061	0.068	negative
S_4_14548115	AL4G25980	139	-0.047	0.224	0.078	0.047	negative
S_4_14549794	AL4G25980	137	-0.097	0.194	0.071	0.097	negative
S_4_16574296	AL4G30860	126	-0.185	0.228	0.026	0.185	negative
S_4_16574326	AL4G30860	125	-0.176	0.229	0.024	0.176	negative
S_4_16574405	AL4G30860	127	-0.073	0.216	0.017	0.073	negative
S_4_16574644	AL4G30860	127	-0.122	0.230	0.016	0.122	negative
S_4_16574686	AL4G30860	126	-0.196	0.215	0.014	0.196	negative
S_4_16582058	AL4G30890	125	-0.128	0.170	0.025	0.128	negative
S_4_16582151	AL4G30890	123	-0.137	0.172	0.026	0.137	negative
S_4_20738763	AL4G40930	436	0.056	0.148	0.019	0.056	positive
S_4_20739049	AL4G40930	430	0.080	0.149	0.020	0.080	positive
S_5_2635116	AL5G14730	301	-0.243	0.124	0.056	0.243	negative
S_5_2636965	AL5G14730	301	-0.187	0.134	0.044	0.187	negative
S_5_11228788	AL5G22750	232	-0.035	0.122	0.016	0.035	negative
S_5_11228803	AL5G22750	236	-0.067	0.125	0.019	0.067	negative
S_5_11228825	AL5G22750	239	-0.045	0.124	0.019	0.045	negative
S_5_11228828	AL5G22750	238	-0.063	0.124	0.021	0.063	negative
S_5_11228856	AL5G22750	239	-0.091	0.124	0.019	0.091	negative
S_5_11228889	AL5G22750	238	-0.009	0.124	0.023	0.009	negative
S_5_12720723	AL5G25490	146	-0.585	0.521	0.072	0.585	negative
S_5_12824835	AL5G25810	148	0.180	0.176	0.060	0.180	positive
S_5_12824880	AL5G25810	147	0.227	0.178	0.067	0.227	positive
S_5_12829737	AL5G25820	146	0.130	0.186	0.086	0.130	positive
S_5_12829742	AL5G25820	146	0.130	0.186	0.086	0.130	positive
S_5_12829745	AL5G25820	146	0.130	0.186	0.086	0.130	positive
S_5_17841024	AL5G37490	146	-0.260	0.167	0.059	0.260	negative
S_5_17841028	AL5G37490	147	-0.268	0.166	0.060	0.268	negative
S_5_17841032	AL5G37490	145	-0.252	0.167	0.055	0.252	negative
S_5_17841033	AL5G37490	148	-0.229	0.164	0.061	0.229	negative
S_5_17841402	AL5G37490	145	-0.313	0.168	0.057	0.313	negative
S_5_20031599	AL5G43050	148	-0.373	0.237	0.072	0.373	negative
S_5_20033833	AL5G43050	146	-0.294	0.252	0.072	0.294	negative
S_5_20040026	AL5G43070	144	-0.399	0.246	0.076	0.399	negative
S_5_20040072	AL5G43070	144	-0.388	0.244	0.070	0.388	negative
S_6_3056651	AL6G18170	124	0.078	0.164	0.065	0.078	positive
S_6_3057392	AL6G18170	124	0.189	0.195	0.052	0.189	positive
S_6_3058982	AL6G18180	122	0.184	0.185	0.070	0.184	positive
S_6_3059319	AL6G18180	123	0.060	0.189	0.051	0.060	positive
S_6_3059426	AL6G18180	124	0.116	0.185	0.067	0.116	positive
S_6_3059442	AL6G18180	122	0.087	0.165	0.065	0.087	positive
S_6_3982203	AL6G20530	287	-0.040	0.206	0.059	0.040	negative
S_6_3982204	AL6G20530	286	-0.047	0.207	0.058	0.047	negative
S_6_5419821	AL6G24050	124	-0.093	0.152	0.039	0.093	negative
S_6_5420607	AL6G24050	125	-0.138	0.151	0.044	0.138	negative

S_6_7079555	AL6G28290	137	0.239	0.190	0.062	0.239	positive
S_6_7079571	AL6G28290	137	0.210	0.189	0.060	0.210	positive
S_6_7079648	AL6G28290	142	0.237	0.187	0.059	0.237	positive
S_6_7080143	AL6G28290	137	0.203	0.187	0.065	0.203	positive
S_6_7080562	AL6G28290	140	0.239	0.188	0.061	0.239	positive
S_6_7081604	AL6G28300	143	0.150	0.179	0.067	0.150	positive
S_6_7082808	AL6G28300	137	0.205	0.180	0.065	0.205	positive
S_6_7082949	AL6G28300	141	0.277	0.185	0.069	0.277	positive
S_6_7083381	AL6G28300	140	0.233	0.193	0.060	0.233	positive
S_6_7083449	AL6G28300	139	0.215	0.187	0.066	0.215	positive
S_6_7083462	AL6G28300	138	0.141	0.182	0.065	0.141	positive
S_6_7083514	AL6G28300	139	0.187	0.185	0.066	0.187	positive
S_6_7083528	AL6G28300	139	0.185	0.186	0.063	0.185	positive
S_6_7083913	AL6G28300	141	0.250	0.183	0.065	0.250	positive
S_6_7084323	AL6G28300	137	0.216	0.188	0.058	0.216	positive
S_6_7763958	AL6G29890	147	0.159	0.266	0.047	0.159	positive
S_6_7763989	AL6G29890	146	0.140	0.264	0.048	0.140	positive
S_6_11089566	AL6G36680	241	0.086	0.116	0.019	0.086	positive
S_6_11089768	AL6G36680	239	0.208	0.113	0.041	0.208	positive
S_6_11089841	AL6G36680	241	0.203	0.113	0.044	0.203	positive
S_6_11089847	AL6G36680	239	0.207	0.114	0.043	0.207	positive
S_6_11089996	AL6G36680	237	0.228	0.114	0.046	0.228	positive
S_6_11090126	AL6G36680	234	0.199	0.116	0.039	0.199	positive
S_6_11090144	AL6G36680	237	0.199	0.114	0.042	0.199	positive
S_6_11090154	AL6G36680	238	0.217	0.114	0.043	0.217	positive
S_6_11090198	AL6G36680	237	0.201	0.114	0.039	0.201	positive
S_6_11090366	AL6G36680	236	0.202	0.115	0.042	0.202	positive
S_6_23209638	AL6G49560	140	-0.120	0.174	0.058	0.120	negative
S_6_23209706	AL6G49560	140	0.001	0.174	0.062	0.001	positive
S_6_23209712	AL6G49560	137	0.006	0.179	0.060	0.006	positive
S_7_2955099	AL7G17280	328	-0.030	0.196	0.023	0.030	negative
S_7_2955174	AL7G17280	323	-0.058	0.203	0.018	0.058	negative
S_7_5095004	AL7G22350	138	-0.214	0.303	0.074	0.214	negative
S_7_5095847	AL7G22350	139	-0.229	0.309	0.066	0.229	negative
S_7_5097245	AL7G22350	140	-0.221	0.311	0.067	0.221	negative
S_7_5097554	AL7G22350	141	-0.290	0.302	0.063	0.290	negative
S_7_5097935	AL7G22350	143	-0.216	0.306	0.067	0.216	negative
S_7_5098056	AL7G22350	141	-0.177	0.285	0.067	0.177	negative
S_7_7653883	AL7G28920	234	0.194	0.149	0.047	0.194	positive
S_7_7654107	AL7G28920	235	0.181	0.145	0.058	0.181	positive
S_7_8498176	AL7G30850	249	-0.229	0.182	0.051	0.229	negative
S_7_8498457	AL7G30850	246	-0.230	0.181	0.051	0.230	negative
S_7_8498458	AL7G30850	246	-0.230	0.181	0.051	0.230	negative
S_7_8498469	AL7G30850	246	-0.239	0.182	0.048	0.239	negative
S_7_8498474	AL7G30850	247	-0.239	0.182	0.048	0.239	negative

S_7_8498504	AL7G30850	249	-0.245	0.180	0.050	0.245	negative
S_7_9657010	AL7G33490	243	-0.090	0.155	0.043	0.090	negative
S_7_9661353	AL7G33490	240	-0.136	0.135	0.072	0.136	negative
S_7_9662939	AL7G33500	250	-0.036	0.138	0.067	0.036	negative
S_7_9662954	AL7G33500	249	-0.107	0.129	0.069	0.107	negative
S_7_9663446	AL7G33500	248	0.016	0.141	0.035	0.016	positive
S_7_9664699	AL7G33510	246	-0.107	0.129	0.069	0.107	negative
S_7_9665238	AL7G33510	245	-0.059	0.140	0.044	0.059	negative
S_7_9665417	AL7G33510	248	0.071	0.147	0.052	0.071	positive
S_7_19836914	AL7G45710	146	0.531	0.205	0.100	0.531	positive
S_7_19837422	AL7G45710	149	0.378	0.207	0.081	0.378	positive
S_8_1238273	AL8G12470	294	-0.259	0.193	0.017	0.259	negative
S_8_1238886	AL8G12470	295	-0.284	0.185	0.025	0.284	negative
S_8_1239032	AL8G12470	289	-0.299	0.189	0.026	0.299	negative
S_8_1239053	AL8G12470	291	-0.290	0.187	0.026	0.290	negative
S_8_4113233	AL8G16610	148	0.021	0.412	0.045	0.021	positive
S_8_4114711	AL8G16610	149	0.028	0.416	0.042	0.028	positive
S_8_4116800	AL8G16620	147	0.100	0.357	0.037	0.100	positive
S_8_4116870	AL8G16620	147	0.183	0.410	0.036	0.183	positive
S_8_18245391	AL8G33680	148	0.176	0.186	0.049	0.176	positive
S_8_18245394	AL8G33680	148	0.176	0.186	0.049	0.176	positive
S_8_18245778	AL8G33680	148	0.296	0.181	0.052	0.296	positive
S_8_18245945	AL8G33680	150	0.313	0.204	0.049	0.313	positive
S_8_21949767	AL8G43030	147	0.019	0.163	0.058	0.019	positive
S_8_21949800	AL8G43030	147	0.050	0.163	0.059	0.050	positive
S_8_21950417	AL8G43030	145	-0.017	0.167	0.055	0.017	negative
S_8_21950580	AL8G43030	145	0.208	0.219	0.084	0.208	positive
S_8_21950636	AL8G43030	147	0.161	0.217	0.094	0.161	positive
S_8_21950643	AL8G43030	147	0.220	0.211	0.086	0.220	positive
S_8_21950696	AL8G43030	148	0.193	0.219	0.081	0.193	positive
S_8_21950700	AL8G43030	147	0.232	0.229	0.076	0.232	positive
S_8_21950748	AL8G43030	147	0.213	0.212	0.085	0.213	positive
S_8_21950839	AL8G43030	149	0.178	0.209	0.093	0.178	positive
S_8_21950841	AL8G43030	149	0.197	0.209	0.089	0.197	positive
S_8_21950852	AL8G43030	149	0.197	0.209	0.089	0.197	positive
S_8_21951151	AL8G43030	148	0.180	0.216	0.092	0.180	positive
S_8_21951348	AL8G43030	150	0.180	0.209	0.090	0.180	positive
S_8_21951468	AL8G43030	146	0.209	0.218	0.085	0.209	positive
S_8_21951563	AL8G43030	147	0.247	0.212	0.074	0.247	positive
S_8_21951901	AL8G43030	146	0.100	0.209	0.076	0.100	positive
S_8_21952027	AL8G43030	145	0.182	0.214	0.091	0.182	positive
S_8_21952034	AL8G43030	145	0.189	0.213	0.090	0.189	positive
S_8_21952111	AL8G43040	145	0.111	0.206	0.109	0.111	positive
S_8_21952537	AL8G43040	147	0.232	0.229	0.072	0.232	positive
S_8_21952839	AL8G43040	146	0.184	0.211	0.093	0.184	positive

S_8_21952878	AL8G43040	148	0.184	0.209	0.091	0.184	positive
S_8_21952972	AL8G43040	147	0.176	0.217	0.091	0.176	positive
S_8_21952974	AL8G43040	147	0.176	0.217	0.091	0.176	positive
S_8_21953095	AL8G43040	150	0.192	0.208	0.088	0.192	positive
S_8_21953352	AL8G43040	148	0.159	0.216	0.092	0.159	positive
S_8_21953463	AL8G43040	149	0.191	0.210	0.089	0.191	positive
S_8_21953554	AL8G43040	150	0.203	0.208	0.088	0.203	positive
S_8_21953773	AL8G43040	147	0.195	0.209	0.092	0.195	positive
S_8_21954069	AL8G43040	146	0.219	0.212	0.085	0.219	positive
S_8_21954945	AL8G43040	145	0.152	0.211	0.103	0.152	positive
S_8_21955029	AL8G43040	145	0.207	0.220	0.079	0.207	positive
S_8_21955227	AL8G43040	145	0.243	0.216	0.084	0.243	positive
S_8_21955358	AL8G43040	146	0.184	0.214	0.089	0.184	positive
S_8_21956298	AL8G43040	147	-0.030	0.201	0.057	0.030	negative
S_8_21956920	AL8G43040	147	0.192	0.216	0.088	0.192	positive
S_8_21957336	AL8G43040	147	0.138	0.207	0.101	0.138	positive
S_8_21957607	AL8G43040	145	0.146	0.208	0.103	0.146	positive
S_8_21957871	AL8G43040	146	0.221	0.210	0.084	0.221	positive
S_8_21957938	AL8G43040	146	0.143	0.214	0.079	0.143	positive
S_8_21957998	AL8G43040	146	0.198	0.211	0.093	0.198	positive
S_8_21958059	AL8G43040	147	0.176	0.210	0.095	0.176	positive

Supporting Information – Chapter II

Fig. S1 Top) Broad-sense heritability (H^2) of each trait with standard error (error bars). **Middle)** Genetic (V_g; circle) and environmental variance (V_e; triangle). **Bottom)** Standardized genotypic (I_g; circle) and environmental variance (I_e; triangle). All measures are shown for the four treatments (colour coded) and the respective growth trait. s_{asym} – asymptotic size. r_{max} – maximum growth rate. x_{mid} – time till fastest growth. Logarithmic y-scales for middle and bottom rows.

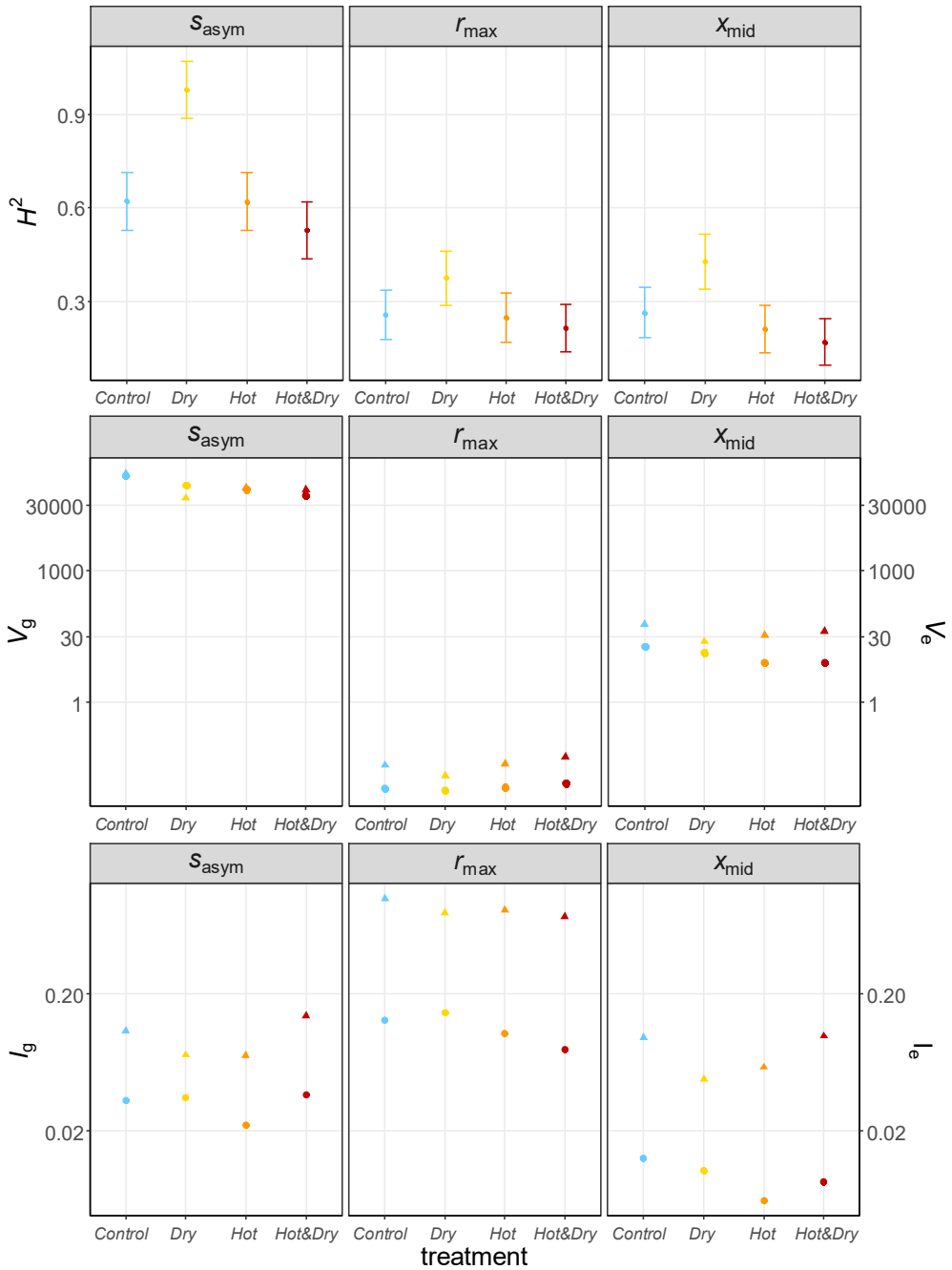

Fig. S2 2D illustration of treatment-specific G-matrices. Top left: r_{max} ~ s_{asym}. Bottom left: x_{mid} ~ s_{asym}. Bottom right: x_{mid} ~ r_{max}. Different colours indicate the four treatments: blue for *Control*, yellow for *Dry*, orange for *Hot*, and red for *Hot&Dry*.

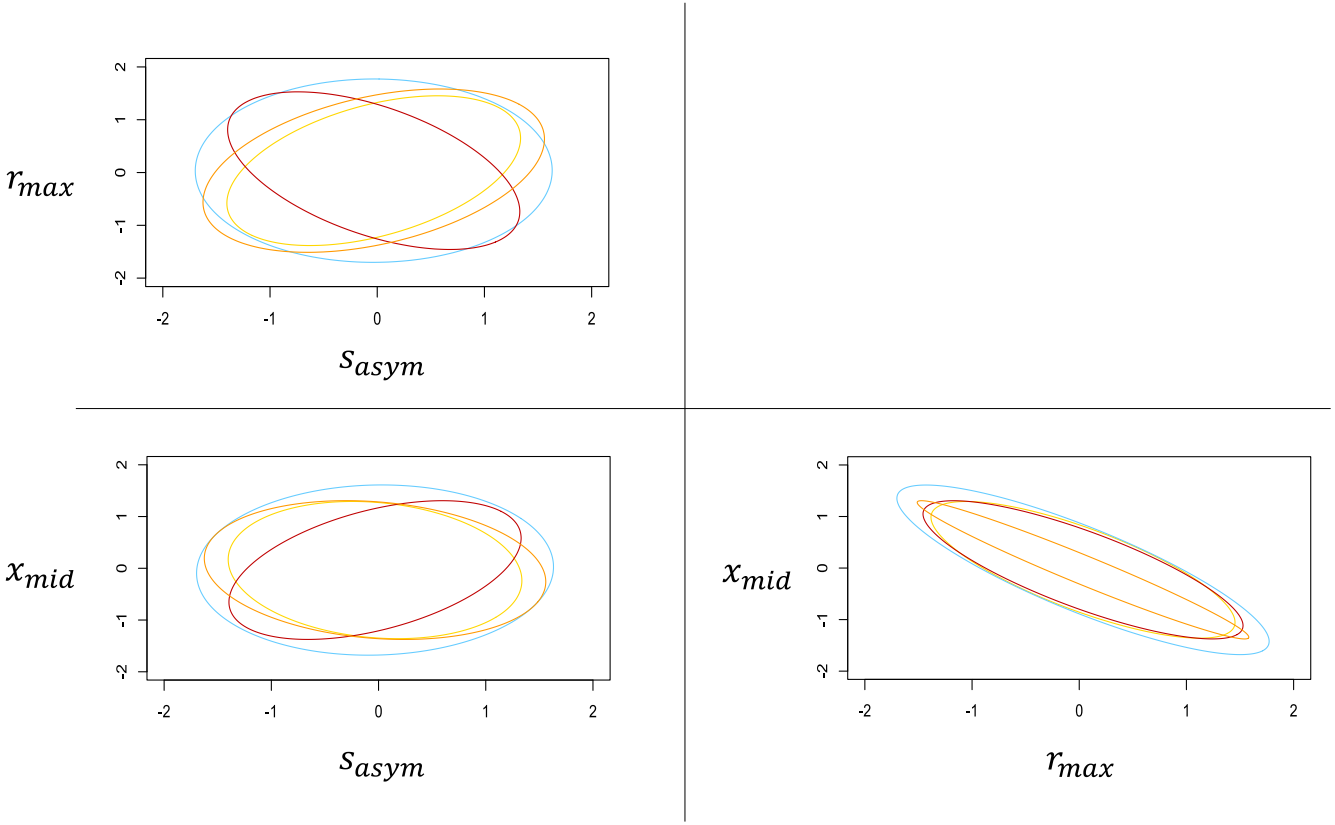

Fig. S3 **a)** Hansen & Houle's measure of evolvability (evo_{HH}) in the four treatments. Letters indicate differentiation between treatments based on ROPE technique (b-d). Posterior distributions of the quotients of genetic variances between **b)** *Dry* and *Control*, **c)** *Dry* and *Hot*, and **d)** *Dry* and *Hot&Dry*. The green band indicates the ROPE (Region of Practical Equivalence), and areas within light-grey regions of the posterior distribution are the 95% HPDs.

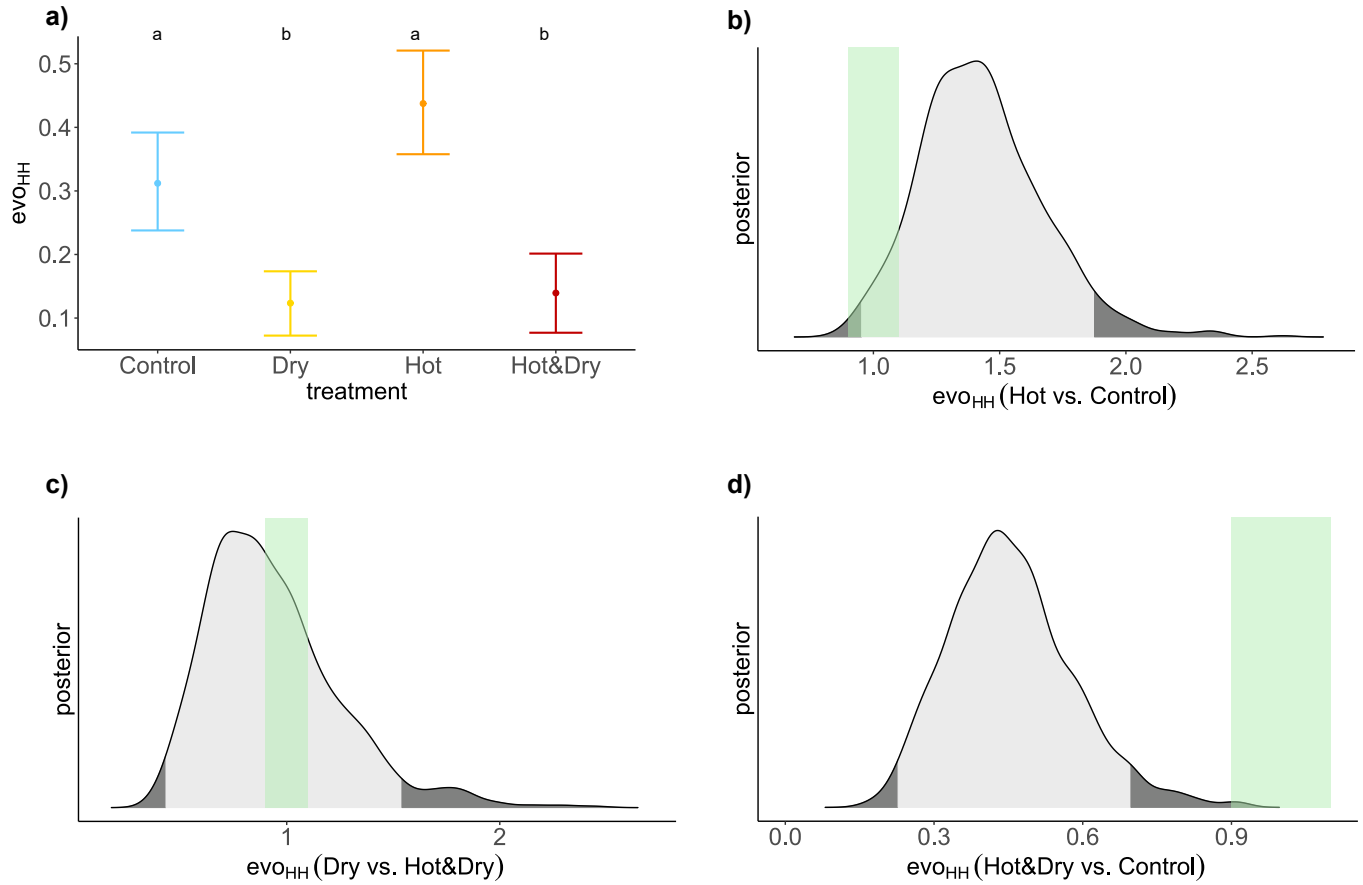

Fig. S4 Trait means for the three latitudinal populations and per treatment. From top to bottom: maximum size – s_{asym}, maximal growth rate – r_{max}, and time till half growth – x_{mid}. Colours and shapes indicate latitudinal belonging.

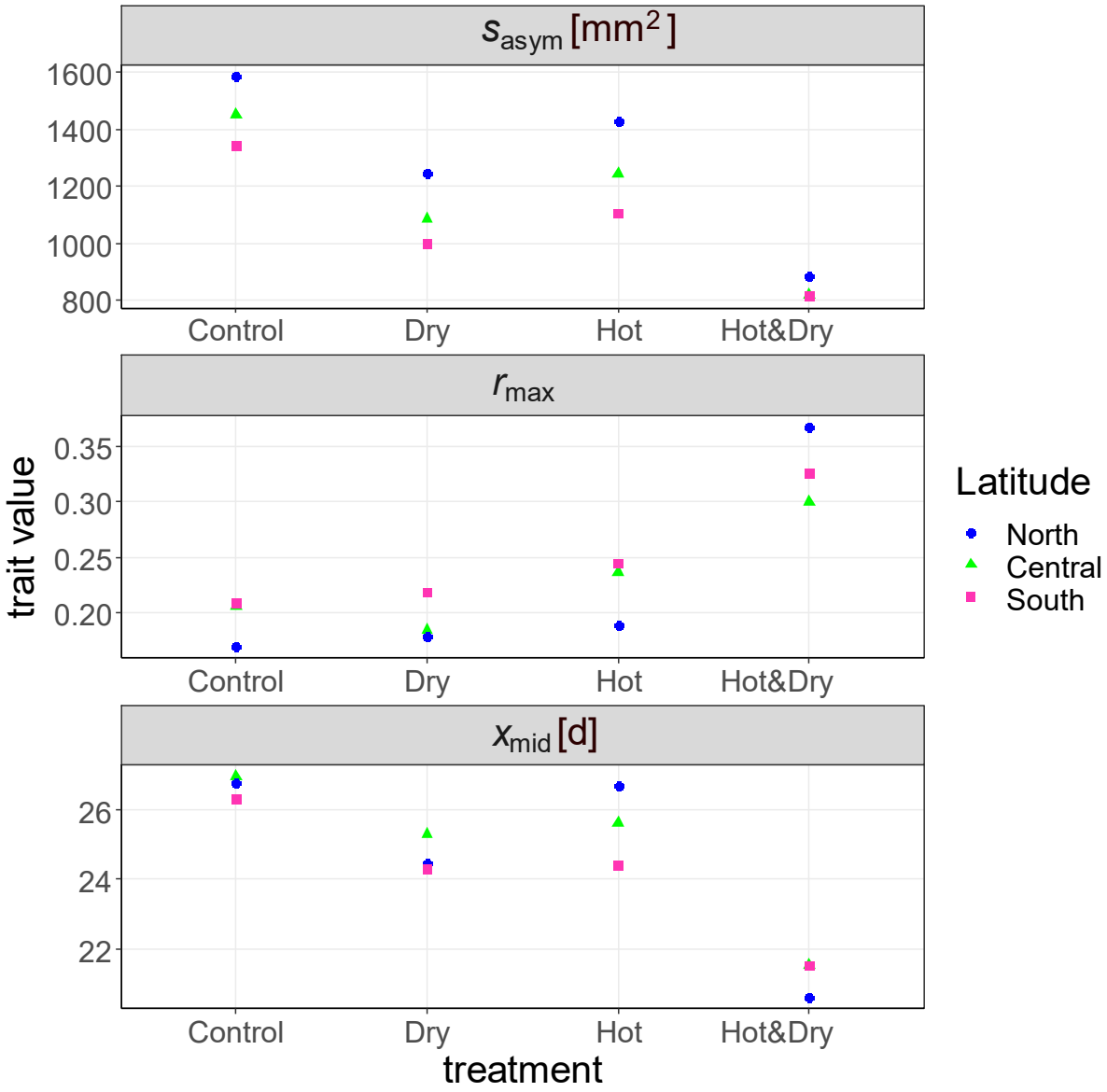

Fig. S5 Comparison of evolutionary and geometric aspects of genetic variance-covariance (G-) matrices estimated under benign and stress conditions for the three allocation traits: *SLA*, *LDMC* and root-shoot ratio (RS_{ratio}) (**a-c**), and G-matrices for allocation and growth traits (**d-f**). Total genetic variance, trace of G - v_t, for allocation (**a**) and all traits (**d**). Number of dimensions - n_d, for allocation (**b**) and all traits (**e**). Deviation distance (*dev*) between selection vector (β) and selection response (Δz) for allocation (**c**) and all traits (**f**). The colours indicate the treatments: blue for *Control*, yellow for *Dry*, and orange for *Hot*. Due to the low sample size the *Hot&Dry* treatment is indicated in grey, if calculation was possible. Dots indicate the predicted model estimate and bars the 95% HPD interval. Letters above the bars indicate differences between treatments based on ROPE (Region of Practical Equivalence).

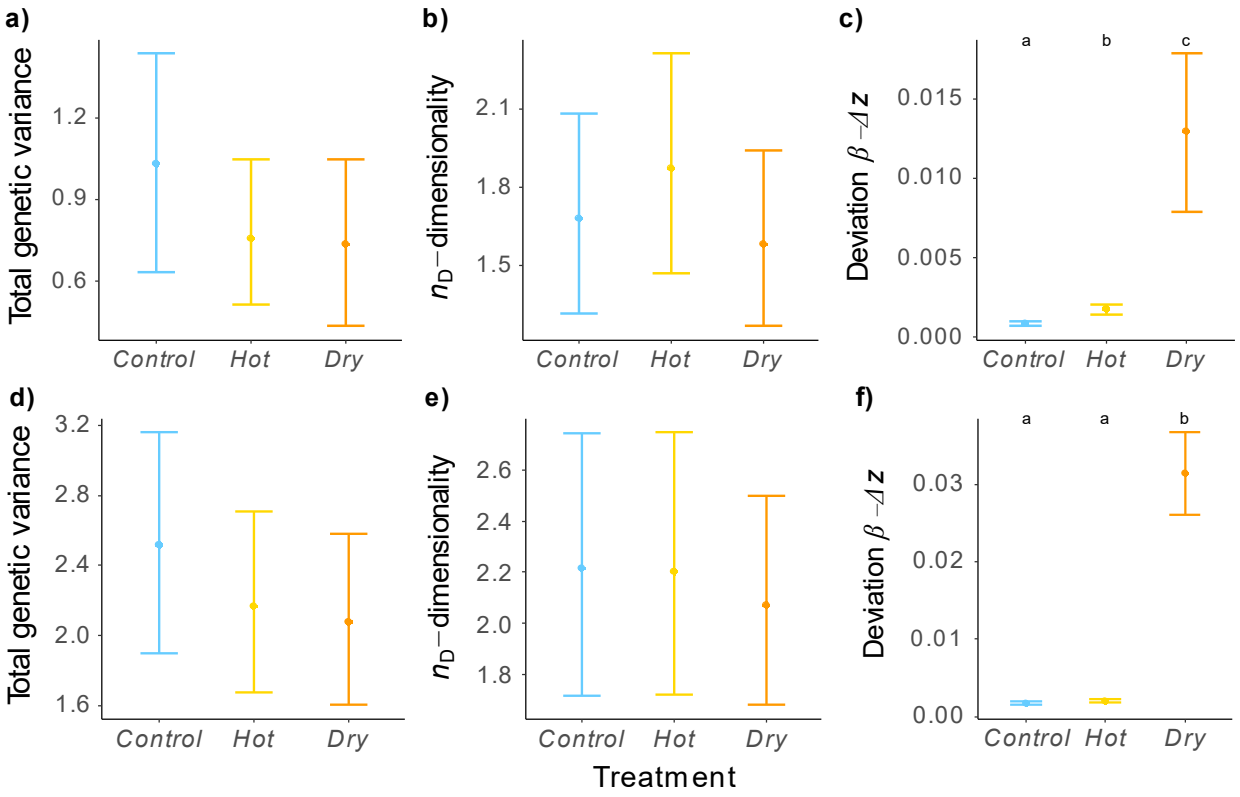

Table S1 Conditions during parental/crossing (**top**) and experimental generation (**bottom**). Stages of each generation are shown and respective day, night and midday peak temperatures, watering amount as well as day length, light intensity, humidity, and duration in each stage are indicated.

parental / crossing generation

stage	place	temp $_{day}$ [°C]	temp $_{night}$ [°C]	day length [h]	light intensity [µMm^{-2}s^{-1}]	humidity [%]	duration
stratification	climate cabinets	-	4	0	-	80	10 d
germination	glasshouse	20	18	8 – 12	150 - 200	80	6 weeks
vernalization	climate cabinets	4	4	10	150	80	6 weeks
growing	glasshouse	22	18	16	200	70	until seed ripening

experimental generation

stage	place	treatment	temp $_{day}$ [°C]	temp $_{midday\ peak}$ [°C]	temp $_{night}$ [°C]	water [ml]	day length [h]	light intensity [µMm^{-2}s^{-1}]	humidity [%]	duration
stratification	climate cabinets	-	-	-	4	-	0	-	80	12 d
germination	glasshouse	-	20	-	18	-	8 - 16	sunlight	80	4 weeks
stress experiment	glasshouse	*Control*	22	25	18	10	16	200	70	6 months
	glasshouse	*Dry*	20	25	18	6	16	200	70	6 months
	glasshouse	*Hot*	27	30	23	10	16	200	70	5 months
	glasshouse	*Hot&Dry*	27	30	23	6	16	200	70	5 months

Table S2 Populations of *Arabidopsis lyrata* included in the study, their coordinates, position within the distribution, cluster assignment, and year of sampling.

Population	Lat	Long	Lat orien	Genetic cluster	Sampling year
MI1 / 07L	42°42'14.20"N	86°12'0.08"W	Central	West	2007, 2009, 2010, 2011, 2014
11V / NY4	42°21'11.52"N	76°23'29.04"W	North	East	2011
11F / NC4	36°24'45.72"N	79°57'44.64"W	South	East	2011
11A / MO1	37°43'24.24"N	92° 3'24.12"W	South	West	2011
11AE / ON12	49°39'2.88"N	94°55'27.84"W	North	West	2011

Table S3 Comparison of growth models, based on AIC and weighted AIC (AIC_{wt}) of the four best models overall and per treatment. Models withing each group are ordered by weighted AIC. Smaller AICs and higher weighted AICs indicate better fitting.

Growth model	treatment	AIC	AIC_{wt}
m.gompertz	*Overall*	322.534	0.327
m.3PL	*Overall*	320.592	0.305
m.2PL	*Overall*	324.909	0.232
m.power	*Overall*	330.497	0.076
m.gompertz	*Control*	333.597	0.385
m.3PL	*Control*	333.205	0.251
m.2PL	*Control*	340.571	0.174
m.vb	*Control*	344.364	0.099
m.3PL	*Dry*	335.062	0.363
m.gompertz	*Dry*	336.294	0.325
m.2PL	*Dry*	339.926	0.194
m.vb	*Dry*	344.117	0.079
m.gompertz	*Hot*	359.394	0.353
m.3PL	*Hot*	359.875	0.311
m.2PL	*Hot*	364.485	0.246
m.vb	*Hot*	373.587	0.069
m.2PL	*Hot&Dry*	254.414	0.312
m.3PL	*Hot&Dry*	253.690	0.294
m.gompertz	*Hot&Dry*	257.551	0.240
m.power	*Hot&Dry*	261.022	0.069

Table S4 Overview of sample sizes for growth and allocation traits within each treatment and each population separately. Sample numbers of *SLA* are similar to the number of individuals surviving the experiment.

range	North		Central	South		North		Central	South		North		Central	South	
pop	11AE	11V	MI1	11A	11F	11AE	11V	MI1	11A	11F	11AE	11V	MI1	11A	11F
trait	s_{asym} [mm^2]					r_{max}					x_{mid} [d]				
Control	8	9	543	7	7	8	9	534	7	6	7	9	522	7	6
Dry	7	9	536	9	9	7	9	518	8	9	7	9	529	9	8
Hot	8	9	542	8	9	8	9	523	8	8	8	8	524	8	9
Hot&Dry	6	10	539	7	8	6	9	536	7	8	6	9	539	7	8
trait	*SLA* [mm^2 mg^{-1}]					*LDMC* [mg g^{-1}]					RS_{ratio}				
Control	4	9	410	5	3	4	9	406	6	5	6	9	496	6	6
Dry	5	8	357	8	6	6	8	357	9	7	6	8	393	7	7
Hot	7	8	412	7	9	5	8	405	7	8	7	8	434	7	9
Hot&Dry	0	0	23	1	2	0	0	23	1	2	0	0	21	0	2

Table S5 Trait means and standard error (SE) for the five latitudinal populations, per treatment and over familiy means.

range	North		Central	South		North		Central	South		North		Central	South	
pop	11AE	11V	MI1	11A	11F	11AE	11V	MI1	11A	11F	11AE	11V	MI1	11A	11F
trait	s_{asym} [mm^2]					r_{max}					x_{mid} [d]				
Control	1390.256 ± 70.4	1796.534 ± 20.4	1449.593 ± 30.3	841.190 ± 9.0	1767.145 ± 26.5	0.191 ± 0.009	0.152 ± 0.002	0.207 ± 0.025	0.280 ± 0.022	0.113 ± 0.002	29.473 ± 0.75	25.445 ± 0.11	26.933 ± 0.74	24.238 ± 0.78	28.270 ± 0.25
Dry	1007.815 ± 2.77	1351.053 ± 8.7	1084.600 ± 13.6	816.696 ± 25.7	1176.562 ± 33.3	0.201 ± 0.002	0.144 ± 0.002	0.187 ± 0.021	0.228 ± 0.002	0.209 ± 0.020	24.311 ± 0.04	24.571 ± 0.06	25.268 ± 0.40	24.404 ± 0.20	23.562 ± 0.19
Hot	1170.752 ± 11.3	1609.854 ± 18.6	1242.841 ± 21.1	853.070 ± 24.3	1336.067 ± 30.4	0.198 ± 0.011	0.187 ± 0.008	0.237 ± 0.025	0.303 ± 0.009	0.185 ± 0.004	28.527 ± 0.29	24.799 ± 0.29	25.604 ± 0.45	22.936 ± 0.70	25.629 ± 0.16
Hot&Dry	829.311 ± 17.9	881.118 ± 30.6	819.014 ± 22.9	600.122 ± 9.3	1019.684 ± 28.6	0.310 ± 0.034	0.399 ± 0.005	0.301 ± 0.025	0.285 ± 0.044	0.311 ± 0.049	22.885 ± 0.67	18.615 ± 0.44	21.521 ± 0.47	21.356 ± 0.36	22.194 ± 0.45

Table S6 Trait correlation of family means per treatment for three growth (s_{asym}, r_{max}, x_{mid}) and three allocation traits (*SLA*, *LDMC*, RS_{ratio}) respectively. Days alive in the experiment (d_{alive}) was not used for G-matrix calculation but for selection response. Bottom and top half of matrix show different treatments. Negative correlations are coloured in blue and positive ones in red. Significant Pearson correlations in bold ($p < 0.05$).

Control \ *Dry*	s_{asym}	r_{max}	x_{mid}	*SLA*	*LDMC*	RS_{ratio}	d_{alive}
s_{asym}		0.06	-0.10	0.09	-0.12	0.04	0.04
r_{max}	**-0.25**		**-0.63**	-0.03	0.05	0.04	**-0.34**
x_{mid}	0.14	**-0.65**		0.09	-0.04	0.09	**0.21**
SLA	0.15	-0.08	-0.05		**0.43**	-0.10	0.03
LDMC	0.09	-0.07	0.04	**0.39**		**-0.49**	-0.18
RS_{ratio}	-0.17	0.16	-0.13	**-0.35**	**-0.47**		**0.21**
d_{alive}	-0.03	-0.07	0.14	-0.10	**-0.19**	0.06	

Hot \ *Hot&Dry*	s_{asym}	r_{max}	x_{mid}	*SLA*	*LDMC*	RS_{ratio}	d_{alive}
s_{asym}		**-0.36**	**0.49**	0.06	-0.06	-0.40	0.17
r_{max}	-0.06		**-0.69**	-0.17	-0.10	0.19	**-0.48**
x_{mid}	-0.02	**-0.59**		0.14	-0.06	-0.28	**0.26**
SLA	0.06	-0.03	-0.03		**-0.60**	0.13	-0.19
LDMC	-0.10	0.07	-0.13	0.17		-0.06	0.36
RS_{ratio}	**-0.20**	0.15	-0.12	0.07	-0.05		0.01
d_{alive}	0.05	-0.03	0.17	0.08	0.05	0.00	

Table S7 Treatment-specific genetic variance-covariance matrices (G-matrices) of the three growth traits. Variances can be found on the diagonal and covariances in the off-diagonal cells.

Control	s_{asym}	r_{max}	x_{mid}
s_{asym}	0.462	0.001	0.017
r_{max}		0.503	-0.402
x_{mid}			0.452

Hot	s_{asym}	r_{max}	x_{mid}
s_{asym}	0.423	0.159	-0.060
r_{max}		0.399	-0.337
x_{mid}			0.300

Dry	s_{asym}	r_{max}	x_{mid}
s_{asym}	0.313	0.141	-0.047
r_{max}		0.336	-0.241
x_{mid}			0.293

Hot&Dry	s_{asym}	r_{max}	x_{mid}
s_{asym}	0.310	-0.176	0.141
r_{max}		0.372	-0.270
x_{mid}			0.300

Table S8 Treatment-specific latitudinal variance-covariance matrices (D-matrices) of the three growth parameters. Variances can be found on the diagonal and covariances in the off-diagonal cells.

Control	s_{asym}	r_{max}	x_{mid}
s_{asym}	1.140	-0.317	0.394
r_{max}		0.117	-0.165
x_{mid}			1.000

Hot	s_{asym}	r_{max}	x_{mid}
s_{asym}	0.690	-0.061	-0.153
r_{max}		0.101	-0.109
x_{mid}			0.317

Dry	s_{asym}	r_{max}	x_{mid}
s_{asym}	0.523	-0.022	0.255
r_{max}		0.087	-0.067
x_{mid}			0.192

Hot&Dry	s_{asym}	r_{max}	x_{mid}
s_{asym}	0.063	-0.172	0.065
r_{max}		1.340	-0.538
x_{mid}			0.217

Methods S1 Crossing design of parental (seed donor) generation

Crossing design

Seeds of field-collected mother plants were raised in the greenhouse, and one seedling was kept per mother plant. For the Saugatuck population, these offspring plants were crossed by accounting for environmental variation in the field and phenotypic trait expression. The goal was to produce good numbers of seeds among plants originating from similar and dissimilar environmental conditions and with similar and dissimilar phenotypic trait expression in the greenhouse. The intention was to produce offspring plants that retained environment- and phenotype-dependent genetic differences versus plants that did not retain such differences. Four environmental variables and one phenotypic variable were considered and allowed to sort plants into the following main groups (number of individuals in brackets):

1. Dune position
    a. Bottom (52 + 1)
    b. Slope (74)
    c. Top (54)
2. Intraspecific density
    a. < 3 individuals per 0.25 m^2 (74)
    b. > 4 individuals per 0.25 m^2 (74 + 1)
3. Vegetation cover on 0.25m^2 surrounding the mother plant
    a. < 25 % (74 + 1)
    b. > 45 % (74 + 1)
4. Distance from trees
    a. Close (< 1.5 m) (28)
    b. Far (> 5 m) (30)
5. Random (late/early flowering)
    a. Flowering between 29/1/20 till 9/3/20 (47)
    b. Flowering between 16/3/20 till 25/5/20 (23)

Within each subgroup and for all the range edge populations, crossing was done randomly whenever two plants were ready to be crossed. All crossings were performed by hand-pollination until six fruits, each with about 20 seeds each, per pair were produced (~ 36.000 seeds). As crosses were mostly possible both directions of a plant pair, they were performed evenly in the two directions. If a pair did not produce any seeds due to incompatibility, plants were paired with others.

Methods S2 Image analysis script

Image analysis of plant growth

We built a "black-box" that fitted quite closely over each of our trays and had a stable camera holding on top. The inside walls were sprayed black/dull to prevent reflection of the flashlight. The camera was a digital 12 MP Panasonic DMC-FS10 with ISO 100 and -2/3 exposure. A Python script was developed to analyse images automatically. The base script followed the image analysis script of Exposito-Alonso *et al.* (2018) with multiple adaptations. Adaptations concerned the colour filtering, especially for distinguishing between healthy plant material and soil as well as tissue colour change, and the smoothing and masking of individual pots/plants. The code, pictures of the black box used, examples of tray position files and test pictures can be found at: https://github.com/HeblackJ/automated_image_analysis.git.

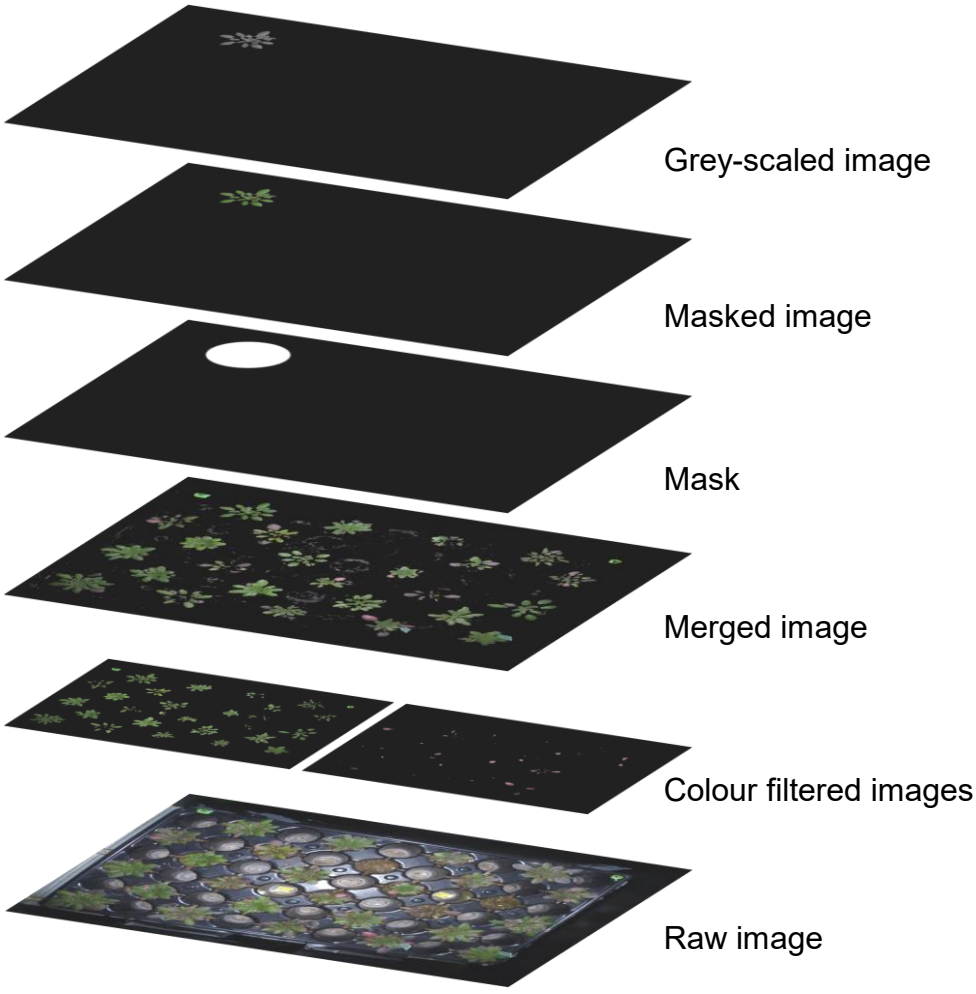

Figure A: Workflow of extracting size data of plants.

Stress caused some of the leaves to turn red/lilac during the experiment. As plant tissue was still viable, we adapted the existing script to also include these colour ranges. First, pictures were separately filtered for all green and red leaf pixels. The two newly obtained images were then merged, and greyscale transformed (Fig. A). To reduce plants that had leaves growing into each other, only every other pot per tray contained substrate and a plant. Furthermore, the layout of the potential pots was not simply per column and row, but every other row had pots shifted by half a pot size, with only 4 instead of 5 pots. This required an adaptation of defining the perimeter of counting pixels. A black mask was produced that had the same size as the raw picture and holes at the positions of interest, where a plant grew.

The program computed date of observation, tray ID, pot position (plant ID) and number of counted pixels per individual as .csv file and saved the obtained filtered picture, separately per pot or for the whole tray.

Method verification

During code development we detected issues of distinguishing between soil and dark green leaves. We addressed the issue by optimizing colour extraction without losing too much of the plant tissue. To assess the quality of our adjustments, we cropped (parts of) images of 72 plants by hand (~3% of all individuals) thereby removing any background of soil and ran the same colour extraction code for full images and hand-cropped images. Differences the two methods varied depending on treatment. In general, we found a tendency to underestimate taller individuals by the automated approach (Fig. B). In the *Hot&Dry* treatment, underprediction was most pronounced (steepest linear regression line). Overall, we saw an average decrease of 4.5% in comparison to the actual size of the plant (*Control*: 3.1%; *Dry*: -11.4%; *Hot*: 2.3%; *Hot&Dry*: -4%). R^2 was 74.5% across treatments, with a range of 65.2% (*Hot*) to 80.8% (*Dry*).

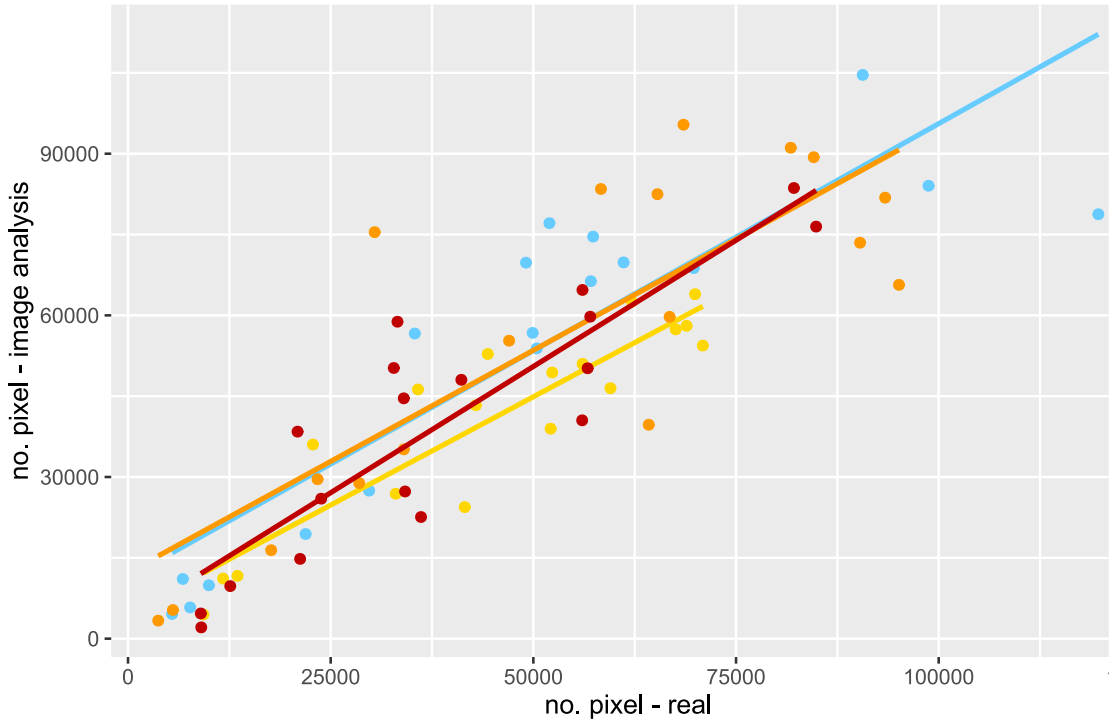

Figure B: Linear regression between pixel number revealed by automated image analysis on pixel number revealed after hand-cropping (real). Different colours indicate the four treatments: blue for *Control*, yellow for *Dry*, orange for *Hot*, and red for *Hot&Dry*.

Supporting Information – Chapter III

Fig. S1 Overlap in outlier genes and enriched GO terms linked to PC1 scores of growth traits among the four treatments in the greenhouse stress experiment.

Fig. S2 Tree map of enriched GO terms for longevity in the greenhouse stress experiment in *control* and *dry*.

Fig. S3 Tree map of enriched GO terms for longevity in the greenhouse stress experiment in *hot* and *hot&dry*.

Table S1 Locations of the selection experiment in the USA.

Table S2 Number of outlier SNPs and outlier genes detected using either of the two approaches: Hidden-Markov-Models (HMM) with > 2 outlier SNPs per gene or a p cut-off value < 0.001 with > 1 outlier SNPs per gene.

Figure S1

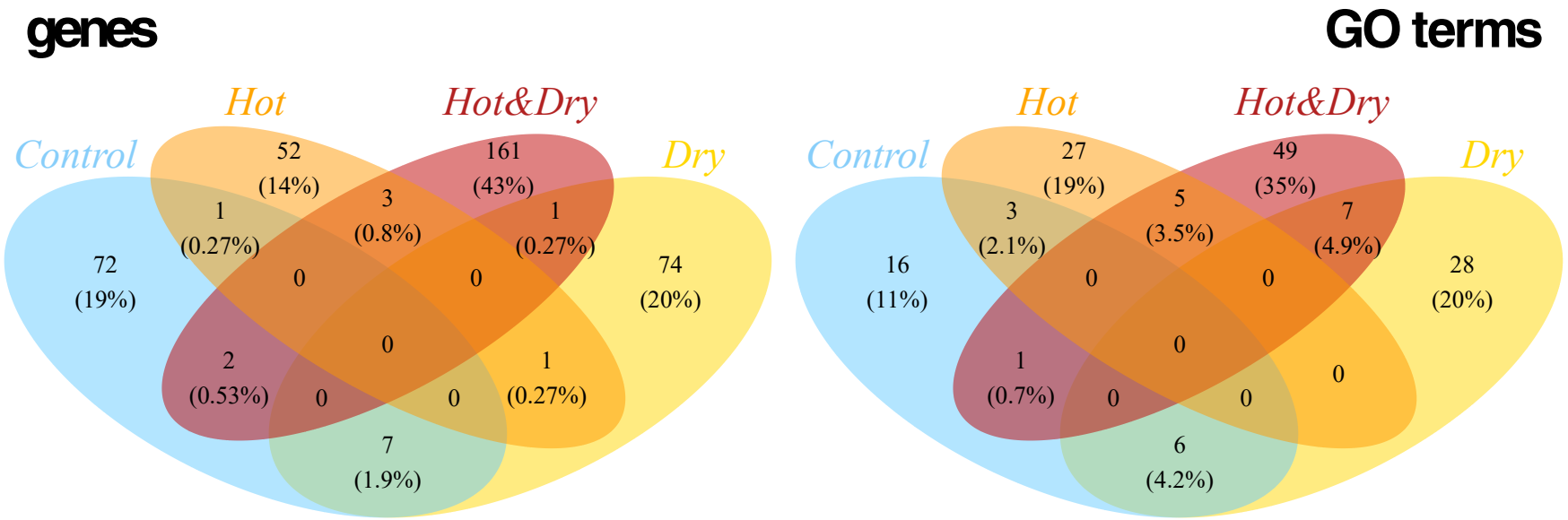

Figure S1: Overlap in outlier genes and enriched GO terms linked to PC1 scores of growth traits among the four treatments in the stress experiment conducted in the greenhouse. The three performance traits were: asymptotic size (s_{asym}), time till half size (x_{mid}), and maximum growth rate (r_{max}). Colours of ellipses indicate the treatments: control in blue, dry in yellow, hot in orange, and hot with dry in red, with mixtures of these colours for outlier genes that overlapped. Percentages are relative to all outlier genes found for a trait.

Figure S2

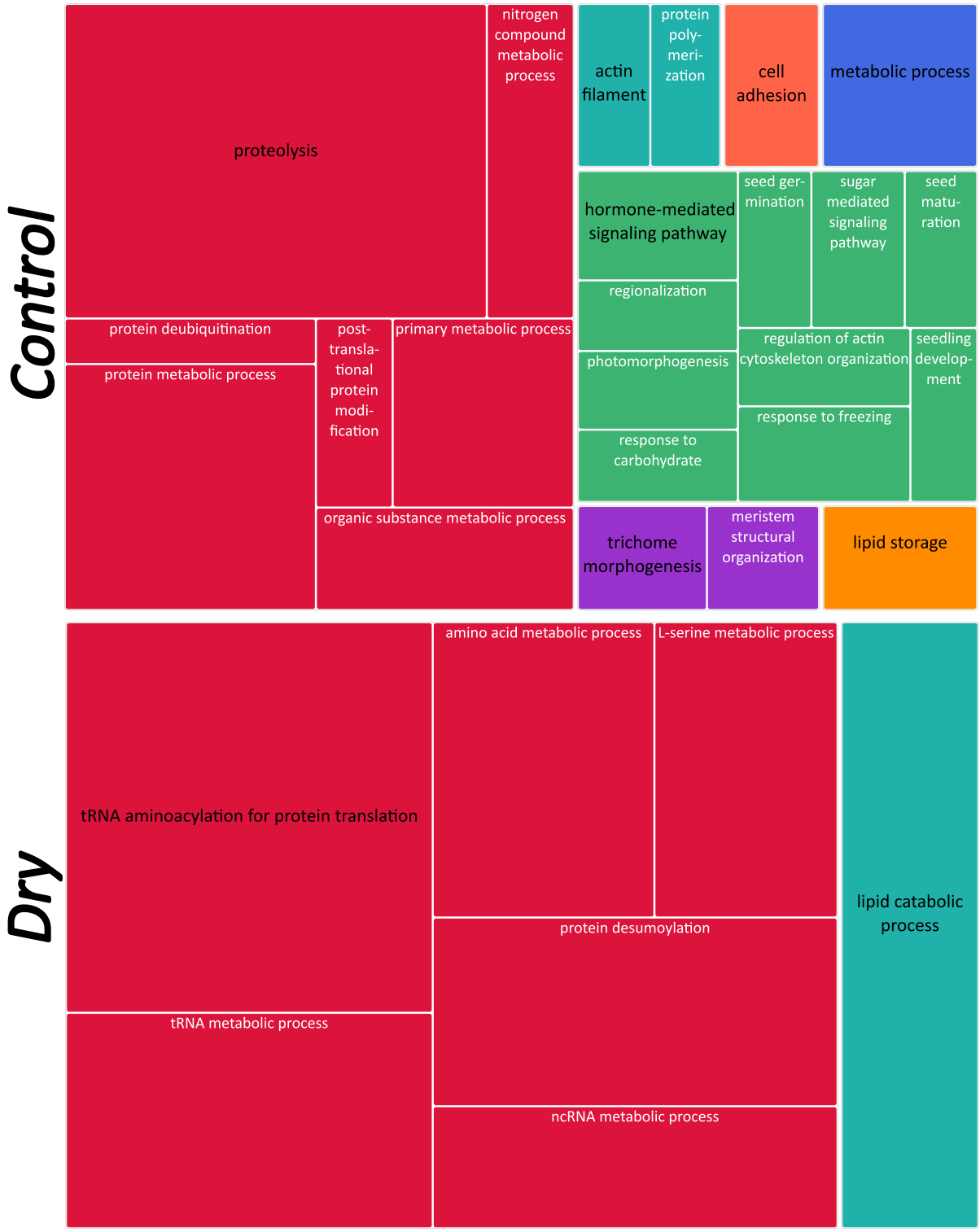

Figure S2: Tree map of enriched GO terms for the performance trait longevity in the stress experiment in the greenhouse for the two treatment: *control* (top) and *dry* (bottom). Same colours within the panel indicate functional group belonging. Group function in black.

Figure S3

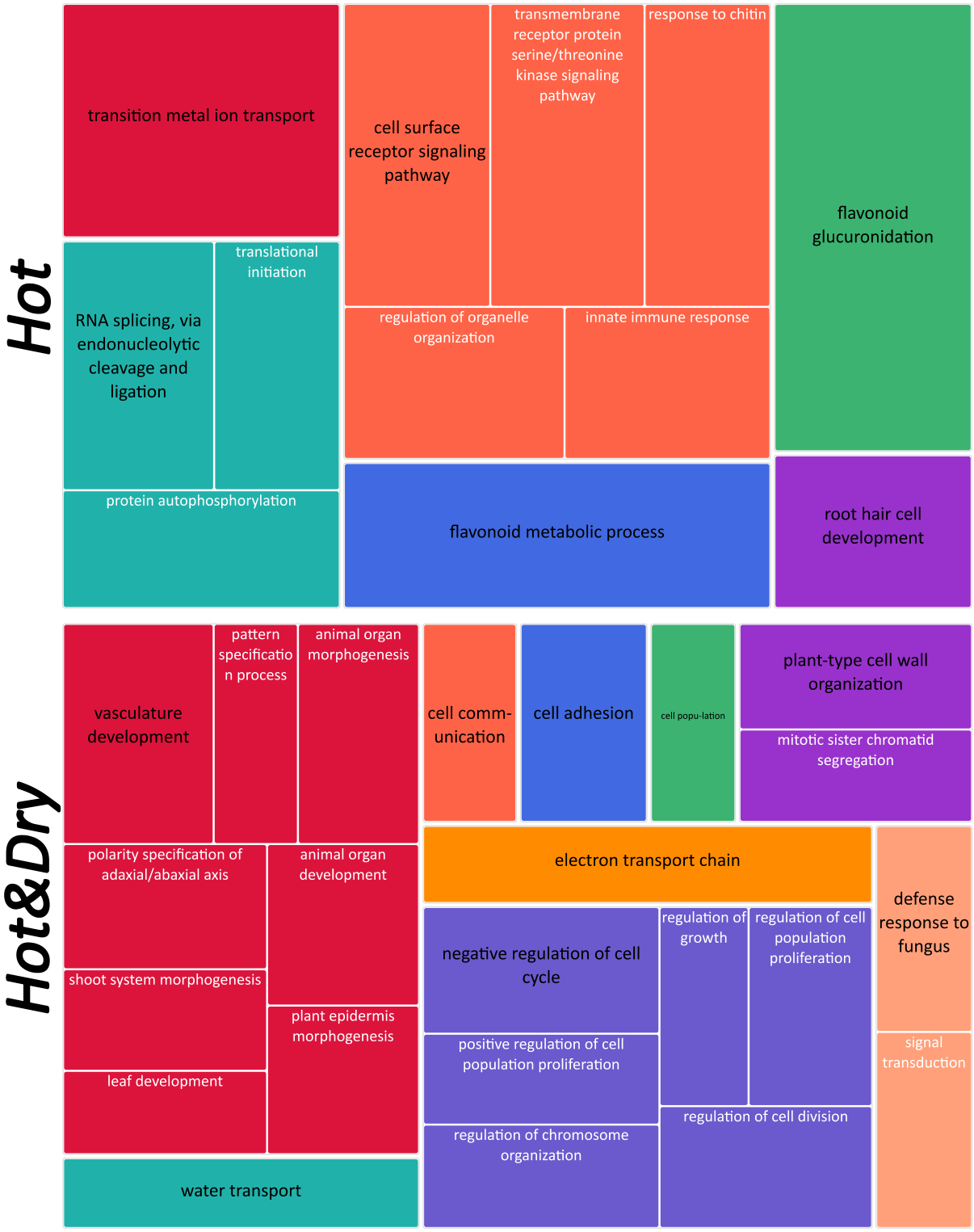

Figure S 3: Tree map of enriched GO terms for the performance trait longevity in the stress experiment in the greenhouse for the two treatment: *hot* (top) and *hot&dry* (bottom). Same colours within the panel indicate functional group belonging. Group function in black.

Table S1: Locations of the selection experiment in the USA. VA – Virginia. NC – North Carolina. Suitability values are based on Lee-Yaw et al. (2018).

	Position	Town	Site	Suitability
Northern transect	Inside	Lexington, VA	Campus Garden, Washington & Lee University	0.569
	Range edge	Williamsburg, VA	York River State Park, Virginia Department of Conservation and Recreation	0.205
	Outside	Norfolk, VA	Hampton Roads AREC, Virginia Tech	0.015
Southern transect	Inside	Blacksburg, VA	Kentland Farm, Virginia Tech	0.587
	Range edge	Durham, NC	Duke Forest, Duke University	0.217
	Outside	Greenville, NC	West Research Campus, East Carolina University	0.013

Table S2: Number of outlier SNPs and outlier genes detected using either of two approaches: Hidden-Markov-Models (HMM) with > 2 outlier SNPs per gene or a p cut-off value < 0.001 with > 1 outlier SNPs per gene. The upper part of the table is on performance traits measured in the stress experiment in the greenhouse, with the four treatments of control, dry, hot, and hot & dry. The lower part of the table reports on performance (whether a seed sown in autumn led to an established plant in spring) estimated in the selection experiment at the southern range edge of *Arabidopsis lyrata*.

	Treatment / site	HMM			p < 0.001		Type
		-log10 (p)	SNPs	genes	SNPs	genes	
Longevity	*Control*	5.081	101	4	1567	118	Stress experiment in greenhouse
	Dry	2.517	826	54	695	73	
	Hot	3.051	551	29	1030	93	
	Hot&Dry	2.449	819	44	668	56	
Biomass	*Control*	2.241	1182	56	594	47	
s_{asym}	*Control*	2.555	550	40	572	72	
	Dry	2.59	811	47	868	78	
	Hot	2.482	870	49	839	68	
	Hot&Dry	2.331	1335	76	911	89	
x_{mid}	*Control*	2.257	1145	69	523	46	
	Dry	2.321	1184	61	737	68	
	Hot	2.557	703	37	567	48	
	Hot&Dry	2.38	1389	92	972	100	
r_{max}	*Control*	2.37	927	50	624	55	
	Dry	2.647	851	41	903	72	
	Hot	2.782	422	25	509	47	
	Hot&Dry	2.525	1164	73	1120	99	
PC1 x_{mid} r_{max}	*Control*	2.241	1162	69	527	48	
	Dry	2.365	1172	60	739	67	
	Hot	2.548	695	37	568	47	
	Hot&Dry	2.389	1384	80	1468	99	
PC1 s_{asym} x_{mid} r_{max}	*Hot&Dry*	2.331	1336	76	911	89	
seed establishment	*Lexington*	2.541	850	55	814	91	Selection experiment
	Williamsburg	2.254	1108	65	532	58	
	Norfolk	2.275	1123	64	576	62	
	Blacksburg	2.891	660	36	1260	111	
	Durham	2.285	1345	66	773	66	
	Greenville	2.317	1072	63	575	62	

Journal of Evolutionary Biology, 2024, **37**, 555–565
https://doi.org/10.1093/jeb/voae045
Advance access publication 10 April 2024
Research Article

JOURNAL OF
Evolutionary Biology

eseb
European Society for Evolutionary Biology

Evolutionary potential under heat and drought stress at the southern range edge of North American *Arabidopsis lyrata*

Jessica Heblack, Judith R. Schepers, Yvonne Willi

Department of Environmental Sciences, University of Basel, Basel, Switzerland

Corresponding author: Jessica Heblack, Department of Environmental Sciences, University of Basel, Schönbeinstrasse 6, 4056 Basel, Switzerland. Email: jessica.heblack@unibas.ch

Abstract

The warm edges of species' distributions are vulnerable to global warming. Evidence is the recent range retraction from there found in many species. It is unclear why populations cannot easily adapt to warmer, drier, or combined hot and dry conditions and locally persist. Here, we assessed the ability to adapt to these stressors in the temperate species *Arabidopsis lyrata*. We grew plants from replicate seed families of a central population with high genetic diversity under a temperature and precipitation regime typical of the low-latitude margin or under hotter and/or drier conditions within naturally occurring amplitudes. We then estimated genetic variance–covariance (G-) matrices of traits depicting growth and allocation as well as selection vectors to compare the predicted adaptation potential under the different climate-stress regimes. We found that the sum of genetic variances and genetic correlations were not significantly different under stress as compared to benign conditions. However, under drought and heat drought, the predicted ability to adapt was severely constrained due to strong selection and selection pointing in a direction with less multivariate genetic variation. The much-reduced ability to adapt to dry and hot-dry conditions is likely to reduce the persistence of populations at the low-latitude margin of the species' distribution and contribute to the local extinction of the species under further warming.

Keywords: adaptation, climatic gradient, evolutionary potential, genetic variation, G-matrix, range edge, trade-offs

Introduction

Species' distribution limits often reflect endpoints of the ecological niche of a species, with the latter defined as the ranges of abiotic factors, availability of resources, and the abundance of interacting species that enable long-term persistence (Hargreaves et al., 2014; Paquette & Hargreaves, 2021). However, for many species, climate alone is a good predictor of where a species reaches its geographical or elevational limit (Lee-Yaw et al., 2016; Patsiou et al., 2021), suggesting that failing climate adaptation at range limits plays a major role in determining distributions. Constrained climate adaptation at range limits is also indicated by the many examples of species that have shifted their distributions under recent climate warming, with expansions at the cold margins and retractions from the warm margins (Chen et al., 2011; Lenoir et al., 2020; Rumpf et al., 2018). In parallel, macroevolutionary studies have revealed that adaptation to climate is evolutionary constrained, particularly adaptation to heat (Bennett et al., 2021; Liu et al., 2020). Still, the causes of constraint are unknown. Here, we focus on the genetic architecture of growth traits under selection and its role in constraining climate adaptation at warm range limits, as species seem mostly unable to adapt there (Parmesan, 2006).

Evolutionary theory has come up with several hypotheses as to why adaptation to changing conditions can fail at range limits (Sexton et al., 2009). These include steepening environmental gradients, too little or too much dispersal, small population size, and, linked with low dispersal and small population size, low genetic variation (Holt, 2003; Kirkpatrick & Barton, 1997; Polechová, 2018; Polechová & Barton, 2015). An aspect that has received relatively less attention is the nature of genetic variation. There may be ample genetic variation for traits under selection when evaluated individually, though genetic variation may still be constraining if selection acts on several traits and these are tied in genetic correlations antagonistic to the direction of selection (Blows & Hoffmann, 2005; Hansen et al., 2019; Lande, 1979). Within a population, genetic correlations antagonistic to the direction of selection, or genetic trade-offs, may be the result either of physical linkage or antagonistic pleiotropy (Falconer & Mackay, 1996, p. 312). Evolutionary trade-offs can be detected within populations if genotypes differ enough in regard to the expression of traits involved in the trade-off, often under stressful conditions (Stearns, 1992) or across habitat types (Falconer & Mackay, 1996, p. 321–324). For the latter scenario, genotypes that are favoured in one habitat are less favoured in another habitat (Fry, 2003), thus preventing the niche expansion of specialized organisms (Holt & Gaines, 1992) and the evolution of favourable traits at distribution margins (Hoffmann & Blows, 1994; Roff et al., 2002).

Genetic variance–covariance (G-) matrices are useful for disentangling correlations among multiple traits, estimating genetic integration, and assessing constraints on recent or future multivariate evolution (Arnold, 1992; Lande, 1979).

Received August 28, 2023; revised March 9, 2024; accepted April 9, 2024

Genetic variances of specific traits are the elements on the main diagonal axis, whereas genetic covariances are the off-diagonal elements of G. G-matrices of different populations or revealed under different environmental conditions can be compared with each other and in regard to how easily they can contribute to a selection response (Roff & Fairbairn, 2012). An important estimate of G capturing genetic correlations in one value is the effective number of dimensions (Kirkpatrick, 2009). If genetic correlations are absent, this number equals the number of traits included in the matrix. The other extreme is when all genetic variation aligns along one axis, with the effective number of dimensions being 1. Angles between G or its components/eigenvectors and other vectors can predict the constraining nature of genetic correlations more specifically. A first such angle involves the vector of population divergence to assess the adaptability in a likely direction of selection (Schluter, 1996). A second involves a selection vector to predict the immediate response to selection (Blows & Hoffmann, 2005).

So far, few studies have assessed the role that genetic trade-offs may play in constraining adaptive evolution at range margins and/or under climate change on a microevolutionary scale (Willi & Van Buskirk, 2022). Paccard et al. (2016) compared the G-matrices of populations of *Arabidopsis lyrata* of a latitudinal gradient and found that populations at range limits had reduced genetic variances, but genetic covariances were such that they constrained evolution less than those of more centrally located populations. Sheth and Angert (2016) imposed artificial selection on scarlet monkeyflowers (*Mimulus cardinalis*) from replicate populations of the latitudinal range, either for early or late flowering. They detected correlated responses in early flowering lines, namely higher specific leaf area (SLA) and leaf nitrogen content. However, population divergence across latitudes did not follow the pattern of correlations, suggesting that past evolution had gone in the direction of less multivariate genetic variation. Etterson and Shaw (2001) performed a quantitative genetics crossing experiment with three populations of *Chamaecrista fasciculata* from a latitudinal gradient, estimated G-matrices at the three sites of origin, and predicted responses to selection based on single traits or G. The predicted multivariate responses were mostly reduced compared to predicted univariate responses due to genetic correlations antagonistic to the direction of selection.

The traits included in the estimation of G need special consideration. Sessile organisms, such as herbaceous plants, seem to respond to environmental stress either by a strategy of escape or tolerance (e.g., Kooyers, 2015; Puijalon et al., 2011; Upadhyay, 2019). Under stress, growth and development may be accelerated to finish an important life-history phase before the effect of stress becomes too severe, a strategy of escape. Alternatively, growth and development may be slowed down in favour of expressing protective traits. Sartori et al. (2019) showed in *A. thaliana* that an acceleration of phenology is related to lower precipitation and higher temperature along the species' range from high to low latitudes, indicating escape from stress under low-latitude conditions. For our study organism, *Arabidopsis lyrata* ssp. *lyrata*, of the many traits that were previously tested for latitudinal clinal variation, only plant size, reproductive development, and thermal resistance were found to vary. Plants of low-latitude areas grew to smaller sizes under benign temperatures and had a slower transition to flowering, higher thermal tolerance, and higher heat resistance, indicating a strategy of slow development and tolerance/protection at low latitudes (Paccard et al., 2014; Wos & Willi, 2015). Hence, adjustments on the continuum of fast versus slow growth or development may be key for coping with stress (Sartori et al., 2019), and aspects of growth and development are, therefore, good candidate traits in investigations on G in the context of low-latitude/warm range limits.

In this study, we compared G-matrices of one large outcrossing population of North American *Arabidopsis lyrata* ssp. *lyrata* (*A. lyrata* in short) grown under experimental temperature and precipitation similar to those at the low-latitude range margin. In climatized glasshouse chambers, we simulated average temperature and precipitation, or extreme conditions, i.e., increased temperature or decreased precipitation, or both types of stressors combined, as they can occur in spring to summer at the southern range edge. Environmental niche modelling revealed that the distribution of the species in the south and north is restricted by climate, and the major climatic factor associated with range limits was the mean minimum temperature in early spring (Lee-Yaw et al., 2018; Sánchez-Castro et al., 2024). Apart from warmer temperatures, we chose drier conditions, as low precipitation during the growing season may reduce the transpiration capacity of plants, which is their typical way of coping with heat (Irvine et al., 1998). We focussed on traits of growth and allocation based on previous findings that indicated the importance of growth progression and allocation in coping with stress. To achieve solid estimates on genetic correlations, we worked with one population only, but we included many replicate families. For the same reason, we chose a population of the southerly centre of distribution with high genetic variation, including in expressed traits. Populations of the southern range limit generally harbour low genomic variation and genetic variation for expressed traits (Paccard et al., 2016; Willi et al., 2018), making the detection of trade-offs difficult. We addressed the following questions: (a) Do genetic variances of traits differ under benign and climate-stress conditions? (b) Are there multivariate genetic constraints? (c) How well can *A. lyrata* respond to selection and adapt under heat, drought, or combined heat drought?

Materials and methods

Seed material and propagation

Arabidopsis lyrata subsp. *lyrata* occurs in temperate eastern and mid-western North America on sand dunes or rocky outcrops with some natural disturbance. It is a short-lived perennial that produces basal rosettes, out of which inflorescences grow in late spring/early summer. We selected a population from the south centre of the *A. lyrata* distribution at Saugatuck Dunes State Park, Michigan, United States (42.70° N, 86.20° W), with high genomic variation and a history of little genetic drift despite some postglacial range expansion (Willi et al., 2018). Furthermore, the population was found to harbour genetic variation in plant size and reproductive development under control conditions and in frost resistance, with traits being associated with environmental gradients of the dune landscape: position on the dune, distance from the canopy, vegetation cover, and intraspecific density (Paccard et al., 2013; Wos & Willi, 2018). The same three traits were confirmed as being variable among populations across the

latitudinal distribution of the species (Paccard et al., 2014; Wos & Willi, 2015).

Seeds of >600 maternal plants were collected between 2007 and 2014 in the field. We assumed that over the 7 years, there had been little change in allele frequencies as the species is common over a large surface area, with a large census size. Seeds of maternal plants were grown in separate pots in a glasshouse and thinned to one plant per pot (conditions in Supplementary Table S1). Plants were cross-pollinated in pairs, with a preference for pairing within one of several habitat aspects, e.g., both plants from dune tops (Supplementary Methods S1). The intention was to keep some of the potentially existent adaptive variants linked to a habitat aspect at a higher frequency in some offspring genotypes. The design resulted in 271 successful cross pairs or "families," of which 120 were randomly selected for offspring raising. Crosses were performed reciprocally, but cross direction was not included in the statistical models. Additionally, the crossing design included three families, each from two northern and two southern populations. These were used later to compare the within-population variation of the Saugatuck population with the within-species and latitudinal trait variation (Supplementary Table S2; Supplementary Figure S1). One pair of northern/southern populations came from the eastern ancestral cluster of *A. lyrata*, and one, together with the Saugatuck population, from the western ancestral cluster (Willi et al., 2018). The obtained seeds were stored in paper bags at 4 °C with silica beads to reduce moisture.

Experimental setup

We designed a 2 × 2 factorial stress experiment with average or extreme temperatures and average or low precipitation occurring in the two populations at the southern range limit (Supplementary Table S1). Low-temperature conditions (*Control* and *Dry*) were close to the average temperature in late spring/early summer, with the corresponding experimental conditions of 18 °C at night, 22 °C during the day, and 25 °C for the daily 1-hr heat peak (Figure 1A; climate data at the two southern edge sites in Schepers et al., 2024). High-temperature conditions (*Hot* and *Hot&Dry*) resembled the summer climate, with 23 °C at night, 27 °C during the day, and 30 °C for the daily 1-hr heat peak. Experimental temperatures during night-time were not as low as those at the two southern sites. The baseline for watering (*Control* and *Hot*) was about average precipitation in late spring/early summer, 100 mm per month. Low watering (*Dry* and *Hot&Dry*) was chosen close to precipitation during the driest month, 60 mm per month. Precipitation amounts were broken down to watering the pots every second day, which was set to either 8.4 or 5 ml per pot. Because some mortality was observed early on, we increased watering after two weeks by ~20% to 10 or 6 ml.

Five replicate plants per family were grown in each of the four treatment combinations (in short, treatments), split over 5 blocks. Seeds were sown in pots (1 per pot, pot diameter/depth: 4/5 cm) of 54-multi-pot-trays filled with a mixture of 1:2 of peat and sand (120 families × 4 environments × 5 replicate blocks = 2,400 pots, plus 3 families × 4 marginal populations × 4 environments × 3 replicates = 144 pots). Pots were watered to saturation and covered with mesh nets, and seeds were stratified at 4 °C in dark climate cabinets for 12 days (ClimeCab 1400, KÄLTE 3000 AG, Landquart, Switzerland). Trays were then moved to the glasshouse for germination and kept moist by spraying from above and keeping the mesh nets until ~75% of seeds had germinated (for 7 days). After 3 weeks, when ~80% of the plants had reached the 4-leaf stage, the stress experiment started. The experiment involved four glasshouse chambers, two with the low-temperature regime and two with the high-temperature regime. Within each of these, five blocks of multiport trays were maintained, with multiport trays allocated to either baseline- or low-watering. To reduce the effects of the glasshouse chamber and position within the block, blocks and trays within blocks were randomly repositioned across the two glasshouse chambers of the same temperature regime twice a week. Plants received fertilizer every fourth week and some insecticide to combat thrips infestation. The stress experiment was terminated after 5 months for plants under the high-temperature regime and after 6 months for plants under the low-temperature regime.

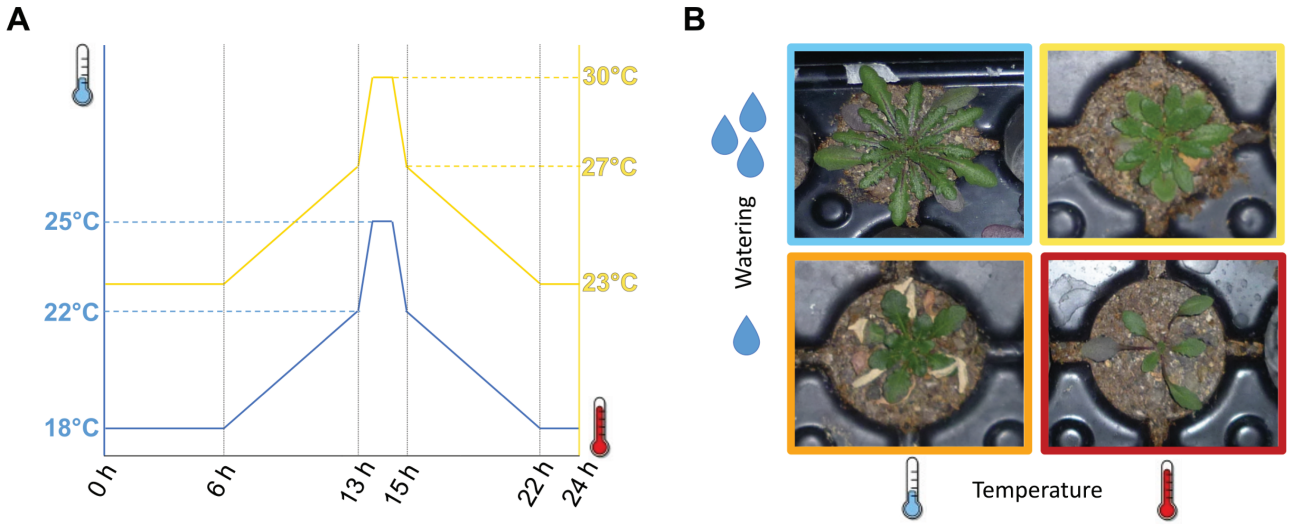

Figure 1. Climate stress experiment with *Arabidopsis lyrata* in the glasshouse. (A) The two temperature treatments were benign (left axis) and high temperature (right axis). Daily temperature profiles included an amplitude of 7 K per day. (B) Differences in performance among plants of the same seed family in the respective treatment combinations (from top left to bottom right)—*Control* (benign temperature and watering), *Hot* (high temperature), *Dry* (low watering), and *Hot&Dry* (high temperature and low watering). Colours indicate the respective treatments.

Trait assessment

Growth

Seed germination was checked every day for the first 2 weeks. The starting size for the day of germination was set to 2 mm^2, representing about four times the mean seed size of *A. lyrata* (Willi, 2013). Growth was tracked by taking pictures of each tray twice a week (every 3–4 days) until at least bolting (Figure 1B). At the same time, mortality was recorded. Camera setup, photo box, and image analysis were based on descriptions by Exposito-Alonso et al. (2018) and were adapted to fit this study design. A detailed description and access to the image analysis script can be found in the Supplementary Methods S2. Overrepresentation of late time points with size data occurred, and therefore, size values that were recorded after the four largest sizes of a plant were removed from the growth curve calculation. All remaining size measures of individual plants were used to fit seven growth models: linear, exponential, power, two- and three-parametric logistic, Gompertz, and von Bertalanffy, using the R package *minpack.lm* (Elzhov et al., 2022). Based on weighted AIC (AIC for each model and plant, and weighted relatively for each plant), the Gompertz model was overall the best but was only in third position for the *Hot&Dry* treatment (Supplementary Table S3). For this reason, the next best model, the three-parameter logistic, was chosen for trait extraction. For 11 plants (0.4%), this model could not be fitted, and the asymptotic size was set to the mean of the four highest size values (no data for growth rate and time to half the asymptotic size). Model output for plant growth included the following three parameters: asymptotic size (s_{asym}, in mm^2), maximal growth rate (r_{max}), and time until half the asymptotic size and fastest growth were achieved (x_{mid}, in days).

Allocation

At the end of the experiment, all available plant material per pot was split into the following categories and weighted separately: green rosette tissue, dead rosette tissue, roots, and inflorescences. Soil particles were washed away, and saturated weight was measured. After 48 hr of drying the material in an oven at 60 °C, the dry weight was measured. We then calculated *SLA* (s_{asym} [mm^2] per green rosette dry matter [mg]), leaf dry matter content (green rosette dry matter [mg] per green rosette saturated weight [g]), and root-shoot ratio (RS_{ratio}; the dry weight of roots to dry weight of all aboveground biomass). Final sample sizes for all populations, growth traits, and allocation traits are listed in Supplementary Table S4.

G-matrices and their analysis

G-matrix

G-matrices were calculated with a focus on growth traits. The first reason for focusing on this set of traits was the modularity among growth and allocation traits (see *Results* section), with considerable correlations within the two sets of traits, but not between them. A second reason was that allocation estimates for the *Hot&Dry* treatment were few (n = 21–23), as many plants died after accelerated growth in this treatment, which precluded the comparison of G for these traits and treatment. For allocation traits and all traits combined, we ran the same set of analyses on G-matrices as for the growth traits but by excluding the *Hot&Dry* treatment (results in the Supplementary Material).

Around 1,800 growth data points per treatment were available: 120 families × 5 replicates × 3 growth traits. Trait estimates were first corrected for the effects of block, tray within block, and position in the multi-pot tray for each treatment separately. The data points were then centred and rescaled across treatments, with a mean of 0 and a variance of 1. We calculated G-matrices for each treatment combination using a Bayesian approach with *MCMCglmm* (Hadfield, 2010). The mixed-effects model was:

$$Y_{ijk} \sim \mu + F_{jk} + \varepsilon_{ijk},$$

where Y_{ijk} is an observation for plant i of family j on trait k, the intercept (μ) is a fixed effect, F_{jk} is the random effect of the family, and ε_{ijk} is the random residuals. Iterations were set to 200,000, with a burn-in of 5,000 and thinning of 50. Priors for G came from a restricted maximum likelihood model (*lme4*; Bates et al. 2015). The significance of family-level covariance and variance estimates was evaluated by comparing deviance information criterion values (DIC; generalization of the Akaike information criterion) of (a) a model with a full G-matrix to (b) one with a matrix with family-level variances only, and (b) to (c) one without variances or covariances on the family level (Paccard et al., 2016; Puentes et al., 2016). For further analyses and presentation, all obtained G-matrices were multiplied by 2 to approximate genetic variances and covariances given the full-sib design.

Comparison of Gs

G-matrices of the four treatment combinations were compared by estimates of G-matrix geometry (Hansen & Houle, 2008; Kirkpatrick, 2009; Milocco & Salazar-Ciudad, 2022; Paccard et al., 2016). The first was the sum of the genetic variances across the traits, the trace of G (Kirkpatrick, 2009). The second was the effective number of dimensions (n_D), calculated as the sum of all eigenvalues of G divided by the first eigenvalue (eq. [2] in Kirkpatrick, 2009). The third measure was the angle between the dominant eigenvector of G, g_{max}, and the dominant eigenvector of the matrix of latitudinal trait divergence (D) among northern and southern populations, d_{max}. D matrices were established for the four environments in the same way as the G matrices, but with the input data of plant traits of the above-mentioned edge populations and including the random effect of southern position (north/south as 0/1). The fourth was the deviation of the predicted selection response from the end point of the selection vector, a measure of adaptive potential. We produced selection vectors using longevity (days of survival) as a fitness proxy. As with the three growth traits, longevity was first corrected for the effects of the block, tray within the block, and position in the multi-pot tray within treatment, followed by dividing by the mean in that treatment. We used *blme* (Chung et al., 2013) to overcome singularity and the model (in *blme* format):

$$\frac{\text{Longevity}}{\text{Mean longevity}} \sim s_{\text{asym}} + r_{\text{max}} + x_{\text{mid}} + (1|j),$$

with family, j, being the random factor. The obtained coefficients of the fixed effects of traits are the selection coefficients, which, taken together, build the selection vector (β) of the specific treatment (Hansen & Houle, 2008). The response to selection (Δz) can now be calculated by multiplying G with the selection vector (β) using the multivariate breeder's equation ($\Delta z = G^*\beta$; Lande, 1979). Selection deviation is the distance of the end points between the selection vector and the predicted response to selection after one generation. As a fifth measure, we calculated evolvability (evo_{HH}) by the method

of Hansen and Houle (2008, eq. [1]), which incorporates the strength of selection (the length of the selection vector) and its orientation. More precisely, evo_{HH} is the projection of the predicted response to selection on the selection vector. All comparisons involving aspects of G were made based on the posterior distribution of 3,900 G-matrices per treatment, following the approach described in Aguirre et al. (2014). Testing was done based on 95% highest posterior density (HPD) intervals, and when HPD intervals were overlapping, a comparison of the region of practical equivalence (Kruschke, 2018) followed. For this, the posterior distributions of the two treatments were divided. If the 95% HPD interval of the distribution of differences did not overlap with ROPE, i.e., a range between 0.9 and 1.1 (±10%; Henry and Stinchcombe, 2023; Kruschke, 2018), then a difference between treatments was assumed to exist.

Heritability

We estimated broad-sense heritability (H^2) by analysis of variance on mean-centred data across treatments. H^2 was calculated as twice the variance explained by family (V_f) over the phenotypic variance ($V_z = V_f + V_{error}$). In a full sib design, $2V_f$ represents an upper-bound estimate of additive genetic variance (V_g), likely inflated by a fraction of dominance variance and variance due to common-environment/maternal effects that also contribute to V_f (Walsh & Chenoweth, 2017). However, maternal effects were shown to be insignificant beyond very early life stages in *A. lyrata* (Paccard et al., 2013), and empirical (Wolak & Keller, 2014) and theoretical results (Clo & Opedal, 2021) show that dominance variance is generally much lower than additive variance. To compare variance estimates among traits and treatments, we standardized them by the square of the trait mean of the specific environment as proposed by Houle (1992)—now I_g and I_e. Standardized genetic variance, I_g, is another measure of evolvability that, compared to heritability, estimates the response relative to the trait mean before selection (Houle, 1992). The standard error of H^2 was approximated based on sample sizes (Walsh & Chenoweth, 2017). All analyses were done in R v. 4.0.5 (R Core Team, 2021).

Results

The four treatment combinations varied in stress, indicated by the varying mean sizes the plants achieved. Plants had declining asymptotic sizes from *Control* (14.5 ± 0.3 cm^2) to *Hot* (12.4 ± 0.2 cm^2), *Dry* (10.8 ± 0.1 cm^2), and *Hot&Dry* (8.2 ± 0.2 cm^2; Supplementary Table S5; Supplementary Figure S1). Correlation analysis among growth and allocation traits within treatments revealed a modular pattern (Supplementary Table S6). Growth traits (s_{asym}, r_{max}, x_{mid}) were often highly correlated with each other, and allocation traits (*SLA*, leaf dry matter content, RS_{ratio}) were often highly correlated, but correlations between the two sets of traits were weak. This, along with the low sample sizes for allocation traits in the *Hot&Dry* treatment (Supplementary Table S4), motivated the focus on growth traits in further analyses.

We found that genetic co-/variances for growth traits were overall significant in all treatments. Models with covariances, as compared to those without covariances, always had significantly lower DIC values, and models with variances only as compared to models without had lower DICs (Table 1). The comparison of the trace and dimensionality of treatment-specific G-matrices revealed little variation among the four environments. Neither the trace of Gs nor their dimensionality significantly differed between any of the four treatments, as 95% of HPD intervals were highly overlapping (Figure 2A and B). Dimensionality varied between averages of 1.3 and 1.6 for the three aspects of the logistic growth trajectory, indicating the presence of considerable correlations. The strongest correlations across treatments were revealed between maximal growth rate and time to the mid-point of growth (Supplementary Tables S6 and S7; Supplementary Figure S2). Plants either grew early (low x_{mid}) and had a high growth rate (r_{max}), or they grew late with a slow growth rate. In the *Hot&Dry* treatment, the two traits were associated with trade-offs with maximum size. Early and fast-growing plants reached small final size, while late and slow-growing plants reached large asymptotic size.

The next five estimates related the direction of G with vectors of population divergence and selection. Two were angles, with higher angles (up to 180°) indicating stronger constraints. The angle between g_{max} and d_{max} (dominant eigenvectors of G and the matrix of latitudinal trait divergence, D) was highest in the *Hot* and *Dry* treatments and lowest in the *Hot&Dry* treatment, with differences being significant (Figure 2C; G-matrices in Supplementary Table S7; D-matrices in Supplementary Table S8). The result indicates a good alignment between G and latitudinal trait divergence under combined stress. The angle between the selection vector and the predicted response to selection based on G required the assessment of selection in each of the experimental environments. We found selection (vector length; $|\beta|$) to be strongest under *Hot&Dry* ($|\beta| = 0.136$), considerably lower under *Dry* ($|\beta| = 0.058$) and lowest under *Control* ($|\beta| = 0.011$) and *Hot* ($|\beta| = 0.007$; Figure 3). The angle between the selection vector and the predicted response to selection revealed for the four treatment combinations decreased in the following order: *Dry* (close to 60°), *Hot&Dry*, *Control*, *Hot* (close to 20°) (Figures 2D and 3). Similarly, the deviation between the endpoints of the selection vector and the predicted response significantly differed between treatments, with the distance decreasing from *Hot&Dry* and *Dry* to *Control* and *Hot* (Figures 2E and 3). Somewhat in line, the projection of the selection response onto the selection vector (evo_{HH}) was lowest in the *Dry* treatment and significantly higher in the other three treatments (Figures 2F; Supplementary Figure S3). This latter estimate indicated the strongest constraints under *Dry*, followed by *Hot&Dry*.

Average broad-sense heritability deviated from the trace of G in predicting genetic variation across the four

Table 1. DIC values for G-matrices that include both variances and covariances on the family level ($DIC_{(co)variances}$), variances only ($DIC_{variances}$), or only family effects (DIC_{null}) for each treatment.

	$DIC_{(co)variances}$	$DIC_{variances}$	DIC_{null}
Control	4,391.379	4,440.294	4,556.135
Hot	3,722.478	3,785.262	4,039.161
Dry	2,951.876	2,982.765	3,410.213
Hot&Dry	3,846.137	3,875.810	4,001.464

Note. Models with smaller DIC are better supported—those with variances and covariances on the family level as compared to variances only and those with variances as compared to none.

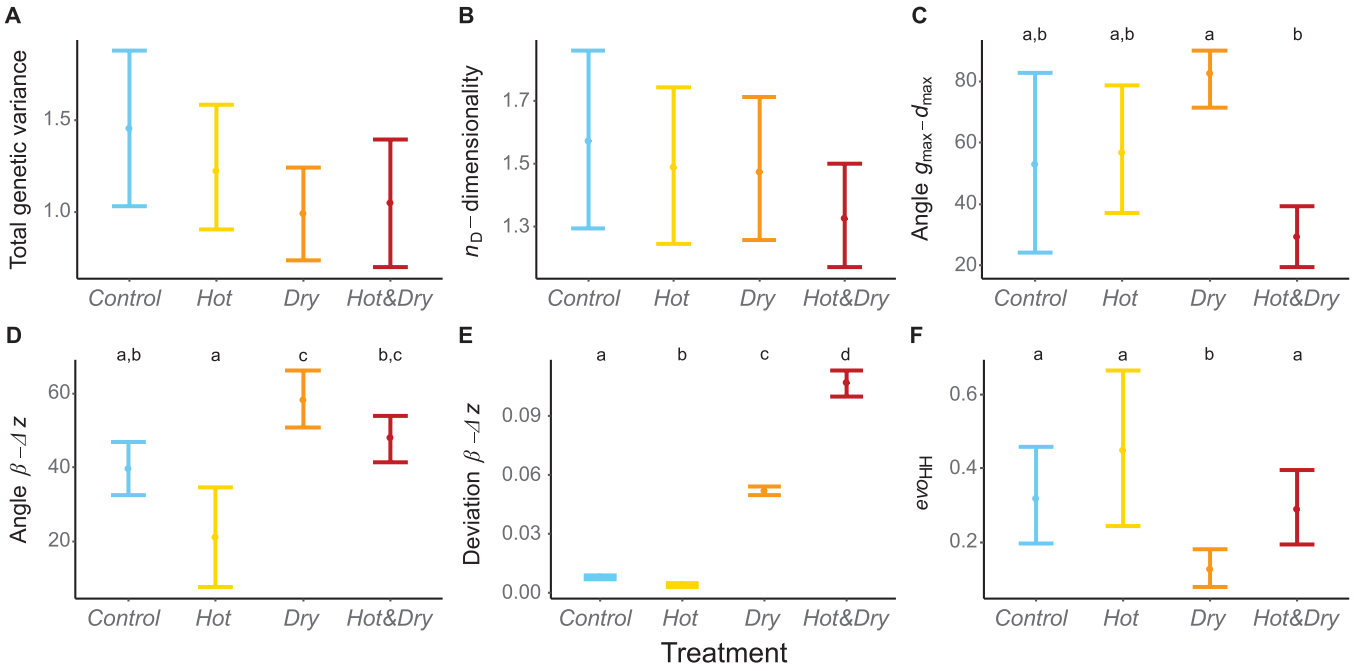

Figure 2. Comparison of geometric aspects of genetic variance–covariance (G-) matrices estimated under benign and stress conditions. (A) Total genetic variance, the trace of G. (B) Effective number of dimensions, n_D. (C) Change in the angle between g_{max}, the dominant eigenvector of G, and d_{max}, the dominant eigenvector of the matrix of latitudinal trait divergence. (D) Angle and (E) deviation distance between selection vector (β) and predicted selection response (Δ*z*). (F) Hansen and Houle's measure of evolvability (evo_{HH}). The colours represent the respective treatments: *Control*, *Hot*, *Dry*, *Hot&Dry*. Dots indicate the predicted model estimates and bars the 95% highest posterior density intervals. The letters above the bars indicate differences between treatments based on the region of practical equivalence.

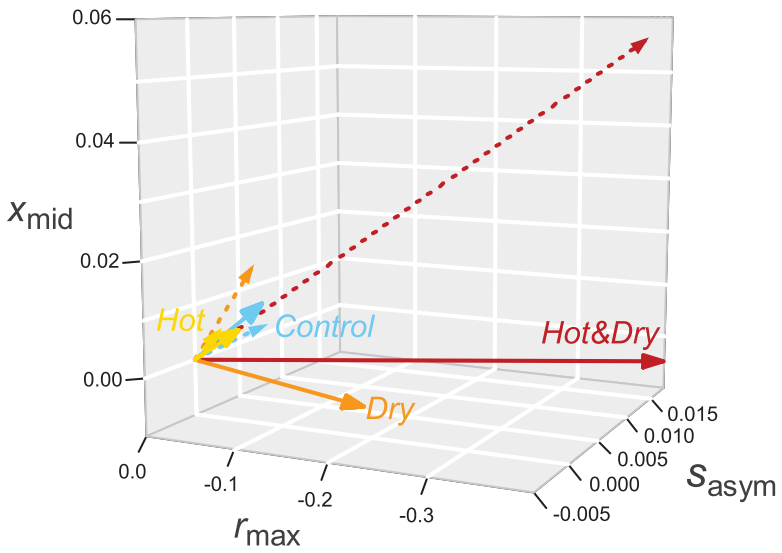

Figure 3. Direction and strength of viability selection (β, solid lines) and predicted selection response after two generations (Δ*z*, dotted lines) for each treatment along the three aspects of logistic growth (asymptotic size—s_{asym}, maximal growth rate—r_{max}, time to fastest growth—x_{mid}).

treatments. Heritability tended to be lower—across traits—in the *Control* (mean: 0.359, range: 0.278—0.440), the *Hot&Dry* treatment (0.370, 0.289—0.451), and the *Hot* treatment (0.477, 0.392—0.561), and higher in the *Dry* treatment (0.567, 0.481—0.653; Supplementary Figure S4). The maximal growth rate and the time to the mid-point of growth had heritabilities that were generally low across the four treatments (mean: 0.431 and 0.292, respectively; mean for asymptotic size: 0.606). Estimates of genetic and environmental variances as well as Houle's *I* varied across traits, with no consistent patterns across the four treatments (no systematic increase or decline with increasing stressfulness; Supplementary Figure S4).

G-matrices for allocation traits, as well as growth and allocation traits combined, revealed similar patterns as for growth traits. The three allocation traits had lower trace values, and differences among treatments were not significant (Supplementary Figure S5A). Furthermore, the dimensionality of G did not differ among treatments (Supplementary Figure S5B). The higher discrepancy between the selection vector and selection response was pronounced under *Dry* (Supplementary Figure S5C). However, the mean was about

four times smaller than for G-matrices with growth traits only. G-matrices, including allocation and growth traits, did not differ in trace or dimensionality among treatments, but the distance between the selection vector and selection response was again pronounced under *Dry* (Supplementary Figure S5D–F). Despite the seemingly low correlation between growth and allocation traits, the dimensionality of G when all six traits were included was considerably lower than the sum of n_D of the two separate matrices with three traits.

Discussion

There is no consensus on the causes of species' distribution limits when species have range limits that equal niche limits, as evolution should progress towards expanding the niche and the range if habitat is generally available (Sexton et al., 2009; Willi & Van Buskirk, 2019). Our study focussed on the potential contribution of genetic correlations constraining adaptive responses to cope with extreme conditions at range limits. We picked conditions typical for the low-latitude range limit of *A. lyrata*, as numerous studies have shown that warm margins of species' distributions are places where constrained evolution becomes most evident under climate change (Clark et al., 2020; Parmesan, 2006). The population studied was from the southerly centre of distribution with high genetic variation, which was assumed to make the detection of genetic correlations more likely. Furthermore, the population was reported to harbour genetic variation for traits that also vary along the latitudinal cline both in the eastern and western ancestral cluster of *A. lyrata* (see *Materials and methods* section, first paragraph). We found support that heat stress imposes multivariate selection to which the specific population can respond by adaptation. However, drought stress or the combination of heat and drought led to strong selection and in a direction away from high multivariate genetic variation, resulting in a high predicted lag of adaptation. We will discuss the results in light of aspects of G, the role of stress in affecting them, and what the results imply for low-latitude populations under climate warming. The focus is on traits of the growth trajectory.

Genetic variation and covariation in growth traits under climate stress

Across treatments, we found significant genetic variation in growth traits (Figure 2A). Similarly, broad-sense heritabilities were considerably too high (range of means across environments: 0.260—0.799), with the lowest for the trait of time to fastest growth. However, the trace of G and average heritabilities did not vary concordantly. While the sum of genetic variances did not differ significantly across treatments (Figure 2A), average heritability tended to be higher in the dry treatment (Supplementary Figure S4). Deviations were the result of environmental variances being relatively reduced under dry conditions. Furthermore, we found genetic covariances to be significant and important. They reduced the number of dimensions or sphericity of G by one-half relative to no correlations, and there was little variation in this among treatments (Figure 2B).

Environmental stress was hypothesized to either increase genetic variances or decrease them (Hoffmann & Merilä, 1999). Our results do not support a systematic increase or decrease of genetic variances or heritabilities under stress. The trace of G for growth and/or allocation traits did not significantly differ between treatments. Heritabilities across traits tended to be lowest in the benign and the most stressful environment. Furthermore, genetic and environmental variances did not reveal a linear-like pattern with stressfulness (Supplementary Figure S4). Another way of depicting genetic variation for individual traits was suggested for fitness-relevant traits, the variance standardized by the square of the trait mean (Houle, 1992). In previous research, those estimates were shown to increase consistently with the level of stress, including thermal stress (Willi et al., 2010, 2011). Here, the mean-standardized variances also did not reveal a linear-like pattern with stressfulness (Supplementary Figure S4), supporting inconsistent responses of genetic variation to stress.

Environmental stress has also been discussed to affect genetic correlations systematically. Empirical studies covering a wide range of taxa have documented that genetic correlations are ubiquitous, with the effective number of dimensions of G often being considerably lower than the number of traits studied (e.g., Chenoweth & Blows, 2008; Eroukhmanoff & Svensson, 2011; Kirkpatrick & Lofsvold, 1992; McGuigan & Blows, 2007; Mezey & Houle, 2005). In a previous study on *A. lyrata* populations of a latitudinal gradient, the dimensionality of Gs was relatively more reduced than shown here (Paccard et al., 2016), possibly because more traits were studied. Stearns (1992) argued that negative correlations between traits in regard to their fitness implications, or trade-offs, might be expressed more likely under considerable stress. Our results and those of Paccard et al. (2016), who applied a dry treatment, suggest that genetic correlations are not necessarily altered by stress. We found no significant changes in the dimensionality of G despite dry and hot-dry conditions being the most stressful (e.g., based on the effect on plant size).

Instead, our results and those of Paccard et al. (2016) point to the increased divergence between the direction of G and the direction of selection under water stress (Figures 2D and 3). Similar results were revealed in a meta-analysis by Wood and Brodie (2015). Despite only small differences in genetic correlations among environments, variation in the discrepancy (angle) between the direction of genetic correlations and the direction of selection was found to be considerable. The direction of multivariate genetic variation relative to the direction of selection plays a major role, as genetic constraints may seriously limit adaptive evolution only if they are directed against selection (Agrawal & Stinchcombe, 2009; Conner, 2002). Therefore, despite very similar G-matrices, the orientation of genetic constraints compared to selection as well as the strength of selection might be the most important factors for a species' adaptive potential under differing selection regimes (Arnold et al., 2008; Phillips & Arnold, 1999).

Lastly, a reason for some consistency in the magnitude of genetic covariances in growth and allocation traits may be their generally high integration. There was one consistent and considerable genetic correlation among growth traits, namely between the time to the mid-point of growth and the maximal growth rate of the logistic growth model (Supplementary Table S6; Supplementary Figure S2). Plants either grew early and fast, or they grew late and slowly. Furthermore, under combined stress, the two traits of time to the mid-point of growth and the maximal growth rate were tied in trade-offs with asymptotic size. Early-growing plants and plants that grew fast had a smaller final size, while late- and slow-growing plants achieved larger sizes. These results are in line with the slow-fast continuum suggested by Grime and

Hunt (1975) and later extended by Stearns (1992, 1983), that organisms either grow fast, have a short lifecycle, and are small, or the opposite. Support for the hypothesis is numerous (e.g., Oliveira et al., 2021; Salguero-Gómez, 2017; Sartori et al., 2019, 2022). Interestingly, a similar trade-off complex among the three growth traits was found in the latitudinal divergence matrices. To variable extents across treatments, time to the mid-point of growth and growth rate were negatively correlated, and, with the exception of one of these traits under heat, early and fast growth implied a smaller final size (Supplementary Table S8). Southern populations had generally smaller sizes within each of the two ancestral clusters, though the association with earlier and faster growth was not consistent (Supplementary Table S5).

Predicted selection response under climate stress at the low-latitude range edge

Unlike genetic variances and genetic correlations, the predicted ability to adapt varied significantly among treatments for growth traits, allocation traits, and all traits combined. On the one hand, selection was stronger both under drought and heat drought as compared to benign or hot conditions. This strongly affected the deviation between ideal and predicted selection response (Figure 2E; for allocation and all traits, see Supplementary Figure S5C and F). Under both drought and heat with drought, the deviation was high. This pattern was also depicted by the estimate of evolvability (evo_{HH}), though only the estimate under drought was significantly lower (Figure 2F; Supplementary Figure S3). On the other hand, the genetic correlations were involved in lowering the ability to adapt. However, and as discussed further up, what changed was that under drought and heat with drought, selection took a direction more antagonistic to the direction of the highest multivariate genetic variation; the genetic correlations changed little (Figures 2D and 3). Results confirm previous results by Lau et al. (2014) on *A. thaliana* that certain stressors, particularly combined stressors, impose strong selection, and combined stress reduces the evolutionary potential along a phenotypic selection gradient. Furthermore, they are in line with the constraining aspect of genetic correlations as found, e.g., in the transplant experiment by Etterson and Shaw (2001). Covering gradients of temperature and water availability, they showed that genetic correlations antagonistic to the direction of selection decreased the evolutionary potential in a plant despite considerable genetic variances and heritabilities in the traits under selection.

If drought and combined heat with drought become more frequent at the low-latitude range limit of *Arabidopsis lyrata*, this will seriously impede population persistence. Niche modelling indicated that temperature was the main driver of distribution limits in the south and north (Lee-Yaw et al., 2018; Sánchez-Castro et al., 2024). This suggests that the species occurs in areas with marginal temperature conditions at the range limit, which was confirmed in a transplant experiment with sites within and beyond the southern and northern range limits (Sánchez-Castro et al., 2024). With climate warming, drought will become an additional stressor. For the southern and eastern United States, climate change has been associated not only with increasing temperature but also with longer periods of drought (Easterling et al., 2017; Schepers et al., 2024; Vose et al., 2017). For several accessions of the closely related *A. thaliana*, Vile et al. (2012) found that the fitness proxy of biomass production was mostly higher under heat than drought conditions, suggesting that drought is more of a stressor than heat. A meta-study on a variety of organisms revealed a more even picture, whereby at low latitudes, water availability is of similar importance for survival than temperature (Pearce-Higgins et al., 2015). Given that temperatures are marginal at the southern range limits for *A. lyrata* and drought phases are increasing, our results of low adaptation potential under these conditions suggest that populations at the low-latitude range limit are at risk of extinction.

Conclusions

Our study shows that drought and combined heat and drought—at magnitudes that may occur in nature at the low-latitude range limit of *Arabidopsis lyrata*—impose strong selection on traits related to the growth trajectory. At the same time, multivariate genetic variation for these traits is reduced due to some consistent genetic correlations. Correlations generally follow the continuum between slow and fast growth and become more constraining under drought and combined heat and drought because selection takes a direction more antagonistic to the direction of high multivariate genetic variation. When occurring together, strong selection and such constrained genetic variation led to a relatively low predicted selection response. If the future climate exposes low-latitude populations of *A. lyrata* to drought or heat with drought more frequently, populations may therefore fail to persist due to excessive deaths linked with selection.

Supplementary material

Supplementary material is available at *Journal of Evolutionary Biology* online.

Data availability

Data will be available on DRYAD: https://doi.org/10.5061/dryad.2rbnzs7sw. The image analysis script (Supplementary Methods S2) is available at https://github.com/HeblackJ/automated_image_analysis.git or https://doi.org/10.5281/zenodo.10897248.

Author contributions

Jessica Heblack (Conceptualization [Equal], Data curation [Lead], Formal analysis [Lead], Methodology [Equal], Software [Lead], Visualization [Lead], Writing—original draft [Equal], Writing —review & editing [Equal]), Judith Schepers (Conceptualization [Equal], Data curation [Supporting], Formal analysis [Supporting], Methodology [Equal], Writing—original draft [Supporting], Writing—review & editing [Supporting]), and Yvonne Willi (Conceptualization [Equal], Formal analysis [Supporting], Funding acquisition [Lead], Methodology [Equal], Writing—original draft [Equal], Writing—review & editing [Equal])

Funding

We were supported by the Swiss National Science Foundation (grant no. 310030_184763 to Y.W.).

Acknowledgments

We thank O. Bachmann, E. Belen, S. Ellenberger, C. Mattson, S. Riedl, F. Schlöth and X. Quinter, and for help with

raising plants and measuring them. K. Lucek and A. Narasimhan gave comments on an early draft of the manuscript.

Conflicts of interest

None declared.

References

Agrawal, A. F., & Stinchcombe, J. R. (2009). How much do genetic covariances alter the rate of adaptation? *Proceedings of the Royal Society of London, Series B: Biological Sciences*, *276*(1659), 1183–1191. https://doi.org/10.1098/rspb.2008.1671

Aguirre, J. D., Hine, E., McGuigan, K., & Blows, M. W. (2014). Comparing G: Multivariate analysis of genetic variation in multiple populations. *Heredity*, *112*(1), 21–29. https://doi.org/10.1038/hdy.2013.12

Arnold, S. J. (1992). Constraints on phenotypic evolution. *The American Naturalist*, *140*(Suppl 1), S85–107. https://doi.org/10.1086/285398

Arnold, S. J., Bürger, R., Hohenlohe, P. A., … Jones, A. G. (2008). Understanding the evolution and stability of the G-matrix. *Evolution*, *62*(10), 2451–2461. https://doi.org/10.1111/j.1558-5646.2008.00472.x

Bates, D., Mächler, M., Bolker, B., & Walker, S. (2015). Fitting linear mixed-effects models using lme4. *Journal of Statistical Software*, *67*(1), 48. https://doi.org/10.18637/jss.v067.i01

Bennett, J. M., Sunday, J., Calosi, P., … Olalla-Tárraga, M. (2021). The evolution of critical thermal limits of life on Earth. *Nature Communications*, *12*(1), 1198. https://doi.org/10.1038/s41467-021-21263-8

Blows, M. W., & Hoffmann, A. A. (2005). A reassessment of genetic limits to evolutionary change. *Ecology*, *86*(6), 1371–1384. https://doi.org/10.1890/04-1209

Chen, I. -C., Hill, J. K., Ohlemüller, R., … Thomas, C. D. (2011). Rapid range shifts of species associated with high levels of climate warming. *Science*, *333*(6045), 1024–1026. https://doi.org/10.1126/science.1206432

Chenoweth, S. F., & Blows, M. W. (2008). Q_{ST} meets the G matrix: The dimensionality of adaptive divergence in multiple correlated quantitative traits. *Evolution*, *62*(6), 1437–1449. https://doi.org/10.1111/j.1558-5646.2008.00374.x

Chung, Y., Rabe-Hesketh, S., Dorie, V., … Liu, J. (2013). A nondegenerate penalized likelihood estimator for variance parameters in multilevel models. *Psychometrika*, *78*(4), 685–709. https://doi.org/10.1007/s11336-013-9328-2

Clark, J. S., Poore, A. G. B., Coleman, M. A., & Doblin, M. A. (2020). Local scale thermal environment and limited gene flow indicates vulnerability of warm edge populations in a habitat forming macroalga. *Frontiers in Marine Science*, *7*, 711. https://doi.org/10.3389/fmars.2020.00711

Clo, J., & Opedal, H. (2021). Genetics of quantitative traits with dominance under stabilizing and directional selection in partially selfing species. *Evolution*, *75*(8), 1920–1935. https://doi.org/10.1111/evo.14304

Conner, J. K. (2002). Genetic mechanisms of floral trait correlations in a natural population. *Nature*, *420*(6914), 407–410. https://doi.org/10.1038/nature01105

Easterling, D. R., Kunkel, K. E., Arnold, J. R., … Wehner, M. F. (2017). Chapter 7: Precipitation change in the United States. In D. J. Wuebbles, D. W. Fahey, K. A. Hibbard, D. J. Dokken, B. C. Stewart, & T. K. Maycock (Eds.), *Climate science special report: Fourth national climate assessment* (Vol. *I*, pp. 207–230). U.S. Global Change Research Program. https://doi.org/10.7930/J0H993CC

Elzhov, T. V., Mullen, K. M., Spiess, A. -N., & Bolker, B. (2022). *minpack.lm: R Interface to the Levenberg-Marquardt nonlinear least-squares algorithm found in MINPACK, Plus support for bounds* (R package version 1.2-2) [Computer software]. https://CRAN.R-project.org/package=minpack.lm

Eroukhmanoff, F., & Svensson, E. I. (2011). Evolution and stability of the G-matrix during the colonization of a novel environment: G-matrix evolution. *Journal of Evolutionary Biology*, *24*(6), 1363–1373. https://doi.org/10.1111/j.1420-9101.2011.02270.x

Etterson, J. R., & Shaw, R. G. (2001). Constraint to adaptive evolution in response to global warming. *Science*, *294*(5540), 151–154. https://doi.org/10.1126/science.1063656

Exposito-Alonso, M., Vasseur, F., Ding, W., … Weigel, D. (2018). Genomic basis and evolutionary potential for extreme drought adaptation in *Arabidopsis thaliana*. *Nature Ecology & Evolution*, *2*(2), 352–358. https://doi.org/10.1038/s41559-017-0423-0

Falconer, D. S., & Mackay, T. (1996). *Introduction to quantitative genetics* (4th ed.). Pearson, Prentice Hall.

Fry, J. D. (2003). Detecting ecological trade-offs using selection experiments. *Ecology*, *84*(7), 1672–1678. https://doi.org/10.1890/0012-9658(2003)084[1672:detuse]2.0.co;2

Grime, J. P., & Hunt, R. (1975). Relative growth-rate: Its range and adaptive significance in a local flora. *The Journal of Ecology*, *63*(2), 393. https://doi.org/10.2307/2258728

Hadfield, J. D. (2010). MCMC methods for multi-response generalized linear mixed models: The MCMCglmm R package. *Journal of Statistical Software*, *33*(2), 22. https://doi.org/10.18637/jss.v033.i02

Hansen, T. F., & Houle, D. (2008). Measuring and comparing evolvability and constraint in multivariate characters. *Journal of Evolutionary Biology*, *21*(5), 1201–1219. https://doi.org/10.1111/j.1420-9101.2008.01573.x

Hansen, T. F., Solvin, T. M., & Pavlicev, M. (2019). Predicting evolutionary potential: A numerical test of evolvability measures. *Evolution*, *73*(4), 689–703. https://doi.org/10.1111/evo.13705

Hargreaves, A. L., Samis, K. E., & Eckert, C. G. (2014). Are species' range limits simply niche limits writ large? A review of transplant experiments beyond the range. *The American Naturalist*, *183*(2), 157–173. https://doi.org/10.1086/674525

Henry, G. A., & Stinchcombe, J. R. (2023). G-matrix stability in clinally diverging populations of an annual weed. *Evolution*, *77*(1), 49–62. https://doi.org/10.1093/evolut/qpac005

Hoffmann, A. A., & Blows, M. W. (1994). Species borders: Ecological and evolutionary perspectives. *Trends in Ecology & Evolution*, *9*(6), 223–227. https://doi.org/10.1016/0169-5347(94)90248-8

Hoffmann, A. A., & Merilä, J. (1999). Heritable variation and evolution under favourable and unfavourable conditions. *Trends in Ecology & Evolution*, *14*(3), 96–101. https://doi.org/10.1016/s0169-5347(99)01595-5

Holt, R. D. (2003). On the evolutionary ecology of species' ranges. *Evolutionary Ecology Research*, *5*, 159–178.

Holt, R. D., & Gaines, M. S. (1992). Analysis of adaptation in heterogeneous landscapes: Implications for the evolution of fundamental niches. *Evolutionary Ecology*, *6*(5), 433–447. https://doi.org/10.1007/bf02270702

Houle, D. (1992). Comparing evolvability and variability of quantitative traits. *Genetics*, *130*(1), 195–204. https://doi.org/10.1093/genetics/130.1.195

Irvine, J., Perks, M. P., Magnani, F., & Grace, J. (1998). The response of *Pinus sylvestris* to drought: Stomatal control of transpiration and hydraulic conductance. *Tree Physiology*, *18*(6), 393–402. https://doi.org/10.1093/treephys/18.6.393

Kirkpatrick, M. (2009). Patterns of quantitative genetic variation in multiple dimensions. *Genetica*, *136*(2), 271–284. https://doi.org/10.1007/s10709-008-9302-6

Kirkpatrick, M., & Barton, N. H. (1997). Evolution of a species' range. *The American Naturalist*, *150*(1), 1–23. https://doi.org/10.1086/286054

Kirkpatrick, M., & Lofsvold, D. (1992). Measuring selection and constraint in the evolution of growth. *Evolution*, *46*(4), 954–971. https://doi.org/10.1111/j.1558-5646.1992.tb00612.x

Kooyers, N. J. (2015). The evolution of drought escape and avoidance in natural herbaceous populations. *Plant Science*, *234*, 155–162. https://doi.org/10.1016/j.plantsci.2015.02.012

Kruschke, J. K. (2018). Rejecting or accepting parameter values in Bayesian estimation. *Advances in Methods and*

Practices in Psychological Science, *1*(2), 270–280. https://doi.org/10.1177/2515245918771304

Lande, R. (1979). Quantitative genetic analysis of multivariate evolution, applied to brain: Body size allometry. *Evolution*, *33*(1, Part2), 402–416. https://doi.org/10.1111/j.1558-5646.1979.tb04694.x

Lau, J. A., Shaw, R. G., Reich, P. B., & Tiffin, P. (2014). Indirect effects drive evolutionary responses to global change. *The New Phytologist*, *201*(1), 335–343. https://doi.org/10.1111/nph.12490

Lee-Yaw, J. A., Fracassetti, M., & Willi, Y. (2018). Environmental marginality and geographic range limits: A case study with *Arabidopsis lyrata* ssp. *lyrata*. *Ecography*, *41*(4), 622–634. https://doi.org/10.1111/ecog.02869

Lee-Yaw, J. A., Kharouba, H. M., Bontrager, M., … Angert, A. L. (2016). A synthesis of transplant experiments and ecological niche models suggests that range limits are often niche limits. *Ecology Letters*, *19*(6), 710–722. https://doi.org/10.1111/ele.12604

Lenoir, J., Bertrand, R., Comte, L., … Grenouillet, G. (2020). Species better track climate warming in the oceans than on land. *Nature Ecology & Evolution*, *4*(8), 1044–1059. https://doi.org/10.1038/s41559-020-1198-2

Liu, H., Ye, Q., & Wiens, J. J. (2020). Climatic-niche evolution follows similar rules in plants and animals. *Nature Ecology & Evolution*, *4*(5), 753–763. https://doi.org/10.1038/s41559-020-1158-x

McGuigan, K., & Blows, M. W. (2007). The phenotypic and genetic covariance structure of drosophilid wings. *Evolution*, *61*(4), 902–911. https://doi.org/10.1111/j.1558-5646.2007.00078.x

Mezey, J. G., & Houle, D. (2005). The dimensionality of genetic variation for wing shape in *Drosophila melanogaster*. *Evolution*, *59*(5), 1027–1038. https://doi.org/10.1111/j.0014-3820.2005.tb01041.x

Milocco, L., & Salazar-Ciudad, I. (2022). Evolution of the G matrix under nonlinear genotype-phenotype maps. *The American Naturalist*, *199*(3), 420–435. https://doi.org/10.1086/717814

Oliveira, R. S., Eller, C. B., Barros, F. D. V., … Bittencourt, P. (2021). Linking plant hydraulics and the fast–slow continuum to understand resilience to drought in tropical ecosystems. *New Phytologist*, *230*(3), 904–923. https://doi.org/10.1111/nph.17266

Paccard, A., Fruleux, A., & Willi, Y. (2014). Latitudinal trait variation and responses to drought in *Arabidopsis lyrata*. *Oecologia*, *175*(2), 577–587. https://doi.org/10.1007/s00442-014-2932-8

Paccard, A., Van Buskirk, J., & Willi, Y. (2016). Quantitative genetic architecture at latitudinal range boundaries: Reduced variation but higher trait independence. *The American Naturalist*, *187*(5), 667–677. https://doi.org/10.1086/685643

Paccard, A., Vance, M., & Willi, Y. (2013). Weak impact of finescale landscape heterogeneity on evolutionary potential in *Arabidopsis lyrata*. *Journal of Evolutionary Biology*, *26*(11), 2331–2340. https://doi.org/10.1111/jeb.12220

Paquette, A., & Hargreaves, A. L. (2021). Biotic interactions are more often important at species' warm versus cool range edges. *Ecology Letters*, *24*(11), 2427–2438. https://doi.org/10.1111/ele.13864

Parmesan, C. (2006). Ecological and evolutionary responses to recent climate change. *Annual Review of Ecology, Evolution, and Systematics*, *37*(1), 637–669. https://doi.org/10.1146/annurev.ecolsys.37.091305.110100

Patsiou, T., Walden, N., & Willi, Y. (2021). What drives species' distributions along elevational gradients? Macroecological and -evolutionary insights from Brassicaceae of the central Alps. *Global Ecology and Biogeography*, *30*(5), 1030–1042. https://doi.org/10.1111/geb.13280

Pearce-Higgins, J. W., Ockendon, N., Baker, D. J., … Tanner, E. V. J. (2015). Geographical variation in species' population responses to changes in temperature and precipitation. *Proceedings of the Royal Society of London, Series B: Biological Sciences*, *282*(1818), 20151561. https://doi.org/10.1098/rspb.2015.1561

Phillips, P. C., & Arnold, S. J. (1999). Hierarchical comparison of genetic variance-covariance matrices. I. Using the Flury hierarchy. *Evolution*, *53*(5), 1506–1515. https://doi.org/10.1111/j.1558-5646.1999.tb05414.x

Polechová, J. (2018). Is the sky the limit? On the expansion threshold of a species' range. *PLoS Biology*, *16*(6), e2005372. https://doi.org/10.1371/journal.pbio.2005372

Polechová, J., & Barton, N. H. (2015). Limits to adaptation along environmental gradients. *Proceedings of the National Academy of Sciences of the United States of America*, *112*(20), 6401–6406. https://doi.org/10.1073/pnas.1421515112

Puentes, A., Granath, G., & Ågren, J. (2016). Similarity in G matrix structure among natural populations of *Arabidopsis lyrata*: G matrix structure in populations of *A. lyrata*. *Evolution*, *70*(10), 2370–2386. https://doi.org/10.1111/evo.13034

Puijalon, S., Bouma, T. J., Douady, C. J., … Bornette, G. (2011). Plant resistance to mechanical stress: Evidence of an avoidance–tolerance trade-off. *The New Phytologist*, *191*(4), 1141–1149. https://doi.org/10.1111/j.1469-8137.2011.03763.x

R Core Team. (2021). *R: A language and environment for statistical computing* [Computer software]. R Foundation for Statistical Computing. https://www.R-project.org/

Roff, D. A., & Fairbairn, D. J. (2012). The evolution of trade-offs under directional and correlational selection: Selection on a trade-off. *Evolution*, *66*(8), 2461–2474. https://doi.org/10.1111/j.1558-5646.2012.01634.x

Roff, D. A., Mostowy, S., & Fairbairn, D. J. (2002). The evolution of trade-offs: Testing predictions on response to selection and environmental variation. *Evolution*, *56*(1), 84–95. https://doi.org/10.1111/j.0014-3820.2002.tb00851.x

Rumpf, S. B., Hülber, K., Klonner, G., … Dullinger, S. (2018). Range dynamics of mountain plants decrease with elevation. *Proceedings of the National Academy of Sciences of the United States of America*, *115*(8), 1848–1853. https://doi.org/10.1073/pnas.1713936115

Salguero-Gómez, R. (2017). Applications of the fast–slow continuum and reproductive strategy framework of plant life histories. *New Phytologist*, *213*(4), 1618–1624. https://doi.org/10.1111/nph.14289

Sánchez-Castro, D., Patsiou, T., Perrier, A., … Willi, Y. (2024). Uncovering the cause of breakup between species' range limits and niche limits under climate warming. *Journal of Biogeography*, 1–14. https://doi.org/10.1111/jbi.14796

Sartori, K., Vasseur, F., Violle, C., … Vile, D. (2019). Leaf economics and slow-fast adaptation across the geographic range of *Arabidopsis thaliana*. *Scientific Reports*, *9*(1), 10758. https://doi.org/10.1038/s41598-019-46878-2

Sartori, K., Violle, C., Vile, D., … Kazakou, E. (2022). Do leaf nitrogen resorption dynamics align with the slow-fast continuum? A test at the intraspecific level. *Functional Ecology*, *36*(5), 1315–1328. https://doi.org/10.1111/1365-2435.14029

Schepers, J. R., Heblack, J., & Willi, Y. (2024). Negative interaction effect of heat and drought stress at the warm end of species distribution. *Oecologia*, *204*(1), 173–185. https://doi.org/10.1007/s00442-023-05497-5

Schluter, D. (1996). Adaptive radiation along genetic lines of least resistance. *Evolution*, *50*(5), 1766–1774. https://doi.org/10.1111/j.1558-5646.1996.tb03563.x

Sexton, J. P., McIntyre, P. J., Angert, A. L., & Rice, K. J. (2009). Evolution and ecology of species range limits. *Annual Review of Ecology, Evolution, and Systematics*, *40*(1), 415–436. https://doi.org/10.1146/annurev.ecolsys.110308.120317

Sheth, S. N., & Angert, A. L. (2016). Artificial selection reveals high genetic variation in phenology at the trailing edge of a species range. *The American Naturalist*, *187*(2), 182–193. https://doi.org/10.1086/684440

Stearns, S. C. (1983). The influence of size and phylogeny on patterns of covariation among life-history traits in the mammals. *Oikos*, *41*(2), 173. https://doi.org/10.2307/3544261

Stearns, S. C. (1992). *The evolution of life histories* (1st ed.). Oxford University Press.

Upadhyay, P. (2019). Climate change and adaptation strategies: A study of agriculture and livelihood adaptation by farmers in Bardiya District, Nepal. *Advances in Agriculture and Environmental Science:*

Open Access (AAEOA), *2*(1), 47–52. https://doi.org/10.30881/aaeoa.00022

Vile, D., Pervent, M., Belluau, M., … Simonneau, T. (2012). Arabidopsis growth under prolonged high temperature and water deficit: Independent or interactive effects?: Plant responses to high temperature and water deficit. *Plant, Cell & Environment*, *35*(4), 702–718. https://doi.org/10.1111/j.1365-3040.2011.02445.x

Vose, R. S., Easterling, D. R., Kunkel, K. E., … Wehner, M. F. (2017). Chapter 6: Temperature changes in the United States. In D. J. Wuebbles, D. W. Fahey, K. A. Hibbard, D. J. Dokken, B. C. Stewart, & T. K. Maycock (Eds.), *Climate science special report: Fourth national climate assessment*. (Vol. *I*, pp. 185–206). U.S. Global Change Research Program. https://doi.org/10.7930/J0N29V45

Walsh, B., & Chenoweth, S. F. (2017). *Summer institute in statistical genetics—Module1: Principles of quantitative genetics*. https://cnsgenomics.com/data/teaching/SISG/module_1/Module01-Lecture-Notes.pdf

Willi, Y. (2013). The battle of the sexes over seed size: Support for both kinship genomic imprinting and interlocus contest evolution. *The American Naturalist*, *181*(6), 787–798. https://doi.org/10.1086/670196

Willi, Y., Follador, R., Keller, N., … McDonald, B. A. (2010). Heritability under benign and stressful conditions in the plant pathogenic fungus *Mycosphaerella graminicola*. *Evolutionary Ecology Research*, *12*, 761–768.

Willi, Y., Fracassetti, M., Zoller, S., & Van Buskirk, J. (2018). Accumulation of mutational load at the edges of a species range. *Molecular Biology and Evolution*, *35*(4), 781–791. https://doi.org/10.1093/molbev/msy003

Willi, Y., Frank, A., Heinzelmann, R., … Ceresini, P. C. (2011). The adaptive potential of a plant pathogenic fungus, *Rhizoctonia solani* AG-3, under heat and fungicide stress. *Genetica*, *139*(7), 903–908. https://doi.org/10.1007/s10709-011-9594-9

Willi, Y., & Van Buskirk, J. (2019). A practical guide to the study of distribution limits. *The American Naturalist*, *193*(6), 773–785. https://doi.org/10.1086/703172

Willi, Y., & Van Buskirk, J. (2022). A review on trade-offs at the warm and cold ends of geographical distributions. *Philosophical Transactions of the Royal Society of London, Series B: Biological Sciences*, *377*(1848), 20210022. https://doi.org/10.1098/rstb.2021.0022

Wolak, M. E., & Keller, L. F. (2014). Dominance genetic variance and inbreeding in natural populations. In A. Charmentier, D. Garant, & L. E. B. Kruuk (Eds.), *Quantitative genetics in the wild*. Oxford University Press.

Wood, C. W., & Brodie, E. D. (2015). Environmental effects on the structure of the G-matrix: Environmental effects on genetic correlations. *Evolution*, *69*(11), 2927–2940. https://doi.org/10.1111/evo.12795

Wos, G., & Willi, Y. (2015). Temperature-stress resistance and tolerance along a latitudinal cline in North American *Arabidopsis lyrata*. *PLoS One*, *10*(6), e0131808. https://doi.org/10.1371/journal.pone.0131808

Wos, G., & Willi, Y. (2018). Genetic differentiation in life history traits and thermal stress performance across a heterogeneous dune landscape in *Arabidopsis lyrata*. *Annals of Botany*, *122*(3), 473–484. https://doi.org/10.1093/aob/mcy090

Oecologia
https://doi.org/10.1007/s00442-023-05497-5

ORIGINAL RESEARCH

Negative interaction effect of heat and drought stress at the warm end of species distribution

Judith R. Schepers[1] · **Jessica Heblack**[1] · **Yvonne Willi**[1]

Received: 23 May 2023 / Accepted: 10 December 2023

Abstract

Geographic range limits of species are often a reflection of their ecological niche limits. In many organisms, important niche limits that coincide with distribution limits are warm and warm-dry conditions. We investigated the effects of heat and drought, as they can occur at the warm end of distribution. In a greenhouse experiment, we raised North American *Arabidopsis lyrata* from the centre of its distribution as well as from low- and high-latitude limits under average and extreme conditions. We assessed plant growth and development, as well as leaf and root functional traits, and tested for a decline in performance and selection acting on growth, leaf, and root traits. Drought and heat, when applied alone, lowered plant performance, while combined stress caused synergistically negative effects. Plants from high latitudes did not survive under combined stress, whereas plants originating from central and low latitudes had low to moderate survival, indicating divergent adaptation. Traits positively associated with survival under drought, with or without heat, were delayed and slowed growth, though plastic responses in these traits were generally antagonistic to the direction of selection. In line, higher tolerance of stress in southern populations did not involve aspects of growth but rather a higher root-to-shoot ratio and thinner leaves. In conclusion, combined heat and drought, as can occur at southern range edges and presumably more so under global change, seriously impede the long-term persistence of *A. lyrata*, even though they impose selection and populations may adapt, though under likely interference by considerable maladaptive plasticity.

Keywords Adaptation · Drought stress · Heat stress · Phenotypic selection · Warm range limit

Introduction

Across the globe, temperatures have been increasing and precipitation has become more variable, with more droughts or extreme rain (IPCC 2023). In turn, warming has been linked to the retreat of some species from the warm limits of their distribution (Parmesan 2006; Cahill et al. 2014; Sánchez-Salguero et al. 2017; Rumpf et al. 2018). Causes of retreat can include the direct effect of abiotic stressors, biotic stressors, or interactions among them (Cahill et al. 2014; Paquette and Hargreaves 2021). Populations often evolve particular strategies to cope with one type of stressor over their evolutionary histories, which can interfere with strategies for coping with more extreme stress or other stressors (Fry 2003; Ågren and Schemske 2012; Santos del Blanco et al. 2013; Willi and Van Buskirk 2022). For example, it was shown that combined stressors, such as heat and drought, can act to amplify negative effects (Craufurd and Peacock 1993; Savin and Nicolas 1996; Dreesen et al. 2012; Zandalinas and Mittler 2022). Consequently, if we aim to understand why species fail to cope with extreme conditions at the warm end of species distributions, stressors need to be studied both individually and in combination (Suzuki et al. 2014).

Plants have evolved various ways of coping with heat, which have been studied in regards to the genes involved, the physiology, morphology, and development (Berry and Bjorkman 1980; Bita and Gerats 2013; Zhao et al. 2021; Sher et al. 2022; Yadav et al. 2022). In many species, a general strategy of coping with heat is leaf cooling through increased transpiration (Crawford et al. 2012; Deva et al. 2020; Sadok et al. 2021). Increased transpiration is achieved by a longer stomatal opening and higher stomatal

Communicated by Susanne Schwinning.

✉ Judith R. Schepers
judith.schepers@unibas.ch

[1] Department of Environmental Sciences, University of Basel, 4056 Basel, Switzerland

Published online: 23 January 2024

conductance (Marchin et al. 2022). Such cooling requires a continuous supply of water, which is ensured, for example, by deep roots, an extensive and complex root system, or by a high root-to-shoot ratio (Parker 1949; Aston and Lawlor 1979; Natarajan and Kuehny 2008; Giri et al. 2017). Strategies affecting morphology are generally targeted at decreasing surface area to reduce the area of water loss by thick stems and leaves, short internode lengths, or smaller leaves (Vile et al. 2012; Stewart et al. 2016; Leigh et al. 2017). Coping with heat may also include a faster phenology, such as early flowering to escape the heat during critical life stages (e.g., in *Arabidopsis thaliana*, Balasubramanian et al. 2006; Taylor et al. 2019). Additionally, leaf pigments can play an important role during heat and high irradiation as paler leaves with less chlorophyll help maintain energy balance and lower the risk of overheating (Kume 2017; Genesio et al. 2020), while carotenoids can dissipate excess energy and thereby protect the chlorophyll apparatus (Kumar et al. 2020).

Plants have evolved also various strategies to cope with drought (Murtaza et al. 2016), which sometimes differ substantially from those of coping with heat (Zhang and Sonnewald 2017). Under drought conditions, an immediate reduction of water-loss is achieved by the closure of the stomata; this ensures that the leaf water potential does not drop to critical levels and that plant metabolic processes are maintained (Verslues and Juenger 2011; Tardieu 2013). In combination with increased water uptake from the soil, the plant can thus maintain the physiological water balance (Rodrigues et al. 2019). Increased water uptake during a short period of drought is achieved by a wider and deeper root system (Dinneny 2019). In addition to longer roots, smaller leaves are a common response of plants growing under drought conditions, leading to an increased root-to-shoot ratio and reduced leaf surface area per dry weight (lower specific leaf area, SLA) (Matsui and Singh 2003; Dovrat et al. 2019). Another adjustment to a dry climate is accelerated reproductive development (Franks et al. 2007). Further strategies related to escape include a shorter growth period, earlier germination, or dormancy during extreme events (Basu et al. 2016; Franks 2011; Verslues and Juenger 2011; Tardieu 2013; Balachowski et al. 2016).

Combined heat and drought may be particularly challenging for plants. Marchin et al. (2022) reported for broadleaf evergreens that stomata closure is of advantage during drought, as it can maintain a high water potential of the leaves, but it can lead to overheating of leaves under heat. Conflicting responses to heat and drought were also reported for *A. thaliana* (cv Columbia) and *Nicotiana tabacum* (Rizhsky et al. 2002, 2004). While plants responded to heat by increased photosynthesis and respiration, they responded to drought by reducing both processes. Under combined heat and drought, plants increased respiration but reduced photosynthesis, leading to senescence. Also in *A. thaliana*, high temperatures and the combination of heat and water deficiency accelerated reproductive development, while water deficiency alone delayed reproduction (Vile et al. 2012). The different responses to heat, drought and both stressors in combination confirm the need to investigate single and combined stressors to reveal the conflicts among strategies that impede their fitness benefits, particularly in the face of global warming.

The response to climatic stress often depends on the climate history of populations and can therefore vary greatly within species (Lexer et al. 2003). Indeed, local climate has been linked with adaptive differences among populations in several studies (e.g., Richardson et al. 2014; Estarague et al. 2022; Sánchez-Castro et al. 2022). Adaptive differences may be expressed under stress, but also when plants grow under ideal climatic growth conditions. In the canopy species *Corymbia calophylla* and in *A. thaliana*, plants originating from hot and/or dry areas differed in trait expression even under benign conditions; they had lower SLA, higher leaf dry matter content (LDMC), or smaller leaf area (May et al. 2017; Ahrens et al. 2020). Another aspect of climate adaptation is that within species or closely related species, there may be differences in how it is achieved. For example European *A. lyrata* subsp. *petraea* of southern range edges was shown to flower earlier and have a higher flowering propensity (Riihimäki and Savolainen 2004), while in North American *A. lyrata* subsp. *lyrata*, plants from northern latitudes have faster reproductive development (Paccard et al. 2014).

The aim of this study was to test whether heat, drought and combined stress had similar effects on growth, leaf and root functional traits, whether populations responded differently depending on their climate of origin, and whether plastic changes were in the direction favoured by selection. The study organism was the North American *Arabidopsis lyrata* spp. *lyrata* (hereafter *A. lyrata*). Environmental niche modelling had revealed that the range limits of *A. lyrata* in the south and the north were associated with climate niche limits, with minimum temperature in early spring being the most niche- and range-limiting factor (Lee-Yaw et al. 2018). But with climate change, temperature and precipitation have changed across the distribution area of *A. lyrata*, resulting in reduced environmental suitability at the southern distribution limit (Online Resource 1 Fig. S1, Online Resource 2 Table S1). We analysed the stress responses of five populations, one from the range centre and two each from the warm and cold ends of the species' distribution (Figs. 1, Online Resource 1 S1, Online Resource 2 Tables S1, S2). Plants were grown in the greenhouse under four distinct temperature and watering conditions, based on average or higher temperature and average or lower precipitation as they occur at the low-latitude range edge during the growing season (Online Resource 2 Table S1). We addressed the following

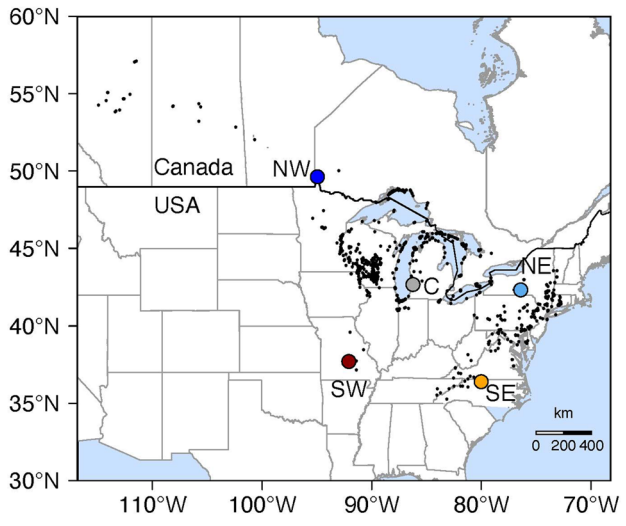

Fig. 1 Range of *Arabidopsis lyrata* in North America. The black dots indicate species occurrences reported since 1960 of a thinned dataset. Coloured dots show the locations of the populations used in this study: one from the centre of the range (C), and the others from the range edges, from the north-east (NE), north-west (NW) south-east (SE) and south-west (SW)

questions: (1) Do heat, drought, and heat-drought differ in how they affect growth, leaf and root functional traits, and do responses vary among populations and seed families within populations? (2) What is the difference in trait expression in populations from the southern edge as compared to central and northern populations? Are trait differences between these groups of populations the same as the plastic changes? And (3) how does selection act on traits? Does selection in the different environments align with plastic changes?

Materials and methods

Plant material

Arabidopsis lyrata subsp. *lyrata* is native to the eastern and mid-western United States and south-eastern Canada, and it is locally restricted to substrates with little water-holding capacity, sand and rocky outcrops (Koch et al. 2001; Al-Shehbaz and O'Kane 2002; Schmickl et al. 2010). Seeds were collected from five *A. lyrata* populations (Fig. 1): a genetically highly diverse one from the centre of the range (**C**) (Wos and Willi 2018), and four from the edges, in the north-east (**NE**), north-west (**NW**), south-east (**SE**), and south-west (**SW**, details in Table S2). Collections were performed between 2007 and 2014, and seeds of field-collected plants were propagated together during one generation in the greenhouse by performing crosses within unique pairs of plants of the same population. For this experiment we considered three pairs of plants for range-edge populations and 120 pairs for the central population; the latter population was used for selection analysis and therefore included many more plants.

Climate data

Climate data at the sites of the five populations were obtained from WorldClim v1.4 (Hijmans et al. 2005), v2.1 (Fick and Hijmans 2017) and CRU-TS 4.06 (Harris et al. 2020) downscaled with WorldClim v2.1. We downloaded monthly average temperature (T_{mean}), maximum temperature (T_{max}), precipitation (P) and precipitation during the driest month (P_{min}, Bio14) for the periods of 1960–1990 and 1970–2000. For 2000–2018, we used the monthly minimum temperature (T_{min}), maximum temperature (T_{max}), and precipitation (P), and calculated monthly average temperature (T_{mean}) and precipitation of the driest month (P_{min}). For T_{mean}, T_{max} and P of the three time periods, we calculated averages for the months of April to June and June to August (using the dplyr and raster packages; Hijmans 2022; Wickham et al. 2022). For the first two periods, the resolution was 30 s, for 2000–2018, the resolution was 2.5 min. Plots and all statistics were done with R (R-Core-Team 2021). Raster plots (Figs. 1, Online Resource 1 S1) were produced with the R packages sp and sf (Pebesma and Bivand 2005; Pebesma 2018).

Experimental design

Offspring plants were grown under four climatic conditions in a two-by-two factorial design, with average or high temperature, and average or low precipitation as occurs at the two warm-end populations (**SE** and **SW**) (Online Resource 1 Fig. S1). We assumed that plants would germinate during fall or early spring and grow and develop thereafter. To imitate average conditions, values close to mean temperature and precipitation for April to June were chosen (data in Online Resource 2 Table S1). For the heat treatment, temperature was set close to the mean of June to August. For the drought treatment, precipitation of the driest month for the two sites was taken.

For each treatment combination, five blocks were set up, each with one replicate seed per cross (edge populations were only represented in three blocks). Seeds were placed into 54-multipot trays within a block, filled with a sand-peat mixture of 2:1. Only every second pot of a tray was used to prevent plants from growing into each other and to facilitate image analysis. Seeds were stratified for 12 days at 4 °C in climate chambers at 70% humidity (ClimeCab 1400, KÄLTE 3000 AG, Landquart, Switzerland) and then transferred to four greenhouse chambers (temperature of 18 °C). During stratification and germination, plants were covered with mesh nets to maintain high humidity. To ensure

a gradual change between stratification and experimental conditions, day length was increased from 8 h to 1 h every 3–4 days until the day length was 16 h, with a light intensity of 200 µM s^{-1} m^{-2}. During the transition phase, day temperature was 20 °C and night temperature was 18 °C, and plants were watered daily by spraying from above. After 7 days, when approximately 75% of the plants had germinated, the mesh nets were removed. After an additional 14 days, when about 80% of germinated plants were at the four-leaf stage, stress treatments began.

Two of the four greenhouse chambers (University of Basel greenhouse) were set to have cold temperatures, and two to have warm temperatures. Each chamber of a particular temperature regime contained either two or three spatial blocks of multi-pot trays with plants of both watering treatments. Based on climate data from the two southern sites (Online Resource 2 Table S1), we set the low-temperature regime to an average of 20.6 °C: 22 °C during the day, a one-hour heat peak of 25 °C at noon, and night temperature at 18 °C for 8 h. The high-temperature regime had an average of 25.2 °C: 27 °C during the day, a heat peak of 30 °C at noon, and a night temperature of 23 °C. The high precipitation/watering regime was initially 8.4 ml of water every second day, corresponding to 100 mm m^{-2} of monthly precipitation. The low-precipitation treatment was 5 ml of water every second day corresponding to 65 mm m^{-2} of monthly precipitation. Due to sudden early dieback in the dry treatment because the soil in the small pots dried out quickly, watering was increased by 20%, to 10 ml and 6 ml in the high and the low precipitation regimes, respectively; in nature, soil bodies where *A. lyrata* grows are typically deeper and less likely to dry out as rapidly. In all chambers, air humidity was set to 70%. Trays were randomized twice per week (within blocks, and block position in the paired chambers), and fertilizer was given every 4 weeks (0.2% Wuxal universal fertilizer, Westland Schweiz GmbH, Dielsdorf, Switzerland). Additionally, after 14 weeks, an insecticide (1.5% Kendo gold, Westland Schweiz GmbH) was applied once a week to protect the plants from insect infestations.

Trait assessment

Performance. After stratification, every day for 2 weeks we recorded the day of germination, when the cotyledons became visible. Afterwards, pots were examined every second to third day for further germination, death (all leaves brown and dry), bolting (visible flowering stem), flowering (first flower), revival of plants (green leaves), and infestation. This approach resulted in data on days to germination, survival, longevity (days until death or harvest), and flowering propensity.

Growth traits. We monitored the growth of rosettes by taking images twice a week starting with germination. Images were taken per multiport tray with a 12 MP Panasonic DMC-FS10 digital camera (Kadoma, Japan) with ISO 100 and -2/3 exposure in a photo box that was placed over individual trays. Imaging stopped when 40% of plants from the control treatment had bolted. Additional images were taken before harvest. Images were analysed by an adapted script of Exposito-Alonso et al. (2018). From each image, two new images were produced, one retaining pixels in the range of green and the other in the range of red. The two images were then merged, the sum of pixels counted for each pot and time point, and the value transformed into mm^2. For each plant, seven growth models were explored (linear, exponential, power, two- and three-parameter logistic, von Bertalanffy, and Gompertz) to fit the size data over time. Of these, the three-parameter logistic model–together with the more complex Gompertz model–was the best supported across plants and treatments. From the three-parameter logistic model we extracted the asymptote (maximum rosette size [mm^2], *size*), the time to the inflection point (time to fastest growth [days], x_{mid}), and the slope at the inflection point (*growth rate*). The script is accessible at github.com/heblackj/image_analysis.

Leaf and root functional traits. We stopped the experiment one month after 40% of the plants of the control group had started flowering. All plants were separated into four components, if present: inflorescences, dead leaves, living leaves, and roots. Leaves and roots were washed to remove attached soil and dried with a paper towel to remove excess water. The fresh weight of inflorescences, living leaves, and roots was taken. Then the material was dried separately for 48 h in an oven at 60 °C. We calculated the specific leaf area (*SLA*, size [mm^2] per dry weight of leaves [mg], excluding dead leaves), the leaf dry matter content (*LDMC*, dry weight leaves [mg] per wet weight leaves [g], excluding dead leaves), and the root-to-shoot ratio (*root:shoot*; dry weight roots per dry weight all leaves and inflorescences). The range of trait values per treatment and family are presented in Online Resource 2 Table S3.

Statistical analysis

To approach normality of the dependent variables, we $\log_{10}$-transformed growth rate, root:shoot ratio, SLA, and LDMC. An initial analysis of variance was performed to reveal the effects of days to germination, block, and tray within block on variables (Anova in car package; Fox and Weisberg 2019). If considerable variance was explained, variables were corrected for the specific effects. Furthermore, we looked into trait dependencies by correlating all traits within the central population at the level of the plant for each treatment separately (Fig. 3, rcorr in Hmisc; Harrell

2022) and performed a principal component analysis for each treatment (Online Resource 1 Fig. S2, factoextra package; Kassambara and Mundt 2020).

In the main analysis, we tested for the effect of temperature, watering and the interaction term on aspects of performance and functional traits using linear mixed effects models for continuous data or generalized linear models for binary data (lmerTest package; Kuznetsova et al. 2017). The random effects included population and family nested within population, but the precise structure was set based on model selection. The models that were compared by Akaike information criterion (AIC) varied from: including intercept, slope on temperature, slope on watering, and all covariances for population and family nested within population, to including intercepts only (results in Online Resource 2 Table S4). For each dependent variable the best model was chosen for final analysis. The random effects were evaluated by likelihood ratio testing (Table 1; lrtest in the lmtest package; Zeileis and Hothorn 2002). Differences in plant performance and traits between low- (SE, SW) and high-latitude populations (NE, NW, C) were tested by Wilcoxon rank sum tests (Table 2).

We conducted univariate and multivariate phenotypic selection analyses on the growth and functional traits of the central population with generalized linear models (de Jong 1995; Scheiner and Callahan 1999; Callaway et al. 2003). Trait data was standardized (mean = 0, deviation = 1) within treatment, and models were run for each treatment separately. An exception was the combined heat and drought treatment. As we lacked data on SLA, LDMC and root:shoot ratio of the many plants that had died in this treatment, we replaced values; we calculated family means for these traits under drought or heat treatment, averaged those values over the two treatments, and used this trait data instead in the selection analysis of the combined stress treatment. In models including single traits, we first evaluated the inclusion of both the linear and quadratic term by AIC (Table 3). As the inclusion of the quadratic term was rarely better, the multivariate models were built by only including linear terms (packages mcglm and htmcglm; Bonat 2018; de Freitas 2022). As fitness variables, we used the propensity to flower for the control treatment, survival for single stress treatments, and longevity for the combined stress treatment.

Results

Climate change

For the five populations studied, the climate had shifted between the periods of 1960–1990 and 2000–2018 (Online Resource 1 Fig. S1, Online Resource 2 Table S1). The change in mean temperature for the growing season of

Table 1 Effect of heat and drought on performance and leaf and root functional traits of *Arabidopsis lyrata*

Variable	Estimates of fixed effects				Difference in log-likelihood					
	Intercept	Heat	Drought	Heat + Drought	Pop	Pop.*Heat	Pop.*Drought	Fam	Fam.*Heat	Fam.*Drought
Survival	**3.51*****	**− 1.62*****	**− 1.84****	**− 2.71*****	0.81			2.96		
Flowering	− 0.33		**− 1.76*****		0.89			**113.32*****		
Size	**1464.85*****	− 209.25	**− 374.06***	**− 62.10****	< 0.01	1.85	2.51	< 0.01	**43.02*****	**25.98*****
x_{mid}	**27.12*****	**− 1.48*****	**− 1. 38*****	**− 2.30*****	< 0.01	< 0.01	< 0.01	< 0.01	**32.43*****	**14.89****
Growth rate	**0.08*****	**0.01****	**< − 0.01*****	**0.03*****	< 0.01			**109.62*****		
SLA	**1.04*****	0.07	− 0.07	**0.53*****	< 0.01	1.87	1.9	< 0.01	**43.64*****	**13.44****
LDMC	**2.46*****	**− 0.06*****	**− 0.04*****	0.04	< 0.01	< 0.01	< 0.01	< 0.01	**12.70****	1.73
Root:shoot	**0.13****	**0.06***	**0.05***	0.01	**29.92****			54.64		

Estimates of fixed effects and the difference in log-likelihood for random effects are reported. Significance is indicated in bold (*P < 0.05, **P < 0.01, ***P < 0.001). Models for size, x_{mid} (time to fastest growth), SLA (specific leaf area) and LDMC (leaf dry matter content) assessed variances of intercepts, slopes on temperature and watering, and all covariances, for population and family (testing of an aspect included its variance and the two covariances). Models for survival, flowering, growth rate and root:shoot ratio assessed variances of intercepts only, for population (Pop.) and family (Fam.). The random-effects structure of models was determined based on model selection (Online Resource 2 Table S4)

Table 2 Effect of heat and drought on performance and leaf and root functional traits differing between southern and northern/central populations

Variable	P-values			
	Intercept	Heat	Drought	Heat + Drought
Survival	0.394	0.138	0.200	**0.004**
Flowering	0.721		0.964	
Size	0.252	0.268	0.483	0.661
x_{mid}	0.781	0.417	0.806	0.621
Growth rate	0.515	0.760	0.081	0.495
SLA	**0.003**	0.064	0.133	**0.018**
LDMC	0.431	0.989	0.384	0.880
Root:shoot	**0.037**	**< 0.001**	**< 0.001**	0.312

x_{mid} is the time to fastest growth, SLA the specific leaf area, and LDMC the leaf dry matter content. P-values based on pairwise Wilcox tests are shown. Significant differences are indicated in bold ($P < 0.05$)

April to June and the summer months of June to August had increased by 0.4 °C and 0.6 °C, respectively. Change varied considerably among sites, e.g. for the summer means from + 0.1 °C to + 1.1 °C. At the same time, mean precipitation during April to June and June to August increased by 11 mm and 8.6 mm, respectively, again with some variability among sites. However, precipitation during the driest month of the year, which tends to be in late winter at the southern edge of *A. lyrata*, had declined by 14.5 mm. Under the conditions chosen in the experiment, we simulated average spring compared to summer temperature at the southern edge, and average spring precipitation compared to dry conditions, assuming that such extreme events may become more likely under global warming already during spring, when plants grow and start flowering.

Heat and drought stress

The treatments, temperature and watering, had strong additive and interaction effets (Table 1). Heat and drought lowered survival, and both stressors combined lowered survival even further (Fig. 2A). Longevity and the propensity to flower generally followed this pattern. The variable of longevity had low values and high variability in the treatment with combined stress (Online Resource 2 Table S3). For treatments with low temperatures, there was considerable flowering, and plants showed a lower propensity to flower under dry compared to control conditions (Fig. 2B).

Patterns for plant size were similar to those for survival. Maximum plant size was negatively affected by drought and – as a trend – by heat, and under combined heat and drought, their negative effect was exacerbated (Fig. 2C, Table 1). In turn, time to mid-size was shorter under single stress and interacted to be much shorter under combined stress (Fig. 2D). Furthermore, maximal growth rate was higher under heat and lower under drought, though the interaction term was again positive, indicating highly accelerated growth rates under combined heat and drought (Fig. 2E). LDMC decreased and the root:shoot ratio increased under single stress, indicating more water relative to dry weight in leaves and more relative investment into roots (Figs. 2G, H). However, the interaction term was not significant for the two traits. For SLA, only the interaction term was significant, indicating that plants had thinner leaves under combined heat and drought (Fig. 2F).

Populations did not differ significantly in traits across treaments nor in response to drought or heat stress, except in the root:shoot ratio (Table 1). All other significant random effects involved families or how families reacted to heat and watering. Nevertheless, some trends of population differences could be detected based on contrasts between the southern and the more northerly populations, including the central population (Table 2). Survival was similar among populations across treatment combinations except for combined heat and drought; in that treatment, southern populations tended to perform better, indicating some adaptation to extreme heat combined with drought (Fig. 3A). Other traits that differed between the southern and all other populations were SLA and the root:shoot ratio. Plants of southern populations had higher SLA, particularly under combined heat and drought (Fig. 3B), as well as higher root:shoot ratios, and the ratio increased more under single stress (Fig. 3C).

Correlations among traits were investigated for patterns within treatments by considering plants of the central population only (Figs. 4, Online Resource 1 S2). A few correlations were rather consistent across treatments, such as the negative correlation between maximal growth rate and both asymptotic plant size and time to mid-size, and the positive correlation between time to mid-size and plant size. There were two additional, consistently negative correlations both involving the root:shoot ratio, with plant size and LDMC.

Traits under selection

Lastly, we investigated the traits under phenotypic selection under the different treatments (Table 3). Only the diverse central population was included in this analysis, as it covered most of the variation in traits of the edge populations. Under heat alone, no evidence for a trait under selection could be found, neither in the univariate nor in the multivariate selection analyses. Under drought, high x_{mid}/late vegetative growth and a low growth rate were selectively favoured, though this was only found under univariate selection. Under combined heat and drought stress, we found evidence for positive linear selection favouring late maximal growth (univariate selection only), slow growth, large final size, and small SLA (multivariate selection only). Finally, under

Table 3 Selection analysis of plant growth, leaf and root functional traits under the four treatments, based on the performance measures [W] of flowering, survival or longevity

Variable	Univariate selection				Multivariate selection
	$AIC_{lin.}$	$AIC_{quad.}$	$Coef._x$	$Coef._x^2$	$Coef._x$
Control; W = *flowering [0/1]*					
Size	755	758	**0.06****		− 0.02
x_{mid}	761	761	0.02		− 0.02
Growth rate	761	761	− 0.01		− 0.03
SLA	290	309	**0.33*****		**0.29*****
LDMC	499	466	**0.22*****		**0.10*****
Root:shoot	624	567	**− 0.19*****		**− 0.04***
Heat; W = *survival [0/1]*					
Size	553	552	< 0.01		< 0.01
x_{mid}	546	547	0.03		< 0.01
Growth rate	549	549	− 0.03		< 0.01
SLA	− 27,626	− 27,621	< 0.01		< 0.01
LDMC	− 27,366	− 27,372	< 0.01	< 0.01	< 0.01
Root:shoot	− 27,385	− 27,394	< 0.01	< 0.01	< 0.01
Drought; W = *survival [0/1]*					
Size	623	623	0.02		< 0.01
x_{mid}	613	621	**0.06****		< 0.01
Growth rate	608	619	**− 0.07*****		< 0.01
SLA	− 24,473	− 24,476	< 0.01		< 0.01
LDMC	− 24,472	− 24,474	< 0.01		< 0.01
Root:shoot	− 24,805	− 24,806	< 0.01		< 0.01
Heat + Drought; W = *longevity*					
Size	1497	1512	**0.18*****		**0.14****
x_{mid}	1494	1502	**0.16*****		− 0.12
Growth rate	1448	1466	**− 0.32*****		**− 3.6*****
$SLA_{Heat\&Drought}$	1429	1429	− 0.07		**− 0.11***
$LDMC_{Heat\&Drought}$	1432	1434	0.06		0.06
$Root:shoot_{Heat\&Drought}$	1449	1447	− 0.01		0.02

x_{mid} is the time to fastest growth, SLA the specific leaf area, and LDMC the leaf dry matter content. In the univariate selection models, each trait was explored for the importance of the linear and quadratic term by AIC, and for the model with the lower AIC, estimated coefficients are reported. The last column shows the estimated coefficients of a model of multivariate selection, with all six traits as linear effects. Significant coefficients (coef.) are indicated in bold (*P < 0.05, **P < 0.01, ***P < 0.001)

control conditions, we found evidence for positive linear selection favouring larger size (univariate selection only), higher SLA, higher LDMC, and lower root:shoot ratio.

Discussion

Populations from the southern edge of the distribution of *A. lyrata* are affected by climate change, warmer average temperatures and more variable precipitation (Online Resource 2 Table S1). In our experimental study, we found that an increase in temperature and lower precipitation/watering had a negative effect on plant survival, and combined stress had a worse than additive effect on survival (Fig. 2A). Parallel findings were revealed for vegetative growth. Under single stress, plants had fast growth earlier and reached or tended to reach a smaller final size, while under combined stress, fastest growth happened even earlier and final size was smaller than if stressors had acted additively (Figs. 2C, D). Moreover, southern populations had a higher survival under combined stress compared to northern populations, indicating some adaptation to such extreme climatic conditions. We discuss these and further results below in regard to strategies for coping with climatic extremes and conflicts among strategies under variable climatic extremes at the low latitudinal edge.

Single stressors, heat or drought, lowered survival to a similar extent, though other aspects of performance differed.

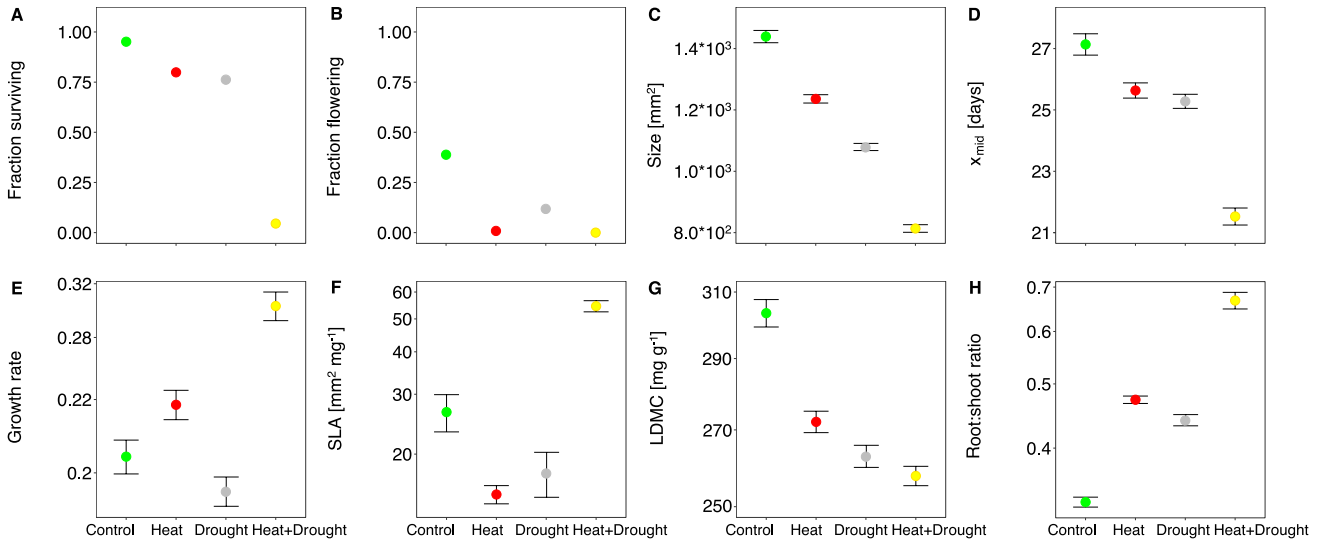

Fig. 2 Effect of heat, drought and combined stress on performance and leaf and root functional traits of *Arabidopsis lyrata*. For each of the four treatment combinations of Control, Heat, Drought, and Heat + Drought, the overall corrected means with standard error (for non-binary traits) are shown. Please note the $\log_{10}$ scale for growth rate, SLA, LDMC, and root:shoot ratio

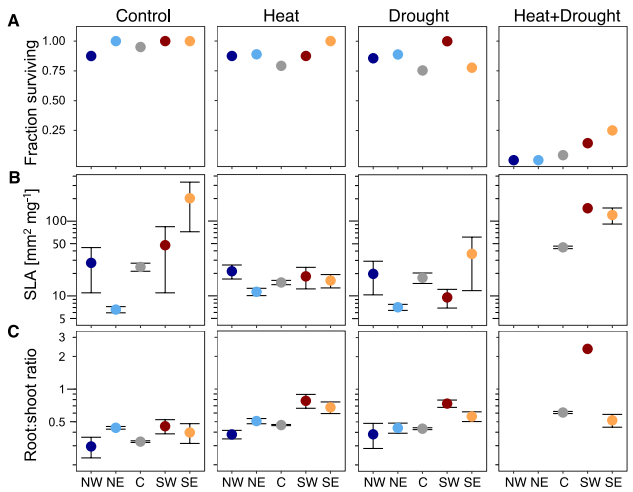

Fig. 3 Effect of heat, drought and combined stress on performance and leaf and root functional traits of *Arabidopsis lyrata*. For each of the four treatment combinations, population corrected means with standard error are shown. The five populations are sorted on the x-axis from left/north to right/south. Please note the $\log_{10}$ scale for SLA and root:shoot ratio. SLA had a wider than usual range of values because leaf area was approximated by rosette surface area, resulting in particularly low values in the case of overlapping leaves and particularly high values in the case leaves had long petioles

Size was reduced more under drought, but hardly any plants flowered under heat (Fig. 2B, C). The combination of heat and drought was then particularly devastating for plant survival, as stressors interacted in a synergistic manner. *Arabidopsis lyrata* must regularly experience very hot and dry conditions where it occurs. The species thrives in relatively open vegetation, on active sand dunes and on rocks with little vegetation cover, which heat up on sunny days. Furthermore, sandy soils typically have little water-holding capacity, and rocky outcrops have hardly any, except for cracks that may be filled with organic substrate. Given these features of the habitat, one would assume that the species can cope with both stressors, but apparently not when they co-occur as in our pot-design experiment. The result is in line with many studies showing that stressors multiply in their effect on plant performance (Mittler 2006; Zhang and Sonnewald 2017; Zandalinas and Mittler 2022).

We observed a number of plastic responses to heat, drought, and combined stress along the slow-fast continuum that did not seem adaptive. Plants exposed to heat or drought had the fastest growth early, a higher maximal growth under heat, and they reached a smaller final size (Figs. 2C–E, Table 1). This pattern of earlier and faster growth together with reduced size was strengthened under combined stress. Therefore, results suggest that *A. lyrata* generally responds to heat and/or drought by a strategy of escape in time (Levitt 1980; Ludlow and Muchow 1990) that seems to come at the cost of small size, in line with the concept of the slow-fast continuum (Reich 2014). The study of phenotypic selection indicated that these induced responses in vegetative growth were not adaptive or even maladaptive, with selection favouring opposite trait responses (Table 3). Under drought and combined heat and drought, selection tended to favour late and slow growth. Furthermore, under combined heat and drought, selection favoured large size. A reason could be that the plastic responses evolved in environments of short stress exposure, whereas the one applied in our study lasted

longer and might have possibly favoured adaptations increasing climate tolerance (or resistance). Divergence between strategies of escape and tolerance have often been reported in response to drought stress. While early growth can be a drought escape or avoidance strategy with a short life cycle, plants with a tolerance strategy commonly grow more slowly under long-term drought stress and over a longer period of time, and thus live longer (Franks 2011; Tardieu 2012; Bouzid et al. 2019; Csilléry et al. 2020; Burnette and Eckhart 2021).

Small size need not necessarily be a cost of early and rapid growth but could be beneficial under heat and drought. Under heat, small leaves rather than large ones are more likely to maintain a low leaf temperature by higher transpiration (Vile et al. 2012; Stewart et al. 2016; Saini et al. 2022). Under drought, small leaf size can be beneficial as water loss is lower (Lin et al. 2017). Such benefits may have also partially existed in our experiment, as under heat or drought alone we found no sign of positive selection for larger size (Table 3). Moreover, small size seems largely a cost of early and fast growth. Phenotypic correlation analysis on the central population supported that the three traits of time to fastest growth, maximal growth rate and final plant size, were strongly integrated in each of the four treatment combinations used in our study, with the strongest found under combined stress (Fig. 4). Therefore, while small size may be of some advantage under single stress, it is a serious cost to early and rapid growth under combined stress.

We also observed plastic responses in leaf and root functional traits. Plants had a higher root:shoot ratio and more water in leaves (lower LDMC) under single stress and thinner leaves (higher SLA) under combined stress (Table 1). Morphological adaptations to maintain a high water potential under stress are typically achieved by increased root systems, reduced vegetative growth or reduced stomatal transpiration loss, e.g. by thicker leaves (Sicher et al. 2012; Maggio et al. 2018; Seleiman et al. 2021). Alternatively, tolerance strategies are associated with maintaining hydrostatic pressure, by osmotic adjustments, and cavitation resistance (Delzon 2015; Blum 2017). Except for thinner leaves being disfavoured under combined heat and drought (in multivariate selection analysis only), none of the three leaf and root functional traits were found to be under selection under single or combined stress while they were under control conditions. Under control conditions, a high root:shoot ratio was negatively selected against, indicating costs. Furthermore, thin leaves (higher SLA) with a high dry matter content (higher LDMC) – potentially photosynthetically highly active – were favoured. Plants seem to adjust plastically in response to stress mainly by trait expression away from what is favoured under benign conditions.

However, southern populations, which had the highest survival under combined heat and drought, differed exactly

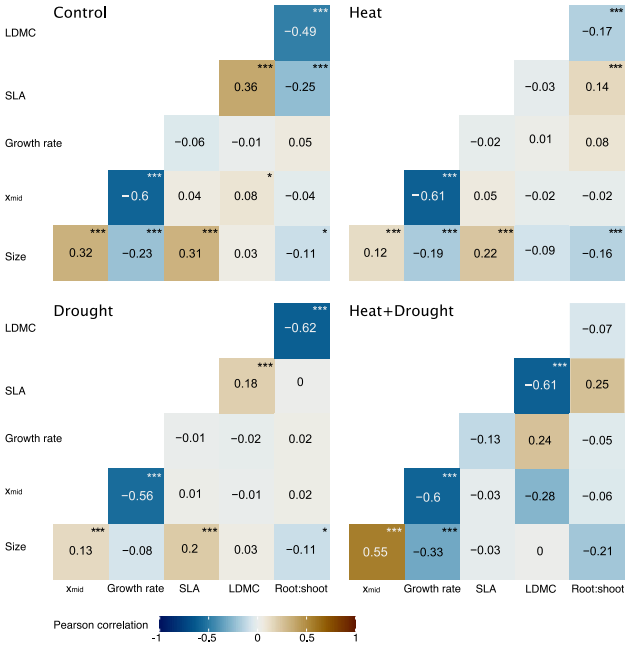

Fig. 4 Phenotypic correlations between all trait pairs of the central population in the four treatments. Negative correlations are indicated in shades of blue, positive ones in brown. Colour intensity indicates the strength of the correlation. Significance is indicated (*P < 0.05, **P < 0.01, ***P < 0.001)

in leaf and root functional traits. The two northern populations had no survival under combined stress, the central population, represented by many more plants in the experiment, had some survival, and the two southern-range-edge populations had considerable survival (Fig. 3A, Table 2). The southern populations seem to have been pre-exposed to similar stress conditions in the past and adapted to them. Therefore, traits that we found divergent between southern and more northern populations can indicate the traits of adaptation (Estarague et al. 2022). Southern populations differed in the expression of a higher root:shoot ratio, especially under stress (Fig. 3C). This response of low-latitude populations in the root system should allow the cooling by transpiration while maintaining the leaf water potential and photosynthesis (Stewart et al. 2016; Berny Mier y Teran et al. 2019; Csilléry et al. 2020; Marchin et al. 2022). Furthermore, under combined heat and drought, plants mainly from a southern population had thinner leaves (higher SLA, Fig. 3B, Table 2). This latter finding is hardly an adaptation, however, as thicker leaves were shown to be better at heat buffering and low water loss by evaporation (Wright et al. 2005; Leigh et al. 2012; Zhou et al. 2020), leaving the root:shoot ratio as the most likely candidate.

In fact, the combination of results of the different analyses suggests some important differences in the root:shoot ratio between southern and northern populations. At a first glance, the presumably adaptive differences between the southern

and northern populations are in line with induced responses by stress – higher root:shoot ratio under single stress and higher SLA under combined stress (Table 1), but with selection not found to act on these traits (Table 3). However, a high root:shoot ratio can be achieved by either investing less in shoots or investing more in roots. The plastic response of an increased root:shoot ratio under single stress may have been the result of smaller plant size and lower investment in shoots, which was neither disfavoured nor favoured by selection in those environments. In line with this, thin leaves, as found under combined heat and drought, may indicate less investment in above-ground structures as compared to roots (Wright et al. 2005; de Castro et al. 2019), which was not an adaptation but actually disfavoured in that environment (under negative selection in multivariate selection analysis). It is important to emphasize that these results were found with a focus on the central population. Southern populations are probably different in that they had a high root:shoot ratio owing to a higher investment in root structures and that is why they performed better under stress. Evidence in favour of this is their higher root:shoot ratio, particularly under stress, that is not paralleled with a lower investment in above-ground plant size (Table 2). The results clearly indicate the need to study the evolutionary potential of root traits in the context of southern range limits and climate change (Zhou et al. 2019; Taseski et al. 2021).

Conclusion

We studied replicate *A. lyrata* populations from across its distribution for their ability to cope with single stress, heat or drought as well as combined heat and drought as can be expected at the southern range edge under global warming. Our results led to two main conclusions for the species. First, the combination of heat and drought reduces plant survival more than predicted by the additive effects of heat and drought. Second, while plants from the north cannot persist under such conditions, plants originating from the southern end of the range have some survival, indicating the potential for adaptation. Selection analysis with a focus on the central population suggested that plastic responses to heat and drought followed a strategy of escape, which was not favoured under any of the stress environments. In line with this, the higher stress tolerance of the southern populations did not involve adjustments on the slow-fast continuum but was probably achieved by a higher allocation into roots as compared to shoots.

Supplementary Information The online version contains supplementary material available at https://doi.org/10.1007/s00442-023-05497-5.

Acknowledgements We thank O. Bachmann, E. Belen, S. Ellenberger, C. Mattson, S. Riedl, F. Schloeth, and X. Quinter for help with the experiment and data collection, and A. Newton for grammatical improvements. Collection permits were granted by the New York State Office of Parks and the United States National Park Service.

Author contributions statement YW, JH and JS designed the study. YW collected seeds in the field, and JH propagated the seeds. JH and JS performed the experiment. JS did the analysis and wrote the manuscript, with inputs by YW. All authors read and agreed on the manuscript.

Funding Open access funding provided by University of Basel. This project was supported by the Swiss National Science Foundation (grant no. 310030_184763 to Yvonne Willi). Schweizerischer Nationalfonds zur Förderung der Wissenschaftlichen Forschung

Data availability The data will we available at figshare (https://doi.org/10.6084/m9.figshare.23104481).

Code availability The code will be available on figshare (https://doi.org/10.6084/m9.figshare.23104481).

Declarations

Conflict of interest The authors declare that they have no conflict of interest.

Ethics approval Not applicable.

Consent to participate Not applicable.

Consent for publication Not applicable.

References

Ågren J, Schemske DW (2012) Reciprocal transplants demonstrate strong adaptive differentiation of the model organism *Arabidopsis thaliana* in its native range. New Phytol 194:1112–1122. https://doi.org/10.1111/j.1469-8137.2012.04112.x

Ahrens CW, Andrew ME, Mazanec RA et al (2020) Plant functional traits differ in adaptability and are predicted to be differentially affected by climate change. Ecol Evol 10:232–248. https://doi.org/10.1002/ece3.5890

Al-Shehbaz IA, O'Kane SL (2002) Taxonomy and phylogeny of *Arabidopsis* (Brassicaceae). Arab B 1:1–22. https://doi.org/10.1199/tab.0001

Aston MJ, Lawlor DW (1979) The relationship between transpiration, root water uptake, and leaf water potential. J Exp Bot 30:169–181

Balachowski JA, Bristiel PM, Volaire FA (2016) Summer dormancy, drought survival and functional resource acquisition strategies in California perennial grasses. Ann Bot 118:357–368. https://doi.org/10.1093/aob/mcw109

Balasubramanian S, Sureshkumar S, Lempe J, Weigel D (2006) Potent Induction of *Arabidopsis thaliana* flowering by elevated growth temperature. PLOS Genet 2:e106. https://doi.org/10.1371/journal.pgen.0020106

Basu S, Ramegowda V, Kumar A, Pereira A (2016) Plant adaptation to drought stress. F1000 Res. https://doi.org/10.12688/f1000research.7678.1

Berry J, Bjorkman O (1980) Photosynthetic response and adaptation to temperature in higher plants. Annu Rev Plant Physiol 31:491–543. https://doi.org/10.1146/annurev.pp.31.060180.002423

Bita C, Gerats T (2013) Plant tolerance to high temperature in a changing environment: scientific fundamentals and production of heat stress-tolerant crops. Front Plant Sci 4:273. https://doi.org/10.3389/fpls.2013.00273

Blum A (2017) Osmotic adjustment is a prime drought stress adaptive engine in support of plant production. Plant Cell Environ 40:4–10. https://doi.org/10.1111/pce.12800

Bonat WH (2018) Multiple response variables regression models in R: the mcglm package. J Stat Softw 84:1–30. https://doi.org/10.18637/jss.v084.i04

Bouzid M, He F, Schmitz G et al (2019) *Arabidopsis* species deploy distinct strategies to cope with drought stress. Ann Bot 124:27–40. https://doi.org/10.1093/aob/mcy237

Burnette TE, Eckhart VM (2021) Evolutionary divergence of potential drought adaptations between two subspecies of an annual plant: Are trait combinations facilitated, independent, or constrained? Am J Bot 108:309–319. https://doi.org/10.1002/ajb2.1607

Cahill AE, Aiello-Lammens ME, Fisher-Reid MC et al (2014) Causes of warm-edge range limits: systematic review, proximate factors and implications for climate change. J Biogeogr 41:429–442. https://doi.org/10.1111/jbi.12231

Callaway RM, Pennings SC, Richards CL (2003) Phenotypic plasticity and interactions among plants. Ecol 84:1115–1128. https://doi.org/10.1890/0012-9658(2003)084[1115:PPAIAP]2.0.CO;2

de Castro JN, Muller C, Almeida GM, Costa AC (2019) Physiological tolerance to drought under high temperature in soybean cultivars. Aust J Crop Sci 13:976–987. https://doi.org/10.21475/ajcs.19.13.06.p1767

Craufurd PQ, Peacock JM (1993) Effect of heat and drought stress on sorghum (*Sorghum bicolor*). II Grain Yield Exp Agric 29:77–86. https://doi.org/10.1017/S0014479700020421

Crawford AJ, McLachlan DH, Hetherington AM, Franklin KA (2012) High temperature exposure increases plant cooling capacity. Curr Biol 22:R396–R397. https://doi.org/10.1016/j.cub.2012.03.044

Csilléry K, Buchmann N, Fady B (2020) Adaptation to drought is coupled with slow growth, but independent from phenology in marginal silver fir (*Abies alba Mill.*) populations. Evol Appl 13:2357–2376. https://doi.org/10.1111/eva.13029

de Jong G (1995) Phenotypic plasticity as a product of selection in a variable environment. Am Nat 145:493–512

Delzon S (2015) New insight into leaf drought tolerance. Funct Ecol 29:1247–1249. https://doi.org/10.1111/1365-2435.12500

Deva CR, Urban MO, Challinor AJ et al (2020) Enhanced leaf cooling is a pathway to heat tolerance in common bean. Front Plant Sci. https://doi.org/10.3389/fpls.2020.00019

Dinneny JR (2019) Developmental responses to water and salinity in root systems. Annu Rev Cell Dev Biol 35:239–257. https://doi.org/10.1146/annurev-cellbio-100617-062949

Dovrat G, Meron E, Shachak M et al (2019) Plant size is related to biomass partitioning and stress resistance in water-limited annual plant communities. J Arid Environ 165:1–9. https://doi.org/10.1016/j.jaridenv.2019.04.006

Dreesen FE, De Boeck HJ, Janssens IA, Nijs I (2012) Summer heat and drought extremes trigger unexpected changes in productivity of a temperate annual/biannual plant community. Environ Exp Bot 79:21–30. https://doi.org/10.1016/j.envexpbot.2012.01.005

Estarague A, Vasseur F, Sartori K et al (2022) Into the range: a latitudinal gradient or a center-margins differentiation of ecological strategies in *Arabidopsis thaliana*? Ann Bot 129:343–356. https://doi.org/10.1093/aob/mcab149

Exposito-Alonso M, Vasseur F, Ding W et al (2018) Genomic basis and evolutionary potential for extreme drought adaptation in Arabidopsis thaliana. Nat Ecol Evo 2:352–358. https://doi.org/10.1038/s41559-017-0423-0

Fick SE, Hijmans RJ (2017) WorldClim 2: New 1-km spatial resolution climate surfaces for global land areas. Int J Climatol 37:4302–4315. https://doi.org/10.1002/joc.5086

Fox J, Weisberg S (2019) An R companion to applied regression, 3rd edn. Sage, Thousand Oaks CA

Franks SJ (2011) Plasticity and evolution in drought avoidance and escape in the annual plant *Brassica rapa*. New Phytol 190:249–257. https://doi.org/10.1111/j.1469-8137.2010.03603.x

Franks SJ, Sim S, Weis AE (2007) Rapid evolution of flowering time by an annual plant in response to a climate fluctuation. Proc Natl Acad Sci 104:1278–1282. https://doi.org/10.1073/pnas.0608379104

de Freitas LC (2022) _htmcglm: Hypothesis Testing for McGLMs. R package version 0.0.1. https://CRAN.R-project.org/package=htmcglm. Accessed 22 Nov 2023

Fry JD (2003) Detecting ecological trade-offs using selection experiments. Ecology 84:1672–1678. https://doi.org/10.1890/0012-9658(2003)084[1672:DETUSE]2.0.CO;2

Genesio L, Bassi R, Miglietta F (2020) Plants with less chlorophyll: a global change perspective. Glob Chang Biol 27:959–967. https://doi.org/10.1111/gcb.15470

Giri A, Heckathorn S, Mishra S, Krause C (2017) Heat stress decreases levels of nutrient-uptake and -assimilation proteins in tomato roots. Plants 6:6. https://doi.org/10.3390/plants6010006

Harrell Jr F (2022) Hmisc: Harrell Miscellaneous. R package version 5.1–0, https://hbiostat.org/R/Hmisc/. Accessed 22 Nov 2023

Harris I, Osborn TJ, Jones P, Lister D (2020) Version 4 of the CRU TS monthly high-resolution gridded multivariate climate dataset. Sci Data 7:109. https://doi.org/10.1038/s41597-020-0453-3

Hijmans RJ, Cameron SE, Parra JL et al (2005) Very high resolution interpolated climate surfaces for global land areas. Int J Climatol 25:1965–1978. https://doi.org/10.1002/joc.1276

Hijmans RJ (2022) Raster: geographic data analysis and modeling. R package version 3.6–20. https://rspatial.org/raster/. Accessed 22 Nov 2023

Intergovernmental Panel on Climate Change (IPCC) (2023) Climate change 2021 – The physical science basis: Working group I contribution to the sixth assessment report of the intergovernmental panel on climate change. Cambridge University Press, Cambridge

Kassambara A, Mundt F (2020) Factoextra: extract and visualize the results of multivariate data analyses. R package version 1.0.7.999, https://CRAN.R-project.org/package=factoextra. Accessed 22 Nov 2023

Koch M, Haubold B, Mitchell-Olds T (2001) Molecular systematics of the Brassicaceae: evidence from coding plastidic *mat*K and nuclear *Chs* sequences. Am J Bot 88:534–544. https://doi.org/10.2307/2657117

Kumar P, Yadav S, Singh MP (2020) Possible involvement of xanthophyll cycle pigments in heat tolerance of chickpea (*Cicer*

arietinum L.). Physiol Mol Biol Plants 26:1773–1785. https://doi.org/10.1007/s12298-020-00870-7
Kume A (2017) Importance of the green color, absorption gradient, and spectral absorption of chloroplasts for the radiative energy balance of leaves. J Plant Res 130:501–514. https://doi.org/10.1007/s10265-017-0910-z
Kuznetsova A, Brockhoff PB, Christensen RHB (2017) lmerTest package: tests in linear mixed effects models. J Stat Softw 82:1–26. https://doi.org/10.18637/jss.v082.i13
Lee-Yaw JA, Fracassetti M, Willi Y (2018) Environmental marginality and geographic range limits: a case study with *Arabidopsis lyrata* ssp. *lyrata*. Ecography (Cop) 41:622–634. https://doi.org/10.1111/ecog.02869
Leigh A, Sevanto S, Ball MC et al (2012) Do thick leaves avoid thermal damage in critically low wind speeds? New Phytol 194:477–487. https://doi.org/10.1111/j.1469-8137.2012.04058.x
Leigh A, Sevanto S, Close JD, Nicotra AB (2017) The influence of leaf size and shape on leaf thermal dynamics: does theory hold up under natural conditions? Plant Cell Environ 40:237–248. https://doi.org/10.1111/pce.12857
Levitt J (1980) Responses of plants to environmental stress. Chilling freezing, and high temperature stresses, vol 1, 3rd edn. Academic Press, New York
Lexer C, Randell RA, Rieseberg LH (2003) Experimental hybridization as a tool for studying selection in the wild. Ecology 84:1688–1699. https://doi.org/10.1890/0012-9658(2003)084[1688:EHAATF]2.0.CO;2
Lin H, Chen Y, Zhang H et al (2017) Stronger cooling effects of transpiration and leaf physical traits of plants from a hot dry habitat than from a hot wet habitat. Funct Ecol 31:2202–2211. https://doi.org/10.1111/1365-2435.12923
Ludlow MM, Muchow RC (1990) A critical evaluation of traits for improving crop yields in water-limited environments. Adv Agron 43:107–153. https://doi.org/10.1016/S0065-2113(08)60477-0
Maggio A, Bressan RA, Zhao Y et al (2018) It's hard to avoid avoidance: uncoupling the evolutionary connection between plant growth, productivity and stress "tolerance." Int J Mol Sci 19:11. https://doi.org/10.3390/ijms19113671
Marchin RM, Backes D, Ossola A et al (2022) Extreme heat increases stomatal conductance and drought-induced mortality risk in vulnerable plant species. Glob Chang Biol 28:1133–1146. https://doi.org/10.1111/gcb.15976
Matsui T, Singh BB (2003) Root characteristics in cowpea related to drought tolerance at the seedling stage. Exp Agric 39:29–38. https://doi.org/10.1017/S0014479703001108
May R-L, Warner S, Wingler A (2017) Classification of intra-specific variation in plant functional strategies reveals adaptation to climate. Ann Bot 119:1343–1352. https://doi.org/10.1093/aob/mcx031
Berny Mier y Teran JC, Konzen ER, Medina V et al (2019) Root and shoot variation in relation to potential intermittent drought adaptation of Mesoamerican wild common bean (*Phaseolus vulgaris* L.). Ann Bot 124:917–932. https://doi.org/10.1093/aob/mcy221
Mittler R (2006) Abiotic stress, the field environment and stress combination. Trends Plant Sci 11:15–19. https://doi.org/10.1016/j.tplants.2005.11.002
Murtaza G, Rasool F, Habib R et al (2016) A review of morphological, physiological and biochemical responses of plants under drought stress conditions. Imp J Interdiscip Res 2:1600–1606
Natarajan S, Kuehny JS (2008) Morphological, physiological, and anatomical characteristics associated with heat preconditioning and heat tolerance in *Salvia splendens*. J Amer Soc Hort Sci 133:527–534. https://doi.org/10.21273/JASHS.133.4.527
Paccard A, Fruleux A, Willi Y (2014) Latitudinal trait variation and responses to drought in *Arabidopsis lyrata*. Oecologia 175:577–587. https://doi.org/10.1007/s00442-014-2932-8
Paquette A, Hargreaves AL (2021) Biotic interactions are more often important at species' warm versus cool range edges. Ecol Lett 24:2427–2438. https://doi.org/10.1111/ele.13864
Parker J (1949) Effects of variations in the root-leaf ratio on transpiration rate. Plant Physiol 24:739–743. https://doi.org/10.1104/pp.24.4.739
Parmesan C (2006) Ecological and evolutionary responses to recent climate change. Annu Rev Ecol Evol Syst 37:637–669. https://doi.org/10.1146/annurev.ecolsys.37.091305.110100
Pebesma E, Bivand R (2005) Classes and methods for spatial data in R. R News 5:9–13
Pebesma E (2018) Simple features for R: standardized support for spatial vector data. R J 10:439–446. https://doi.org/10.32614/RJ-2018-009
R-Core-Team (2021) R: A language and environment for statistical computing, Vienna. https://www.R-project.org. Accessed 22 Nov 2023
Reich PB (2014) The world-wide 'fast–slow' plant economics spectrum: a traits manifesto. J Ecol 102:275–301. https://doi.org/10.1111/1365-2745.12211
Richardson JL, Urban MC, Bolnick DI, Skelly DK (2014) Microgeographic adaptation and the spatial scale of evolution. Trends Ecol Evol 29:165–176. https://doi.org/10.1016/j.tree.2014.01.002
Riihimäki M, Savolainen O (2004) Environmental and genetic effects on flowering differences between northern and southern populations of *Arabidopsis lyrata* (Brassicaceae). Am J Bot 91:1036–1045. https://doi.org/10.3732/ajb.91.7.1036
Rizhsky L, Liang H, Mittler R (2002) The combined effect of drought stress and heat shock on gene expression in tobacco. Plant Physiol 130:1143–1151. https://doi.org/10.1104/pp.006858
Rizhsky L, Liang H, Shuman J et al (2004) When defense pathways collide. The response of *Arabidopsis* to a combination of drought and heat stress. Plant Physiol 134:1683–1696. https://doi.org/10.1104/pp.103.033431
Rodrigues J, Inzé D, Nelissen H, Saibo NJM (2019) Source–sink regulation in crops under water deficit. Trends Plant Sci 24:652–663. https://doi.org/10.1016/j.tplants.2019.04.005
Rumpf S, Hülber K, Klonner G et al (2018) Range dynamics of mountain plants decrease with elevation. Proc Natl Acad Sci 115:1848–1853. https://doi.org/10.1073/pnas.1713936115
Sadok W, Lopez JR, Smith KP (2021) Transpiration increases under high-temperature stress: potential mechanisms, trade-offs and prospects for crop resilience in a warming world. Plant Cell Environ 44:2102–2116. https://doi.org/10.1111/pce.13970
Saini K, Dwivedi A, Ranjan A (2022) High temperature restricts cell division and leaf size by coordination of PIF4 and TCP4 transcription factors. Plant Physiol 190:2380–2397. https://doi.org/10.1093/plphys/kiac345
Sánchez-Castro D, Perrier A, Willi Y (2022) Reduced climate adaptation at range edges in North American *Arabidopsis lyrata*. Glob Ecol Biogeogr 31:1066–1077. https://doi.org/10.1111/geb.13483
Sánchez-Salguero R, Camarero JJ, Gutiérrez E et al (2017) Assessing forest vulnerability to climate warming using a process-based model of tree growth: bad prospects for rear-edges. Glob Chang Biol 23:2705–2719. https://doi.org/10.1111/gcb.13541
Santos del Blanco L, Bonser S, Valladares F et al (2013) Plasticity in reproduction and growth among 52 range-wide populations of a Mediterranean conifer: adaptive responses to environmental stress. J Evol Biol 26:1912–1924. https://doi.org/10.1111/jeb.12187
Savin R, Nicolas ME (1996) Effects of short periods of drought and high temperature on grain growth and starch accumulation of two malting barley cultivars. Funct Plant Biol 23:201–210

Scheiner SM, Callahan HS (1999) Measuring natural selection on phenotypic plasticity. Evol 53:1704–1713. https://doi.org/10.1111/j.1558-5646.1999.tb04555.x

Schmickl R, Jørgensen MH, Brysting AK, Koch MA (2010) The evolutionary history of the *Arabidopsis lyrata* complex: a hybrid in the amphi-Beringian area closes a large distribution gap and builds up a genetic barrier. BMC Evol Biol 10:98. https://doi.org/10.1186/1471-2148-10-98

Seleiman MF, Al-Suhaibani N, Ali N et al (2021) Drought stress impacts on plants and different approaches to alleviate its adverse effects. Plants 10:259. https://doi.org/10.3390/plants10020259

Sher A, Asghar Y, Qayum A et al (2022) A review on strong impacts of thermal stress on plants physiology, agricultural yield; and timely adaptation in plants to heat stress. J Bioresour Manag 9:15

Sicher RC, Timlin D, Bailey B (2012) Responses of growth and primary metabolism of water-stressed barley roots to rehydration. J Plant Physiol 169:686–695. https://doi.org/10.1016/j.jplph.2012.01.002

Stewart JJ, Demmig-Adams B, Cohu CM et al (2016) Growth temperature impact on leaf form and function in *Arabidopsis thaliana* ecotypes from northern and southern Europe. Plant Cell Environ 39:1549–1558. https://doi.org/10.1111/pce.12720

Suzuki N, Rivero RM, Shulaev V et al (2014) Abiotic and biotic stress combinations. New Phytol 203:32–43. https://doi.org/10.1111/nph.12797

Tardieu F (2012) Any trait or trait-related allele can confer drought tolerance: just design the right drought scenario. J Exp Bot 63:25–31. https://doi.org/10.1093/jxb/err269

Tardieu F (2013) Plant response to environmental conditions: assessing potential production, water demand, and negative effects of water deficit. Front Physiol 4:17. https://doi.org/10.3389/fphys.2013.00017

Taseski GM, Keith DA, Dalrymple RL, Cornwell WK (2021) Shifts in fine root traits within and among species along a fine-scale hydrological gradient. Ann Bot 127:473–481. https://doi.org/10.1093/aob/mcaa175

Taylor MA, Cooper MD, Schmitt J (2019) Phenological and fitness responses to climate warming depend upon genotype and competitive neighbourhood in *Arabidopsis thaliana*. Funct Ecol 33:308–322. https://doi.org/10.1111/1365-2435.13262

Verslues PE, Juenger TE (2011) Drought, metabolites, and *Arabidopsis* natural variation: a promising combination for understanding adaptation to water-limited environments. Curr Opin Plant Biol 14:240–245. https://doi.org/10.1016/j.pbi.2011.04.006

Vile D, Pervent M, Belluau M et al (2012) *Arabidopsis* growth under prolonged high temperature and water deficit: Independent or interactive effects? Plant Cell Environ 35:702–718. https://doi.org/10.1111/j.1365-3040.2011.02445.x

Wickham H, François R, Lionel K, Müller H (2022) dplyr: a grammar of data manipulation. R package version 1.1.2. https://dplyr.tidyverse.org. Accessed 22 Nov 2023

Willi Y, Van Buskirk J (2022) A review on trade-offs at the warm and cold ends of geographical distributions. Philos Trans R Soc B Biol Sci 377:20210022. https://doi.org/10.1098/rstb.2021.0022

Wos G, Willi Y (2018) Genetic differentiation in life history traits and thermal stress performance across a heterogeneous dune landscape in *Arabidopsis lyrata*. Ann Bot 122:473–484. https://doi.org/10.1093/aob/mcy090

Wright IJ, Reich PB, Cornelissen JHC et al (2005) Modulation of leaf economic traits and trait relationships by climate. Glob Ecol Biogeogr 14:411–421. https://doi.org/10.1111/j.1466-822x.2005.00172.x

Yadav MR, Choudhary M, Singh J et al (2022) Impacts, tolerance, adaptation, and mitigation of heat stress on wheat under changing climates. Int J Mol Sci 23:5. https://doi.org/10.3390/ijms23052838

Zandalinas SI, Mittler R (2022) Plant responses to multifactorial stress combination. New Phytol 234:1161–1167. https://doi.org/10.1111/nph.18087

Zeileis A, Hothorn T (2002) Diagnostic checking in regression relationships. R News 2:7–10

Zhang H, Sonnewald U (2017) Differences and commonalities of plant responses to single and combined stresses. Plant J 90:839–855. https://doi.org/10.1111/tpj.13557

Zhao J, Lu Z, Wang L, Jin B (2021) Plant responses to heat stress: physiology, transcription, noncoding RNAs, and epigenetics. Int J Mol Sci 22:117. https://doi.org/10.3390/ijms22010117

Zhou M, Wang J, Bai W et al (2019) The response of root traits to precipitation change of herbaceous species in temperate steppes. Funct Ecol 33:2030–2041. https://doi.org/10.1111/1365-2435.13420

Zhou H, Zhou G, He Q et al (2020) Environmental explanation of maize specific leaf area under varying water stress regimes. Environ Exp Bot 171:103932. https://doi.org/10.1016/j.envexpbot.2019.103932